



විදුලිබල හා බලශක්ති අමාත්‍යාංශය  
மின்வலு சக்தி அமைச்சு  
Ministry of Power & Energy



# NATIONAL ENERGY SYMPOSIUM 2019



ශ්‍රී ලංකා සුනිත්‍ය බලශක්ති අධිකාරිය  
மினிசக்தி மற்றும் மீள்சக்தி அமைச்சு  
Sri Lanka Sustainable Energy Authority





Peer Reviewed Journal on  
Vidulka  
**National Energy Symposium**  
**2019**

13<sup>th</sup> and 14<sup>th</sup> December 2019

BMICH, Colombo 07, Sri Lanka

Organised by



**Sri Lanka Sustainable Energy Authority**  
**Ministry of Power and Energy**



## **REVIEW PANEL**

Prof. H. Y. Ranjith Perera

Prof. Parakrama Karunaratne

Prof. W.D. Anura S. Wijayapala

Dr. Narendra De Silva

Eng. D. D. Ananda Namal

## **CORRESPONDENCE**

Email : [symposium@energy.gov.lk](mailto:symposium@energy.gov.lk) / [ravini@energy.gov.lk](mailto:ravini@energy.gov.lk)

Tel : +94 112677445

Fax : +94 112682534

Web Link of the Publications:

<http://www.energy.gov.lk/en/energy-management/vidulka-energy-exhibition>

**General Chair**

Dr. Asanka S. Rodrigo

**Programme Chair**

Prof. H. Y. Ranjith Perera

Prof. Parakrama Karunaratne

Dr. Narendra De Silva

Eng. Chamila Jayasekera

**Publications Chair**

Eng. Harsha Wickramasinghe

Eng. Ravini Karunaratne

**International Relations Chair**

Eng. H. A. Wimal Nadeera

**Financial Chair**

Mr. Densi Rathnayake

**Publicity Chair**

Mr. P. P. K. Wijethunga

Mr. Chaminda Liyanage

**Special Sessions Chair**

Prof. W. D. Anura S. Wijayapala  
(Renewable Energy)

Eng. D.D. Ananda Namal (Energy  
Efficiency)

**Innovations Chair**

Eng. K. Sanath Kithsiri

**Local Organizing Chair**

Eng. Poornima Kalhari

Eng. Apsara Katugaha

Eng. Madhurika Palatuwa

### **Conference Support**

Eng. Kalanika Hewage

Ms. Sandasara Subashni

Mr. Palitha Abeyrathne

Ms. Buddhika Dananjani

Mr. Chamila Prasanna

Mr. Kasun Hettiwatte

Mr. Sunimal Perera

Mr. B. P. P. J. De Silva

Ms. Anoja Thilakarathne

Mr. S. V. D. Dilshan

Ms. Thusangi Pelawatta

Mr. M. N. M. Nifran

Ms. Nimalka Samarakoon

Mr. R. M. C. L. Gunarathna

# Table of Contents

| Ref | Research Title  | Page No. |
|-----|---|----------|
| 1   | Statistical Assessment of Solar PV Impacts on Distribution Networks   | 1        |
| 2   | Optimum Operation of a Community Cluster using Demand Side Management and Dynamic Line Rating   | 11       |
| 3   | Mitigating Protection Issues of Islanded Rooftop Solar PV Systems   | 23       |
| 4   | Optimization of Energy Saving in Commercial Buildings using DC Microgrid  | 35       |
| 5   | Model for Measuring the Effect of Incentive Schemes, Tariff Regimes and Technological Innovations on Change of Consumer Behaviour on Energy Savings: A Study Based on Sri Lankan Electricity Consumers in Industrial Sector | 51       |
| 6   | Cost Benefit Analysis of Using Battery Energy Storage Systems in Distribution Systems   | 65       |
| 7   | Blockchain Assisted Business Model for Rooftop PV Energy Trading  | 75       |
| 8   | Sky Image-Based Short-Term Solar Power Forecasting Model  | 86       |
| 9   | Geographical Area Identification for Concentrated Solar Power (CSP) Plant in Sri Lanka  | 96       |
| 10  | The Effect of Electricity Supply on Economic Growth in Sri Lanka  | 108      |
| 11  | Sustainable Energy Options for Sri Lankan Transport Sector  | 119      |
| 12  | Importance of Developing a Sri Lankan Wave Energy Resource assessment according to IEC standards  | 128      |

|    |  |     |
|----|--|-----|
| 13 | Wave Energy Resource Assessment for the Coastal Ocean Around Sri Lanka using Satellite Altimeter Data  | 138 |
| 14 | Investigations on Ocean Wave Energy Assessment for Sri Lanka   | 150 |
| 15 | Geothermal Energy – Potential Applications in Sri Lanka  | 161 |
| 16 | Greenhouse Gas Emissions in the Energy Sector and Mitigation by Shifting from Coal to Natural Gas  | 174 |
| 17 | Determination of Suitable Concentration of Non-Digested and Digested Dairy Wastewater for Growing <i>Nannochloropsis</i> Spp. for Biodiesel Production   | 185 |
| 18 | A Rechargeable Banana Pith Bio-Battery   | 191 |
| 19 | Development of Cathode Material for Sodium-ion Rechargeable Battery in Sri Lanka   | 199 |
| 20 | Fabrication and Characterization of CuO Nanocrystalline Thin Films Prepared by Using Colloidal Suspension  | 213 |
| 21 | Torrefied Biomass Combustion in Biomass Powered Boilers: Process Simulation- Based Case Study Analysis of Power Generation and Thermal Energy Generation | 219 |
| 22 | Investigation of the Suitability of on-site Cogeneration Power Plants for Sri Lankan Upcountry Hotels  | 230 |
| 23 | A Tunnel Dryer for Clay Roof Tile; Preliminary Evaluation of Pilot Unit  | 244 |

## **Message from the Director General**

Energy is one of the major aspects contributing to the development of the country. In this respect, all the economic development sectors including industries, commercial establishments, etc. need to have quality and reliable energy supplies at affordable rates. The prospective economic development of the country will have increased energy demands due to the expansion of these sectors. Meanwhile, in the process of uplifting the living standards of people, utilization of more and more equipment and appliances will be there, and with all these there will be increasing energy demands in electricity as well as other forms of energy. So, a sustainable supply of energy at the most competitive prices along-with sound management of the supply side and demand side will be of paramount importance in the long-term sustainable development agenda of the country. As a country devoid of conventional energy resources, Sri Lanka will be able to assure of sustainable supply of energy through systematic approaches in sustainable energy development initiatives. This will be in par with the energy transition for which priority has been received at global level right in the present day context.

Sri Lanka became a party to the global Green House Gas (GHG) emission reduction efforts through ratifying the Nationally Determined Contributions (NDCs) in the aftermath of the 21<sup>st</sup> Conference of Parties (COP21) of the United Nations Framework Convention on Climate Change (UNFCCC). We, the energy sector, are committed to realize the GHG emission reduction as the major sector with 20% reduction targets. We are at a critical juncture in this context as 2020-2030 is the period declared for the NDC implementation. We can be happy of the National Energy Policy & Strategies being gazetted in August 2019, where sustainable energy is well recognized as

a policy element representing several policy pillars. That necessitates the country to have effective sustainable energy development programme implementation in the most economical and effective manner.

Sri Lanka Sustainable Energy Authority (SLSEA) as the focal national entity for the implementation of sustainable energy development programmes in the country has a pivotal role to play in the mentioned background. With the experience of the past 12 years of existence, we are of the understanding that it will be a profound multi-faceted endeavour to align the work towards a sustainable energy future. With this very theme, we conduct Vidulka Symposium 2019 with a view to obtain inputs from the researchers in the universities, research institutes, professional bodies, etc. to make fruitful use of their research outcomes in the sustainable energy development process.

We have a wide spectrum of research papers including the diverse subject areas of energy such as energy policy & planning, electrical engineering, thermal energy systems, chemical engineering, energy management, green buildings, biomass energy, solar energy and the emerging renewable energy resources of the country – wave power and geothermal energy. It is highly commendable that energy research is being carried out by many institutes. As far as the energy sector is concerned, it has good information and data in contrast to any other sector in the country, and we understand that it is attributed to the high research involvement pertinent to the subject of energy. Nevertheless, it would be high time to have a critical review on how policy, R&D, industrial interventions, can be integrated so that the country is benefitted in the long run. When it comes to the sustainable energy development, this will be a key aspect to be concerned in view of the multiple dimensions related to the subject. Primarily, it is becoming more and more important in the background of energy transition being taken place all



around the world. The important factor coming to the scene here is, it is very important to adapt the technologies to the Sri Lankan context in order to have the maximum economic benefits to the country. Further, development of the energy sector can achieve job creation, value addition to resources, etc., which would eventually contribute to the overall economy, going far beyond the energy aspect of it. Also, national infrastructure planning and implementation, industrial development, etc. need to be done with a serious attention towards energy management where support and contribution from many other sectors will be required. In all these interventions, there will be many areas where R&D activities will be involved. So, we will extensively need a wider coordination and networking among the relevant stakeholder communities to maximize the impact of work on the development agenda of the country. Development of innovative mechanisms and approaches will be required in that context, and I will be extremely happy for your cooperation and support in this line.

Let me take this opportunity to express my gratitude to the Hon. Minister, Hon. State Minister and Secretary to the Ministry of Power & Energy and all the officials of the Government institutes and all other stakeholders for extending their fullest support, cooperation and guidance in the related endeavours. I also thank the panel of judges and all the sector experts contributed with the expertise knowledge in the deliberations in the symposium. I thank the academia and researchers for sharing their research outcomes with the peer community and all others, who contributed towards the success of the Vidulka Symposium 2019.

**Dr. Asanka S. Rodrigo**  
**Director General**  
**Sri Lanka Sustainable Energy Authority**

# Statistical Assessment of Solar PV Impacts on Distribution Networks

Dilini Almeida<sup>#1</sup>, Sathsara Abeysinghe<sup>\*2</sup>, Janaka Ekanayake<sup>#3</sup>

*# Department of Electrical and Electronic Engineering, University of Peradeniya,  
Sri Lanka*

<sup>1</sup> dilini.almeida@eng.pdn.ac.lk

<sup>3</sup> jbe@ee.pdn.ac.lk

*\* Institute of Energy, School of Engineering, Cardiff University  
UK*

<sup>2</sup> AbeysingheAM@cardiff.ac.uk

## Abstract

Solar photovoltaic (PV) systems have gained attention around the world in generating greener energy. However, the high integration of PV systems could cause negative impacts on the operation and performance of the electricity distribution networks. Many studies are being carried out globally to analyse these impacts. Most of these studies are based on synthetic and real grid topologies. The research findings of a PV impact study performed for a specific case study network has very limited applicability to the other networks making them unsuitable for deriving generalised conclusions. In this study, a methodology was developed to generate a large number of realistic distribution network models with similar characteristics, and statistical analysis was performed using the generated network models to investigate the impact of solar PV on low voltage (LV) distribution networks. A Monte Carlo based approach has been proposed to evaluate the impacts using voltage unbalances, neutral currents, voltage and thermal limits. The results of the statistical study illustrate the impact of possible PV deployment scenarios for generalised LV distribution networks.

**Keywords:** low voltage distribution networks, solar PV impacts, Monte Carlo analysis

## Introduction

The depletion of fossil fuels and global warming issues have increased the adaptation of Renewable Energy Sources (RESs) such as solar and wind to meet the growing energy demand. Over recent years, power generation using solar PV has shown an exponential rise compared to the other RESs. Moreover, the declining price of solar modules and supporting policies by governments around the world have aided the growth of solar PV to be the one of the most promising RESs.

However, the influx of grid connected solar PV causes new challenges to the operation and performance of the distribution systems. Therefore, it is crucial to investigate these before they occur and develop methods to support high integration of solar PV into the existing grids.

Many studies are being carried out globally to evaluate the potential impact of solar PV on LV distribution networks. It has been widely reported that the possible impacts of grid connected solar PV are voltage rise, voltage fluctuations and unbalances, thermal overloads, and higher levels of harmonics.

The conventional LV distribution networks are radial in configuration and designed to operate on unidirectional power flow feed. Due to the high

proliferation of PV systems, reverse power flows could be seen when PV generation exceeds the load demand [1], [2]. Consequently, a voltage rise could be foreseen along the distribution system feeder causing violations on utility planning limitations and standards [3-5]. The irregular solar irradiation due to weather conditions introduces rapid variations in the output power of PV systems, which could lead to voltage fluctuations at the point of connection to the electric network [6]. Voltage unbalance is one of the common power quality problems that could be caused due to unequal system impedance and single-phase loads. Large penetration levels and unbalanced allocation of single-phase solar PV units installed on rooftops may offset feeder currents and lead to significant voltage unbalances [7], [8].

According to the literature review, most of the studies are focused on synthetic and real grid topologies [2, 9-20]. Therefore, the research findings of such studies have a limited applicability to the other networks making them unsuitable for deriving generalised conclusions. A brief overview of these studies is provided in Table 1. Considering the aforementioned limitations, a statistical analysis was performed using a large number of realistic distribution network models with similar characteristics to investigate the impact of solar PV on LV distribution networks.

*Table 1: Literature review of PV impact studies on LV distribution networks*

| <b>Ref.</b> | <b>Electricity network</b>                | <b>Studied impact</b>                            |
|-------------|---|--|
| [2]         | Canadian benchmark test system            | Reverse power flow and voltage rise              |
| [9]         | A representative LV network from Malaysia | Voltage rise and unbalance                       |
| [10]        | A contrived test network                  | Voltage rise and unbalance                       |
| [11]        | A representative LV network from Belgium  | Voltage rise, unbalance and neutral displacement |
| [12]        | Two LV networks from Australia            | Voltage rise and harmonics                       |
| [13]        | A representative network from UK          | Voltage rise                                     |
| [14]        | A simple 3 node LV system                 | Voltage rise                                     |
| [15]        | IEEE 13 and IEEE 34 bus test system       | Voltage rise and unbalance                       |
| [16]        | IEEE 34 bus test system                   | Voltage rise                                     |

## Methodology

A comprehensive analysis was carried out to investigate the potential impacts on distribution networks with the increasing integration of PV systems using statistically-similar distribution networks. The methodology of the study is illustrated in Figure 1.

### Generic Network Generation

A tool was developed to generate a large number of random, realistic models of LV distribution networks [17]. The tool is capable of generating ensembles of network models which are statistically-similar in terms of a set of topological and electrical properties as defined by the user with some given values. The overall concept of the tool is shown in Figure 2.

The tool was used to generate a number of statistically-similar distribution networks required for the impact assessment.

### LV Network Model

The electrical and topological data of the networks generated by the tool were used to model three phase four wire, unbalanced distribution networks in OpenDSS simulation platform for a realistic analysis.

The network models were used to examine the impact of PV on voltage and thermal limits, neutral current and voltage unbalance factor of distribution networks.

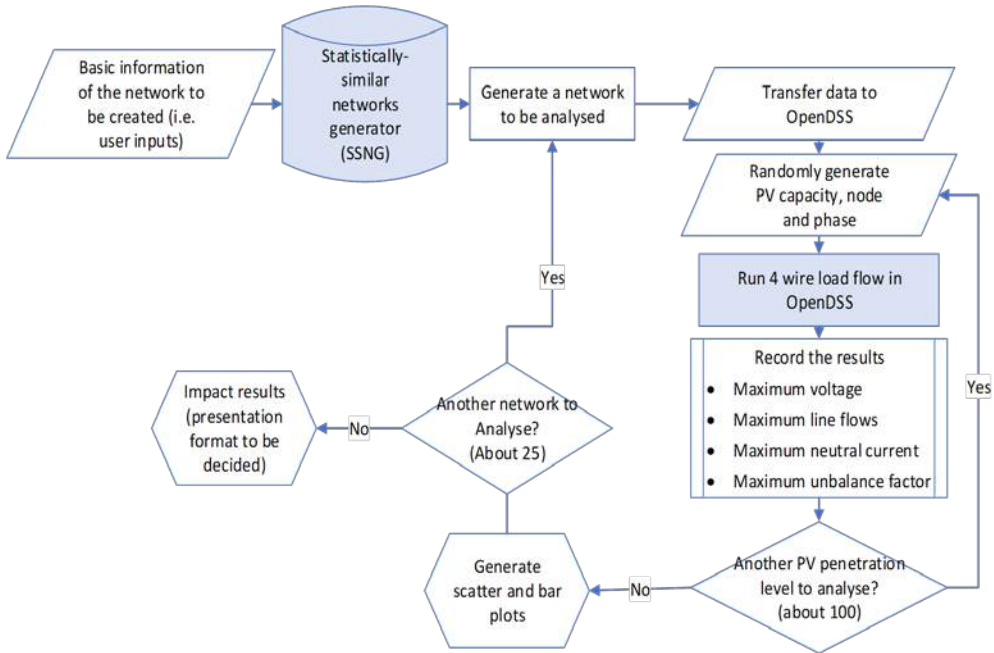


Figure 1: Methodology of the statistical analysis of PV impact

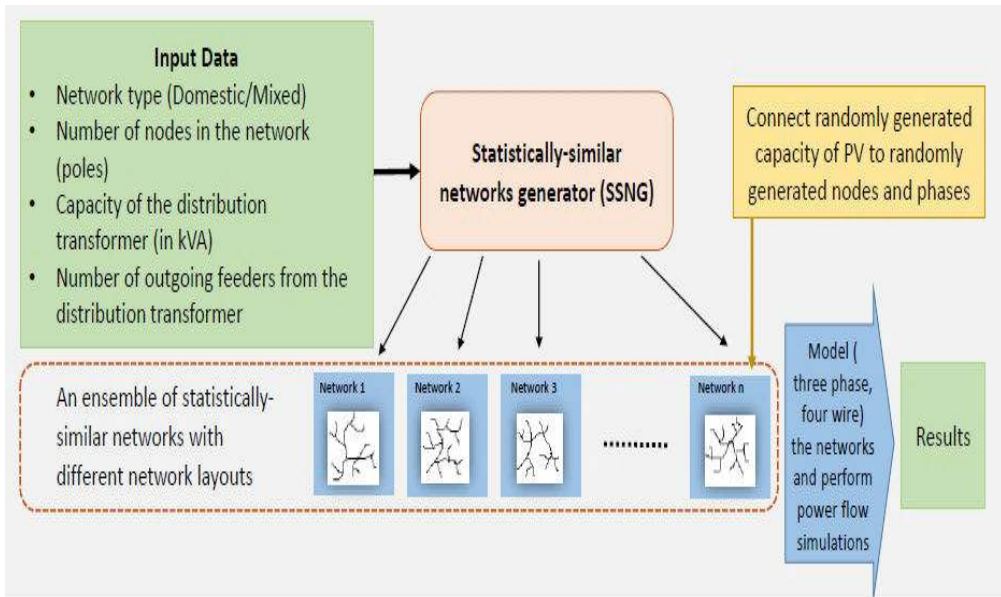


Figure 2: Concept diagram of the tool [17]

## Impact Assessment

To capture the intermittent nature of the electrical systems, a Monte Carlo based stochastic analysis framework was used in the study. A pre-defined number of PV systems with randomly generated PV capacity were connected to randomly generated nodes and phases. In order to investigate the impact of PV penetration in a possible future, a large number of PV deployment scenarios were obtained by varying the capacity and the location of PV installations. For each network model, the maximum voltage, maximum line flow, maximum neutral current and maximum voltage unbalance factor were extracted and stored after every power flow simulation. An impact study was conducted for voltage and thermal limits, voltage unbalance and neutral currents by evaluating the extracted data.

## Case study

### Validation of the tool

In this study, the real network data used for the development of the tool was collected from the Lanka Electricity Company (LECO). A validation stage was carried out to fine-tune the algorithms for

network generation and validate the complete development procedure of the tool. First, a test network was selected (from a different set of networks collected from LECO) and an ensemble of statistically similar distribution networks to the selected test network was generated by the tool. Then, the topological and electrical properties of the networks generated by the tool were compared with that of the selected test network. The user inputs considered for the validation of the tool are shown in Table 2.

*Table 2: Basic user inputs from the test network to the tool*

| <b>Parameter</b>   | <b>Value</b> |
|--|--------------|
| <b>Network type</b>                                      | Domestic     |
| <b>Capacity of the supply transformer</b>                | 100 kVA      |
| <b>Number of nodes</b>                                   | 67           |
| <b>Number of outgoing feeders</b>                        | 2            |
| <b>Conductor type</b>                                    | ABC 70       |
| <b>Number of statistically similar networks required</b> | 20           |

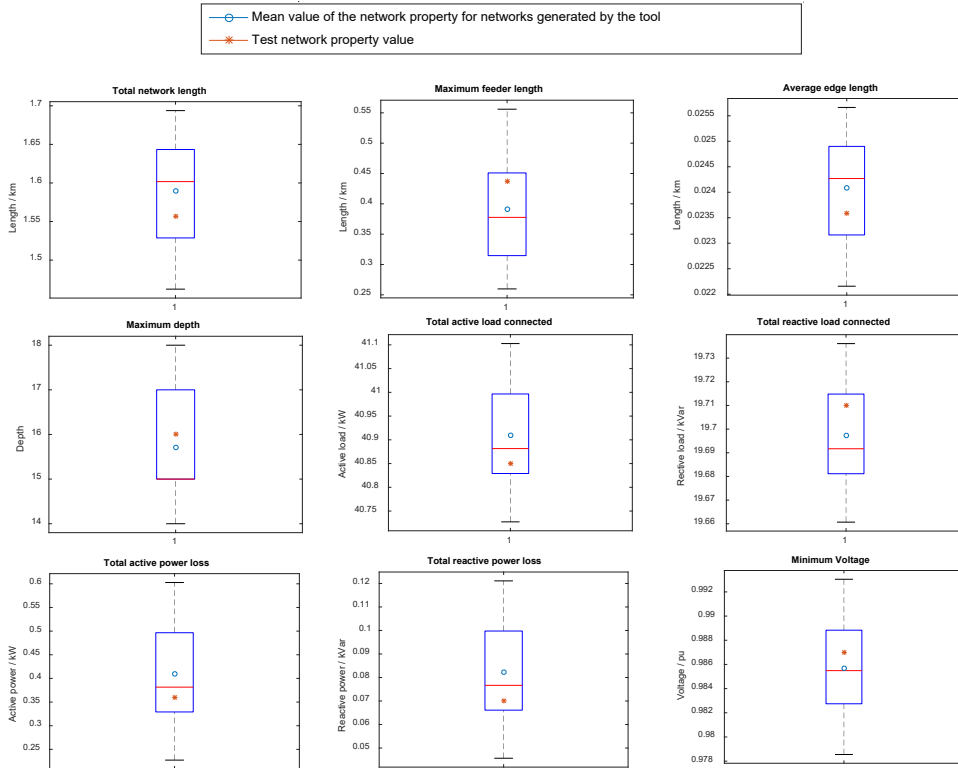


Figure 3: Box-whisker plot representations of the topological and electrical properties of the 20 networks

The box-whisker plot representations of the topological and electrical properties of 20 networks generated by the tool are shown in Figure 3. On each box, the central mark inside the box indicates the median, and the bottom and top edges of the box indicate the 25<sup>th</sup> and 75<sup>th</sup> percentiles, respectively. The whiskers above and below indicate the locations of the minimum and maximum values.

From the box-whisker plots, it can be clearly observed that the networks generated by the tool share very close topological and electrical properties making them statistically similar to each

other. However, these networks have different layouts and any of that is a possible realisation of a real distribution network. Therefore, the random integration of the solar PV can lead to different performances of the statistically-similar networks.

### Statistical Assessment of Solar PV Impacts

A statistical analysis was performed using the networks generated by the tool to investigate the impact of solar PV on LV distribution networks. The methodology of the case study is illustrated in Figure 4.

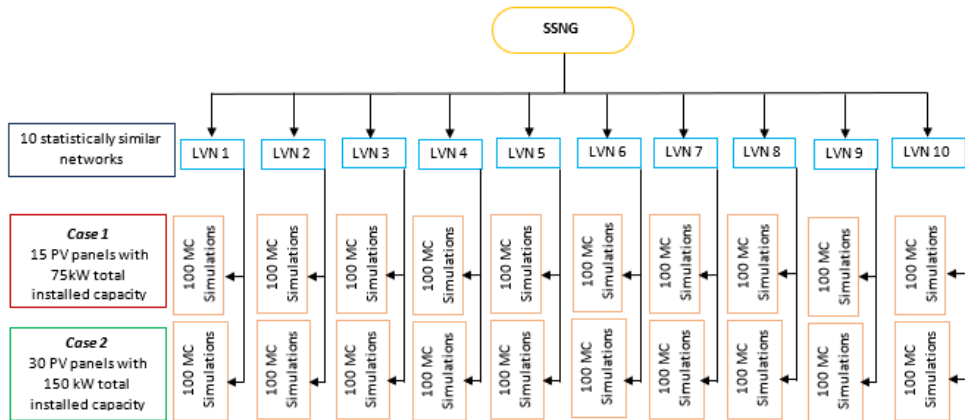


Figure 4: Methodology of the case study

Ten statistically similar networks were generated by the tool considering the user inputs of the networks to be generated. The set of input parameters given to the tool are summarized in Table 3.

Table 3: Input parameters given to the tool

| Parameter   | Value    |
|---|----------|
| Network type                                      | Domestic |
| Capacity of the supply transformer                | 160 kVA  |
| Number of nodes                                   | 72       |
| Number of outgoing feeders                        | 3        |
| Conductor type                                    | ABC 70   |
| Number of statistically similar networks required | 10       |

The impact of solar PV on the generated networks were investigated under two

cases as described below.

- Case 1: 15 PV units with 75 kW total installed capacity
- Case 2: 30 PV units with 150 kW total installed capacity

The number of PV units and the total installed capacity were retained as constants throughout the Monte Carlo implementation. Random numbers were generated corresponding to the location (node and phase) and the capacity of each PV unit. For all ten networks, one hundred Monte Carlo simulations were performed under each case by varying the PV capacity and location. Altogether, one thousand simulations were executed for cases 1 and 2. For the impact assessment, the extracted critical parameters (maximum voltage, maximum neutral current, maximum line flow, maximum voltage unbalance factor) from the load flow results were examined to see whether the voltage and thermal limits, neutral currents and voltage unbalances are within the statutory limits.



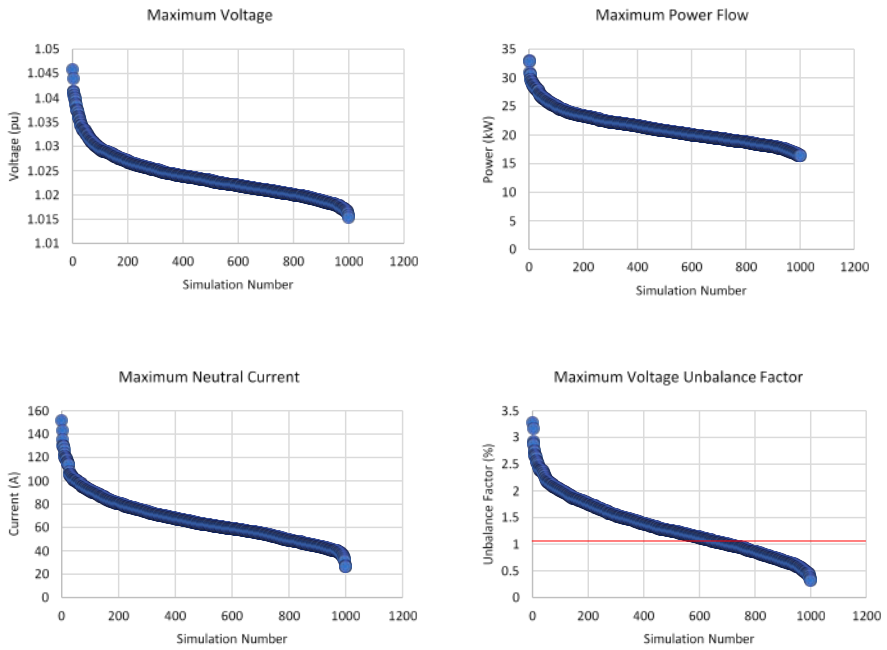


Figure 5: Scatter plots obtained from Monte Carlo simulations for case 1

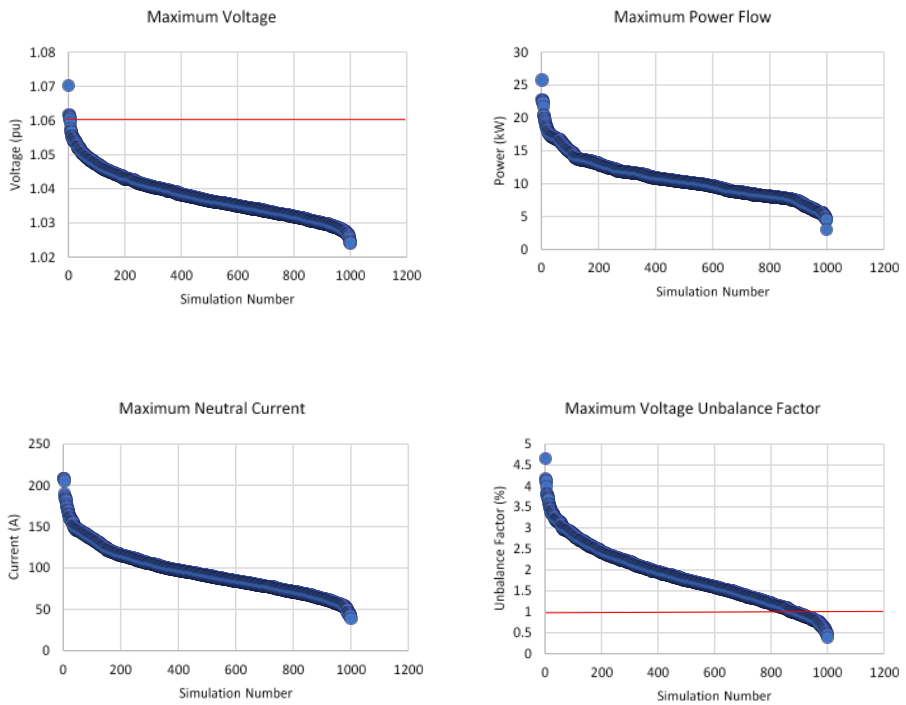


Figure 6: Scatter plots obtained from Monte Carlo simulations for case 2

## Results and Discussion

The extracted parameter values obtained for each network under two cases were arranged in descending order and scatter plots were obtained for each parameter considered. The scatter plots shown in Figures 5 and 6 represent the maximum value variation of one thousand Monte Carlo simulations of cases 1 and 2 respectively.

By examining the results, it can be confirmed that for a generalized domestic network having a transformer capacity of 160 kVA, voltage violation could be seen under a few possible future scenarios. Also, it was revealed that the higher penetration level of PV power generation will lead to more voltage violations. The random allocation of single-phase PV units created high voltage unbalances and neutral currents. This could be minimized to an acceptable limit by introducing a phase balancing technique at the time of connection of these PV units [18].

## Conclusion

This paper presented a statistical analysis of solar PV impacts on LV distribution networks using a large number of realistic distribution network models with similar characteristics. A Monte Carlo based approach was performed to evaluate the impacts using voltage unbalances, neutral currents, voltage and thermal limits. The case study presented, demonstrates how the proposed methodology could be utilized to investigate the impact of possible PV deployment scenarios for generalised LV distribution networks.

## Acknowledgements

The authors would like to thank the officials of Lanka Electricity Company for providing LV distribution data for this study.

## References

- [1] M. Begovic, I. Kim, D. Novosel, J. R. Aguero, and A. Rohatgi, "Integration of photovoltaic distributed generation in the power distribution grid", in *Proc.*, 2011, pp. 1977-1986.
- [2] Tonkoski, R., Turcotte, D., El-Fouly, T. H. M., "Impact of high PV penetration on voltage profiles in residential neighborhoods". *IEEE Transactions on Sustainable Energy*, 2012, 3(3):518–527.
- [3] Y. Hou, J. Magnusson, G. Engdahl, L. Liljestr and, "Impact on voltage rise of PV generation in future swedish urban areas with high PV penetration", in *Proc. ENERGYCON 2014 - IEEE International Energy Conference*, 2014, pp. 904–911.
- [4] Ali, S., Pearsall, N., Putrus, G., "Impact of high penetration level of grid-connected photovoltaic systems on the UK low voltage distribution network". *Renewable Energy and Power Quality Journal*, 2012, 1(10):519–522.
- [5] Patil, A., Girgaonkar, R., & Musunuri, S. K., "Impacts of increasing photovoltaic penetration on distribution grid - Voltage rise case study", in *Proc. ICAGE 2014 - International Conference on Advances in Green Energy*, 2014, pp. 100–105.
- [6] Woyte, A., Thong, V. V., Belmans, R., Nijs, J., "Voltage fluctuations on distribution level introduced by photovoltaic systems", *IEEE Transactions on Energy Conversion*, 2006, 21:202-209.
- [7] Schwanz, D., Moller, F., Ronnberg, S. K., Meyer, J., Bollen, M. H. J., "Stochastic assessment of voltage unbalance due to single-phase-connected solar power". *IEEE Transactions on Power Delivery*, 2017, 32(2):852–861.
- [8] Kharrazi, A., Sreeram, V., Mishra, Y., "Assessment of voltage unbalance due to single phase rooftop photovoltaic panels in

residential low voltage distribution network: A study on a real LV network in Western Australia”, in Proc. AUPEC 2017 - Australasian Universities Power Engineering Conference, 2017, pp. 1–6

[9] Tie, C., Gan, C., “Impact of grid-connected residential PV systems on the Malaysia low voltage distribution network”, in Proc. 2013 IEEE 7<sup>th</sup> Int. Power Engineering and Optimization Conf. (PEOCO), Langkawi Island, Malaysia, 3–4 June 2013, pp. 670–675.

[10] Chen, P., Kezunovic, M., “Analysis of the impact of distributed generation placement on voltage profile in distribution systems”, in Proc. 2013 IEEE Power and Energy Society General Meeting (PES), 2013, pp. 1–5.

[11] Gonzalez, C., Geuns, J., Weckx, S., “LV distribution network feeders in Belgium and power quality issues due to increasing PV penetration levels”, in Proc. 2012 IEEE PES International Conf. and Exhibition on Innovative Smart Grid Technologies (ISGT Europe), 2012, pp. 1–8.

[12] Chant, T.I., Shafiullah, G.M., Oo, A.M.T., Harvey, B.E., “Impacts of increased photovoltaic panel utilisation on utility grid operations – a case study”, in Proc. 2011 IEEE

PES Innovative Smart Grid Technologies Asia (ISGT), Perth, Australia, 2011, pp. 1–7.

[13] Thomson, M., Infield, D.G., “Impact of widespread photovoltaics generation on distribution systems”, in Proc. IET Renewable Power Generation, 2007, 1, pp. 33–40.

[14] Conti, S., Raiti, S., Tina, G., “Simulink modelling of LV photovoltaic grid-connected distributed generation”, in Proc. 18<sup>th</sup> Int. Conf. on Electricity Distribution, Turin, 2005, pp. 6–9.

[15] Jan-E-Alam, M., Muttaqi, K.M., Sutanto, D., “Assessment of distributed generation impacts on distribution networks using unbalanced three-phase power flow analysis”, in Proc. 2011 IEEE Power and Energy Society General Meeting, 2011, pp. 1–8.

[16] Mather, B.A.: ‘Quasi-static time-series test feeder for PV integration analysis on distribution systems’, in Proc. 2012 IEEE Power and Energy Society General Meeting, 2012, pp. 1–8.

[17] Abeysinghe, S., A statistical assessment tool for electricity distribution networks. PhD Thesis, Cardiff University, 2018.

[18] D. W. Almeida, A. H. M. S. M. S. Abeysinghe, and J. B. Ekanayake, “Analysis of Rooftop Solar Impacts on Distribution Networks”, 2018, 48(2):103–11

# Optimum Operation of a Community Cluster using Demand Side Management and Dynamic Line Rating

A.H. Wijethunge<sup>#1 \*2</sup>, J.V. Wijayakulasooriya<sup>\*3</sup>, J.B. Ekanayake<sup>\*4</sup>

*# Faculty of Technology, University of Sri Jayewardenepura*

<sup>1</sup> aki.wijethunga@gmail.com

*\* Department of Electrical and Electronic Engineering, Faculty of Engineering, University of Peradeniya*

## Abstract

With the high penetration of distributed generation and rapid development of new operational strategies, the power system is experiencing decentralized operation mechanisms. To manage different entities having similar attributes in an optimum manner and to obtain optimal operation of the power system, a clustering concept is proposed. Community cluster with locally generated renewable energy is a new paradigm that leads to a system that is more sustainable, secure and cost effective to the community, while enabling connection of more renewable energy resources. Maximising the utilisation of the renewables while maximising the profit of a Community cluster is investigated using the combined operation of dynamic line rating and demand side management through an optimum smart appliances schedule. This ensures the user comfort as it satisfies the user preferences on operating times of smart appliances; maximises the profit to the Community cluster, and provides benefits to the society as it allows the maximum use of the renewable energy sources within the Community cluster.

**Keywords:** Community cluster, Dynamic line rating, Demand side management, Renewable integration, Appliance scheduling

## **Introduction**

### **Integrating renewables into distribution networks**

In response to climate change, many governments have set ambitious targets to increase the use of renewable energy and to reduce greenhouse gas emissions from electricity generation. The integration of Distributed Generation (DG) plays a major role in decarbonising the energy supply in distribution networks. DG connected to the distribution network is considered as a mainstream generation addition as the penetration level of DGs has increased significantly [1]–[3]. Combined Heat and Power (CHP) generation, Renewable Energy Sources (RES) such as small scale hydro generation, wind power generation, PV generation, biomass generation are considered as main DG sources. DGs along with electrical storage such as battery storage and electric vehicles are considered as Distributed Energy Resources (DER) [3].

The main contributions of DGs in distribution network include the reduction of central generation capacity, the reduction of overall generation cost and CO<sub>2</sub> emission, the reduction of power losses, the improvement of voltage profile and reliability, and postponing network upgrades [3], [4]. The rapid growth of DG integration brings energy diversification and increments the security of energy supply [5].

The rapid integration of renewable energy based DGs creates challenges to the utility such as operating the network within thermal limits, voltage regulation, ensuring protection, stability and power quality [1], [6]. The distribution network must be steadily transformed into smart

networks due to the impacts of high penetration of DGs [7].

### **Facilitating renewable integration into Distribution Networks**

#### **Dynamic Line Rating (DLR)**

Relieving network bottlenecks occurred due to thermal limits of network components require a mechanism to increase the power flow capability of the existing system. Even though the simplest method of increasing the capability of a conductor is reconductoring, it is not an economical solution. Therefore, a cost-effective way of harnessing the unused capacity of the existing conductors and components without introducing new infrastructure is required.

The theoretical value of the line rating is usually calculated conservatively by considering the maximum allowable conductor temperature and the pre-determined environmental conditions such as ambient temperature and wind speed. This is called the static rating of the conductor. As the environmental conditions are continuously changing, there will be a margin between the current, a line can actually carry and the static rating. Thus with the maximum allowable temperature unchanged, the practical allowable loading capacity of an overhead line in the natural meteorology is much higher than that determined by the current practice [8].

As the real-time thermal rating of a distribution line depends on the weather condition, real-time measurements of weather conditions such as wind speed and air temperature can be used to calculate the dynamic line rating (DLR) [9]. According to the study reported in [10], operating with DLR needs a rapid

accurate estimation. A 5-20% increment of the line rating over static rating can be achieved with the dynamic estimation of the current carrying capacity of the line.

### **Demand Side management (DSM)**

A significant amount of renewable energy sources are connected to the distribution networks and their output is varying with the resource. Therefore the utilities are introducing different power system operational strategies such as demand-side management to shift the demand to balance the generation and demand [11], [12].

With the integration of ICT, the demand side is now capable of providing more services to DNO. DSM broadly refers to utility activities that influence customers' total electricity usage and usage patterns [12]. The DSM encompasses the planning, implementation, and monitoring of activities designed to encourage customers to change their electricity usage patterns. Economic benefits of a distributed generation could be enhanced by using DSM [13].

DSM has been used to utilise the limited capacity of the distribution networks more effectively. The efficiency of a DSM system has a direct connection with the competence of handling the new loads and generations by the distribution network without exceeding the existing constraints. DSM leads the distribution network operators to avoid underutilisation of network infrastructure and energy generation which increases the capacity of the system effectively [14], [15].

DSM technology increases the effective usage of distribution network infrastructure while managing the system constraints [16].

### **Clustering approach to manage the emerging systems**

With the high penetration of distributed generation and rapid development of new operational strategies, the power system is undergoing transformations such as centralized electricity generation to decentralized generation [17], [18], [19], central markets to distributed ledges [14], [20] and centralized control to decentralized control [11], [21], [22].

With the transformations anticipated in the power system, new electricity market trends and different energy clusters are formed or considered to optimize planning and operating mechanisms of the power system [18], [21], [23], [24], [25]. The optimum planning and operating mechanisms focus on minimising generation and transmission costs, reducing power losses, managing demand and supply according to the user requirements, and minimising the cost of consumption [11], [18], [26].

Considering current trends, five main energy clusters namely, Generation cluster, Consumer/ Prosumer cluster, Community cluster, Hybrid cluster, and Virtual cluster were identified. Table 1 shows some of the entities that can be considered under each of these clusters [11], [21]. The clustering concept allows the optimal operation of the power system by managing different entities having similar attributes in an optimum manner.

Table 1: Energy clusters

| Cluster Type                  | Name   | Description  |
|-------------------------------|--|--|
| <b>Generation</b>             | Array of generation sources                            | Array of PV panels, Array of wind turbines or any other energy sources   |
|                               | Individual Consumers                                   | Consumers who are electrically connected to a single point   |
| <b>Consumer/<br/>Prosumer</b> | Individual Prosumers                                   | Those who consume and generate electricity based on different operating and market mechanisms offered by the utility and connected to a single point   |
|                               | Collaborative Consumption<br>Prosumer energy community | Consumers with social agreement to share the energy sources<br>Players with the right to generate, consume, store and sell energy who have their own operating and market mechanisms in addition to mechanisms introduced by the utility |
| <b>Community</b>              | Smart Building cluster                                 | A group of neighbouring smart buildings that are electrically interconnected and utilise automated approaches to minimise their consumption, CO <sub>2</sub> emissions, impact to the utility, etc.                                      |
|                               | Zero energy neighbourhood                              | Smart buildings that use smart interactions to reach energy balance through on-site renewable energy generation  |
| <b>Hybrid</b>                 | Micro Grid   | A localised group of distributed generators (often not belongs to consumers) and loads synchronous with the main grid but can also disconnect to island mode and function autonomously   |
|                               | Virtually connected Consumers/prosumers                | Group of consumers/prosumers with virtual, market-oriented connection  |
| <b>Virtual</b>                | Virtual Power Plant                                    | Collective generators of renewable energy sources that can act as a large coherent generator   |

## Material and Method

### Operational paradigms and market mechanism for *Community cluster*

There is a growing interest for the community energy projects that have an emphasis on local engagement, local leadership and control, and the local community benefiting collectively from the outcomes [27]. Community power will create a new paradigm; that is locally controlled energy system with distribution technologies and market mechanisms. This paradigm leads to a system that is more sustainable, secure and cost-effective to the community while enabling connection of more and more renewable-based distributed energy resources.

As defined Community cluster which owns the distributed generation of its own could gain benefits from new operating mechanisms so as to achieve optimum consumption cost, optimum generation cost and also the maximum utilisation of the network infrastructure. In a Community cluster, where the loads and generation both are dynamic, increasing the self-utilisation of renewable energy and reducing the peak load in the domestic sector via a localized demand side management system is important [28].

Numerous operational paradigms and market mechanism are reported in the literature for community energy/power systems. Some of the available references that illustrate the operation paradigms and market mechanisms of a cluster that could be categorised as a Community cluster are summarized below.

Reference [29] presents a demonstration of a smart community focusing on the construction of a future-oriented city where advanced energy technologies are utilised to achieve Europe's aggressive environmental target. The suggested community in reference [29] consists of energy generating equipment, energy storage, energy saving, and energy management system. The study introduces Positive Energy Building (PEB) concept for office buildings with renewable generation to match demand and supply to a certain extent. It also suggests an EV car sharing system to charge EV from more renewable energy. Predicted PV output and EV charging time are used to optimize the EV car sharing schedule with grid constraints. Another approach suggested in this study is the Community Management System (CMS) that supports effective and efficient city planning through management of real-time energy usage data of the city.

A new energy system with prosumers and utility providers targeting a 20% energy saving and 50% or more CO<sub>2</sub> emission reduction compared to a typical block in the city is suggested in reference [30]. This smart community achieves energy saving by using Energy Management System (EMS) to households; load levelling by utilizing information technology and storage batteries and combining various types of utility customers to cut and shift peak demand. The community aims to optimize the use of renewable energy and also to provide independent operation for the system during a contingency.

Reference [30] suggests a community energy system with prosumers which has a special supply area where power is supplied over a self-owned line from a cogeneration power station. The



participants are divided into two groups namely controlled group (without implementing demand response), and treatment group (with an implementation of demand response). The Community Energy Management System (CEMS) introduced for this community performs a demand forecast for the next day and delivers the next day power rate table to prosumer EMS and smart meters. Based on this forecast, an operation plan for the next day at the prosumer EMS is generated and sent to CEMS. Based on this information, the power rate table for the next day is determined for the community. The consumer behaviour is based on dynamic pricing. In the community, the surplus of renewable energy will be covered by demand creation.

The smart community defined in reference [31] comprises of houses, offices and independent power generation sources. The suggested local power sources of the community are solar power, fuel cell, regional wind farm, cogeneration using gas as fuel, unused energy in factories (existing, new) and waste power generation. In the community, the demand during peak time periods decreased among the households and the offices with installed Building Energy Management System with dynamic pricing. The results show that introducing dynamic pricing changes the behaviour of some residents in households. However, a reduction of the peak was not seen so much among commercial customers. The importance of the implementation of regional smart community with the development of new energy-related industries is also highlighted in the study.

Smart energy community described in [32] is made up of hundreds of

households with various forms of electric loads (domestic loads, EV) and DG technologies. A local control system will actively manage generation and demand within the community to meet a variety of objectives. The importance of having a local energy management system to control energy consumption and energy flow within the energy communities is highlighted in the study. In this conceptual study, it was shown that implementing global control over the clusters of energy communities will be necessary to regulate the electricity network and optimize central plant generation.

In reference [33] a smart energy community composed of a number of residential users and a neighbourhood coordinator powered by a primary utility along with a small scale local power supplier (LPS) is studied. Renewable energy generation and storage capacity are constraints of the LPS. Real time-varying price signals are given by both suppliers. Users are motivated to control their household appliances' operation time and calculate appropriate portions of power purchased from these two suppliers to achieve bill curtailments. The LPS can decide between either to sell power to the grid or to the users. Minimising total energy cost of the community is achieved using this method with the limited power generation capability of LPS.

The operation of a goal-oriented prosumer community group (PCG) to achieve multiple goals such as demand constraints, cost constraints, and income maximisation using multiple-criteria goal programming is discussed in reference [26]. The collaborative actions of prosumer community groups are inspired

in order to achieve mutual goals for a sustainable system.

Even though the studies highlight the importance of the prosumers as a community, the optimum operation of the community along with DSM and DLR is not analysed. The Community cluster defined in this paper is a novel approach to optimise the operation of the power system as clusters that benefits both consumer and utility.

In this paper a novel Community cluster shown in Figure 1 is defined. This cluster comprises of household or industry prosumers, consumers, renewable energy sources, network infrastructure owned by communities. The operations

of the Community cluster are carried out by the controller owned by the cluster.

For the analysis of optimum operation mechanisms, a generic system of a smart community Figure 2 was used. Based on the modified genetic algorithm based optimisation in [34], the optimum operation for Community cluster is obtained.

The community cluster in Figure 2 consists of 1250 houses each with five shiftable appliances. The optimum appliance schedule to obtain the maximum profit of the Community cluster was gained using the algorithm in [34].

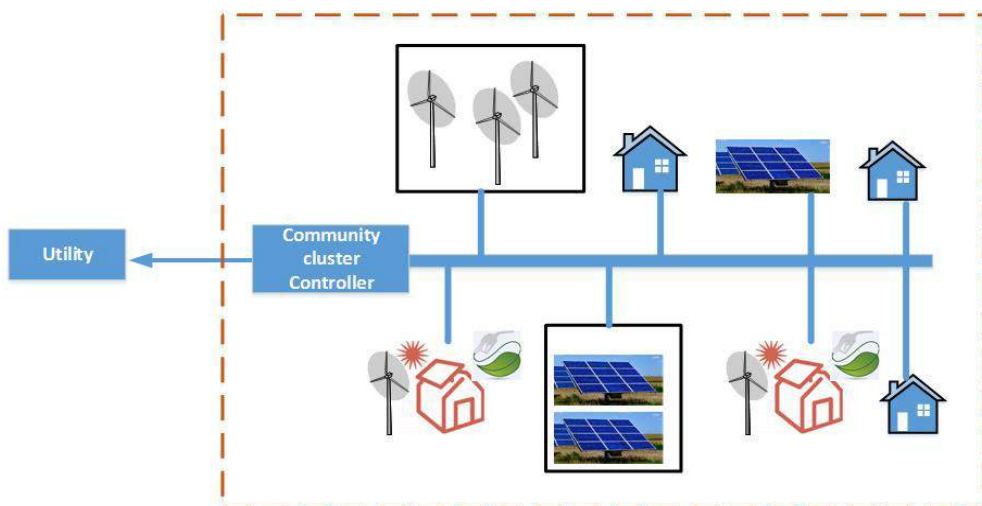


Figure 1: Defined Community cluster

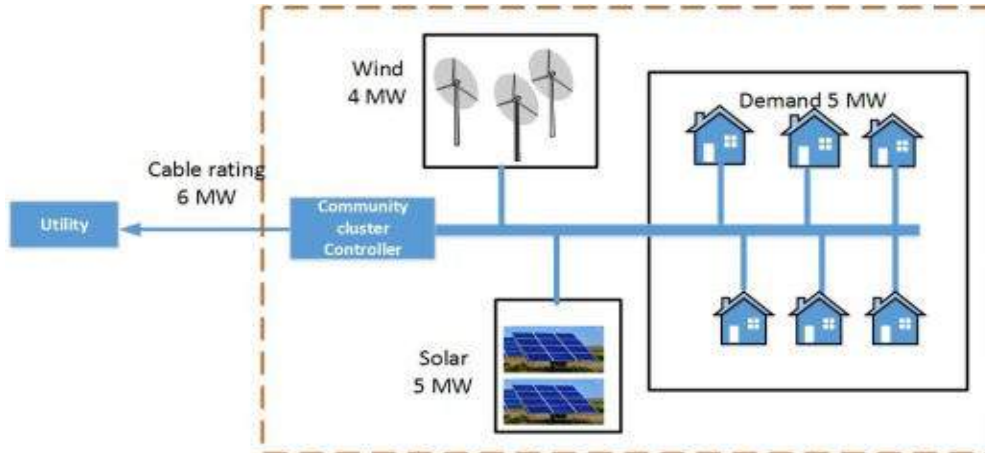


Figure 2: Community cluster components

## Result and Discussion

### Optimum operation of Community Cluster with DLR and DSM

The Community cluster defined in Figure 2 will purchase energy from grid based on the Sri Lanka Time of use tariff as given in Figure 3. The tariff which Community cluster sells generated renewable energy to the grid is also given in Figure 3.

Figure 4 shows the generated energy from the wind farm and solar PV plant owned by Community cluster and the DLR

of the cable which connects the grid and the Community cluster. Optimum power flow of the cable is obtained using the real time DLR which was higher than the conventional current rating.

The optimum appliance schedule of the Community cluster is obtained after 2000 iterations for 128 chromosomes for 6250 appliances. The profit for each iteration is shown in Figure 5. The appliance starting time is shown in Figure 6 for 100 appliances. The demand of the Community cluster at the optimum appliance schedule is given in Figure 7. Energy purchased from the grid and sold to the grid at the optimum schedule is given in Figure 8.

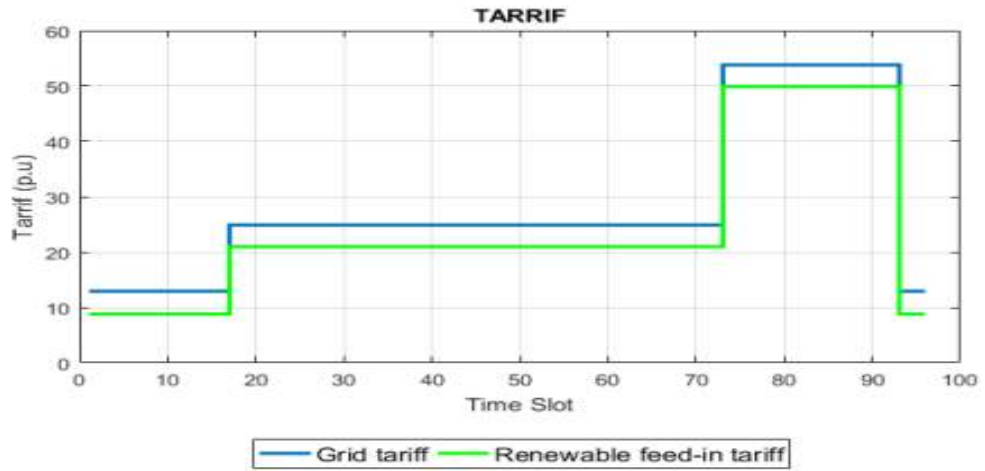


Figure 3: Time of use tariff

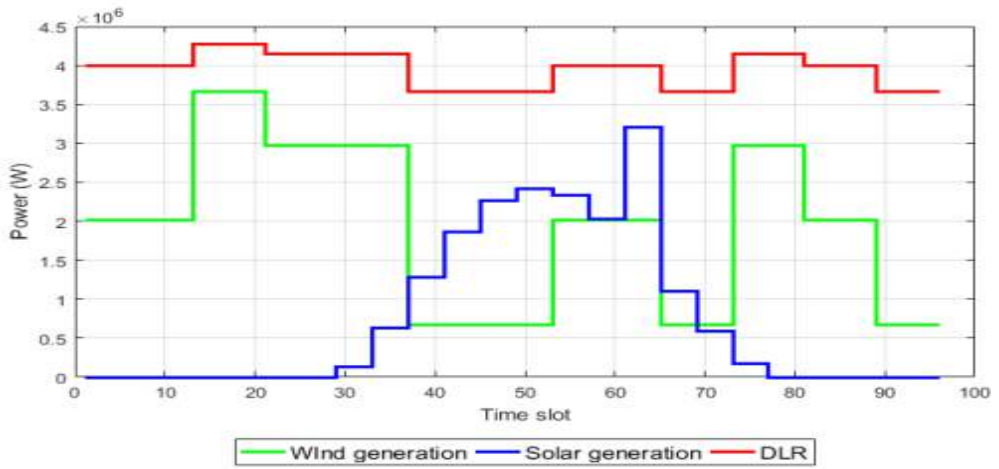


Figure 4: Renewable generation and DLR

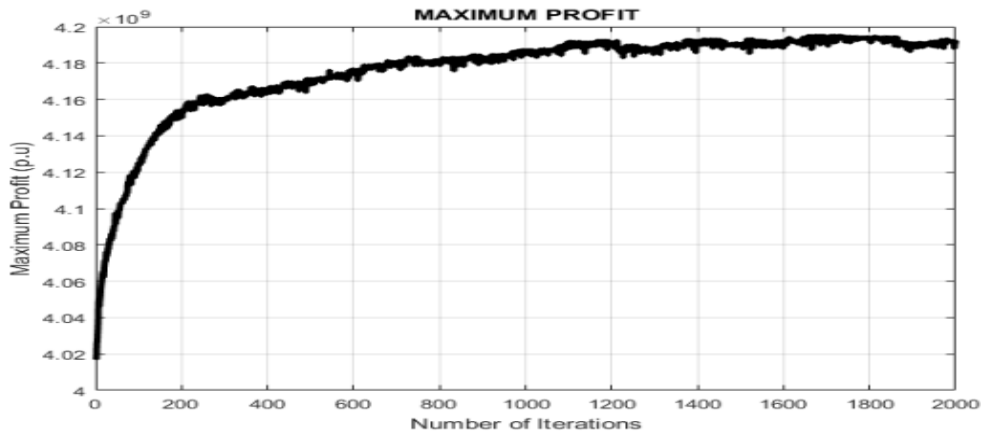


Figure 5: Profit of the Community cluster for each iteration

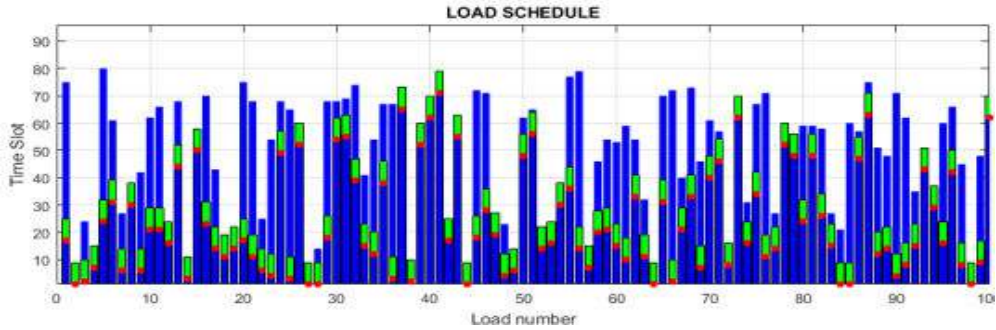


Figure 6: Appliance starting and maximum allowable end time

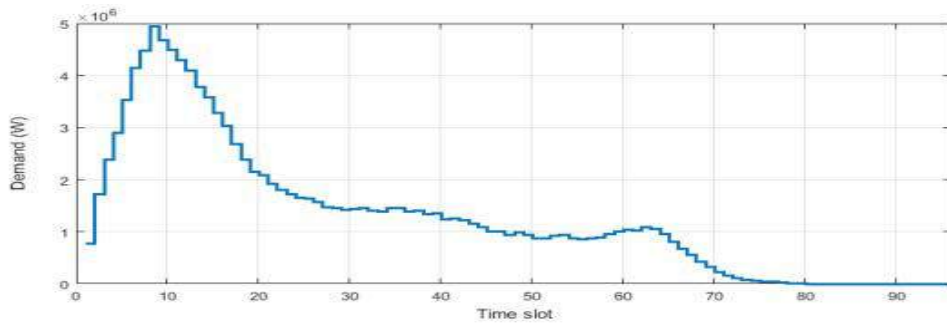


Figure 7: Demand of the Community cluster at optimum schedule

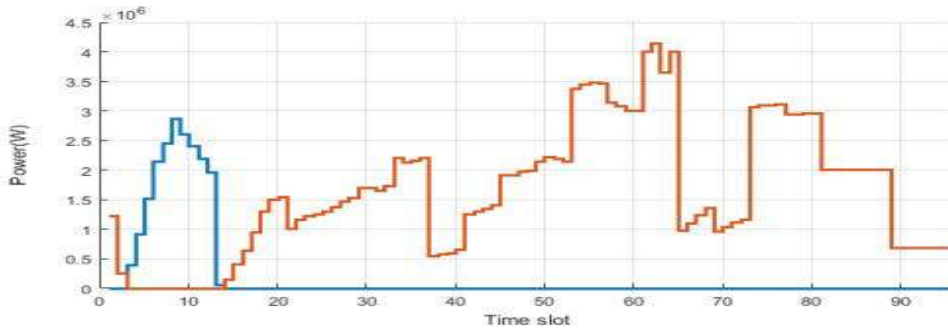


Figure 8: Power purchased from the grid and power sold to grid

## Conclusions

The impact of connecting distribution generation to distribution networks plays a major role in power system. A novel clustering approach is then introduced to manage and operate distribution networks with distributed generation with optimum manner. The optimum appliance schedule is obtained with wind

generation and solar generation along with the dynamic line rating and demand side management for the defined Community cluster based on the modified genetic algorithm optimisation. The results shows that coordinated operation of prosumers, renewable generation, network infrastructure and utility leads to an effective, sustainable power system with the emerging technologies.

## Future Works

The Community cluster defined can be implemented in the existing power system with the higher penetration of distributed solar PV and wind energy generation. This clustering approach will be used to define the economic transactions and energy transactions in the future studies.

## References

- [1] J. M. Bloemink and T. C. Green, "Benefits of Distribution-Level Power Electronics for Supporting Distributed Generation Growth," pp. 1–9, 2012.
- [2] T. Aziz, U. P. Mhaskar, T. K. Saha, and S. Member, "An Index for STATCOM Placement to Facilitate Grid Integration of DER," pp. 1–10, 2013.
- [3] Jenkins, Nicholas, J. B. Ekanayake, and G. Strbac, Distributed Generation. IET, 2009.
- [4] S. Abapour, B. Mohammadi-ivatloo, and K. Zare, "Evaluation of technical risks in distribution network along with distributed generation based on active management," IET Gener. Transm. Distrib., vol. 8, no. 4, pp. 609–618, 2014.
- [5] C. Deckmyn, T. L. Vandoorn, B. Meersman, L. Gevaert, L. Vandeveldel, and J. Desmet, "A coordinated voltage control strategy for On-Load Tap Changing transformers with the utilisation of Distributed generators," 2016 IEEE Int. Energy Conf. ENERGYCON 2016, 2016.
- [6] R. K. Varma, V. Khadkikar, and R. Seethapathy, "Nighttime Application of PV Solar Farm as STATCOM to Regulate Grid Voltage," vol. 24, no. 4, pp. 983–985, 2009.
- [7] M. Barragán-Villarejo, E. Romero-Ramos, A. Marano-Marcolini, J. M. Maza-Ortega, and A. Gómez-Expósito, "Voltage source converter-based topologies to further integrate renewable energy sources in distribution systems," IET Renew. Power Gener., vol. 6, no. 6, pp. 435–445, 2012.
- [8] IEEE Standard for Calculating the Current-Temperature Relationship of Bare Overhead Conductors, vol. 2006, no. January. IEEE Power Engineering Society, 2013.
- [9] M. W. Davis, "A new thermal rating approach: The real time thermal rating system for strategic overhead conductor transmission lines: Part II: Steady state thermal rating program," IEEE Trans. Power Appar. Syst., vol. 96, no. 3, pp. 810–825, 1977.
- [10] R. Adapa and D. A. A. Douglass, "Dynamic thermal ratings: monitors and calculation methods," Proc. Inaug. IEEE PES 2005 Conf. Expo. Africa, no. July, pp. 163–167, 2005.
- [11] J. Ni and Q. Ai, "Economic power transaction using coalitional game strategy in micro-grids," IET Gener. Transm. Distrib., vol. 10, no. 1, pp. 10–18, 2016.
- [12] P. Palensky and D. Dietrich, "Demand side management: Demand response, intelligent energy systems, and smart loads," IEEE Trans. Ind. Informatics, vol. 7, no. 3, pp. 381–388, 2011.
- [13] A. Daraeepour, S. J. Kazempour, D. Patino-Echeverri, and A. J. Conejo, "Strategic Demand-Side Response to Wind Power Integration," IEEE Trans. Power Syst., pp. 1–11, 2015.
- [14] F. Ye, Y. Qian, and R. Q. Hu, "A Real-Time Information Based Demand-Side Management System in Smart Grid," IEEE Trans. Parallel Distrib. Syst., vol. 27, no. 2, pp. 329–339, 2016.
- [15] T. Luo, G. Ault, and S. Galloway, "Demand Side Management in a Highly Decentralized Energy Future," 2010, pp. 1–6.
- [16] E. R. Stephens, D. B. Smith, and A. Mahanti, "Game Theoretic Model Predictive Control for Distributed Energy Demand-Side Management," IEEE Trans. Smart Grid, vol. 6, no. 3, pp. 1394–1402, Dec. 2014.
- [17] D. J. Vergados, I. Mamounakis, P. Makris, and E. Varvarigos, "Prosumer clustering into virtual microgrids for cost reduction in renewable energy trading markets," Sustain. Energy, Grids Networks, vol. 7, pp. 90–103, 2016.
- [18] R. Lahon and C. P. Gupta, "Energy Management of Cooperative Microgrids with High-Penetration Renewables," Iet, vol. 12, pp. 680–690, 2018.
- [19] T. Luo, G. Ault, and S. Galloway, "Demand Side Management in a highly decentralized

- energy future," Univ. Power Eng. Conf. (UPEC), 2010 45th Int., pp. 1–6, 2010.
- [20] Y. Liu, C. Yuen, S. Huang, N. Ul Hassan, X. Wang, and S. Xie, "Peak-to-average ratio constrained demand-side management with consumer's preference in residential smart grid," IEEE J. Sel. Top. Signal Process., vol. 8, no. 6, pp. 1084–1097, 2014.
- [21] I. Vigna, R. Perneti, W. Pasut, and R. Lollini, "New domain for promoting energy efficiency: Energy Flexible Building Cluster," Sustain. Cities Soc., vol. 38, no. December 2017, pp. 526–533, 2018.
- [22] A. Amato, M. Calabrese, V. Di Lecce, and V. Piuri, "An intelligent system for decentralized load management," Proc. 2006 IEEE Int. Conf. Comput. Intell. Meas. Syst. Appl. CIMSAS 2006, no. July, pp. 70–74, 2006.
- [23] G. Tsaousoglou, P. Makris, and E. Varvarigos, "Electricity Market Policies for Penalizing Volatility and Scheduling Strategies: the Value of Aggregation, Flexibility, and Correlation," Sustain. Energy, Grids Networks, 2017.
- [24] K. Gaiser and P. Stroeve, "The impact of scheduling appliances and rate structure on bill savings for net-zero energy communities: Application to West Village," Appl. Energy, vol. 113, pp. 1586–1595, 2014.
- [25] E. A. Martínez Ceseña, N. Good, A. L. A. Syrri, and P. Mancarella, "Techno-economic and business case assessment of multi-energy microgrids with co-optimization of energy, reserve and reliability services," Appl. Energy, vol. 210, no. April 2017, pp. 896–913, 2018.
- [26] A. J. D. Rathnayaka, V. M. Potdar, T. Dillon, and S. Kuruppu, "Framework to manage multiple goals in community-based energy sharing network in smart grid," Int. J. Electr. Power Energy Syst., vol. 73, pp. 615–624, 2015.
- [27] Department for Business, Energy & Industrial Strategy, "Guidance Community Energy," Jan-2015. .
- [28] T. Rajeev and S. Ashok, "Dynamic load-shifting program based on a cloud computing framework to support the integration of renewable energy sources," Appl. Energy, vol. 146, pp. 141–149, May 2015.
- [29] I. Lyon and C. Management, "Case Study : Smart Community Demonstration Project in Lyon , France," 2016.
- [30] O. G. A. Eiji and K. Akihiro, "Social System Demonstration of Dynamic Pricing in the Kitakyushu Smart Community Creation Project," vol. 59, no. 3, pp. 152–160, 2013.
- [31] K. Smart and C. Creation, "Result of the Kitakyushu Smart Community Creation," 2015.
- [32] A. Fazeli, E. Christopher, C. M. Johnson, M. Gillott, and M. Sumner, "Investigating the Effects of Dynamic Demand Side Management within Intelligent Smart Energy Communities of Future Decentralized Power System."
- [33] N. Yu, L. Mu, Y. Miao, H. Huang, H. Du, and X. Jia, "Distributed load scheduling in smart community with capacity constrained local power supplier," 2015 IEEE 30th Int. Perform. Comput. Commun. Conf. IPCCC 2015, pp. 8590–8599, 2016.
- [34] A. H. Wijethunge, J. V. Wijayakulasooriya, J. B. Ekanayake, and A. Polpitiya, "Coordinated Operation of the Constituent Components of a Community Energy System to Maximize Benefits While considering the Network Constraints," vol. 2019, 2019.

# Mitigating Protection Issues of Islanded Rooftop Solar PV Systems

<sup>1</sup>M.J.C.S. Siriwardena, <sup>2</sup>R.M.D.V. Obeysekara, <sup>3</sup>R.W.I.A. Welikumbura,  
<sup>4</sup>A.D.A.D. Rajapaksha, <sup>5</sup>P.J. Binduhewa, <sup>6</sup>J.B. Ekanayake

*Department of Electrical and Electronic Engineering,  
Faculty of Engineering,*

*University of Peradeniya, Sri Lanka*

<sup>1</sup> charith.siriwardena@ceb.lk

<sup>2</sup> rmvimukthi95@gmail.com

<sup>3</sup> rwinduni95@gmail.com

<sup>4</sup> adarajaksha@gmail.com

<sup>5</sup> prabathb@ee.pdn.ac.lk

<sup>6</sup> jbe@ee.pdn.ac.lk

## Abstract

In view of enhancing renewable energy portfolio in electricity generation in Sri Lanka, Government has launched an island-wide program to promote rooftop solar installations, under which nearly 20,000 PV plants have been installed and operated in grid-tied mode. In TT earthing topology used in Sri Lankan distribution network, grid-tied inverters are designed to quickly disconnect from the grid if utility fails, to eliminate the risk of energising grid side conductors in case of maintenance. Consequently, consumers are unable to utilise their rooftop PV plants during an interruption. A key factor for this limitation is lack of provisioning proper earth fault protection scheme during off-grid operation.

If both L&N conductors are disconnected from the grid, utility earthing at distribution transformer will be disconnected hence become an unearthed system. Even if unearthed distribution systems detect earth faults through capacitive currents, domestic wiring incorporates very small capacitance so that the fault could persist undetected.

In this paper, how Earth-fault-protection is ensured with minimum modifications to the existing systems while inverter is operating in islanded mode is discussed.

**Keywords:** Photovoltaic, Islanded Operation, Inverter, Earth Fault Protection, TT Earthing System, PSCAD Simulation



## Introduction

A photovoltaic system can operate in any of the following modes; i.e. Grid-Tied, Autonomous or Off-Grid, as per the standard connection schemes described in G59 Engineering Recommendations, for Generators to be integrated in distribution network [1]. On-grid systems are permanently connected to the national grid and the direct current (dc) produced by the solar module is converted into grid-compatible (50/60 Hz) alternating current (ac), where a Phase Locked Loop (PLL) is used to synchronize the inverter's voltage and current to that of the grid. More than 90% of PV systems worldwide are currently implemented as grid-connected systems where the power conditioning unit monitors the functioning of the PV and the grid and switches off the system in case of grid failure or Loss of Mains (LoM) protection which is provided by 83 relay as per ANSI codes) is detected [1].

Recently the Government of Sri Lanka (GoSL) has launched an islandwide program to promote rooftop solar installations in the country, under three schemes (Net-Metering, Net-Accounting and Net-Plus). Accordingly, nearly 170 MW PV capacity is grid-connected by the end of 2018 [4]. Only off-grid plant available then was the pilot project in Eluwathivu island, which is basically operated in the form of a Micro-grid, comprised of a large capacity centralized PV plant. Most of the domestic PV consumers have installed small capacities under Net-Metering, ranging from 1 to 10 kW (single phase). Some bulk consumers have installed 10 – 42 kW (three phase) PV plants under Net-Accounting or mostly Net-Plus. With frequent and long power interruptions in Sri Lankan

distribution network, it is important to investigate whether the installed rooftop PV can be operated in “Off-Grid” or “Autonomous” mode during grid interruptions thus supplying fully or partly the domestic power demand.

## Existing Schemes in TN Earthing Systems

Regulations for LV earthing vary among countries [2] and such arrangements (TN, TT & IT) are standardized in IEC 60364-4-44-2015 [3]. In any of the three sub-categories of TN earthing system (TN-C, TN-S and TN-C-S) the Utility provides both Neutral (N) the Earth (PE) conductors to consumers separately or combined as PEN, where earthing shall only be done at the utility side at a single point (point ‘c’ of Figure 1) or additional earth shall be decided by the utility depending on distance (point ‘d’ of Figure 1), in multiple source arrangements [3].

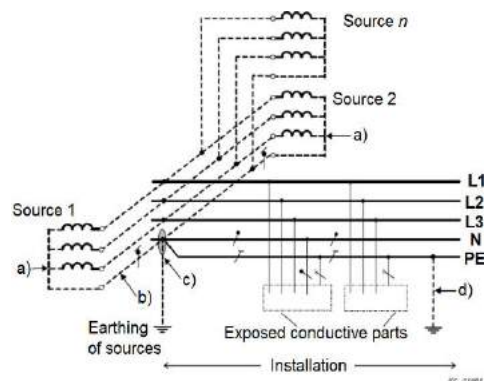


Figure 1: TN Earthing Arrangement for Multiple-Source Power Supplies [3]

For example, in countries like UK, USA and Germany where TN-C earthing is used [2], the autonomous operation of distributed PV is convenient (even in smaller PVs) as Earth Fault Leakage Protection is ensured in Off-Grid operation. As in Figure 1, conductor ‘b’

provides both N and PE functions (PEN), hence a proper low impedance earth leakage loop is maintained continuously, even during a grid failure while PV is operating in Off-Grid mode. In Autonomous operation, when loss of mains is detected, the PV switches automatically driven by an internal oscillator.

### Practical Problem for Off-Grid PV in TT Earthing Systems

Already installed grid-tied inverters in TT earthing system are designed to quickly disconnect from the grid if the utility fails (Loss of sampling signal from grid voltage for synchronizing of frequency, phase & magnitude), so as to eliminate the risk of energizing the grid side conductors in case of maintenance.

If loss of mains is detected and both L & N conductors are disconnected from grid, the utility earthing at distribution transformer will be disconnected hence become an unearthed system. Even if unearthed distribution systems detect earth faults through capacitive currents (line to earth capacitances), domestic wiring incorporates very small capacitance values (almost negligible) so that the fault could persist undetected.

There is a high possibility that a domestic earth fault could persist and undetected due to,

1. High earth fault loop impedance, hence less earth fault current.
2. Insufficient and fast decaying earth fault current contribution of small PV inverters.

As shown in Figure 2, compared to a synchronous generator the fault current

contribution from a PV inverter is small in magnitude and diminishes quickly [5]. Hence conventional RCD / RCCB with prevailing earthing mechanism may not provide intended protection without modifications.

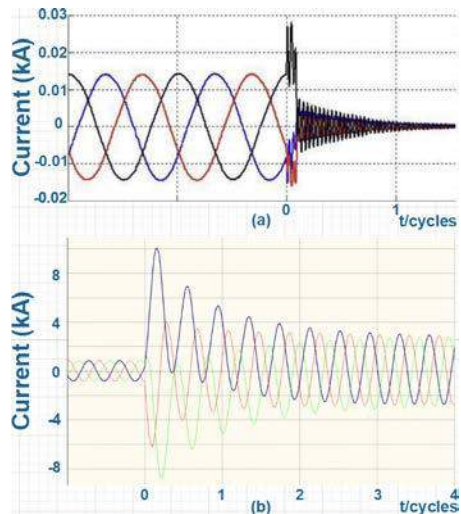


Figure 2: a) PV Inverter 3-Ph Fault Current @ PCC vs b) 32 MVA Synchronous Generator 3-Ph Short Circuit Current @ Terminals [5]

Even if a 30 mA RCD is recommended for human safety, a persisting fault current as small as 20  $\mu$ A could be severe for internal organs of human body which even could lead to death. PV generation with less fault current contribution scenarios could lead to such unattended persisting earth faults.

Considering the above limitations, two solutions are proposed to establish proper earth fault protection in “autonomous /off-grid” operating mode and each case is validated with schematics and modelled circuits, calculations and results obtained using PSCAD software.

## Methodology

For fault current analysis of Off-Grid PV inverter, an internal / stand-alone oscillator-based gate driver needed to be designed for modelling. So, it is assumed that during islanded operation the reference signal is fed from a pre-defined source to the Phase Locked Loop (PLL) of the closed loop controller of the inverter. Since the primary focus is on Fault Current Contribution, the variation of irradiance and temperature was neglected, assuming the PV is producing maximum power. The PV plant with the dc-dc converter is represented by a dc-Link Voltage Source for modelling purpose. Since the model is developed for small sized single-phase PVs, all calculations were done for 3 cases: 1, 5 & 10 kW.

### Derivation of Inverter & Closed Loop Controller Parameters

The following equations were used to calculate the inverter parameters and all the notations will be as per Figure 3.

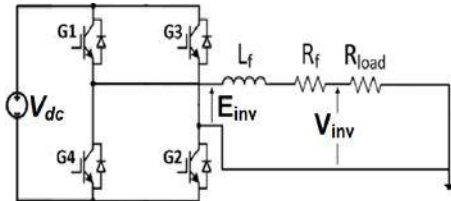


Figure 3: Schematic of Inverter for Modelling

$$V_{inv} = \frac{m_a * V_{dc}}{2 * \sqrt{2}} \quad \text{Eq. (1)}$$

Where,

- $V_{inv}$  = Inverter Output Voltage (Vrms)
- $V_{dc}$  = DC-Link Voltage (V)
- $m_a$  = Modulating Index

$$P = \frac{E_{inv} * V_{inv} * \sin \delta}{2\pi f_{sys} * L_f} \quad \text{Eq. (2)}$$

Where,

- $P$  = Inverter Nominal Power (kW)
- $E_{inv}$  = Gate Output Voltage (Vrms)
- $V_{inv}$  = Inverter Output Voltage (Vrms)
- $\delta$  = Load Angle (deg)
- $f_{sys}$  = Nominal Frequency (Hz)
- $L_f$  = Filter Inductance (mH)

Filter Resistance ( $R_f$ ) is calculated as,

$$R_f = \frac{2\pi f_{sys} * L_f}{10} \quad \text{Eq. (3)}$$

The controller parameters are derived using the following transfer function, where its poles are given by P1 & P2.

$$G(s) = S^2 + \frac{K_p S}{L_f} + \frac{K_i}{L_f} \quad \text{Eq. (4)}$$

Where,

- $K_p$  = Proportional Gain of Controller
- $K_i$  = Integral Gain of Controller
- $L_f$  = Filter Inductance (mH)

Above controller parameters are designed such that,

$$P_1 = \frac{2\pi f_s}{10} = 4 * P_2 \quad \text{Eq. (5)}$$

Where,

- $f_s$  = Carrier Frequency (Hz)

The rated load of the inverter in each case is represented by a resistor value  $R_{load}$ ,

$$R_{load} = \frac{V_{inv}^2}{P} \quad \text{Eq. (6)}$$

Where,

- $V_{inv}$  = Inverter Output Voltage (Vrms)
- $P$  = Inverter Nominal Power (kW)

The data used for example calculations are:  $V_{dc} = 720$  V;  $V_{inv} = 230$  V (RMS);

Inverter Nominal Power ( $P$ ) = 1, 5 & 10 kW; Carrier Frequency ( $f_s$ ) = 5 kHz; Nominal / Modulating Freq. ( $f_{sys}$ ) = 50 Hz First the circuit was developed in PSCAD (Figure 4) for each case with calculated parameter values as per above equations and run the system with respective rated loads,  $R_{load}$  (no-fault condition), and a harmonic analysis was conducted. Based

on the dominant harmonic component for each case, the shunt capacitor value ( $C_f$ ) of L-C filter was calculated for relevant resonant frequency ( $f_{res}$ ). All calculated parameters for each case are tabulated in Table 1.

$$2\pi f_{res} = \frac{1}{\sqrt{L_f * C_f}} \quad \text{Eq. (7)}$$

Table 1: Calculated Inverter and Controller Parameter Values

| Parameter             | 1 kW     | 5 kW     | 10 kW   |
|-----------------------|----------|----------|---------|
| $V_{dc}$ / V          | 720      | 720      | 720     |
| $V_{inv}$ / V         | 230      | 230      | 230     |
| $f_s$ / kHz           | 5        | 5        | 5       |
| $P$ / kW              | 1        | 5        | 10      |
| $m_a$                 | 0.903    | 0.903    | 0.903   |
| $L_f$ / mH            | 32.20    | 6.44     | 3.22    |
| $R_f$ / $\Omega$      | 1.01     | 0.20     | 0.10    |
| $K_p$                 | 126.37   | 25.27    | 12.64   |
| $K_i$                 | 79401.87 | 15880.37 | 7940.19 |
| $R_{load}$ / $\Omega$ | 53       | 10.6     | 5.3     |
| $C_f$ / $\mu\text{F}$ | 109.9    | 549.4    | 1098.9  |

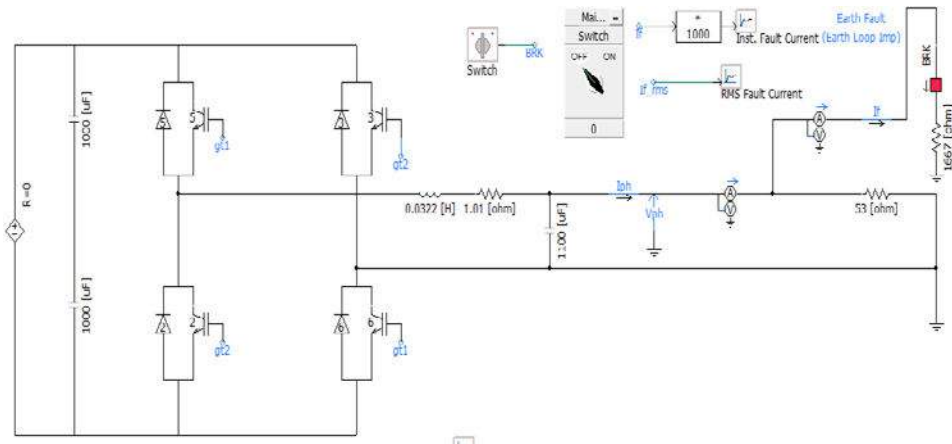


Figure 4: PSCAD Schematic for Simulation



### A) Worst-Case Earth Fault Loop Impedance

For the worst-case, the standard limit for human safety, during an earth fault shall be considered. Hence, the maximum potential rise of the entire system shall be limited to 50 V. If standard RCD ( $I_{\Delta N} = 30$  mA for domestic applications) is selected for the protection scheme, the maximum Earth Fault Loop Impedance,  $Z_m$  is given by,

$$Z_m = \frac{50}{I_{\Delta N}} \quad \text{Eq. (8)}$$

Hence,  $Z_m = 1,667 \Omega$ . Here the maximum allowable resistance value for installation (consumer) side earth electrode is  $200 \Omega$ , where it should be as low as practicable [6].

### B) Typical Values Incorporating Earth Fault Loop Impedance

The following assumptions were made for the calculations:

- i) Typical Impedance of Utility Transformer earth electrode is  $10 \Omega$ .
- ii) Typical Impedance of Installation / consumer earth electrode is  $10 \Omega$ .
- iii) Wiring length for a large sized commercial building is  $1000$  m.
- iv) Conductors are  $2.5 \text{ mm}^2$ , Copper conductors, PVC sheath and PVC Insulation

Relevant data for conductors were extracted from Kelani Cables Catalogue and IEE Wiring Regulations are tabulated in Table 2 [7] [8]. For the worst-case scenario a fault at the farthest end was considered, hence the cable resistance counted was twice. Therefore, as per Table 2 the maximum resistance of domestic wiring,  $R_{wm}$ , is  $34 \Omega$ .

Similarly, the capacitance between L & E conductor can also be calculated within the building premises, assuming the

similar worst-case scenario considered earlier, and based on Eq. (9) and as per data in Table 3 [7] [8].

$$C = \frac{2\pi * \epsilon_0 * \epsilon_r}{\ln\left(\frac{b}{a}\right)} \quad \text{Eq. (9)}$$

Hence the maximum capacitance of domestic wiring ( $C_{wm}$ ) calculated is  $216.19 \text{ pF}$ , and the reactance ( $X_{wm}$ ) is  $14.7 \text{ M}\Omega$ , which may be negligible compared to other impedance values in later calculations.

The resistance and reactance of overhead neutral conductor was calculated assuming that the conductor is a fly conductor. As per the data collected from Distribution Planning Branch, Central Province, Ceylon Electricity Board, the maximum length of the Fly conductor feeder in urban area is assumed to be  $1.8 \text{ km}$ . Therefore, the calculated resistance ( $R_{line}$ ) is  $0.915 \Omega$  and the reactance ( $X_{line}$ ) is  $0.524 \Omega$ .

Based on the calculated values (sections i-iv), the total Resistance ( $R_{total}$ ) and Reactance ( $X_{total}$ ) values in the earth fault loop are derived as  $54.915 \Omega$  and  $0.524 \Omega$  respectively.

The domestic wiring capacitance,  $C_{wm}$  is negligible, as it represents a very large reactance compared to that of overheadline ( $X_{wm} \gg X_{line}$ ). Further, line reactance is also negligible ( $X_{total} \ll R_{total}$ ) hence earth fault loop impedance is  $54.915 \Omega$ .

### Approach-2 for Proposed Off-Grid Earth Fault Protection Scheme

Approach-2 to isolate both L & N conductors from the grid whenever loss of grid supply is detected and to connect a new local earth connection by means of an Earth Switch controlled by the change-over mechanism.

Table 2: Extracted Data for Cable Resistance &amp; Line to Earth Capacitance Calculations [7] [8]

| Symbol               | Parameter  | Value                        | Unit   |
|----------------------|--|------------------------------|--|
| <b>a</b>             | Core Diameter  | 1.78                         | mm   |
| <b>b</b>             | Sheath + Insulation Diameter                                 | 4.98                         | mm   |
| <b>ε<sub>0</sub></b> | Permittivity of Free Space                                   | $8.85418782 \times 10^{-12}$ | $\text{m}^{-3} \text{kg}^{-1} \text{s}^4 \text{A}^2$ |
| <b>ε<sub>r</sub></b> | Relative Permittivity of PVC                                 | 4.0                          | -  |
| <b>R'</b>            | Max Allowable Resistance @ 70 °C<br>(As per IEE Regulations) | 17                           | Ω / km   |

By this method the prevailing earthing arrangement is supposed to be modified; i.e. the utility transformer neutral earthing will be disconnected and a new local earth for the Inverter will be introduced, while customer side domestic earthing is kept unchanged. Hence the Earth Fault Loop will be changed but the same domestic RCD is supposed to provide expected earth fault protection. The modified earth fault loop is shown in Figure 6.

### Calculations

The maximum allowable earth fault loop impedance,  $Z_m$  is given by Eq. (10).

$$Z_m = \frac{U_0 * f_s}{I_{>(RCD)}} \quad \text{Eq. (10)}$$

Where,

$U_0$  = Nominal Voltage Ph-E (V)

$f_s$  = Safety Factor

$I_{>RCD}$  = RCD Operating Current (mA)

$I_{>(RCD)}$  is the current causing the operation of the protective device at the maximum time threshold, obtained from the time-current curve of the device. This was selected as 30 mA. With a safety factor of 0.95 accounted for voltage variations,  $Z_m$  was calculated as 7.28 kΩ. However, as calculated in Section 2.2.1 (B),  $R_{wm}$  is 34 Ω, well within the above limit and resulting in a fault current of 6.76 A at the nominal voltage, thus demanding a current limiting resistor. As per BS 6004, the peak current rating of 2.5 mm<sup>2</sup> 450/750 V flexible cables (reference method A; enclosed in conduit in thermally insulating wall) is 20 A [9]. Even if 6.76 A short time fault current is permissible within above limit, core-saturation in existing RCD / RCCB (depending on B-H characteristics) is possible in such high residual currents (with harmonics).

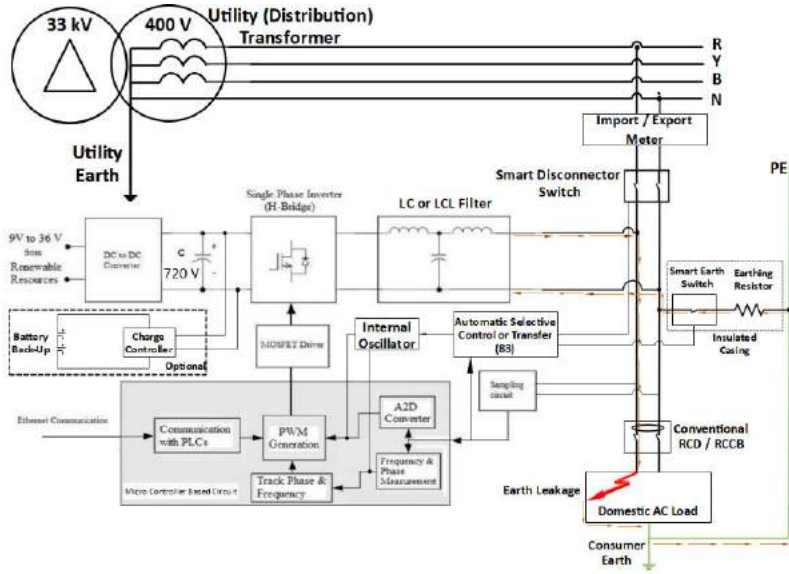


Figure 6: Schematic for Basic Protection Arrangement – Approach 2








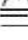
| Residual current form   | Area of application by type |   |   |        |   |   | Tripping current  |
|---|-----------------------------|---|---|--------|---|---|---|
|   | AC                          | A | F | B / B+ |  |  kHz |   |
|    | •                           | • | • | •      | •   | •   | 0.5 to 1.0 $I_{\Delta n}$   |
|   |                             | • | • | •      | •   | •   | 0.35 to 1.4 $I_{\Delta n}$  |
|  |                             | • | • | •      | •   | •   | Contact angle 90°:<br>0.25 to 1.4 $I_{\Delta n}$<br>Contact angle 135°:<br>0.11 to 1.4 $I_{\Delta n}$ |
|  |                             | • | • | •      | •   | •   | max. 1.4 $I_{\Delta n}$ + 6 mA DC <sup>1)</sup>   |
|  |                             |   | • | •      | •   | •   | 0.5 to 1.4 $I_{\Delta n}$   |
|  |                             |   |   | •      | •   | •   | 0.5 to 2.0 $I_{\Delta n}$   |

Figure 7: Limits of Tripping Currents for Various Types and Forms of Current [10]

As per Figure 7 for selection of RCDs (depending on the harmonic waveforms included), Selected fault current ( $I_f$ ) is  $1.4 * I_{\Delta n} = 42 \text{ mA}$ . A fault close to earth switch was considered.

Hence, Current Limiting Resistor required is  $5.47 \text{ k}\Omega$ . Continuous and short time (1 & 3 sec) ratings shall be specified for the Current Limiting Resistor accordingly within above limits. Cost can be reduced by optimizing the rating of the resistor.

The complete compartment including Smart Earthing Switch and Earthing Resistor shall be insulated and covered by a properly earthed casing, since earth link potential could rise up to Phase voltage; i.e.  $230 \text{ V}_{ac}$  during an earth fault. In case of a fault within the Inverter-Distribution board area (which is not exposed to human touch), the fault can prevail undetected until the utility supply recovers.



## Modelling Results and Conclusions

PSCAD Schematic in Figure 4 was developed with respect to different Cases (as in Table 1) for Approach 1 (Typical & Worst-Case) and Approach 2 with the calculated values of earth fault impedance and other parameters. For each simulation the system is allowed to stabilize with full load currents and voltages. Then the earth fault resistance for each scenario calculated in section 2 was used and the transient waveforms were observed. The results are recorded as tabulated in Table 3. Further, the rms fault current waveforms for the 1 kW inverter are illustrated in Figure 8.

## Observations

Based on the results in Table 3, for each scenario, the average fault current was plotted against RCD characteristics ( $I_{\Delta N} = 30 \text{ mA}$ ) in Figure 9, hence following observations are made.

- i) The time taken to settle for the fault current in each scenario is approximately 20 ms, hence the fault is detectable within 1 cycle.
- ii) The fault current is high enough to trigger the protective device (RCD / RCCB) in each scenario hence performance is satisfactory.
- iii) The fault currents in the proposed solutions are not varied in considerable margins with the capacity of the inverter in the selected domestic range (1 to 10 kW), hence a rugged system.

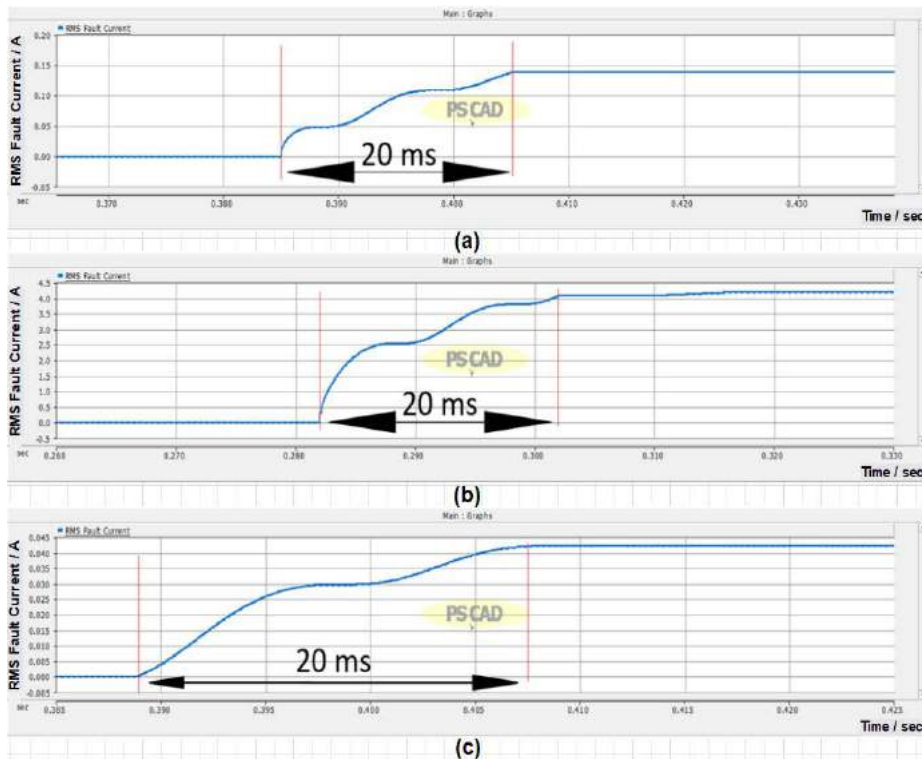
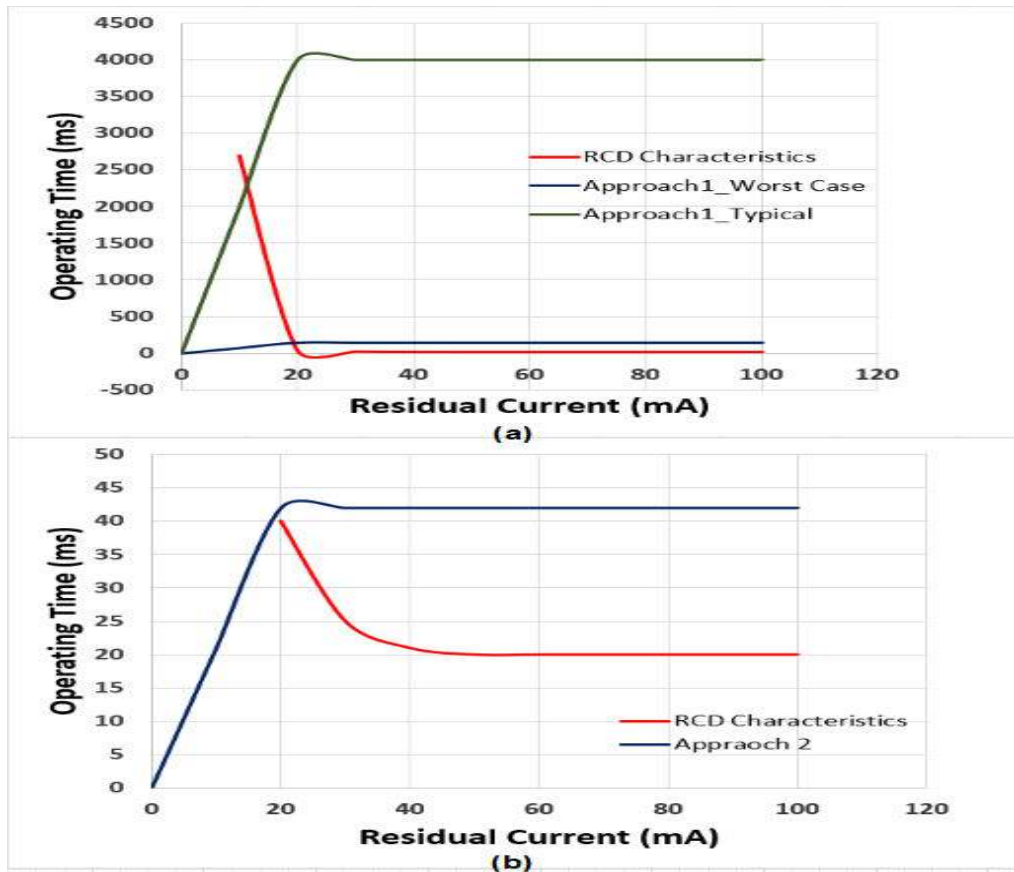


Figure 8: RMS Fault Currents for Case1 a) Approach1 Worst Case; b) Approach1 Typical; c) Approach

Table 3: Comparison of Fault Currents in Different Scenarios Calculated in Section 2

| Scenario                         | Case | RMS Fault Current / mA | Fault Rise Time / ms |
|----------------------------------|------|------------------------|----------------------|
| Approach1                        | 1    | 140                    | 20                   |
| Worst Case                       | 2    | 145                    | 20                   |
| ( $R_f = 1667 \Omega$ )          | 3    | 145                    | 20                   |
| Approach1                        | 1    | 4000                   | 20                   |
| Typical Case                     | 2    | 4000                   | 20                   |
| ( $R_f = 54.915 \Omega$ )        | 3    | 4300                   | 20                   |
| Approach2                        | 1    | 42                     | 20                   |
| ( $R_f = 5.47 \text{ k}\Omega$ ) | 2    | 42                     | 20                   |
|                                  | 3    | 42                     | 20                   |

Figure 9: Performance Comparison: Operating Characteristics of Type B ( $I_{\Delta N} = 30 \text{ mA}$ ) RCD vs (a) Typical & Worst-Case Scenarios for Approach 1; (b) Approach 2

## Conclusions

A reliable earth fault protection scheme for the islanded operation of small-sized roof mounted domestic PV inverters ranging from 1 to 10 kW is proposed. Using simulations under different operating conditions it was shown the proposed arrangement is operating satisfactory. It is important that RCD of domestic application rating with  $I_{\Delta N} = 30$  mA of Type B to be used for this scheme as PV inverter during the Off-Grid mode may generate harmonics.

## Acknowledgements

This work was supported by the Distribution Planning Branch, Central Province, Distribution Division 2 and Protection – Generation Branch, Generation Division of Ceylon Electricity Board.

## References

[1] “Engineering Recommendation G59 - recommendations for the connection of generating plant to the distribution systems of licensed distribution network operators” September 2015 Publication by Energy Networks Association, London

[2] “Earthing Systems Worldwide and Evolutions” by Bernard Lacroix; In-charge of prescription for LV Power distribution, Merlin Gerin & Roland Calvas, In-charge of technical communication for the groupe Schneider.

[3] IEC 60364-4-44-2015: Low-voltage electrical installations - Part 4-44: Protection for safety - Protection against voltage disturbances and electromagnetic disturbances

[4] “Long Term Generation Expansion Plan (Draft) for 2020-2039” May 2019 Publication by Transmission and Generation Planning Branch, Transmission Division, Ceylon Electricity Board, Sri Lanka.

[5] “Fault Current Contribution from DG”; Synchronous generator, Asynchronous generator, PV inverter (and other converters with low power rating), Nordic Workshop on Power System Protection and Control Trondheim-Norway May 25, 2016, Tor Inge Reigstad, SINTEF Energi

[6] “The RCD Handbook”; BEAMA Guide to the Selection and Application of Residual Current Devices, September 2010 [7] IEE Wiring Regulations - Requirements for Electrical Installations; Seventeenth Edition

[8] <http://www.kelanicables.com/product-categories/indoor-cables/> (Accessed on June 29<sup>th</sup>, 2019)

[9] BS6004: 2012: Electric cables. PVC insulated and PVC sheathed cables for voltages up to and including 300/500 V, for electric power and lighting.

# Optimization of Energy Saving in Commercial Buildings using DC Microgrid

Dilini Almeida<sup>\*1</sup>, Amani Weerasinghe<sup>§2</sup>, Ashan Imantha M.H. Bandara<sup>#3</sup>,  
Janaka Ekanayake<sup>#4</sup>

*\* Department of Electrical Power Engineering, University Tenaga Nasional,  
Kajang, Malaysia*

<sup>1</sup> dilinialmeida2@gmail.com

*§ Sri Lanka Sustainable Energy Authority*

<sup>2</sup> amaniweerasingha@gmail.com

*# Department of Electrical and Electronic Engineering, University of Peradeniya,  
Sri Lanka*

<sup>3</sup> ashanimhb31@gmail.com

<sup>4</sup> jbe@ee.pdn.ac.lk

## Abstract

Improvement of energy efficiency in electrical equipment is a widespread practice among many industries nowadays. The commercial buildings such as banks and offices are using variety of dc-powered equipment such as LED lights, and inverter-driven air-conditioners and/or refrigerators with ac-dc converters to improve their energy utilisation. On the other hand, these entities uptake solar photovoltaic (PV) and battery storages with dc-ac conversions to reduce the usage of electricity from the grid. The use of dc in source and load ends opens up an opportunity to improve the energy efficiency by using dc power distribution instead of ac power.

In this study the conventional ac powered LED lights, air-conditioners, computer power supplies and solar PV systems were analysed and compared the power consumption against dc operated counterparts. The power architecture of these devices was analysed and converted them to operate in dc without using ac-dc or dc-ac converters. A prototype dc Micro Grid in a commercial building environment was used to demonstrate the applicability of the proposed idea. The power consumption and efficiency improvement with dc power distribution were recorded and presented.

**Keywords:** dc distribution; Microgrid, Solar PV; Renewable Energy; dc Microgrid

## Introduction

Energy conservation is a prime concern in the world. Out of various types of energy, electricity is a vital commodity of modern society. The statistical research studies revealed that more than 70% of electricity is generated using fossil fuel [1], [2]. At the same time, carbon emission increases by 2% compared to the previous decade ended in 2017 [3]. This increment is caused by the dramatic increase in the demand for electricity. Moreover, the excessive growth of the demand for energy caused by the depletion of fossil fuel reserves [4].

To overcome the anticipated energy challenges, energy optimization in commercial buildings becomes a forefront perspective in the industry. Buildings, other than industrial and private dwellings, are categorized as commercial buildings. Offices and apartment buildings, hotels, schools, and churches, marine, air, railway, and bus terminals, department stores, and buildings in similar capacity can be recognized as examples for commercial buildings [5]. In USA, among the different kinds of commercial buildings, office buildings have the most significant energy consumption, which is similar worldwide [6], [7].

In this research, electrical loads in several commercial buildings were analyzed using energy audit reports. Existing power distribution and ac powered dc

operating devices were analyzed, and efficiency gain was evaluated. The cost benefit analysis was done considering two case studies and outcomes are presented.

## Commercial building as a Microgrid

Microgrid is a small power system which has its own local generation, energy storages and loads. With the plug and play capability within the Microgrid, RES can be connected or disconnected seamlessly without changing the structure of the Microgrid. Due to the unpredictability of RES plug and play capability becomes an attractive feature when connecting RES to the Microgrid. Moreover, Microgrid can be operated in grid connected mode or autonomously (islanded mode). During the islanded mode operation in the absence of utility support, in order to maintain the inertia an energy storage is essential for a Microgrid. The power distribution architecture of Commercial buildings enables us to treat them as Microgrids [8]–[10].

In current ac Microgrids where the power distribution is ac, dc sources and loads such as solar PV, energy storage systems, LED lights, computer power supplies and inverter driven air conditioners are connecting to ac system as presented in Figure 1. As in Figure 1 dc sources such as solar PV supply power to dc loads while sending power through multiple ac-dc and dc-ac conversion stages.

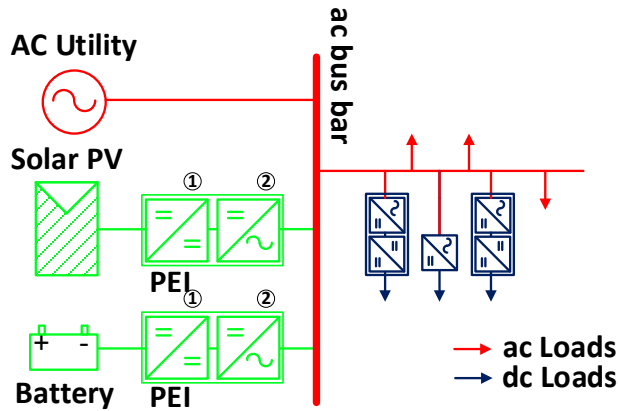


Figure 1: Integration of dc sources and loads to ac distribution system

However, using a dc Microgrid these unwanted conversion stages can be eliminated. Since most of the energy storages and sources are naturally having dc output or intermediate dc power stage it is easier to connect them with a dc Microgrid than its ac counterpart. Furthermore, the ac-dc conversion stages in consumer electronics such as LEDs and computer power supply units can be eliminated when they are connecting to a dc Microgrid. Outline of the proposed dc Microgrid is given in Figure 2.

The dc-dc converters have power conversion efficiency in the range of 90%

to 99% which is comparatively much higher than ac-dc or dc-ac converters. Hence dc Microgrid enables to utilize renewable energy source more efficiently than ac system.

### Loads and sources in commercial buildings

In commercial buildings, most of the electricity is utilized for air conditioning, lighting, and computing. [11]–[13]. Conventionally these devices are connected to ac electric system. However, the advancement in power electronics makes them to working in dc electricity.

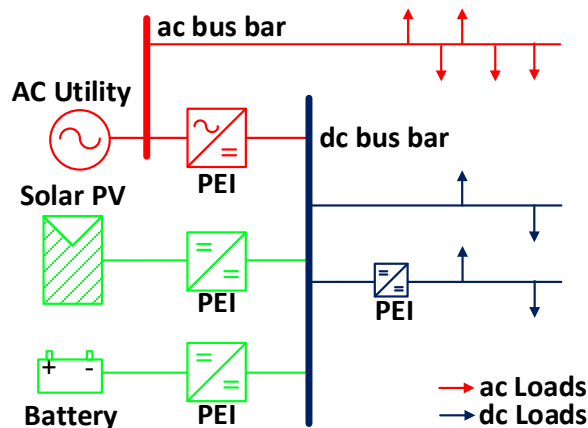


Figure 2: Proposed system to integrated dc loads and sources

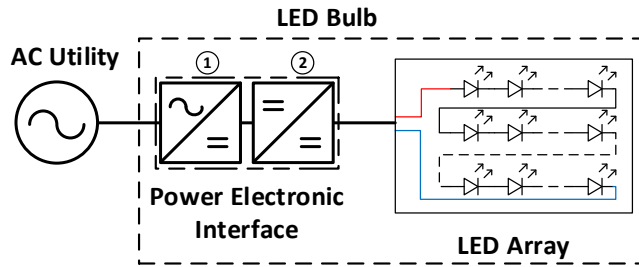


Figure 3: Block diagram of the circuit of LED bulb connected to ac system

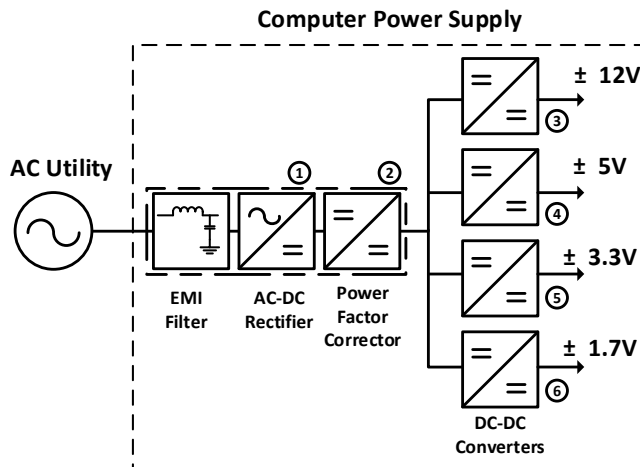


Figure 4: Block diagram of the circuit of computer power supply connected to ac system

### LED Lights

As per the existing research studies, the use of LED lights can reduce the electricity consumption for lighting by 85% compared to incandescent lamps, and by 20% - 40% compared to fluorescent and CFL bulbs [14]–[18]. A block diagram of a conventional power circuitry of an ac LED system is presented in figure 3. [19], [20].

If these lights are powered using dc electricity supply, the ac-dc rectifier (marked as 1 in figure 3) can be removed. This improves the power consumption of LED lights. Therefore, the use of dc powered LEDs can further decrease the power consumption compare to ac powered LEDs by 10% - 20% [16], [19], [20].

### Computer Power Supply

Analysis on computer power supplies confirmed that it is a device comprise of dc-dc converters with different voltage ratings. These converters are powered using common dc link which is connected to ac power system through an ac-dc rectifier followed by a power factor corrector (PFC) module. Conventional power architecture of the computer power supply is presented in the Figure 4 [21]–[23].

The ac-dc rectifier and PFC converters are marked as 1 and 2 in Figure 4. By eliminating ac-dc and PFC circuitries power consumption of computer power supply can be improved by 10% - 20% using dc electricity.

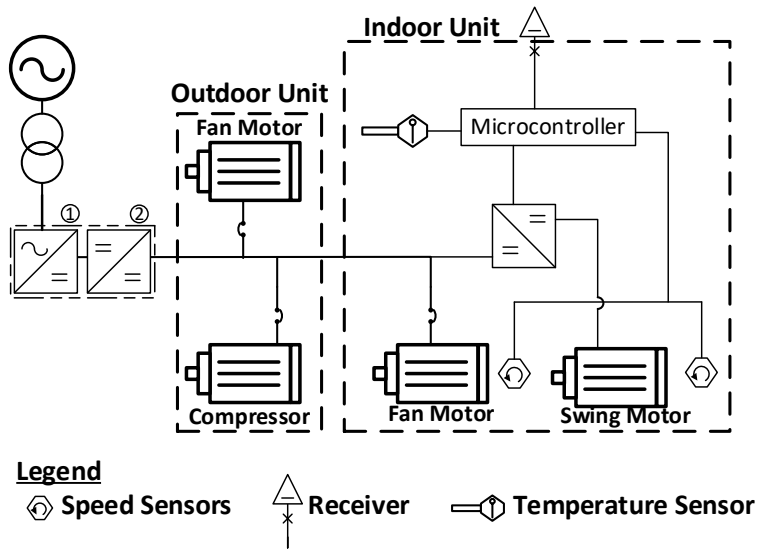


Figure 5: Block diagram of the circuit of inverter driven air conditioner

### Air-conditioners

Conventional air conditioners are equipped with ac induction motors. However modern inverter driven air conditioners are equipped with brushless dc motors which are more efficient compared to conventional ac induction motors. The flat efficiency vs load characteristics of BLDC motors ensures overall efficiency between 80%-90% which is better than ac induction motors under partial load conditions.

Even though these inverter driven air-conditioners are equipped with BLDC motors they are interfaced to ac power system through couple of converter stages which is possible to eliminate using dc power supply.

Figure 5 presents the power flow diagram of inverter driven air conditioner with BLDC motors.

### Solar PV

Natural output of solar PV panel is dc electricity. Typical configuration followed to connect solar PV to ac system is presented in Figure 6. These intermediate ac-dc and dc-ac conversion stage contributes 10% - 40% conversion loss [24], [25]. Furthermore, the efficiency of the inverter is varying with its loading conditions. This can be vary from 50% at slight load conditions to 90% at heavy load conditions [26]. Exemplary efficiency variation is presented in Figure 7.

However, in dc Micro Grid PV can be interfaced to the dc bus using single dc-dc converter. Hence power losses in inverter can be eliminated.

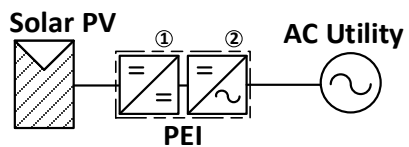


Figure 6: Connection of solar PV and to ac



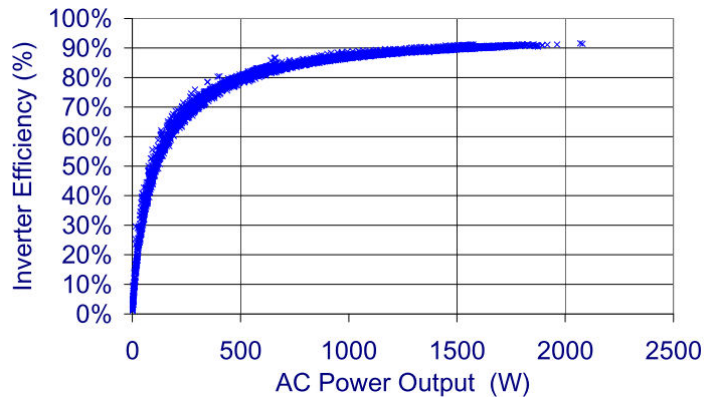


Figure 7: Efficiency variation of PV inverter

## Methodology

### Load Surveys

Energy audit reports were collected from number of commercial buildings designated for different purposes. The daytime energy compensation was audited and identified the different load categories having the most significant power consumption.

Table 1 shows the mean values of energy consumption for each load category as a percentage of total consumption. In general, highest energy consumption was recorded for air conditioning. Also, the total consumption of air-conditioning, lighting and computers vary between

60% ~ 90% and overall average is about 75 %. However, for some of the building categories the sample space is small to evaluate the load share to identify possible dc operated loads.

By analyzing further, building categories with the highest combined energy consumption for air-conditioning, lighting and computers were identified. As per the details in

Table 1, banks are the entities with highest combined energy compensation value of 98%. Universities and private office buildings have the second and third highest combined energy compensation. The distribution of energy consumption is presented in Figure 8.

Table 1: Energy consumption in various building categories

| Category           | Air conditioning | Lighting | Computers | Other |
|--------------------|------------------|----------|-----------|-------|
| Government Offices | 52.8             | 20.0     | 9.8       | 17.5  |
| Private Offices    | 50.8             | 33.4     | 4.5       | 11.4  |
| Hospitals          | 41.7             | 19.1     | 0.6       | 38.7  |
| Hotels             | 60.0             | 2.3      | 0.0       | 37.7  |
| Universities       | 70.5             | 9.1      | 15.5      | 5.0   |
| Super Markets      | 32.0             | 6.1      | 0.0       | 61.9  |
| Banks              | 78.9             | 10.4     | 8.4       | 2.3   |

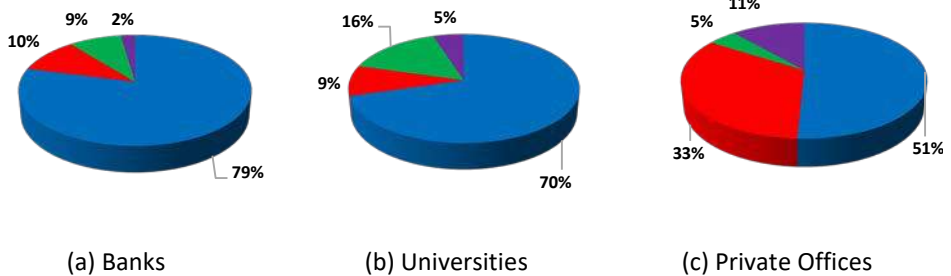


Figure 8: Distribution of Energy Consumption {Blue – Air-conditioning/Red-Lighting/Green-Computers/Purple-Other utilities}

### Analysis of energy saving potential

Considering the buildings with highest combined energy compensation for air-conditioning, lighting and computers, banks seems the best candidate to install a dc Microgrid. Four bank buildings were considered for the load analysis.

The potential energy saving using dc Microgrid for each building is given in Table 2. As per the evaluation it can be seen that about 24% energy saving is possible by operating a bank building through a dc Microgrid.

### Case Study

Two case studies were conducted to evaluate the energy conservation using a dc Microgrid. In the first case study the energy saving possible with dc LED lights was evaluated. New building of the Department of Electrical and Electronic Engineering (DEEE), University of Peradeniya was selected to conduct the case study 1. Layout of the new building-DEEE is shown in Figure 9. The second case study was conducted using the load data of the Bank of Ceylon-Independence Square branch.

Table 2: Variation of monthly energy saving potential

| Building                             | Current Consumption in ac (kWh/month) | Consumption after conversion to dc (kWh/month) | Total Saving (kWh/Month) | Percentage Energy Saving (%) |
|--------------------------------------|---------------------------------------|--|--------------------------|------------------------------|
| Bank of Ceylon – Peradeniya          | 4339                                  | 3288   | 1051                     | 24.2                         |
| Bank of Ceylon – Independence Square | 4061                                  | 3049   | 1012                     | 24.9                         |
| Bank of Ceylon – Ganemulla           | 5045                                  | 3837   | 1208                     | 23.9                         |
| Bank of Ceylon – Gampaha             | 2985                                  | 2288   | 697                      | 23.3                         |

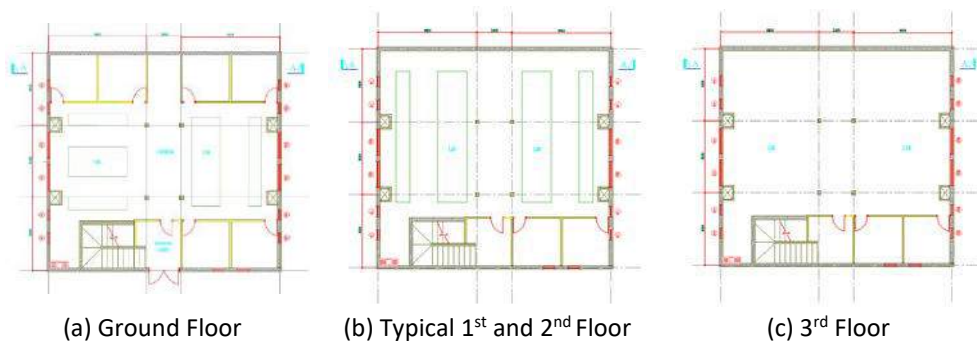


Figure 9: Floor plans of the new building-DEEE

### Case Study 1

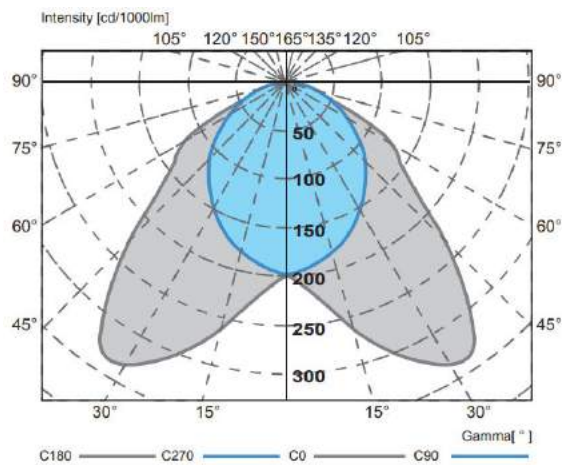
The existing luminaire arrangement of the new building - DEEE was examined as per the layouts given in Figure 9. A sample picture and intensity map of the existing luminaire is given in Figure 10. Specifications of the same luminaire is presented in Table3.

Table 3. Specification of ac luminaire

| Parameter       | Specification              |
|-----------------|----------------------------|
| Luminaire Name  | SJ LITE SAC 240<br>MOL(AH) |
| Electrical Data | 240V, 50Hz, 0.9 pf         |
| Light Source    | Fluorescent TLD<br>lamp    |
| Power (W)       | 36W x 2Nos.                |



(a) Sample luminaire



(b) Intensity map

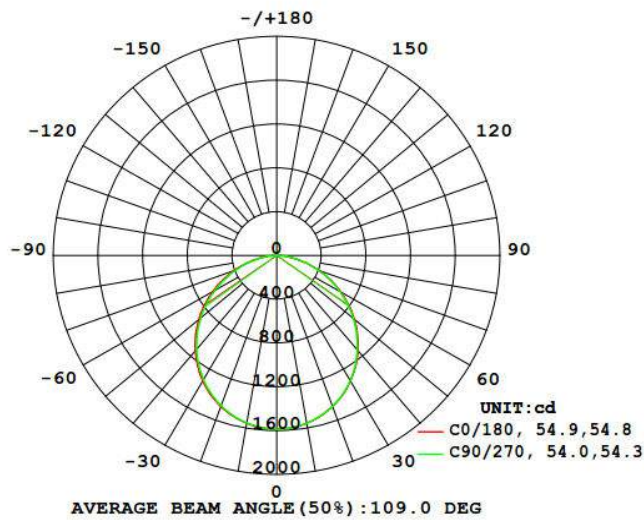
Figure 10: AC Luminaire

Next the luminaire arrangement was modeled and simulated using "DIALux" software (version 4.13) platform. A number of luminaires for each floor was decided according to the standard lux level. Number of luminaires and energy consumption were calculated using simulated results.

Next the existing luminaires were replaced using dc LED luminaires and did the simulations again. As in previous step number of luminaires and energy consumption for dc luminaires were recorded. Sample picture and intensity map of the dc luminaire is presented in Figure 11.



(a) Sample luminaire



(b) Intensity map

Figure 11. DC Luminaire

Observations of the two simulation studies were compared to analyse the energy conservation and cost saving between the use of ac luminaires and dc LED luminaires. The results of the comparison are presented in Table 5.

Table 4. Specification of dc luminaire

| Parameter              | Specification   |
|------------------------|-----------------|
| <b>Luminaire Name</b>  | OKT FS22-DM-35E |
| <b>Electrical Data</b> | 42 VDC          |
| <b>Light Source</b>    | Single lamp     |
| <b>Power (W)</b>       | 40              |

Table 5: Variation of monthly energy saving potential

| Floor Name            | AC luminaires     |           | DC luminaires     |           | Savings (W) | Percentage Saving (%) |
|-----------------------|-------------------|-----------|-------------------|-----------|-------------|-----------------------|
|                       | No. of Luminaires | Power (W) | No. of Luminaires | Power (W) |             |                       |
| Ground Floor          | 30                | 2160      | 30                | 1178      | 982         | 45.5                  |
| 1 <sup>st</sup> Floor | 32                | 2304      | 32                | 1258      | 1046        | 45.4                  |
| 2 <sup>nd</sup> Floor | 32                | 2304      | 32                | 1258      | 1046        | 45.4                  |
| 3 <sup>rd</sup> Floor | 32                | 2304      | 32                | 1258      | 1046        | 45.4                  |

Table 6: Energy saving comparison between ac and dc luminaries

| Item  | Specification |
|---|---------------|
| Total requirement for ac luminaries (kW)            | 9.07          |
| Total requirement for dc luminaries (kW)            | 4.95          |
| Energy consumption per year for ac luminaries (kWh) | 8709          |
| Energy consumption per year for dc luminaries (kWh) | 4754          |
| Total savings per year (kWh)                        | 3955          |
| Percentage total savings per year (%)               | 45.4          |
| Cost saving per year (LKR)                          | 56,754.00     |

Assuming that the lights would be operated for 20 hours per week and energy cost is LKR 14.35 /kWh, cost savings were calculated for case study 1.

As per the results, the annual savings of 45.4% can be achieved by converting existing ac luminaires to dc LED luminaries. For the considered building it was found out that the cost reduction is nearly LKR 56,000/=.

### Case study 2

BOC-Independence Square was considered for the second case study to observe the financial viability of using a dc Microgrid. The 2<sup>nd</sup> entry of the Table 2 shows the energy saving potential of the building when dc Microgrid is implemented. The power consumption pattern shown in Figure 12 was assumed to estimate the financial gain by employing the proposed system.

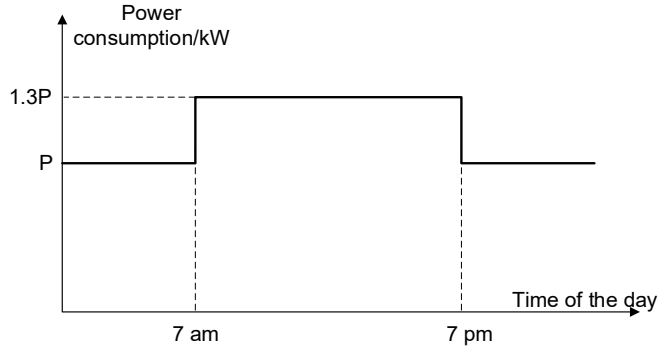


Figure 12: Consumption pattern of the Bank

The following assumptions were made to conduct the case study.

1. Time of use (in 24h format)
  - Idle hours – 07 h – 21h
  - Office hours – 21h – 07h (next day)
2. Office hour power consumption is 30% more than the idle power consumption
3. Energy losses in wires in ac distribution is 5% and it can be eliminated using dc Microgrid.
4. Number of peak sun hours is 5.
5. The bank is operated in GP2 tariff. Charge per kWh;
  - Block 1 – From 5.30 hr to 18.30 hr is LKR 21.80
  - Block 2 – From 18.30 hr to 22.30 hr is LKR 26.60
  - Block 3 – From 22.30 hr to 5.30 hr is LKR 15.40.

Idle load of the building was calculated using Eq.1.

$$P_{Pk} = 1.3P_{Idl}$$

$$P_{Idl} = \frac{E_{Month} + E_{Loss}}{N_d(T_{Idl} + 1.3T_{Pk})} \quad (\text{Eq.1})$$

where,

$E_{Month}$  = Monthly energy consumption  
 $E_{Loss}$  = Monthly energy losses  
 $N_d$  = Number of days

$P_{Pk}$  = Power consumption during office hours

$P_{Idl}$  = Power consumption during idle hours

$T_{Pk}$  = Number of office hours

$T_{Idl}$  = Number of Idle hours

If the solar power installed capacity is  $P_{Sol}$  considering the power consumption pattern shown in Figure 12, the energy cost per day was calculated using (Eq.2).

$$EC_{day} = \alpha_1 t_1 P_{Idl} + \alpha_2 (P_{Pk} t_2 - P_{Sol} t_s) + \alpha_3 t_3 P_{Idl}$$

$$EC_{day} = P_{Idl} \left( \sum_{i=1}^3 \alpha_i t_i + 0.3 \alpha_2 t_2 \right) - P_{Sol} \alpha_2 t_s \quad (\text{Eq.2})$$

where,

$EC_{day}$  = Energy cost per day

$P_{Pk}$  = Power consumption during office hours

$P_{Idl}$  = Power consumption during idle hours

$P_{Sol}$  = Solar power installed capacity

$\alpha_1$  = Tariff for block 1

$\alpha_2$  = Tariff for block 2

$\alpha_3$  = Tariff for block 3

$t_1$  = Number of hours in block 1

$t_2$  = Number of hours in block 2

$t_3$  = Number of hours in block 3

$t_s$  = Number of sun hours

Table 7: Comparison between Energy and power consumption in AC and DC.

| Item  | Specification      |                        |
|---|--------------------|------------------------|
|   | Existing ac system | After converting to dc |
| Monthly energy consumption ( $E_{Month}$ ) (kWh)        | 4061               | 3049                   |
| Monthly energy loss in wires ( $E_{Loss}$ ) (kWh)       | 203                | 0                      |
| Power consumption during idle hours ( $P_{Idl}$ ) (kW)  | 5.15               | 3.68                   |
| Power consumption during office hours ( $P_{Pk}$ ) (kW) | 6.70               | 4.78                   |

Power consumption during idle and office hours is presented in Table 7.

Considering the installed solar capacity as 10 kW in existing ac system, using (Eq.2) Energy charge per day ( $EC_{day}$ ) can be calculated as LKR 1999.5 /day.

The required solar capacity to acquire the same  $EC_{day}$  in dc MicroGrid can be calculated using (Eq.4). All the parameters have usual meaning as in Eq.2. The variation of Electricity charge per day with ac system and dc Microgrid is presented in Figure 13.

$$K = P_{Idl} \left( \sum_{i=1}^3 \alpha_i t_i + 0.3\alpha_2 t_2 \right)$$

$$P_{Sol} = \frac{K - EC_{day}}{\alpha_2 t_s} \quad (\text{Eq.3})$$

where,

$EC_{day}$  = Energy cost per day

$K$  = Constant derived from electricity charges

$P_{Sol}$  = Solar power installed capacity.

$t_s$  = Number of sun hours

By solving Eq.4 it was found that the required solar capacity to operate as a dc MicroGrid is 1.91 kW.

Next the payback period was calculated for both cases using the Eq.4. The average number of days per month is selected as 30.

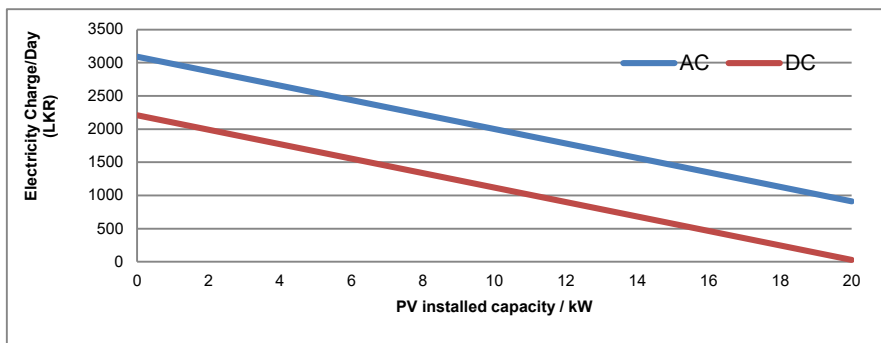


Figure 13: Electricity charge



$$T_{PB} = \frac{P_{Sol} \times \beta_{Sol}}{EC_{Day} \times 30} \quad (\text{Eq.4})$$

where,

- $T_{PB}$  = Payback period in months  
 $P_{Sol}$  = Solar Capacity in kW  
 $\beta_{Sol}$  = Cost per kW of solar  
 $EC_{Day}$  = Energy cost per day after solar installation

If the cost per 1 kW solar capacity is LKR 100,000, with the current payment,

- The payback period for the PV plant connected to the bank with ac would be 18 months
- The payback period for the PV plant connected to the bank with dc would be 4 months.

## Discussion and Conclusions

This paper outlines the possible savings with the dc Microgrid to which solar PV, LED lights, many consumer loads, and air conditioners are connected with lesser number of conversion stages.

Solar PV installations that are connected as roof top schemes utilize an inverter to interface them to the ac grid. These inverters have a typical efficiency about 85% and drop drastically when the power output of the inverter is less than 20%. Therefore, interfacing PV to a dc network through a dc-dc converter brings more than 10% energy saving.

In order to obtain the maximum gain from solar PV connected to a dc network, the loads such as LED lights, computer equipment and air conditioners that have dc bus should be directly interfaced to the dc bus.

LED lamps which are inherently run on dc are interfaced to existing ac network

through a converter that reduced the efficiency of operation. In this research, it was assumed that about 15% of energy can be saved if LED lamps are directly interfaced to a dc network.

When computer equipment is directly interfaced to a dc network, the PFC unit, bridge rectifier, and HF transformer could be eliminated. Assuming that the dc connection needs one extra dc-dc converter having typical efficiency of 85%, the efficiency gain with dc connection is approximately 32%. This will further increase if the power supply is part-loaded.

Modern inverter driven air conditioners utilise brushless dc motors bringing about 25% energy savings if they are directly connected to a dc bus.

Nearly 30 buildings were considered under this research and it was found that the Banks are the ideal candidates for the proposed dc Microgrid. The share of lighting, computers and air conditioners in a number of banks are around 98% of the total load. Analyzing the data from four different banks, it was found that about 24% of energy can be saved if LED lamps, dc fed air conditioners and computer power supplies are connected to a dc Microgrid.

The case study conducted at the bank shows that the simple payback period reduces to 4 months in the proposed dc Microgrid while ac supplied system required 17 month payback period. These are attractive figures for the project, and thus the study reveals that operating dc operated equipment in commercial buildings using dc Microgrid is going to be a feasible project to be implemented in the future.

Within the background mentioned above, the technological intervention considered under the study will be an appropriate approach in the prevailing context. So, dc supply through Microgrid powered by solar PV is observed to be an applicable technology to the country.

## Acknowledgement

Authors would like to acknowledge Sri Lanka Sustainable Energy Authority for providing financial support for this project.

## References

- [1] World Energy Council, "World Energy Resources 2016," World Energy Resource. 2016, 2016.
- [2] "Energy Statistics Pocketbook," New York, 2018.
- [3] British Petroleum, "BP Statistical Review 2015," no. June, p. 2015, 2015.
- [4] IEA, "Key World Energy Statistic 2017," Int. Energy Agency, p. 95, 2017.
- [5] C. B. P. S. C. I. I. A. Society, IEEE recommended practice for electric power systems in commercial buildings, vol. 1990. The Institute of Electrical and Electronics Engineers, Inc., 1983.
- [6] Ö. Boydak, "Commercial Buildings Energy Consumption Survey (CBECS) and Its Comparison with Turkey Applications," J. Clean Energy Technol., vol. 5, no. 1, pp. 69–72, 2017.
- [7] C. B. Dandridge, J. Roturier, and L. K. Norford, "Energy policies for energy efficiency in office equipment Case studies from Europe, Japan and the USA," Energy Policy, vol. 22, no. 9, pp. 735–747, 1994.
- [8] A. Raza and T. N. Malik, "Energy management in commercial building microgrids," J. Renew. Sustain. Energy, vol. 11, no. 1, 2019.
- [9] F. Gonzalez-Espin, V. Valdivia, D. Hogan, D. Diaz, and R. F. Foley, "Operating modes of a commercial and industrial building microgrid with electrical generation and storage," 2014 IEEE 5<sup>th</sup> Int. Symp. Power Electron. Distrib. Gener. Syst. PEDG 2014, pp. 2–6, 2014.
- [10] Y. Wang, Z. Yi, D. Shi, Z. Yu, B. Huang, and Z. Wang, "Optimal Distributed Energy Resources Sizing for Commercial Building Hybrid Microgrids," IEEE Power Energy Soc. Gen. Meet., vol. 2018-Augus, pp. 1–5, 2018.
- [11] N. Luewarasirikul, "A Study of Electrical Energy Saving in Office," Procedia - Soc. Behav. Sci., vol. 197, no. February, pp. 1203–1208, 2015.
- [12] H. Sun, L. Zhang, W. Zhang, and S. Wang, "Research on the energy-controlling system for the terminal electric equipment in office building," Procedia Eng., vol. 205, pp. 281–287, 2017.
- [13] D. Griego, M. Krarti, and A. Hernandez-Guerrero, "Energy efficiency optimization of new and existing office buildings in Guanajuato, Mexico," Sustain. Cities Soc., vol. 17, pp. 132–140, 2015.
- [14] M. Chotiner, "Comparing energy-efficient light bulbs with old-tech lamps," McKnight's Long-Term Care News, 2016. [Online]. Available: <https://www.mcknights.com/marketplace/comparing-energy-efficient-light-bulbs-with-old-tech-lamps/>. [Accessed: 02-May-2019].
- [15] M. I. Zaidy, "Renewable Energy Efficient Solar Lighting System Design for Buildings in UAE," Int. Res. J. Electron. Comput. Eng., vol. 2, no. 1, pp. 13–17, 2016.
- [16] A. Jayaweera, A. Malmquist, and M. T. A. P. Wickramarathna, "Energy Analysis & Effects on Power Utility of LED's compared to Conventional Bulbs," Royal Institute of Technology, Sweden, 2014.
- [17] A. A. El-khalek, K. Youssef, and I. Yassin, "Opportunities of energy saving in lighting systems for public buildings," Renew. Energy Sustain. Dev., vol. 3, no. 1, pp. 95–98, 2017.
- [18] A. Muneeb, S. Ijaz, S. Khalid, and A. Mughal, "Research Study on Gained Energy Efficiency in a Commercial Setup by Replacing Conventional Lights with Modern Energy Saving Lights," J. Archit. Eng. Technol., vol. 6, no. 2, 2017.
- [19] S. A. S. Mohamed, Y. S. Lee, and S. Choi, "Advanced efficiency of DC-LED lighting systems to replace the conventional AC-LED lighting systems Advanced Efficiency of DC-

LED Lighting Systems to Replace the Conventional AC-LED Lighting Systems," no. September, 2018.

[20] A. Jhunjhunwala, K. Vasudevan, P. Kaur, and B. Ramamurthi, "Energy Efficiency in Lighting : AC vs DC LED Lights," pp. 7–10, 2016.

[21] S. Singh, B. Singh, G. Bhuvaneswari, and V. Bist, "A power quality improved bridgeless converter-based computer power supply," IEEE Trans. Ind. Appl., vol. 52, no. 5, pp. 4385–4395, 2016.

[22] S. Singh, B. Singh, G. Bhuvaneswari, and V. Bist, "Power factor corrected zeta converter based improved power quality switched mode power supply," IEEE Trans. Ind. Electron., vol. 62, no. 9, pp. 5422–5433, 2015.

[23] S. Kawaguchi and T. Yachi, "Adaptive power efficiency control by computer power

consumption prediction using performance counters," IEEE Trans. Ind. Appl., vol. 52, no. 1, pp. 407–413, 2016.

[24] S. B. Kjaer, J. K. Pedersen, and F. Blaabjerg, "A Review of Single-Phase Grid-Connected Inverters for Photovoltaic Modules," IEEE Trans. Ind. Appl., vol. 41, no. 5, pp. 1292–1306, 2005.

[25] D. R. Prasad, B. R. Kamath, K. R. Jagadisha, and S. K. Girish, "Smart DC Micro-grid for Effective Utilization of Solar Energy," Int. J. Sci. Eng. Res., vol. 3, no. 12, pp. 1–5, 2012.

[26] F. Vignola, F. Mavromatakis, and J. Krumsick, "Performance of PV inverters," Am. Sol. Energy Soc. - Sol. 2008, Incl. Proc. 37<sup>th</sup> ASES Annu. Conf., 33<sup>rd</sup> Natl. Passiv. Sol. Conf., 3<sup>rd</sup> Renew. Energy Policy Mark. Conf. Catch Clean Energy Wave, vol. 1, pp. 628–650, 2008.

# **Model for Measuring the Effect of Incentive Schemes, Tariff Regimes and Technological Innovations on Change of Consumer Behaviour on Energy Savings: A Study Based on Sri Lankan Electricity Consumers in Industrial Sector**

W. Jayaratne<sup>1</sup>, Prof. Dasanayaka S.W.S.B.<sup>2</sup>, Dr. D.Mudalige<sup>3</sup>

<sup>1</sup>PhD Candidate, University of Moratuwa, Chief Engineer, Ceylon Electricity Board  
witharamalage@gmail.com, 168016A@uom.lk

<sup>2</sup>sarathd@uom.lk

<sup>3</sup>Department of Management of Technology, University of Moratuwa  
dmmudalige@gmail.com

## **Abstract**

The main objective of this research study is to develop a new model to find answers to three questions of why Ceylon Electricity Board (CEB)'s interventions are ineffective in motivating consumers on energy savings, what are the intervening factors effecting the electricity conservation behaviours of consumers and how to make the intervention more effective. To explain the mediating effects of consumer behaviour towards energy conservation, three major factors have been identified in this study. These comprise incentive schemes, tariff regimes and technological innovations. Each of these components acts as an antecedent to change the consumer mindset on energy conservation. Evidence showed that many of the recent attempts to conserve electricity by means of different incentive mechanisms have prematurely failed due to very many facts. Theory of Planned Behaviour (TPB) and Technology Acceptance Model (TAM) have been used as the basic scientific ladder to reach the goal. The Structural Equation Modelling (SEM) technique is used as the main analytical tool to explain the behaviour of input variables with different sensitivity levels in this study. Four hundred industrial consumers of electricity in Colombo, Kalutara and Gampaha Districts were used as the sample by administering structured questionnaire. Findings show that utilities have failed to match incentives, tariff regimes, regulations and new energy saving products scientifically in order to achieve a successful level of energy savings. Therefore, the model developed by this study formulates the guidelines for policy makers to introduce different incentive schemes which sustainably match with other two parameters like regulatory frameworks and tariff regimes whilst supporting the available energy saving technologies.

**Key words:** Energy conservation, incentive schemes, regulatory framework, structural equation modelling, tariff regimes, technology management

## **Introduction and Background for the Study**

Ceylon Electricity Board (CEB) is the government owned electricity provider in Sri Lanka, who is struggling to cater to the increasing demand at an affordable cost. In overall, 10% - 15% electricity is wasted due to technical and non-technical losses in Sri Lanka [1]. As a short-term measure to decrease the electricity wastage and unnecessary consumption, CEB has introduced three types of interventions; Incentive schemes, Tariff regimes and efficient technologies. CEB has implemented several initiatives under these three themes to encourage electricity users to manage their electricity consumption in a way that would positively contribute to reduce the national cost of electricity generation. However, demand for electricity has continuously increased and CEB electricity saving stimulus has proven to be ineffective at current state [2]. Further, this phenomenon also indicates that people and industries have not changed their behaviors relating to electricity usage and do not consider electricity conservation as their social obligation.

This scenario has paved the way to explore answers to questions such as why CEB's interventions are ineffective, what are the intervening factors effecting the electricity conservation behaviors of consumers and how to make the intervention more effective? Normally, people would continually engage in a behavior, if they psychologically feel positive about the outcome of that behavior [3]. If they do not behave as expected, that indicates they do not feel positive about the outcome of the expected behavior. With this contradictory behavior, it is observed that

there is a clear mismatch between CEB's electricity conservation policies and consumer psychological and behavioral concerns on energy consumption and savings. Therefore, this research study aims to theoretically explain why CEB's energy saving stimulus are unable to influence on electricity conservation behavior among the consumers by testing the mediating effect of consumer motivation and behavior.

Normally, efficiency involves cost while conservation involves behavior [4]. Many people are keen on electricity savings as it reflects to the monthly expenses despite the requirement of various energy intensive appliances for this task. Conservation comes from the behavioral domain of the human brain and it does not necessarily guide the consumer to move away from the comfort zone but it excels the social requirement of conserving energy for future use. Today people understand that the most feasible option to move away from high energy prices and bad environmental consequences is to conserve electricity by reducing consumption with whatever means [5].

## **Research Gap and the Significance of the Study**

Recently, several incentive mechanisms have been introduced by the CEB in order to conserve electricity in Sri Lanka. However, many of them failed prematurely due to the lack of consumer awareness and their willingness to accept the offered financial incentives. In this case, consumer's awareness and perceived willingness to adhere to the given mechanism might be insufficient. Documented research [6] showed that there were several determinants with respect to the energy conservation by

means of different motivational activities. Some researchers [7] explain that there exist several social and political factors related to energy conservation and furthermore, they explain that administrative and political issues, firm behavior on different policy instruments and multiple overlapping factors may contribute to the decision on energy conservation [8]. New group of researchers explain that it is difficult to develop, convince and diffuse new policy instruments for different kinds of motivational activities on energy conservation [9].

Researchers have developed some relationship for demand function of electricity as follows [9], [10];

$$\log Y = \log(\beta_1 * P) + \log(\beta_2 * I) + \log(\beta_3 * R) + \log(\beta_4 * B) + \varepsilon \quad (\text{Eq.1})$$

Where,

- Y = Electricity Demand
- P = Electricity Price
- I = Monthly Income of the consumer
- R = Cost of other commodity (Energy Resources)
- B = Consumer behaviors and usage pattern
- $\beta_1$  = Price Elasticity of Demand
- $\beta_2$  = Income Elasticity of Demand
- $\beta_3$  = Cross Price elasticity of Demand
- $\beta_4$  = Incentive Elasticity of Demand
- $\varepsilon$  = Other unknown factors

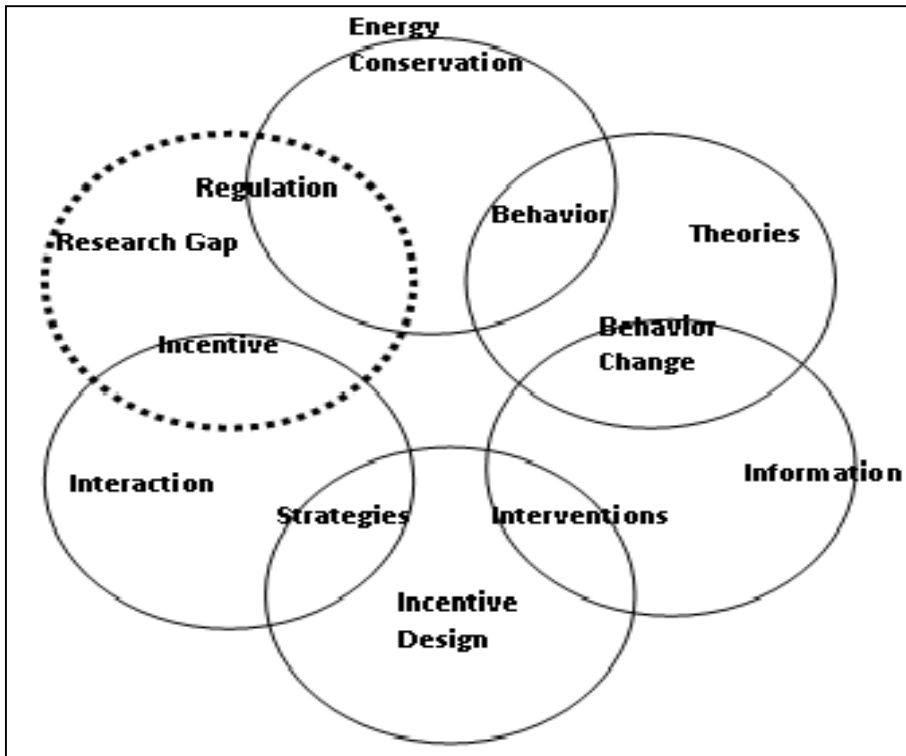


Figure 1: Identification of research gap (Source: Developed by the Author)

Considering the Equation (1), it is found that consumer's behavior (B) effect the energy demand whilst other three factors (P), (I) and (R) all related to tariff regimes also influence the end result. Figure 1, depicts that energy conservation can be achieved by means of changing behavior. However, in order to change the behavior, the related concepts are to be interconnected with the energy conservation. For this task, information on how the consumer behaves during the use of energy is to be studied and interconnected to behavioral functions. In order to change the consumer's attitude and behavioral norms towards the conservation of energy, some form of motivation is necessary. This is achieved by means of incentive schemes and regulatory frameworks which are to be introduced by the government as well as utilities. Some strategies are to be identified in order to motivate the consumers towards the available incentive schemes and thereby to conserve the energy. Therefore, the incentive scheme is to be interconnected with appropriate strategies, interventions and interactions as shown in Figure 1. Finally, all those components are to be bundled to close the prevailing gap for conservation of energy as shown in dotted circle of same figure. The theory of planned behavior (TPB) has significantly been used for systematically identifying the determinants that influence decision making in various behavioral studies including energy conservation, green consumerism, environmental behavioral aspects, etc. [11]. Accordingly, there exists a knowledge gap for conservation of energy using different behavioral aspects in Sri Lanka. The theory of planned behavior [3] stated that a behavior is obtained by interaction between motivation which can be triggered by means of an incentive

scheme, and ability to control. The TPB assumes that intension can directly predict the behavior. Whenever, new technology is introduced to the market, there is certain delay in diffusing same throughout the domain due to the reluctance of consumers to accept the new knowledge. This phenomenon has been fully explained by Technology Acceptance Model (TAM) [9] which is used in this study to develop a new model which is the consolidated and improved extended version of TPB and TAM.

In order to save electricity, consumer behavioral changes are to be made by means of incentive schemes and regulatory framework. This is considered as the prevailing problem. Therefore, the model developed by this study formulates the guideline for policy makers to introduce different incentive schemes which sustainably match with other two parameters like regulatory frameworks and tariff regimes whilst supporting available technologies. Findings of this study can be extended on similar situations in other countries as well. Energy conservation is the saving of energy without wasting whereas energy efficiency is the use of less energy for same kind of work effectively. Approximately, 1.6 Billion of world population do not have the privilege of accessing to national grid connected electricity where as 80 Million population of India do not experience the luxury of this versatile energy resource [12]. Therefore, it is vital to expand the existing generation, transmission and distribution capacities cater to balance 1.6 Billion of un-served population in the world. The major reason for high cost of electricity is due to the volatility of fuel prices, technology cost and high wastage of limited people. Therefore, human behavioral changes are to be inculcated in

their mind in order to conserve energy while averting the severe environmental consequences.

### **Incentive Schemes in CEB; Limitations and Present Situation**

In CEB, most of the incentive schemes and regulatory frameworks on energy conservation are introduced only when there is severe power shortage. Sometimes, whenever there is a severe drought period which results poor hydroelectric power generation, it will remind authorities to go for energy conservation. In the event of an unexpected failure of major equipment in power plant or transmission system, it will create the space for emergency power requirement. Sometimes, during contingency situation in operational activities, energy conservation may be needed. However, during all such occasions, most of the programs have been hurriedly designed and sometimes many of them have failed prematurely due to ad-hoc planning. This proves the lack of empirical novelty on the decisions which have been derived in absence of proper R&D and technology management strategy. Therefore, witnessing the existence of severe gap in the body of knowledge pertaining to this area. CEB's incentive schemes on energy conservation have failed in certain instances whenever it has been implemented without scientific approach. This kind of failure was experienced in 2005 in CEB. According to the findings, two branded CFL has been issued to each individual electricity consumer and the cost of the bulbs was debited to the respective electricity bill in 12 months installment. However, finally it has been found that local suppliers have

issued sub-standard bulbs having lower life time for the sake of achieving high profits. Finally, that mechanism was unpopular among the electricity consumers and failed prematurely. It is learnt that this kind of incentive schemes should be well structured with proper scrutiny prior to implementation. Therefore, it is understood that scientific research is needed in order to ascertain the economic feasibility and sustainability of such systems before the implementation. Many incentive schemes involve large amount of capital investment. The cost benefit ratio and payback period will be the critical factors of such investment decision. Governments can obtain long term loans from financial institutions and invest them in incentive schemes. The total investment can be distributed among the entire consumers of interest for a certain period of time. Whenever the consumers are benefitted with different kinds of incentives and regulatory frameworks, there will be more and more investments flowing towards energy conservation activities, efficiency improvements and technology developments, etc. This will reduce the ultimate energy consumption, energy wastage and thereby can create a new financial model on utilities. The total revenue (top line) and the net profit (bottom line) of the utility business model will be shifted and therefore, careful study is needed to ascertain the limitations and influence of the proposed schemes on demand and supply equilibrium of such institutions. CEB is presently at the verge of termination of net plus and net metering mechanisms for future installations due to the heavy losses incurred to the organization with the inception of new incentive model without proper R&D strategy.



*Table 1: Present situation of consumer base in CEB (Source: Annual Report of CEB -2013, 2015)*

| <b>Tariff Category</b> | <b>Number of Customers in 2013</b> | <b>Number of Customers in 2015</b> | <b>Percentage Sales in 2013</b> | <b>Percentage Sales in 2015</b> | <b>Percentage to total number of consumers, 2015</b> |
|------------------------|------------------------------------|------------------------------------|---------------------------------|---------------------------------|--|
| <b>Domestic</b>        | 4,589,929                          | 4,966,395                          |                                 |                                 |  |
| <b>Religious</b>       | 31,627                             | 34,710                             | 33%                             | 33.5%                           | 88.5%  |
| <b>General Purpose</b> | 535,267                            | 588,063                            | 19%                             | 19.7%                           | 10.4%  |
| <b>Industrial</b>      | 53,162                             | 56,681                             | 32%                             | 30.6%                           | 1.0%   |
| <b>Hotel</b>           | 465                                | 489                                | 2%                              | 1.8%                            | 0.01%  |
| <b>Government</b>      | 309                                | 1792                               | 1%                              | 1.2%                            | 0.03%  |
| <b>LECO</b>            | 1                                  | 1                                  | 13%                             | 12.3%                           | Negligible   |
| <b>Street Lamp</b>     | 1                                  | 1                                  |                                 | 0.9%                            | Negligible   |
| <b>Total</b>           | <b>5,210,761</b>                   | <b>5,648,132</b>                   | <b>100%</b>                     | <b>100%</b>                     | <b>100%</b>  |

Therefore, scientifically designed instrument is highly necessary at this juncture to analyze incentives together with tariff regimes and prevailing energy saving technologies. This issue is addressed within this research. Table 1 shows the different consumer segments by tariffs category-wise [1]. Very important observation could be found in Table 1 with respect to total energy sales in industrial and hotel consumer categories; i.e. the total energy demand in industrial sector has gone down from 32% in 2013 to 30.6% in year 2015. This may be due to the energy conservation options adopted by industries during the period 2013-2015.

### Research Questions and Objectives

Research questions and objectives are:

- What is the influence of incentive schemes to change the consumer behavior intention on energy conservation in industrial sector in Sri Lanka?
- What is the influence of tariff regimes to change the consumer

behavior intention on energy conservation in industrial sector in Sri Lanka?

- How technological innovations influence on consumer behavior intention on energy conservation in industrial sector in Sri Lanka?
- What is the mediating effect of consumer behavior intention on energy conservation with respect to incentive schemes, different tariff regimes and technological innovations?
- How to derive appropriate incentive schemes and regulatory framework to match tariff regime and prevailing technology in Sri Lanka?

Based on the above research questions the following research objectives have been derived.

- To explore the mediating effect of consumer behavior intention on energy conservation over the different incentive schemes available in industrial sector in Sri Lanka.

- To explore the mediating effect of consumer behavior intention on energy conservation over the different tariff regimes available in industrial sector in Sri Lanka.
- To explore the mediating effect of consumer behavior intention on energy conservation over the different technological innovations available in industrial sector in Sri Lanka.
- To explore the behavior of new model with varying parameters of incentives, tariff regimes and technological innovations towards energy conservation in Sri Lanka.
- To develop a model to match appropriate incentive mechanisms, policy guidelines with available technologies and tariff regimes on energy conservation in industrial sector in Sri Lanka.

## Literature Review

Several studies are available on savings of energy in different sectors with different aspects. In this research, the mediating effect of consumer behavior intention on incentive schemes, tariff regimes and technology improvements towards energy savings is studied. Technology changing aspects involve use of efficient equipment at an additional cost whereas tariff regimes and incentive schemes involve energy conservation by way of reducing wastage or avoiding unnecessary usage. Therefore, different mechanisms are explored to find out the theoretical background on this study and thereby, formulate a sound scientific model for describing the concepts with respect to electricity conservation. In order to explore the existing body of knowledge, literature review is performed and thereby the conceptual model is developed.

Many studies have shown that various types of incentives are prevailing to motivate consumers to conserve energy around the world. Among them, investment subsidies, loan schemes, tax credits and emission allowances are the most popular ones. More specific studies explain that the available mandatory regulations and incentive schemes must greatly be cost effective in order them to be implemented by the firms [7]. Specially, tax credits, subsidies and loan schemes must greatly be cost effective and low burden to consumers or the firms.

Some researchers have explained that although many incentive schemes have been introduced all over the world, most of them have not been studied scientifically and comprehensively [13], [14] and [15]. However, it rarely defined the specific design or mechanisms as to how the selected solution will penetrate in to the market. Ultimately, many instruments have failed prematurely and hence, rigorous scientific study needs to be carried out on all those aspects. Many researchers have pointed out that the incentive design is composed of six components; Efficiency criteria, size of incentive, incentive recipients, form of incentive, eligibility requirements and whether program has exit criteria or continuing with recycling mechanism [16].

Some studies showed that incentives work properly than stringent regulations and therefore, governments need to follow effective incentive mechanisms rather than strict regulations to change the behavior of public and furthermore, tariff regimes influence the consumer to conserve energy with different price signals [3].

There are three prominent mechanisms to make behavioral changes in electricity consumers that could be achieved by means of incentive schemes as per [1]. One is the monetary rewards. The second is information feedback to consumers about their usage pattern and third is information receiving from the consumers about the conservation [1]. It has been reported that institutional guidance on energy conservation means of educational, informational and financial tactics may not work as expected unless the continuous monitoring by the authorities [13].

Technology development has increased the energy efficiency in electrical and electronic devices. However, there is less motivation to introduce energy efficient equipment, which is cost effective to consumers and as a result, energy conservation policies need to close this gap towards the sustainable saving of energy at the user end. The barriers and difficulties prevailing against the consumer's decision on investment on energy efficient equipment and changing mindset to use them have been researched by [11]. They reported that lack of financial commitment, lack of information on energy saving equipment, lack of low cost equipment in the market,

lack of technical expertise and difference in financial gain between landlord and renters may have moved the consumers away from the conservation attempts. Furthermore, [13] explains that higher up-front cost of energy saving equipment may discourage electricity consumers on electricity conservation. [17], suggests that technological innovation alone is insufficient to reduce energy consumption and need change of energy related behavior too. This brief literature survey proved that development of a mechanism to change the behavior on energy usage has the empirical novelty and hence knowledge gap prevails in the body of science.

## Methodology and Conceptual Model

Since the literature supports the three major components as the determinants of energy conservation which has real knowledge gap, the conceptual model in figure 2 is developed based on the findings from the existing body of knowledge. Integration of TPB and TAM models to explain the behavior of consumers towards energy conservation is depicted in the conceptual model as given in figure 2.

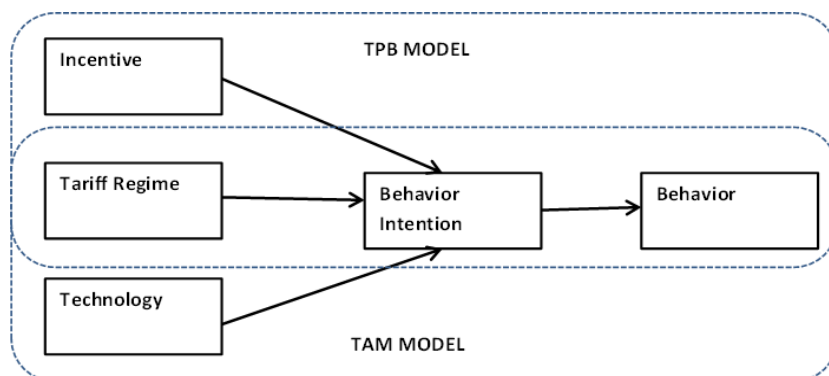


Figure 2: Research Design

In this research, positivism, realism and interpretivism are used to study electricity consumer behavior with respect to incentive schemes, tariff regimes and technological innovations. Data collected by using structured questionnaire survey and series of face to face interviews. Basically, this research is composed of both inductive as well as deductive approaches and hence it is of a mixed method. The research strategy adopted in this study is that it is started from exploratory method to build up a model to integrate consumer behaviors on different aspects and thereby to measure the performance of the instrument on explanatory means. The mediating effect of consumer behavior intention on energy conservation is formulated with the principle of observations based on the integrated TPB and TAM models through an inductive research process. Finally, the new model

is re-evaluated with collected user observations and thereby the entire research becomes a mixed method. Sample size is determined by the conceptual model and the scientific tool which is being used to analyze the hypothesized model. As per the AMOS software requirements [19], the sample size should be large enough to get at least 10 respondents for one parameter to be estimated in the model. In this context, SEM techniques incorporated with AMOS 25<sup>th</sup> version software is used to analyze the hypothesized model and accordingly, sample size is determined by the number of parameters in the model. The size of the sample is re-assured with formula which has been accepted by many scholars in recent literature [20]. In this research, sample size is found to be 400 numbers of industrial consumers which assures the 40 independent variables as identified in the conceptual model.

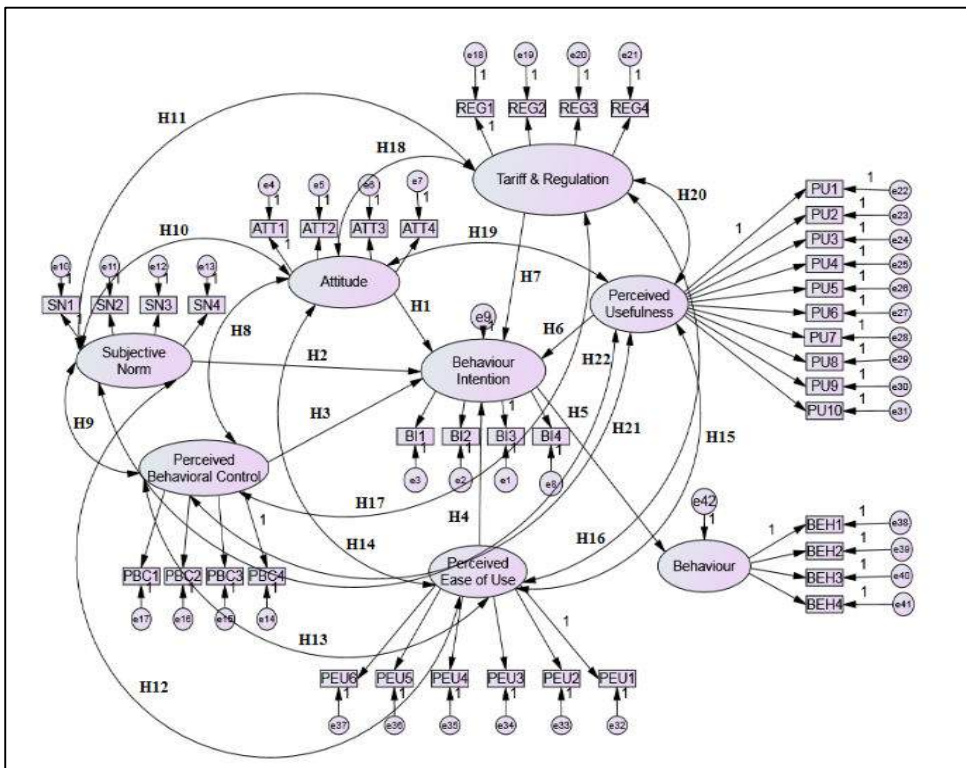


Figure 3: Conceptual model Prepared for SEM

The conceptual model of this study is focused on three independent variables namely incentives, tariff regimes and new technology products and processes while consumer behavior intention on energy conservation act as mediating variable towards the dependent variable which has been identified as energy conservation behavior. However, each variable has unique observable and un-observable variables as given in the Figure 3. Using the TPB and TAM models, factors affecting the consumer behavior intention on energy conservation are measured using Structural Equation Modelling (SEM) techniques available in 25<sup>th</sup> Version of AMOS Software. 27 hypotheses are identified as given in figure 3. All those are tested with the help of Structural Equation Modeling technique available in 25<sup>th</sup> version of AMOS software.

### Data Analysis and Interpretation of the Results

The data collected from 400 consumers in industrial segment by way of structured questionnaire were tabulated in SPSS software and analyzed with AMOS package of 25<sup>th</sup> version. In order to test the reliability of collected data, Cronbach's alpha, Construct reliability, and Average Variance Extracted (Composite Reliability) were measured. It is found that Cronbach's Alpha is above 0.7 and according to [21], [22], reliability prevails in the data set. Further, the Average Variance Extracted is greater than the correlations squared of the two constructs in all cases and hence discriminant validity prevails and multicollinearity absents. Linearity of data set is observed by comparing the means of independent variables using

SPSS software and found that p value is greater than 0.05 and hence linearity prevails. Further Q-Q plot and P-P plot show the straight-line behavior of variables and hence linearity prevails in the collected dataset. Normal distribution of collected data set is observed using Z values of Kurtosis and Skewness and found that both values are within -1.96 and +1.96 and hence normality prevails. Further, Shapiro-Wilk Test and Kolmogorov-Smirnov Test shows p value greater than 0.05 and hence normality prevails in the dataset. All the steps involve in SEM techniques such as Confirmatory Factor Analysis (CFA), measurement analysis, discriminant analysis and direct indirect relationship analysis were carried out. All the construct show relatively good fit as illustrated by CMIN/D.f<5 (i.e. 2.451), p Value < 0.05 (i.e. 0.000), GFI >0.8 (i.e.0.817), RMSEA<0.08 (i.e. 0.06) Chi-Square value at 1795 (small is better) and therefore, proposed model converges and gives new instrument for explaining the behavior of three independent variables which comprise of 40 observable variables, one mediating variable and several dependent variables on consumers behavior intention towards energy conservation. It is also found that incentives has positive influence over conservation intention as  $\beta = 0.603$ , CR = 12.32 and p Value< 0.05. Further, tariff regime has negative impact on perceived usefulness of prevailing technologies as  $\beta = -(0.042)$ , CR =  $-(1.248)$  and p Value > 0.05 (i.e. p Value = 0.212). Therefore, it is understood that existing tariff regime should be re-adjusted in such a way that it will encourage consumers to use new technologies on energy conservation actions by way of proper incentive mechanisms.

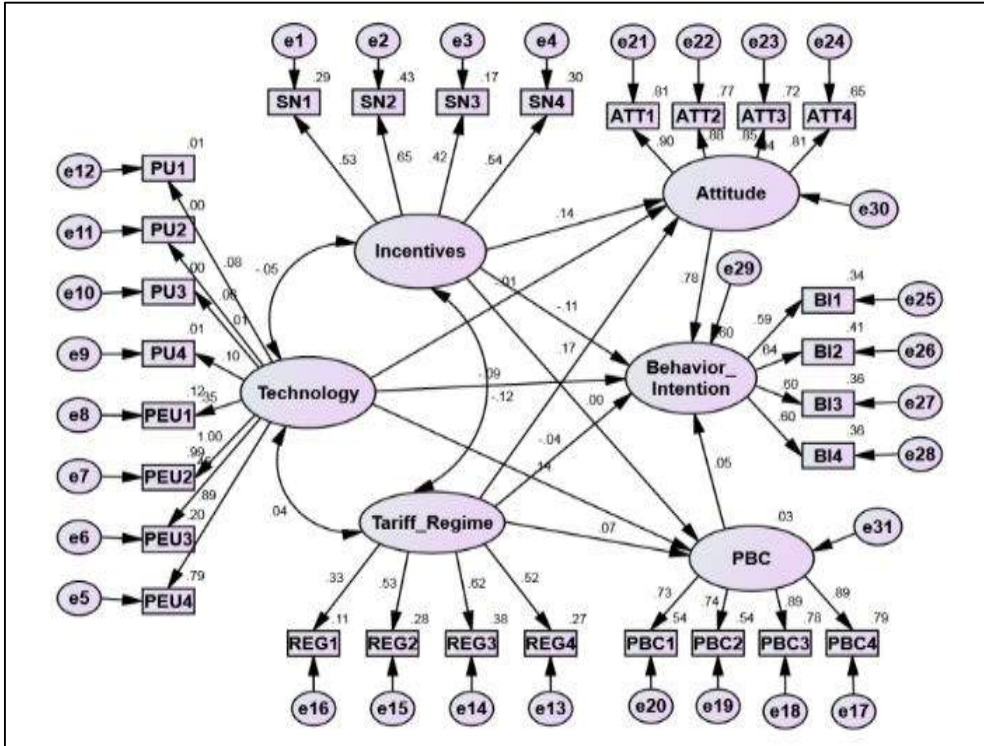


Figure 4: Standardized AMOS Output

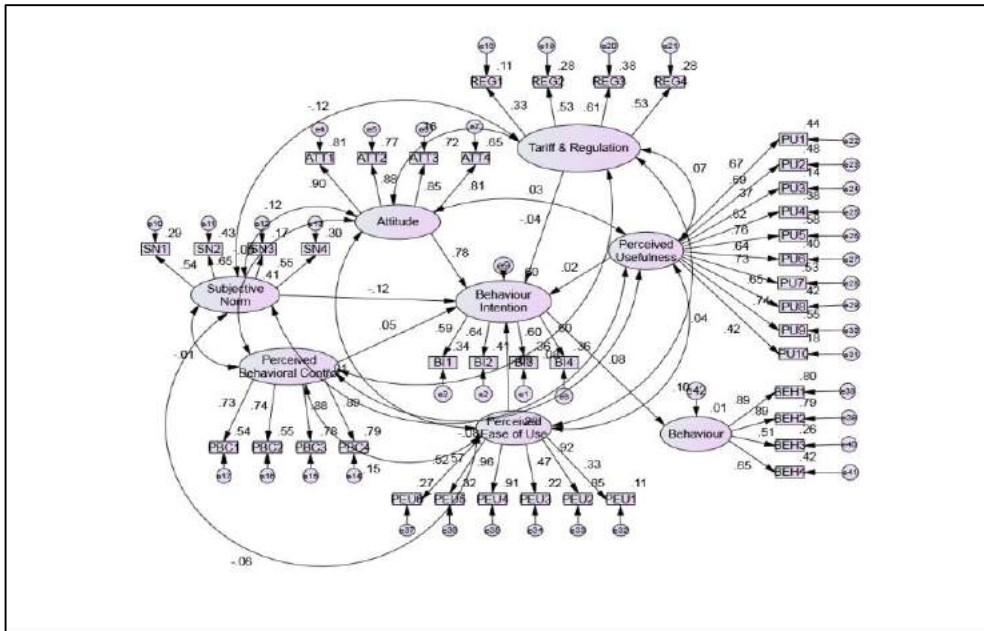


Figure 5: Re-Specified Model

### **Standardized AMOS Output and Re-specified Model**

Re-specified model given in the Figure 5 successfully converged with AMOS requirements and thereby considered as the scientific instrument which can explain the behavior of dependent variables with respect to independent variables. With the fixed values of different components, behavior of other components can be observed. Further the important parameters of the population could be obtained with the use of this instrument. The results found that consumer behavior intention mediates the consumer's attitude, available incentives, tariff system over the energy conservation. However, it was found that perceived ease of use of technology and perceived usefulness of available technologies are poorly mediated by the consumer intention on energy conservation.

With the re-specified model, different values of tariff regime and technology input were calculated at a given incentive level and thereby observed the behavior of the instruments at user defined operating points. This is the new finding of this research and same can be used to evaluate the future incentive mechanisms intend to be introduced by electricity utilities.

### **Conclusions, Policy Recommendations and Agenda for Future Research**

CEB introduces different kinds of incentives to encourage customers to conserve electricity in time to time. However, many of those have become a white elephant in the long run. This is because of the unavailability of proper scientific model and instruments to

measure the behavior of individual components with respect to the given incentive mechanism. Therefore, the developed new model and instruments by this research fill the knowledge gap prevailing in the system and definitely it will add new knowledge for the body of the science. By using this model recently failed solar net metering and net plus mechanisms can be re-evaluated and the convergence values could be obtained. At different level of incentives converging points of tariff system and the technology input can be predicted and thereby future incentive mechanisms could be evaluated in advance before encountered the premature failures.

Especially, the tariff system should be introduced in such a way that it would encourage the energy conservation intention on consumers mindset while offering different incentives which will combine with the available energy saving new technologies. End of the day, consumer may feel free to conserve energy while adhering to the available incentive schemes rather than worrying about the heavy burden created by the tariff system. This kind of new model support utilities to understand how these parameters could be integrated to reach a converging solution.

The policy makers could get use of this new model to decide different values of incentive levels which would balance the available technology and the tariff system. It is observed that introduction of 10% incentive level over the total energy usage will encourage the consumers to conserve energy which is equivalent to the level which could be achieved by only enhancing tariff system by 57%. This would be a very important finding and a parameter while designing future tariff systems.

In order to use the proposed new model, CEB shall simply apply the intended incentive level with respect to expected saving from the energy conservation. For example, if CEB introduces 10% incentive for industrial consumers on the intention of changing behavior, the same result can only be achieved by changing the tariff system by 57%. The changing tariff by 57% is not a viable solution especially on industrial consumers and hence introduction of 10% incentive is the best solution for changing the consumer behavior on energy conservation. Similar situation prevails with respect to the technology inputs as well.

This research covers only the industrial segment of the Western Province (Colombo, Kalutara and Gampaha districts) in the country. This can be extended to commercial and domestic segments as well. Further, the developed model will explain how the consumer behavior can be changed towards the energy conservation aspects by varying incentives, tariff regimes and new technology products and processes. However, the economics aspects too should be incorporated to the model which is identified as the main limitation of this study and reserve for future research.

## References

- [1] Ceylon Electricity Board, Annual Reports 2013-2015.
- [2] Ceylon Electricity Board, Statistical Digests ,2013-2017.
- [3] Ajzen, I. (1991). The theory of planned behavior. *Organizational Behavior and Human Decision Processes*, 50(2), 179-211.
- [4] Rudin, A. (2000), Let's Stop Wasting Energy on Efficiency Programs as Energy Conservation as a Noble Goal, *Energy & Environment*. 11(5), 539-551.
- [5] Dasanayaka, S., Jayaratne, W. (2012), Economic Feasibility of Carbon Emission Reduction in Electricity Generation in Sri Lanka, *International Journal of Global Warming*, 4((2):148-172).
- [6] Geller, H. 2003. *Energy Revolution: Policies for a Sustainable Future*. Washington, DC: Island Press.
- [7] Goulder, Lawrence H, and Robert N Stavins. "Challenges from State-Federal Interactions in Us Climate Change Policy." *American Economic Review* 101 (2011): 253–257. Publisher's Version
- [8] Anthoff, D. and Hahn, R. (2010), "Government failure and market failure: on the inefficiency of environmental and energy policy", *Oxford Review of Economic Policy*, 26(2), pp. 197-224.
- [9] Gillingham K, Harding M and Rapson D 2012 Split incentives and household energy consumption *Energy J.* 33 37–62.
- [10] Prindle, W., & Angel, S. (2010). Customer Incentives for Energy Efficiency Through Program Offerings. *National Action Plan for Energy Efficiency*, (February). Retrieved from [www.epa.gov/eeactionplan](http://www.epa.gov/eeactionplan)
- [11] Herring, R. J. (1987). Sri Lanka Economic Liberalisation Policies International Pressures, Constraints and Supports. *Economic and Political Weekly*, 22(8), 325–333.
- [12] Harland, P. and Staats, H. and Wilke, H., 2006. Explaining Pro environmental intention and Behavior: *Journal of Applied Social Psychology* Vol.29 (12), p.2505-2528.
- [13] Eto, E. Vine, L. Shown, R. Sonnenblick, C. Payne the total cost and measured performance of utility-sponsored energy efficiency programs *Energy J.*, 17 (1) (1996), pp. 31-51.
- [14] IEA (2004). A geographically and socio-economically disaggregated local household consumption model for the UK2008. *Journal of Cleaner Production* 870-880.
- [15] Attari S, D. M. (2010). Public perceptions of energy consumption and savings. *PNAS*, pp. 16054-9.
- [16] Goulder, Lawrence H., Ian W. H. Parry, Roberton C. Williams III, and Dallas Burtraw. 1999. The cost-effectiveness of alternative instruments for environmental protection in a second-best setting. *Journal of Public Economics* 72(3): 329–60.
- [17] Rosenberg and Hoefgen, 2009 Rosenberg, M., Hoefgen, L., 2009. Market Effects and Market Transformation: Their Role in Energy



Efficiency Program Design and Evaluation. California Institute for Energy and Environment. March.

[18] Abrahamse, W.; Steg, L. Factors related to household energy use and intention to reduce it: The role of psychological and socio-demographic variables. *Hum. Ecol. Rev.* 2011,18, 30–40.

[19] Arbuckle, J. (1997), *Amos Users' Guide Version 3.6*, Chicago IL: Small waters Corporation.

[20] Cochran, W.G. (1977) *Sampling Techniques* (3rd ed.) New York: John Wiley & Sons.

[21] Nunnally, J.C. *Introduction to Psychological Measurement*. New York: McGraw-Hill; 1970.

[22] Sentosa, I., Ming, W.C., Soebyakto, B.B., Nik Mat, N.K. (2012). A Structural Equation Modeling of Internet Banking Usage in Malaysia. *Journal of Arts, Science and Commerce* Vol.III Issue 1, pp.75-86.

# Cost Benefit Analysis of Using Battery Energy Storage Systems in Distribution Systems

Angela De Silva<sup>#1</sup>, Udayakumar K.A.C.\*<sup>2</sup>, Dinesh Dissanayake<sup>#3</sup>

*#Department of Electrical and Computer Engineering, The Open University of Sri Lanka,  
Nawala, Nugegoda, Sri Lanka, Ceylon Electricity Board*

<sup>1</sup> angeladilrukshi@gmail.com

<sup>3</sup> eeikaduwela@gmail.com

*\*Department of Electrical and Computer Engineering, The Open University of Sri Lanka,  
Nawala, Nugegoda, Sri Lanka*

<sup>2</sup> kauda@ousl.lk

## Abstract

This work analyzes the cost benefit using Battery Energy Storage Systems (BESS) for peak shaving in distribution systems. Other than the use of BESS for peak shaving, which is the major benefit of use, utilization of BESS for providing emergency power to the customers also has been discussed. Different types of batteries have been analyzed and most suitable BESS for grid application has been presented. A mathematical formula has been presented to determine cost for usage of BESS depending on the capacity of batteries. This work also suggests to provide emergency power from the BESS to the selected customers during the power interruptions. A formula has been presented to calculate this additional cost benefit by providing the emergency power. This work also proposes to allocate BESS at the proximity of the solar PV customers to energize solar PV during the power interruption in LV side. The net cost benefit due to utilization of BESS has been presented as a mathematical formula. The cost benefit of the usage of BESS has been calculated for one of the selected distribution systems in a semi-urban area and the results have been presented herein.

**Keywords:** Battery energy storage systems, peak shaving, emergency power

## Introduction

Instantaneous generation – demand balance has been one of the major constraints in electrical systems for many years. This is due to the fact that electrical energy could not be stored in large amount. Reduction of peak power, which usually last for few hours per day, is one of the objectives of utility organizations to reduce installed capacity. At present Sri Lankan power system is facing difficulties to meet peak demand with the available installed capacity, especially during dry season when major hydro power plants do not deliver maximum power to the national grid. Use of energy storage device to store energy during off-peak hours and dispatch it during peak hours can be a part of solution for this problem.

Pumped storage plant, which is a location specific plant, was the only the option for storage of electrical energy till recent past. However, with the development of battery technology, the storage of electrical energy at the distribution level becomes possible. The idea is to consume the electrical energy from the grid to charge the batteries during the off-peak time and deliver the energy stored in batteries during the peak hours enabling dispatch less energy from the grid. From the economical point of view, utility companies are benefitted from this because the cost of energy during the peak hours is greater than off-peak hours. The reduction of peak load in a system results reduction of installed capacity, which means the reduction of unit cost of generation.

Utilization of Battery Energy Storage system (BESS) comprising series parallel connected batteries, converters, transformer and other accessories, involves capital investment and

periodical maintenance cost [1]. Therefore, the optimum capacity of BESS in electrical systems need to be properly analyzed considering cost for batteries and saving due to reduction of peak energy.

At present electricity becomes an essential requirement for almost all the consumers and expect uninterrupted supply from the utility. Therefore, utility organizations search the possibilities of providing part of the electricity during power interruptions to selected consumers. This is known as emergency power. BESS that have been installed in a system for the purpose of peak shaving can provide additional benefit by supplying part of the power during the power interruption. In addition to this, solar PV customers may energize their solar PV panels using BESS during power outages. Utility organizations can gain additional financial benefit by providing this emergency power utilizing the available BESS.

Only limited number of studies have been carried out on usage of BESS in distribution networks in Sri Lanka. Power system of Sri Lanka may face shortage of peak power in near future due to delay in construction of new power plants to meet future demand. Therefore, utilization of BESS for peak leveling can be one of the possible solutions to reduce the peak power in near future.

## Operation of BESS in Electrical Systems

Grid intergraded BESS consists of batteries, converters, and a step-up transformer. Principle diagram of BESS is shown in figure 1 [1].

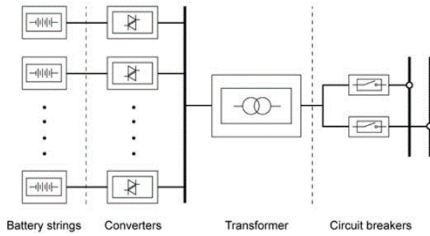


Figure 1: Principal diagram of the BESS [1]

BESS comprises large number of series-parallel connected batteries and therefore considerable space is occupied by BESS. Specific energy density (kWh/kg), capital cost, life cycle, depth of discharge are key parameters that decide the type of battery suitable for electrical systems. Different types of batteries are commercially available and lead acid battery is being used in many of electrical system applications [2].

### Methodology

This study analyses economic viability of battery capacity for LV distribution system. The cost incurred due to installation and maintenance of BESS and money saving by purchasing less amount of power from the grid during peak hour has been compared to determine suitable capacity of BESS.

### BESS capacity determination

Capacity of BESS has been determined to get the maximum economic benefit out of its use. Since part of the peak power is met by discharging BESS, less amount of peak power is purchased from the grid. Therefore, there is a money saving ( $C_{saving}$ ) for the utility organization. However, utility organization requires to bare additional cost for Installation, operation and maintenance of BESS ( $C_{BESS}$ ). Utilization of BESS for peak shaving in distribution systems is

economically justifiable when the saving by peak leveling ( $C_{saving}$ ) is greater than cost for BESS ( $C_{BESS}$ ) over the lifetime of BESS.

This cost benefit ( $C_{benefit}$ ) over the lifetime of BESS (T) is calculated by using equation (1)

$$C_{benefit}|_T = C_{saving}|_T - C_{BESS}|_T \quad (1)$$

Both cost for BESS and saving due to peak shaving are function of reduction of peak power ( $P_{pwr}$ ) as shown in figure 2.

The energy of peak power reduction is equal to the depth of discharge of BESS. Generally, depth of discharge is 70% of BESS capacity. BESS capacity has been calculated using equation (2).

$$B_{cap} = (P_{pwr} \cdot \Delta T) / 0.7 \quad (2)$$

Where,

- $B_{cap}$  = BESS capacity (kWh)
- $P_{pwr}$  = Peak shaving power (kW)
- $\Delta T$  = Duration of peak power (hrs)

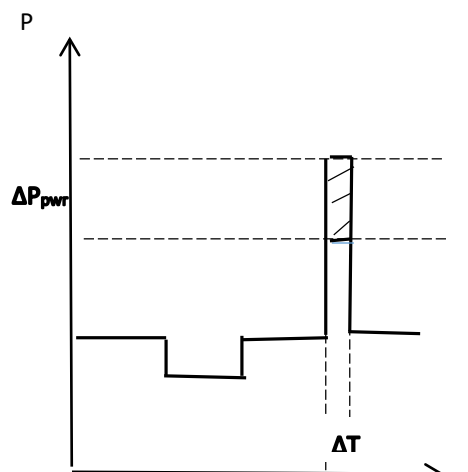


Figure 2: Reduction of peak power [1]

In this work for different values of peak shaving power, BESS capacity ( $B_{cap}$ ) has been calculated using equation (2) and the cost benefit of use of BESS has been calculated using equation (1). The most suitable battery capacity has been determined when  $C_{benefit}$  is maximum.

### Cost of BESS

BESS consist of batteries, converter, transformer and other associated equipment such as breakers. Capital cost of BESS consists of cost for batteries, converter, transformer and other associated equipment. Battery rating is calculated based on the battery capacity ( $B_{cap}$ ) of the equation (2) considering the number of series parallel units. Rating of transformer and converter depends on the capacity of batteries and therefore the cost of those equipment is expressed as a percentage of battery cost. Other than capital investment, battery needs periodical maintenance and operation and maintenance cost is given as percentage of battery power [2],[4]. The cost for BESS is calculated using equation (3).

$$C_{BESS}|_T = C_1 \cdot B_{rated} + C_{op} \cdot P_{rated} \cdot T + C_1 B_{rated} \cdot k/100 \quad (3)$$

Where,

- $C_{BESS}$  = Total cost for BESS (LKR)
- $B_{rated}$  = Rated capacity of the batteries (kWh)
- $P_{rated}$  = Battery power (kW)
- $C_1$  = Capital Cost of Batteries (LKR/kWh)
- $C_{op}$  = Operation and maintenance cost per annum (LKR/ kW)
- $T$  = Battery life time (number of years)
- $k$  = Percentage of cost of associated equipment

### Saving by peak power leveling

In electrical systems the cost of energy depends on the time of use. The cost of energy during peak hours is expensive and off-peak hours' energy is cheaper. Therefore, reduction of purchase of peak power (by discharging the BESS) results the saving. However, there is an additional cost for purchasing energy to charge the battery during off-peak time. The saving over the life time of battery can be calculated using equation (3).

$$C_{saving}|_T = [P_{pwr} \cdot (\Delta - \Delta T_{discharge} C_{offpeak})] \cdot T \cdot 365 \quad (3)$$

Where,

- $C_{saving}|_T$  = Saving due to peak Leveling over the lifetime of BESS (LKR)
- $P_{pwr}$  = The battery discharges power (kW)
- $\Delta T$  = Discharge duration (hrs)
- $\Delta T_{charge}$  = Charge duration (hrs)
- $C_{peak}$  = Unit energy cost during peak hours (LKR/kWh)
- $C_{offpeak}$  = Unit energy cost during off-peak hours (LKR/kWh)

After determining both cost of BESS and saving by peak leveling over the life time of BESS, net saving has been calculated using equation (1). This has been repeated for different amount of peak power shaving.

### Additional cost benefit by providing emergency power

#### Emergency power during the interruption at MV side

Once the capacity of BESS has been decided based on the financial benefit by peak shaving, this BESS can be utilized to supply part of the energy to the selected

customers of the system during power interruptions. During the power interruptions at MV side, LV network remains healthy and the BESS installed at LV side can dispatch energy to interested (selected) customers at higher cost. This is known as emergency power [5]. The emergency power is a fixed value which is sufficient for basic energy needs of the customer. There should be a mechanism to control the power from the distribution transformer station to the customers who purchase this emergency power. Income of the utility company by selling emergency power is calculated as ( $C_{emg\ total(MV)}$ ) shown in equation (4).

$$C_{emg\ total(MV)} = C_{emg} \cdot n_e \cdot P_{emg\ avg} \cdot t_{fault(MV)} \quad (4)$$

Where,

- $C_{emg\ total(MV)}$  = The income of the utility company by selling emergency power during power interruption in MV faults (LKR)
- $C_{emg}$  = Charge for emergency power (LKR/kWh)
- $n_e$  = Number of customers who wish to get emergency power
- $P_{emg\ avg}$  = Average emergency power consumed by a customer (kW)
- $t_{fault(MV)}$  = Average MV fault duration over the life time of BESS (h)

In this work emergency power per customer is taken as 3 kW estimating that this is sufficient to provide power for number of lighting loads, TV and a water pump. It is assumed that the domestic consumers ( $n_e$ ) whose monthly bill is greater than 150 kWh will purchase this

emergency power. Non-domestic consumers have been excluded assuming that they have standby supply in case of power failure. The charge for emergency ( $C_{emg}$ ) power is taken as three times of the peak hour charge.

### Energizing the solar PV during power outages at LV network

Many LV distribution systems do have grid connected, customer based solar PV panels. However, these solar PV panels do not provide power to the consumer when the system is not live. This work proposes energize these solar PV panels during outages with the help of BESS. This is possible only when the BESS are located at the proximity of the solar PV customer. This is possible only for the day time when solar PV generate electricity. The fault can be either day time or night time. Therefore this is possible only for the power outages during day time.

Consumers do not get the electricity during schedule maintenance work of the LV network. During schedule maintenance work of the LV network the consumer based BESS can provide voltage to the solar PV to generate electricity. The income of the utility company for energizing solar PV consumers ( $C_{LV}$ ) can be calculated using equation (6).

$$C_{LV} = C_f \cdot (t_{mnt} \cdot T + t_{LV\ fault}) \quad (5)$$

Where,

- $C_f$  = Fixed cost for voltage supply during LV maintenance period (LKR)
- $t_{mnt}$  = Total schedule maintenance duration per year (h)
- $t_{LV\ fault}$  = Average daytime LV faults Over the BESS lifetime (h)

The total financial benefit is calculated using equation (6)

$$\begin{aligned}
 \text{Net benefit} = & C_{\text{benefit}} + \\
 & C_{\text{emg total(MV)}} + \\
 & C_{\text{emg total(LV)}} + \\
 & C_{\text{LV mnt}} \quad (6)
 \end{aligned}$$

The methods of allocation of BESS at the proximity of customer premises were presented in number of research works [4].

## Results and Discussion

### Case study

Case study for this method was carried out for Kalalgoda LV distribution system. The distribution system is fed through 160 kVA, 33 kV/ 400 V three-phase transformer. The entire network consists of six hundred thirty nine (639) number of consumers and most of them (98%) are domestic consumers.

### Measurement and data collection

Load measurement has been taken at the transformer feeder point at every 15 minutes for twenty four hours of a weekday.

Number of customers for different range of monthly electricity bill is given in table 1. MV and LV fault duration are given in table 2.

|   | Range of units<br>(kWh) | No. of<br>consumers |
|---|-------------------------|---------------------|
| 1 | 0 - 30                  | 102                 |
| 2 | 31 - 60                 | 79                  |
| 3 | 61 - 90                 | 136                 |
| 4 | 91 - 120                | 110                 |
| 5 | 121 - 180               | 128                 |
| 6 | 181 - 280               | 60                  |
| 7 | Non domestic            | 24                  |

Table 1: Consumer data

| Type of<br>fault         | Average<br>duration<br>per fault | No. of<br>faults<br>per year |
|--------------------------|----------------------------------|------------------------------|
| MV fault                 | 6 hrs and<br>15 mins             | 3                            |
| LV fault                 | 2 hrs and<br>30 mins             | 96                           |
| Scheduled<br>maintenance | 8 hrs                            | 24                           |

Table 2: Details of LV and MV faults

### Cost for BESS

Cost and other details of lead acid batteries are given in table 3 [2].

**Cost for energy**

The cost for energy during peak hour and off-peak hours are taken as LKR 22.50 per kWh and LKR 8.80 per kWh [5]. Cost for emergency power is three times of the cost of energy and equal to LKR 67.50 per kWh.

**Load Curve**

Stepwise load curve (assuming that the load is constant during one hour period) and constant power factor is shown in figure 3. Evening and morning peaks are 161.71 kW with duration of 4 hours and 114.57 kW with 1 hour duration (respectively).

Table 3: Details of BESD

| Parameter                      | Value                                |
|--------------------------------|--------------------------------------|
| Capital cost                   | LKR 9000/kWh                         |
| Operation and maintenance cost | LKR 750/kWh-year                     |
| Cost for other accessories     | 15% of the capital cost of batteries |
| Battery lifetime               | 5 years                              |
| Unit capacity                  | 2.4kWh (200 Ah x 12 V)               |

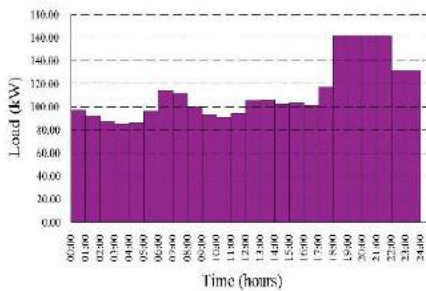


Figure 3: Daily Load Curve of distribution system

The cost benefits by peak shaving using BESS has been summarized in table 3. The results show that the cost benefit is high when more power is delivered by the BESS during the peak hour time. Load curves with improved load factor after installing BESS are illustrated in figures 4-6. Cost variation and saving with BESS capacity is shown in figure 8.

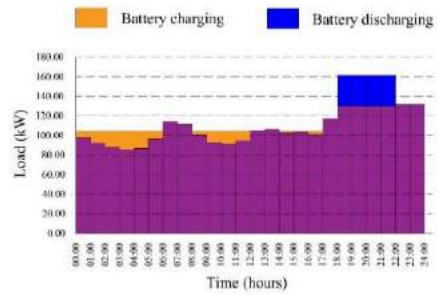


Figure 4: Improved load curve with 182.4 kWh batteries (76 units)

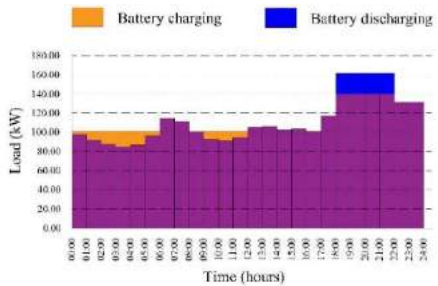


Figure 5: Improved load curve with 124.8 kWh batteries (52 units)

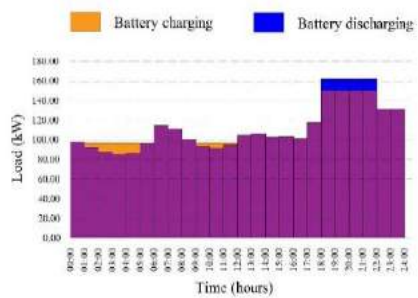


Figure 6: Improved load curve with 67.2 kWh batteries (28 units)



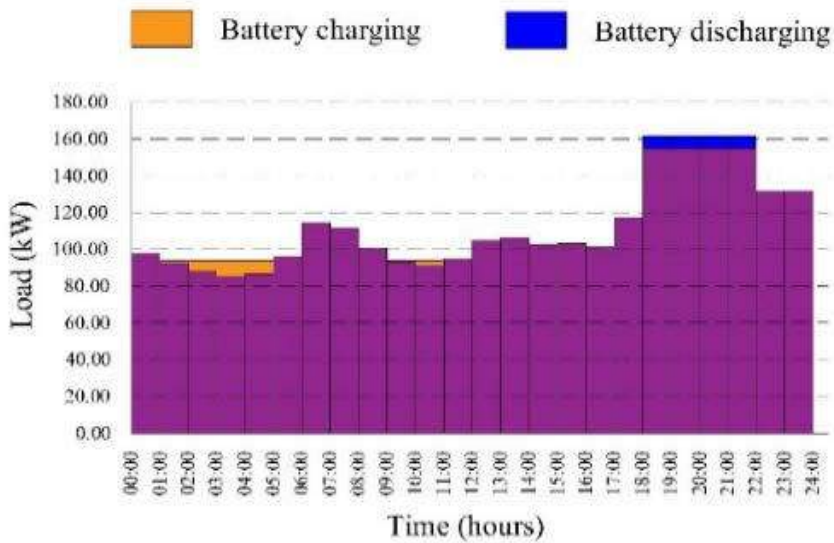


Figure 7: Improved load curve with 38.4 kWh batteries (16 units)

Table 4: Table of results

| $P_{shave}$<br>(kW) | $B_{pwr}$<br>(kW) | No. of<br>battery<br>units | Rated<br>capacity<br>(kWh) | Total cost<br>$C_{total}$ (LKR) | Net saving<br>$C_{net}$ (LKR) | $C_{benefit}$<br>(LKR) | Load<br>factor |
|---------------------|-------------------|----------------------------|----------------------------|---------------------------------|-------------------------------|------------------------|----------------|
| 130                 | 31.71             | 76                         | 182.40                     | 2,571,840.00                    | 3,171,317.10                  | 599,477.10             | 85.44%         |
| 140                 | 21.71             | 52                         | 124.80                     | 1,759,680.00                    | 2,171,217.10                  | 411,537.10             | 80.26%         |
| 150                 | 11.71             | 28                         | 67.20                      | 947,520.00                      | 1,171,117.10                  | 223,597.10             | 74.91%         |
| 155                 | 6.71              | 16                         | 38.40                      | 541,440.00                      | 671,067.10                    | 129,627.10             | 72.49%         |

The suitable capacity of BESS for this system is taken as 240 kWh. Additional benefit by providing emergency power to the consumers have been calculated for this capacity. The income of the utility

company by selling emergency power during MV faults is LKR 759,375.00.

The income of the utility company by energizing solar PV during LV faults is LKR 4,131,000.00.

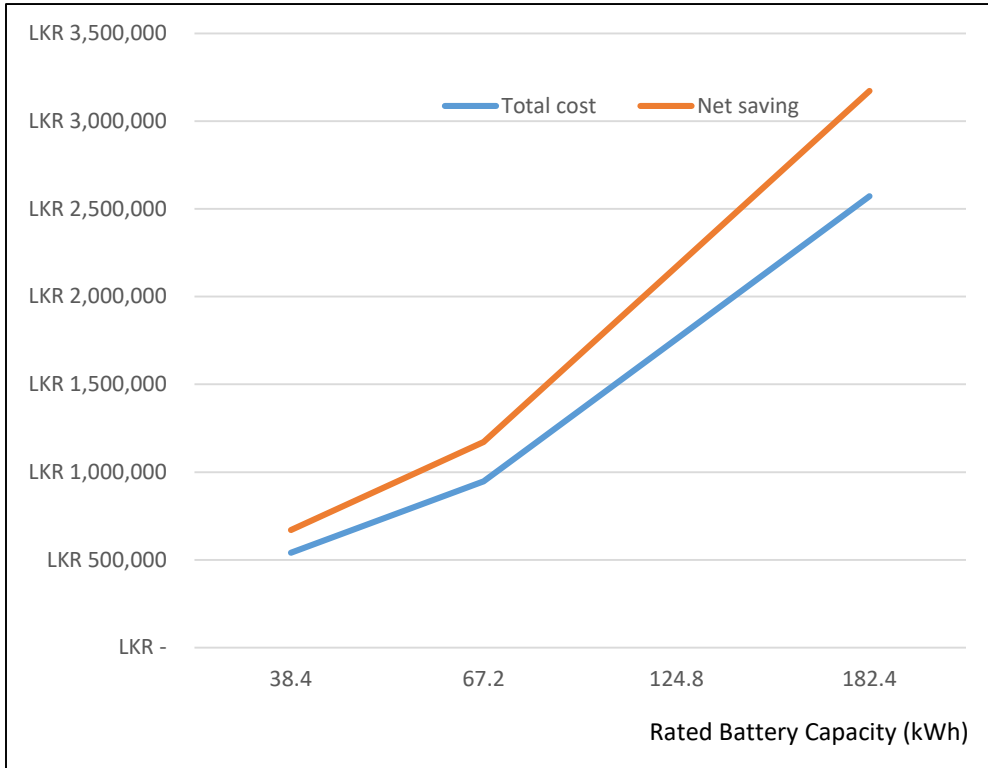


Figure 8: The graph of Total cost and Net saving versus Rated battery capacity.

The income of the utility company by energizing solar PV during schedule maintenance work in LV network is LKR 1,101,600.00.

Total financial benefit is LKR 6,779,392.10.

**Conclusion**

The results of this work show that there is considerable financial benefit of use of BESS in the system. BESS also has been used to provide emergency power to the part of the customers in the system. Since the country is facing energy crisis, BESS helps to reduce the peak power. In long time respective use of BESS reduces the total installed capacity of the system.

The project did not pay much attention on technical feasibility of realization of some of the suggestions. The project proposed that the batteries are to be allocated near the PV solar customers so that batteries can provide the supply during LV outages. One of the main issues is where these batteries are located. This depends on the area required to locate the batteries. On the other hand there should be a strong controlling mechanism between batteries, substation and loads to provide emergency power during outages. These two critical issues remain to be addressed in future projects.

In real scenario, it is expected that the consumers who are willing to get the emergency power need to pay registration fee. Maximum cost benefit by selling emergency power can be

achieved by selling emergency power during the power cut at different cost on demand. This is in contrary to have a fixed registration fee for all the consumers. In economics this is known as “consumer surplus”. In this project this cost benefit analysis has not been carried out. However, it should be mentioned that in real scenario the cost benefit should be increased.

In summary, the use of BEES in distribution systems, which is not a new concept, is timely requirement of many of distributions systems of the country. The reduction of peak power with the help of BESS will reduce the total installed capacity of the entire power systems of the country.

### **Acknowledgement**

Authors wish to gratefully acknowledge Dr. Narendra De Silva, and staff of the Ceylon Electricity Board for their support at various stages of this work.

### **References**

- [1] Alexandre Oudalov, Rachid Cherkaoui, Antoine Beguin. Sizing and Optimal Operation of Battery Energy Storage System for Peak Shaving Application, 2007, IEEE Lausanne Power Tech, 1-5 July 2007, Lausanne, Switzerland
- [2] K.C. Divya, Jacob Ostergaard, 11th December 2008. Battery energy storage technology for power systems, Electrical Power Systems Research, vol.79, Issue 4, April 2009, pp 511-520
- [3] Wei-Fu Su, Shyh-Jier Huang, Chin-E Lin, February 2001. Economic Analysis for Demand-Side Hybrid Photovoltaic and Battery Energy Storage System, Thirty Forth IAS annual meeting, 3-7 Oct 1999, Phoenix,AZ,USA
- [4] P.Bakos, Life Cycle Cost Analysis for Utility Scale Energy Storage Systems. The journal of Undergraduate Research at University of Illinois at Chicago, Vol 7, No2, 2016, pp 52-55
- [5] Thomas E. Hoff, Richard Perez, Robert M. Margolis, Maximizing the value of customer-sited PV systems using storage and controls, Solar Energy, Volume 81, Issue 7, July 2007, pp 940-945
- [6] Ceylon Electricity Board, [Online] Available: <https://www.ceb.lk/commercial-tariff/en>

# Blockchain Assisted Business Model for Rooftop PV Energy Trading

Dhananjaya R.A.D.\*<sup>1</sup>, Edirisinghe E.A.T.H.\*<sup>2</sup>, Madushan W.W.I.\*<sup>3</sup>,  
Ekanayake J.B.\*<sup>4</sup>, Muthukumarasamy V.#

*\*University of Peradeniya, Sri Lanka.*

<sup>1</sup>dhananjayarad@gmail.com

<sup>2</sup>thilok.edir@eng.pdn.ac.lk

<sup>3</sup>wwimk13@gmail.com

<sup>4</sup>jbe@ee.pdn.ac.lk

*#Griffith University, Australia.*

v.muthu@griffith.edu.au

## Abstract

Due to development of small scale renewable energy resources such as solar PVs, decentralized energy trading is expected to be a key feature of the next generation power systems. Electronic smart contracts based on blockchain technology are believed to be a promising solution to create a competitive and interactive market among consumers and prosumers. In this paper, we discuss a peer to peer energy trading system based on Continuous Double Auction method which can give maximum monetary profit to participants when compared to traditional prices given by local authority. This study addresses the question regarding decentralized energy trading among consumers and prosumers along with the existing grid facilities.

**Keywords:** Blockchain, P2P energy trading, Continuous Double Auction, Smart Contract, Hyperledger

## Introduction

Today, renewable energy sources such as Solar PV and Wind Energy are extensively added to our power system. As most of these renewable additions are emerging in the distribution voltage levels with a large number of customers, the optimum trading of this green reserve is a must.

Blockchain or Distributed Ledger Technologies (DLT) has been used in order to design a distributed transaction without 'Central Management'. Using this method, we can have digital transactions without using a central point of authorisation. Because of that, instead of managing the ledger by a single trusted center, smart contract is involved by engaging parties and finally reaches an agreement.

Within a small community, there are two main engaging parties namely, Prosumers and Consumers who could use the smart contract addition the National Grid [1]. Prosumers are the parties that are enable to supply excess energy from their renewable energy generation sources. Consumers are the parties who supposed to buy energy from prosumers for a lower cost than the grid price. Prosumers can submit their excess allowed energy units and offer prices for that, also the consumers can submit their required energy units and offer prices. Finally, it undergoes a smart contract and reaches an agreement prices for each units. Excess energy from prosumers after the smart contract can be sold to the national grid and excess energy requirements of

the consumers after the smart contract can be bought from the national grid. [2]

In this paper a blockchain assisted commercial arrangement and a business model for people to engage in a direct automated execution of peer to peer smart contract without any central management are introduced.

## Proposed P2P Energy Trading Platform

### A. Hyperledger Fabric Blockchain

Hyperledger fabric [3] is an open source collaborative effort created to advance cross-industry blockchain technologies and is governed by the Linux Foundation. It is the first distributed ledger platform to support smart contracts authored in general purpose programming languages such as Java, Go and Node js. Hyperledger fabric supports pluggable consensus protocols which enables the platform to be more efficiently customized to fit particular use cases and trust modes. Hyperledger fabric use Practical Byzantine Fault Tolerance (PBFT) as the consensus algorithm. [3]

For the implementation of the P2P Energy trading platform, Hyperledger fabric was selected in this study due to the following facts.

1. Participants are identifiable
2. Network is permissioned
3. High transaction throughput
4. Low latency of transaction confirmation

## B. Entities of Energy Trading Platform

1. Consumers - Homeowners who do not have any power generating method are considered as consumers and they only consume energy.
2. Prosumers - Homeowners who have some method of power generation such as rooftop solar or diesel generators and they both produce and consume energy.
3. Grid - Existing power grid is also a participant of the proposed energy trading platform. In our study the power grid was considered as an infinite bus. If there are excess energy on the platform it can be sold to the grid and if there is a shortage, energy can be bought from the grid.

## C. Timeline of the Transaction

Energy is traded in one-hour time periods and at the beginning of each and period start trading transactions is initiated by the system. Then, consumers and prosumers can submit PV Offers and bids

to the platform. Every five minutes matching transaction is performed and the market is continuously cleared. At the end of the trading period stop trading transaction occurs and the unmatched offers and bids are matched with the grid. [3]

## D. Smart Contract

Smart contract will receive PVOffers from prosumers to sell energy and bids from consumer to buy energy. PVOffers and Bids include the following information as shown in Figure 2.

In Figure 2, transaction class of the implemented hyper ledger blockchain is shown as the class. Iteration is the number of times the same bid / offer submitted to the smart contract with increase / decreased price. The smart contract then clears the market using continuous double auction (CDA) market mechanism [4]. In CDA, PV offers are sorted from minimum offer price to maximum offer price and bids are sorted from maximum bid price to minimum bid price as shown in Figure 3.

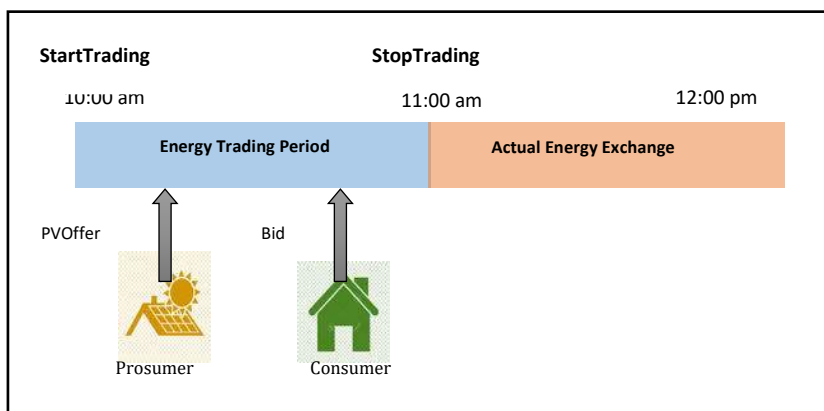


Figure 1: Time line of transaction

If, max bid price is greater than or equal to min offer Price, then the PV Offer and bid are matched [5]. Market clearing price (MCP) is calculated for each and every match according to the formula shown in Figure 4 and its algorithm is shown in Figure 5. The last MCP value calculated in each trading period is considered as the MCP of that trading period.

## E. User interface

In order to interact with the smart contract which is running on computer network, a user interface is essential [6]. Hence, android application which was built by using android studio was used to place bids and offers and know about the market details.

```

"$class": "org.pv.tradenetwork.PV_Offer",
"Iteration": 5,
"reservePrice": 23.2,
"kWh_available": 1.85,
"list": "resource:org.pv.tradenetwork.OffersAndBids#2019-11-04%7C07:00",
"prosumer": "resource:org.pv.tradenetwork.Prosumer#P02",
"transactionId": "000836d2abc6e24302ff47367b79139e10e76bb3dc327b0e313d84e62873fa83",
"timestamp": "2019-11-04T19:42:11.323Z"

"$class": "org.pv.tradenetwork.Bid",
"Iteration": 4,
"BidPrice": 23.6,
"kWh_required": 0.15,
"list": "resource:org.pv.tradenetwork.OffersAndBids#2019-11-04%7C07:00",
"consumer": "resource:org.pv.tradenetwork.Consumer#C02",
"transactionId": "2edce0a608fba5a51164890a12d669e2fbf00ad7302a12d8eb1206ac522c2980",
"timestamp": "2019-11-04T19:41:50.835Z"

```

Figure 2: Content of 'PVOffer' and 'Bid'

| Consumer | Quantity (kWh) | Bid Price (lkr/kWh) | Prosumer | Quantity (kWh) | Offer Price (lkr/kWh) |
|----------|----------------|---------------------|----------|----------------|-----------------------|
| C02      | 1.24           | 8.95                | P01      | 2.52           | 8.80                  |
| C01      | 2.10           | 8.75                | P02      | 3.68           | 8.85                  |
| C03      | 1.35           | 8.45                |          |                |                       |

Diagram illustrating the Order book. The table shows Consumer and Prosumer data. An arrow labeled *max BidPrice* points to the Bid Price of 8.95 for Consumer C02. Another arrow labeled *min OfferPrice* points to the Offer Price of 8.80 for Prosumer P01.

Figure 3: Order book

$$MCP = \max BidPrice - k(\max BidPrice - \min OfferPrice)$$

$$k = \frac{\text{total kWh available}}{\text{total kWh available} + \text{total kWh required}} ; 0 \leq k \leq 1$$

Figure 4: MCP calculation formula

```

Input: Offers, Bids
WHILE listing state = 'AcceptOffers' and Offer/Bid list = current list
    Add Offer/Bid to list
    IF  $maxBidPrice \geq minOfferPrice$ 
        Match Offer with Bid
        Update Offer kWh available
        Update Bid kWh required
    END_WHILE
IF listing State = 'Closed Bidding'
    Match the remaining Offers / Bids with Grid
END_IF

```

Figure 5: Pseudo code of market mechanism

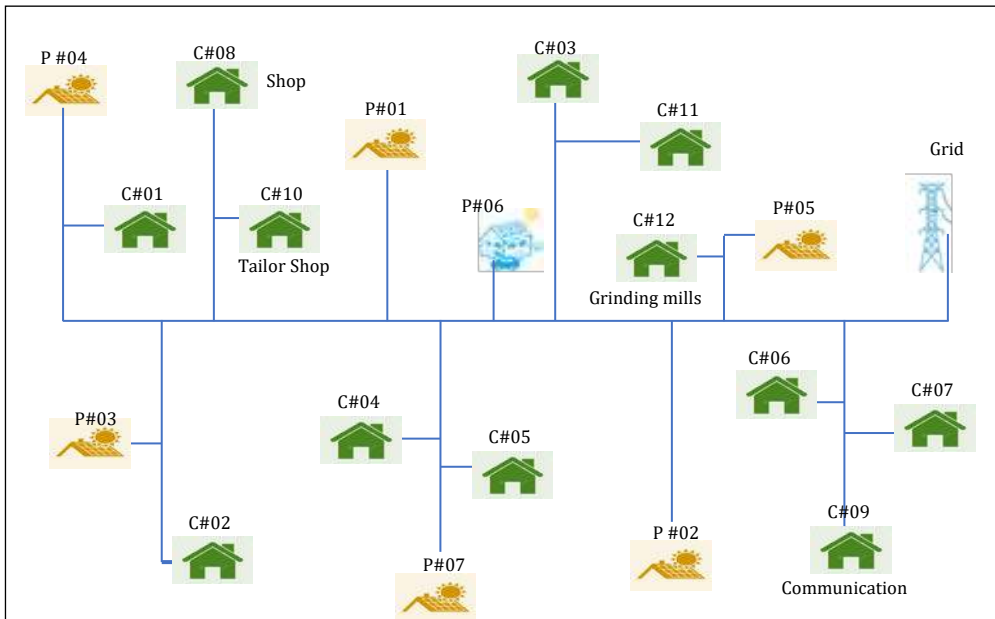


Figure 6: Proposed community - diagram

## Proposed Community

Consumers and prosumers of the community were designed according to a typical urban area in Sri Lanka as shown in Figure 6. Considering the occupations of the consumers and their family or organization status, the power consumptions were calculated.

Consumer #01 and #02 are considered as zero intelligent agents [6] who don't place bids rationally and others are considered as rational.

### A. Assumptions

All consumers and prosumers in the community use selected electrical equipment and energy generation equipment and they were used to



Table 1: Tariff charges

| Time of Use (ToU)     | Unit Charge (LKR/kWh) | Fixed Charge (LKR/Month) |
|-----------------------|-----------------------|--------------------------|
| Peak(18.30-22.30)     | 54.00                 |                          |
| Day(5.30-18.30)       | 25.00                 | 540.00                   |
| Off-Peak(22.30-05.30) | 13.00                 |                          |
| Night                 | 22.00                 | 600.00                   |

calculate energy consumption and generation of the community. For these calculations, 06:00-23:00 time period was only considered and grid selling price was taken from the Ceylon Electricity Board Time of Use electricity tariff shown in Table 1.

Table 2: Maximum prices for bids and offers

| Time      | Maximum price for 1 unit (LKR) |
|-----------|--------------------------------|
| 0006-0007 | 25                             |
| 0007-0008 | 25                             |
| 0008-0009 | 25                             |
| 0009-0010 | 25                             |
| 0010-0011 | 25                             |
| 0011-0012 | 25                             |
| 0012-0013 | 25                             |
| 0013-0014 | 25                             |
| 0014-0015 | 25                             |
| 0015-0016 | 25                             |
| 0016-0017 | 25                             |
| 0017-0018 | 54                             |
| 0018-0019 | 54                             |
| 0019-0020 | 54                             |
| 0020-0021 | 54                             |
| 0021-0022 | 54                             |
| 0022-0023 | 54                             |
| 0023-0024 | 13                             |

Grid buying price was taken as 22 LKR. It was assumed that the rational consumers and prosumers don't place bids and offers higher than the grid selling price and it was taken as the maximum bid and offer prices for each trading period and are summarized in Table 2.

## B. Electrical equipment used in community

Table 3: Energy consumption of equipment

| Electrical equipment | Energy consumption for one hour time (kWh) |
|----------------------|--|
| Refrigerator         | 1(For a day)                               |
| Water pump           | 0.09                                       |
| Rice cooker          | 0.37                                       |
| Computer             | 0.1  |
| Ceiling Fan          | 0.06                                       |
| AC machine           | 1  |
| Grinder              | 0.25                                       |
| Iron                 | 0.25                                       |
| Washing machine      | 0.4  |
| Television           | 0.11                                       |
| LED bulb             | 0.012                                      |
| Sewing machine       | 0.1  |
| Photocopy machine    | 0.6  |
| Electric vehicle     | 30 kWh Lithium Ion battery                 |
| Electric motor       | 0.8  |

Table 4: Cost of energy generation

| Energy Generation Equipment | Cost for one-hour generation (approximately) / (LKR) |
|-----------------------------|--|
| Solar PV                    | 12   |
| Diesel Generator            | 28   |
| Electric Vehicle            | -  |

Major electrical equipment which is basically used in the houses in Sri Lanka was selected to do the calculations. These are shown in Table 3 and energy generation equipment with estimated cost per one-hour generation are in Table 4.

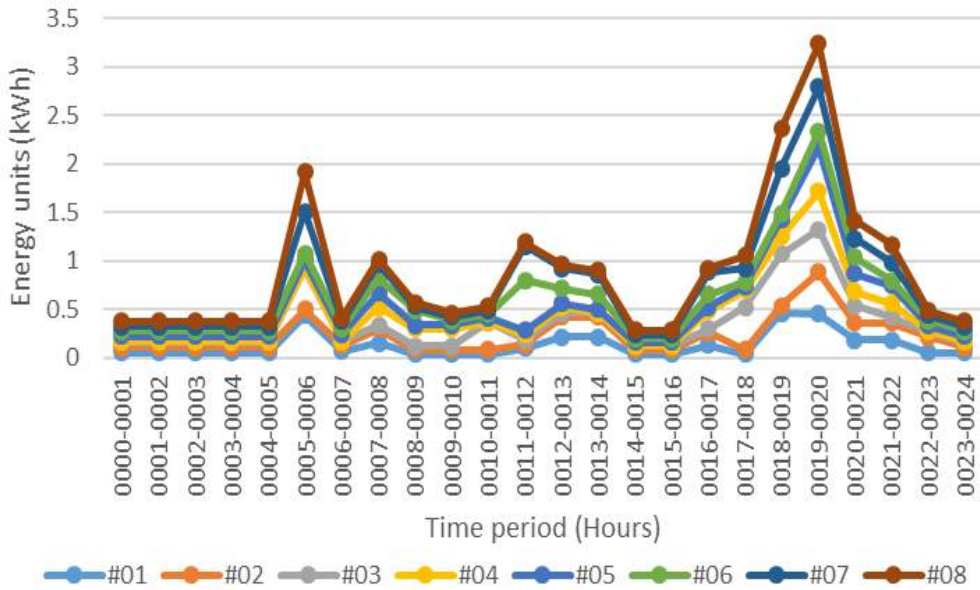


Figure 7: Load demand of the domestic consumers in the community

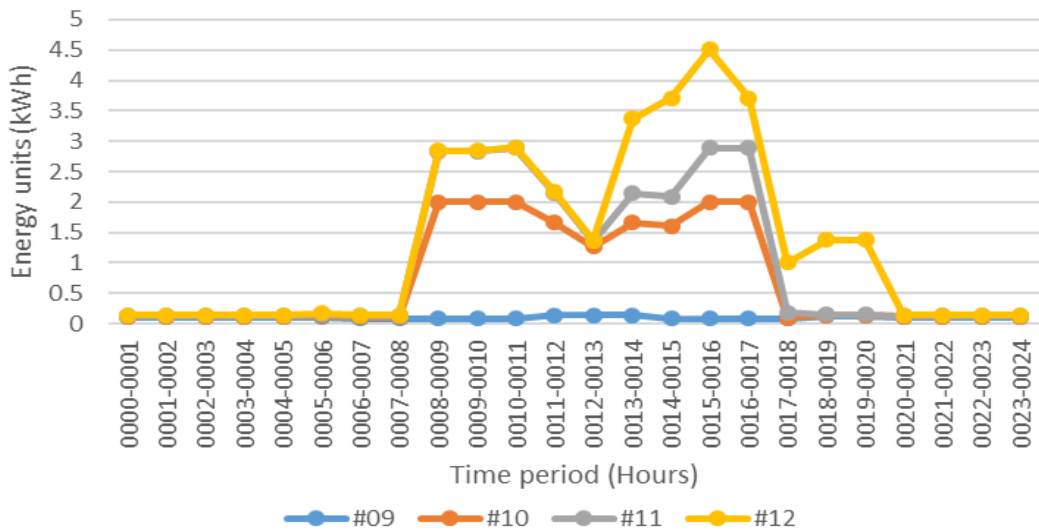


Figure 8: Load demand of the small scale business organizations in the community

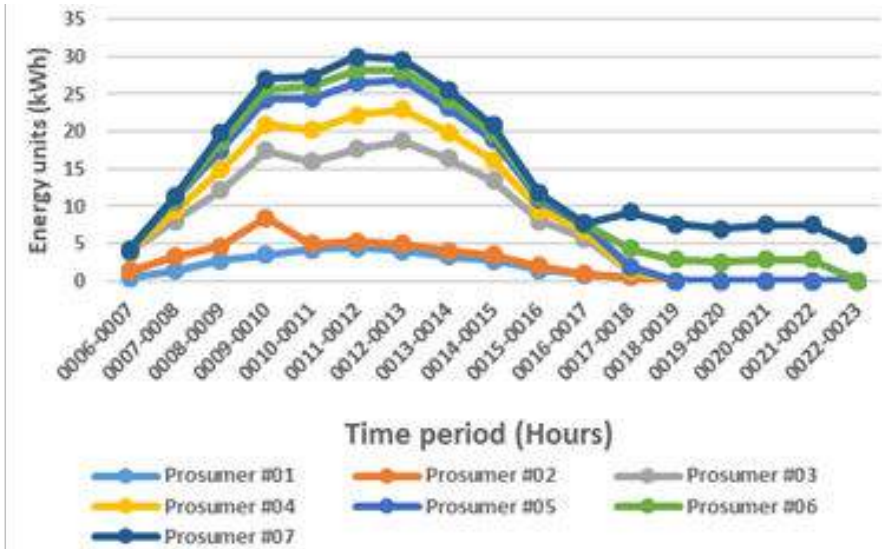


Figure 9: Excessive energy of the prosumers in the community

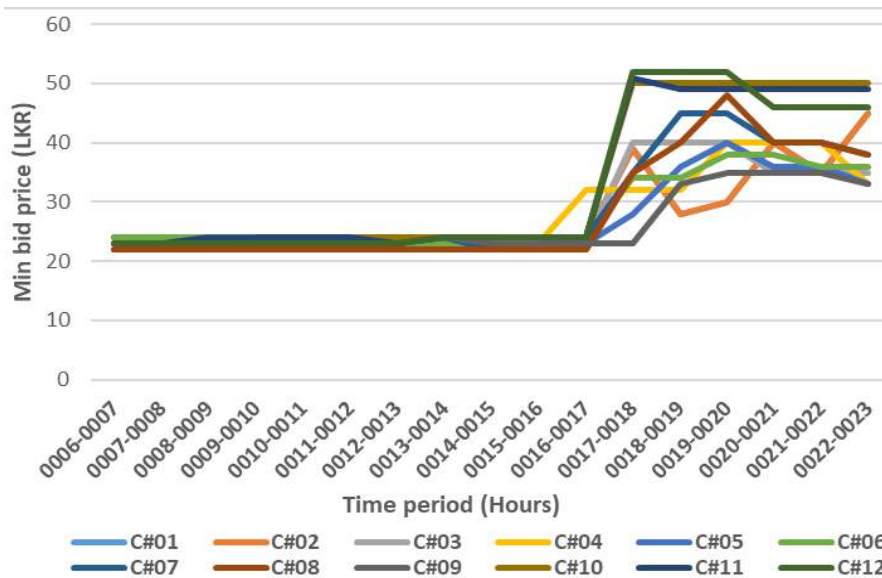


Figure 10: Variation of minimum bid price of consumers in the community

By using these data, the load demand of the consumers and energy generation of the prosumers were estimated and shown in Figure 7, Figure 8 and Figure 9. Thereafter, the load demand and energy generation values were used to test the system. Minimum bid prices of consumers should be higher than the

grid buying price. Minimum offer prices were decided considering their cost of generation and the grid buying price. Considering above assumptions, variation of minimum bid and offer prices are shown in Figure 10 and Figure 11.

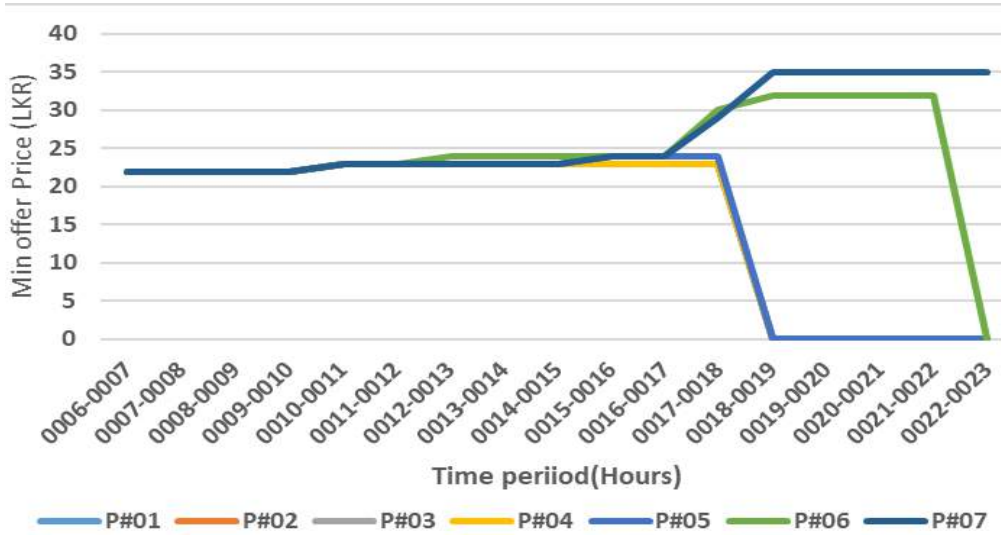


Figure 11: Variation of minimum offer price of prosumers in the community

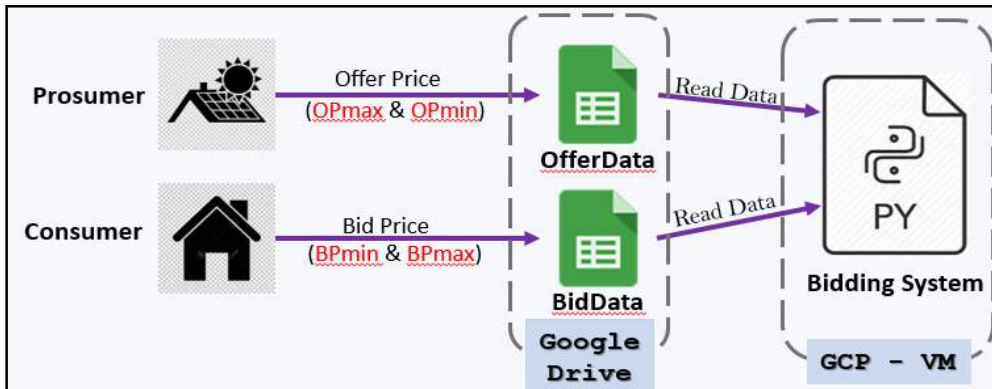


Figure 12: Test implementation - diagram

## Experiments

To run the test, maximum and minimum prices which were submitted by the participants for each trading period and this data is stored in some Google spreadsheets. Those prices were taken from the case study discussed previously. A bidding system shown in Fig 12, which is a python program running on a google

cloud platform virtual machine was used to submit the price range specified by participants to the smart contract in 10 steps. Bids and offers are submitted to smart contract from minimum price to maximum price by this system which is built based on Continuous Double Auction.

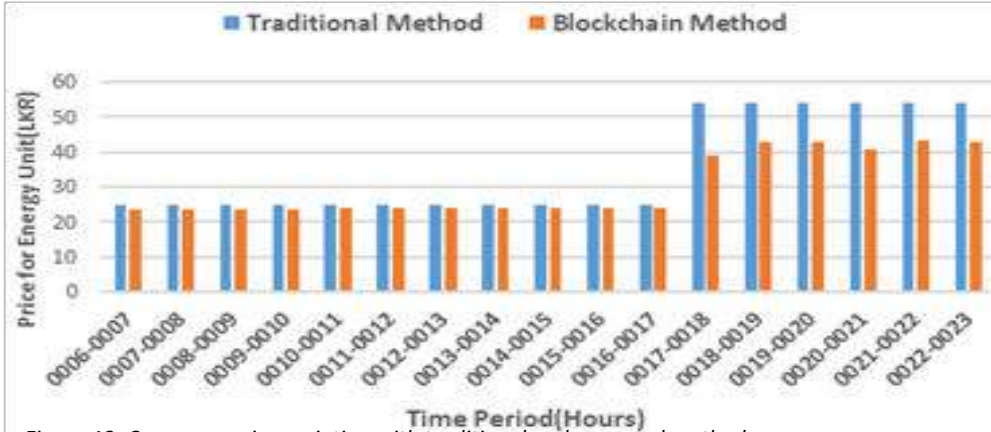


Figure 13: Consumer price variation with traditional and proposed method

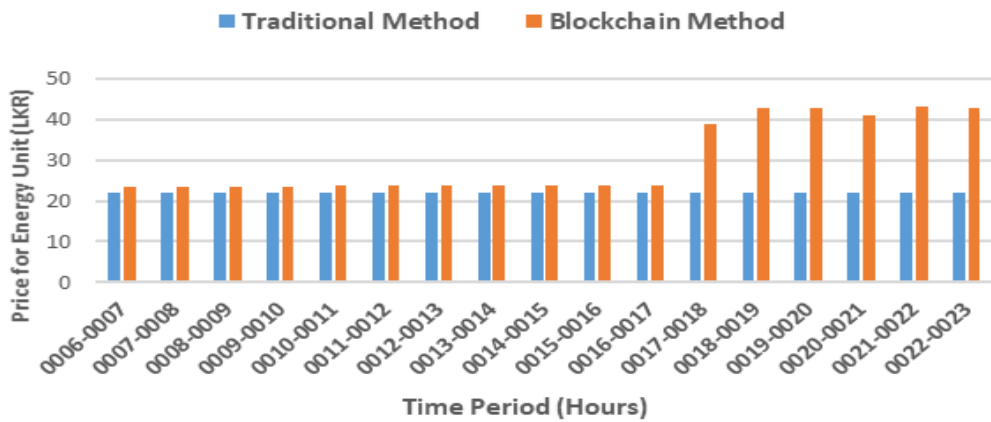


Figure 14: Prosumer price variation with traditional and proposed method

## Results

Energy cost per unit in proposed trading platform is lower than the traditional energy market as shown in Figure 13. Prosumers get higher monetary gain from the proposed trading platform as shown in Figure 14. It can be clearly seen that, at the end both parties could get higher profit compared to the traditional energy market. Further, generated energy of the prosumer#03 was distributed with consumer#01 to consumer #10 shown in Figure 15 and the peer to peer nature can also be observed in it.

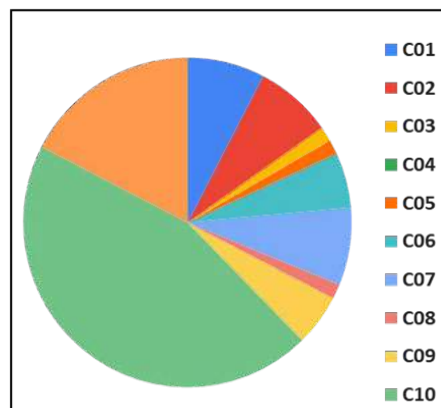


Figure 15: P2P energy trading – Prosumer#03 at 13:00

## Conclusion

In this paper, a blockchain assisted business model to trade energy in a competitive market while ensuring every participant get more profit without direct intervention of a third party was proposed. In addition to that, a community was selected as a case study and the P2P system was tested. Furthermore, the potential benefits of integrating P2P energy trading in local power infrastructure while encouraging the maximum participation of renewable energy resources were demonstrated. However, implementation of this system requires amendments on the current energy policies and laws.

## References

- [1] M. N. Faqiry and S. Das, "A Budget Balanced Energy Distribution Mechanism among Consumers and Prosumers in Microgrid," in 2016 IEEE International Conference on Internet of Things (iThings) and IEEE Green Computing and Communications (GreenCom) and IEEE Cyber, Physical and Social Computing (CPSCom) and IEEE Smart Data (SmartData), 2016, pp. 516–520. Cyber, Physical and Social Computing (CPSCom) and IEEE Smart Data (SmartData), 2016, pp. 516–520.
- [2] A. Salian, S. Shah, J. Shah, and K. Samdani, "Review of Blockchain Enabled Decentralized Energy Trading Mechanisms," in 2019 IEEE International Conference on System, Computation, Automation and Networking (ICSCAN), 2019, pp. 1–7.
- [3] M. Pipattanasomporn, M. Kuzlu, and S. Rahman, "A Blockchain-based Platform for Exchange of Solar Energy: Laboratory-scale Implementation," in 2018 International Conference and Utility Exhibition on Green Energy for Sustainable Development (ICUE), 2018, pp. 1–9.
- [4] N. Farajian and K. Zamanifar, "Market-Driven Continuous Double Auction Method for Service Allocation in Cloud Computing," in Advances in Computing, Communication, and Control, 2013, pp. 14–24.
- [5] C. Long, J. Wu, C. Zhang, L. Thomas, M. Cheng, and N. Jenkins, "Peer-to-peer energy trading in a community microgrid," in 2017 IEEE Power Energy Society General Meeting, 2017, pp. 1–5.
- [6] P. Vytelingum, S. Ramchurn, T. Voice, A. Rogers, and N. Jennings, "Agent-based modeling of smart-grid market operations," in 2011 IEEE Power and Energy Society General Meeting, 2011, pp. 1–8.

# Sky Image-Based Short-Term Solar Power Forecasting Model

Lasanthika H. Dissawa<sup>#\*1</sup>, Janaka B. Ekanayake<sup>#2</sup>, A. P. Agalgaonkar<sup>\*3</sup>,  
Duane Robinson<sup>\*4</sup>, Sarath Perera<sup>\*5</sup>, R. I. Godaliyadda<sup>#6</sup>, P. B. Ekanayake<sup>#7</sup>

*# Department of Electrical and Electronic Engineering, University of Peradeniya,  
Sri Lanka*

<sup>1</sup> lhddm993@uowmail.edu.au

<sup>2</sup> ekanayakej@cardiff.ac.uk

*\* School of Electrical, Computer and Telecommunications Engineering, University of  
Wollongong, Australia*

<sup>3</sup> ashish@uow.edu

## Abstract

Solar photovoltaic generation continues to be a viable alternative in the overall generation mix in many countries around the world. Although this is the case, due to its variability and uncertainty, the increased penetration levels of installed PV systems can lead to power system operational issues.

The main factor affecting the PV output is solar irradiance, which follows a predictable and seasonal pattern. However, the amount of solar radiation at the ground level varies by the local weather conditions, including the intermittency of cloud cover. As an example, intermittent clouds cause the power generation from large scale solar farms to vary by up to 80% in a 5 min period. To mitigate these effects caused by PV generation, relevant mitigation strategies need to be introduced. In this regard, approaches that can be used for forecasting solar irradiance at ground level and associated power output from the localised PV systems will take a prominent place.

Therefore, a short-term irradiance forecasting technique centred on cloud motion estimation employing ground-based sky images captured from two inexpensive sky camera systems is proposed. Based on the cloud motion vectors, the solar irradiance is forecasted 1 min, 5 min and 15 min ahead of time in near locations.

**Keywords:** Short-term irradiance forecast, Fast cross-correlation, Sky imaging, solar PV power forecasting, Sky camera

## Introduction

Solar photovoltaic (PV) generation continues to be a viable alternative in the overall generation mix in many countries. Although this is the case, due to its variability and uncertainty, increased penetration levels of installed PV systems can impact on power system operation and management.

It is well known that solar irradiance levels follow a predictable and seasonal pattern. However, the amount of solar radiation at the ground level varied by the local weather conditions including the intermittency of cloud cover thus impacting the solar PV output. To mitigate the effect of variability and intermittency of PV generation, relevant mitigation strategies need to be introduced. In this regard, approaches that can be used to forecast solar irradiation levels at ground level and associated power output from local PV generation systems can be expected to take a prominent place in future power systems which will see increased levels of solar PV integration.

Typically, the time horizon for solar power forecasting can be categorised into intra-hour, intra-day and day-ahead commensurate with grid operator activities [1]–[3]. Intra-hour, from a few seconds to minutes, or in other words, very short-term forecasts can be used for ramp up/down event predictions, PV inverter and energy storage management. Also, such forecasts can be used as inputs to energy market operations, such as the Australian National Electricity Market (NEM) which uses 5 minute PV forecasts [4].

Techniques used for forecasting solar irradiance depends on the desired time scale of the forecast [5]. Numerical

Weather Prediction Models (NWP) based models can give accurate predictions in the range of 6 hours to several days ahead [6] whereas, in a time horizon smaller than 6 hours, satellite data-based models typically outperform the NWP based models. Due to time and space availability of the satellite data, the satellite data-based PV prediction models have been developed covering forecasting intervals from 30 minutes up to 6 hours [6].

In intra-hour or real-time predictions, the use of cloud information from ground-based sky images and/ or time series models based on historical data are described in [7]–[14]. These methods derive accurate solar irradiance forecasts with much higher spatial and temporal resolution compared with the satellite image-based forecasting models or NWP based forecasting models in short time horizon. Sky image-based forecasting models use cloud motion vector estimations and/ or the changes in the sky image features, such as mean and variance of the image pixel colour values, image mean intensity level [10] over the time to predict future PV power/irradiance variations.

Cross-Correlation based methods (CCM) are used in [15] to find cloud motion vectors whereas [12], [13] describes Lucas-Kanade optical flow algorithm or variational optical flow algorithm based methods to find the cloud motion vectors where it is applied to cloud feature points such as corners or well-defined lines located on the edges between the cloud and the sky. It assumes that there is an even local flow around the neighbourhood of pixels around the feature and that the displacement of the feature is small between two consecutive frames. In the cross-correlation method covered in [15], [16], the image is



partitioned into subsets of pixels of equal size and by assuming spatial homogeneity of cloud velocity an average cloud velocity across the image is found. Further, [17] introduces a cross-correlation based method to identify multiple cloud velocities which uses a cloud boundary tracking algorithm. As CCM does not depend on the cloud feature points errors are reduced caused by cloud boundary or feature point deformations over time.

Despite the number of techniques described above, the main problem in short-term solar irradiance forecasting/power forecasting is the prediction of cloud shadows on PV arrays. These shadows naturally create changes in PV power output. Considering the very-short-term forecasting horizon, this paper proposes a new methodology for irradiance forecasting based on ground-based sky images. The method has the ability to provide forecasts in different locations covering a few minutes ahead of time by incorporating cloud base height calculations into the cloud motion tracking model. The shadow movement

or ray-tracing method enables forecasting of irradiance in multiple PV sites.

## Materials

To capture the ground-based sky images, visual measurement of the whole skydome with the high spatial and temporal resolution is required. Figure 1 shows newly designed, inexpensive whole sky imagers, installed on the rooftop of the Sustainable Buildings Research Centre (SBRC) at the innovation campus, University of Wollongong and at the rooftop of Building 35, main campus, University of Wollongong, Australia.

The two sky imagers were developed employing Raspberry Pi (3<sup>rd</sup> Generation, Model B) boards. A high resolution fully programmable Raspberry pi camera module with a wide-angle lens was connected to the Raspberry Pi board to capture a wide area of the sky. The camera and the Raspberry Pi board were enclosed with a waterproof weather enclosure.

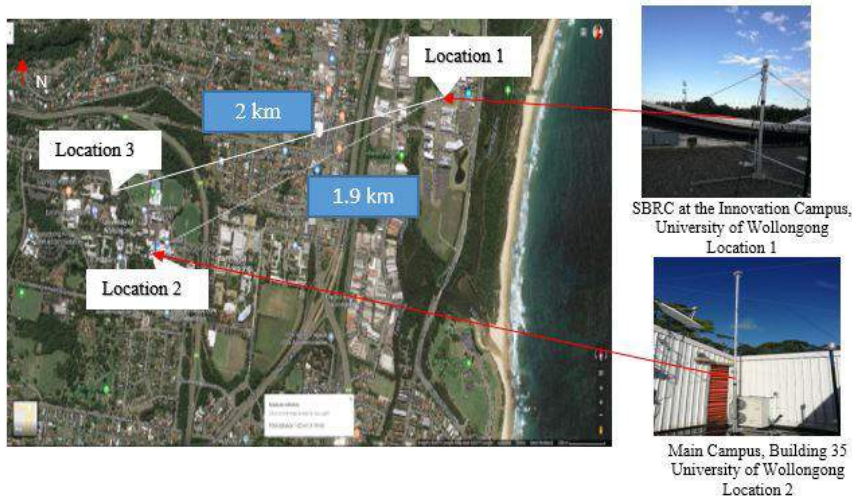


Figure 1: Locations of the two cameras, camera 1 in Location 1 is installed on the rooftop of the Sustainable Buildings Research Centre (SBRC) of the Innovation Campus and rooftop PV system at location 1, and the other installed on the roof of Building 35, Main Campus ('camera 2' - Location 2), of the University of Wollongong, Australia. Location 3 is the 2<sup>nd</sup> PV plant at on the roof of Building 28, Main Campus)

The sky imager is operated remotely, and it automatically captures the images at a pre-defined rate. In the present case, the images were captured every 10 seconds and were stored in JPEG format which has a resolution of 1024x768 pixels. In the beginning, the images were divided into 1 min image sets according to their timestamps. For each image set, the average time between two image frames was calculated.

In addition to the sky images, power/irradiance measurements are needed to evaluate the results. Therefore, a location which is 2 km away from the main camera (Camera 1 at location 1) is selected for evaluation, the building 28 of Main Campus rooftop PV system (Location 3). The locations are shown in figure 1. The power measurements were saved in 1 min time interval.

To forecast the irradiance associated with cloud shadow movement, (a) the camera orientation with respect to true north (b) the zenith angle of the sun (c) the azimuth angle of the sun (d) the clear sky irradiance values, (e) both latitude and longitude of the camera and PV location and (f) cloud base height (height above ground level) at the camera location are required. The zenith angle, azimuth angle, and clear sky irradiance values were calculated employing the information in [18]–[20] using date, time, latitude and the longitude of the locations. The cloud base height was calculated using a new sky image-based CBH calculating method.

### Cloud Segmentation and Tracking

A new technique is introduced to segment the clouds where the clouds are classified into three categories based on

image pixel's YCbCr (Y is the luma component, and Cb and Cr are the blue-difference and red-difference chroma components) colour component. By applying different thresholds to the Cb image component, the white and gray regions in the sky image were identified. After obtaining the binary image, Matlab® median filter function was applied to the binary image to obtain a smooth cloud boundary where small white blobs (blob area < 1000 pixels) were removed from the image. To track each individual cloud movement from frame to frame, individual cloud areas in the first image frame in each image set was identified by applying the connected component algorithm to the cloud binary image obtained through the cloud segmentation process. Then, according to the Cb values of the cloud areas, the pixels are classified into three categories. The RGB image and the selected cloud areas, and the three cloud categories are shown in Figure 2, respectively.

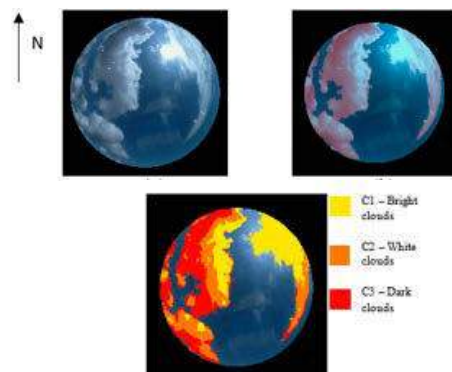


Figure 2: RGB raw image, selected cloud areas are marked on the RGB image, categorized clouds using the threshold method into three categories

Before applying the cloud tracking algorithm, the first sky image in each image set was categorised into one category; clear sky, partially cloudy sky or overcast depending on the number of

white blobs and on the percentage of white pixels (PR) (contains clouds and the sun) in the binary image. If the first sky image is categorized into the partially cloudy condition ( $15\% < PR < 80\%$  and more than one blob are detected), then to apply cloud tracking algorithm, clouds and the sun areas were separately identified by mapping the location of the sun onto the sky image.

Following this, the clouds were selected one by one and set of points inside each cloud boundary were selected for tracking. The selected total number of points depends on the cloud size. Figure 3 (a) shows a cloud with the selected points  $[X_i, Y_i]$ . The distance between each point is 50 pixels.

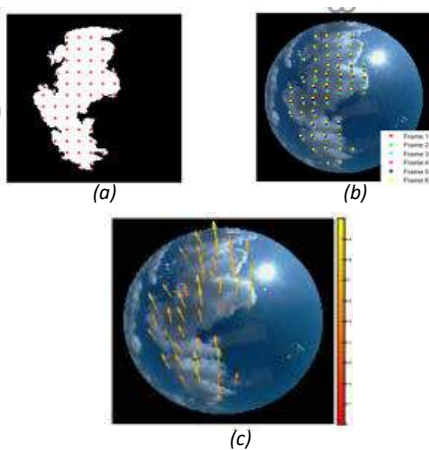


Figure 3: a) selected cloud points inside a cloud  $[X_i, Y_i]$ , b) the tracked cloud points over a 1 min period over a 1 min time interval (from frame 1 to frame 6), and c) the average motion vectors of the selected points

Fast cross-correlation (CCM) based cloud motion tracking algorithm is introduced to estimate the cloud motion vectors. Without considering only the cloud boundary points or whole cloud region as one segment, the CCM was applied to the selected points inside each cloud region separately. This method enables the

determination of multiple layer cloud movements.

Following the tracking of points, cloud moving velocity was calculated. Before calculating the velocity, the lens distortion of the selected points was removed according to the camera mapping function and CBH (rather than undistorting the whole image at the initial stage, at this stage the undistorted process was implemented). Then, the motion velocities were calculated using the time between two image frames. To establish the cloud velocity from the point velocities, the point moving speed and the direction were considered separately. The median speed of the point moving speeds (median of non-zero values) and median of the point moving direction (median of non-zero values) were obtained. The median speed and median angle were assigned as the cloud moving velocity vector.

### Cloud base height

To calculate the CBH, a technique based on two camera system was introduced. For this, the same cloud should be captured by two cameras from two different locations. After capturing two images from two locations, in one image few cloud boundary points were selected (image captured from Camera 1), and the CCM was used to identify the common cloud areas captured in the second image (captured from Camera 2). Both images are captured simultaneously. Figure 4 shows (a) Image taken from the camera at location 1 and selected boundary points, (b) selected single point  $[x, y]$ , (c) Image taken from the camera at location 2 with  $[x, y]$  position for different cloud base heights  $[x', y'] = [(x'_1, y'_1), (x'_2, y'_2), \dots, (x'_n, y'_n)]$ .

The point which has the maximum correlation and minimum distance from each point's search window centre location was assumed as the cloud base height. Figure 4 (d) shows the maximum CC for different cloud-based heights (blue) and the distance between search window centre-point to maximum cross-correlation point for the selected boundary point  $[x,y]$  (brown). The CBHs were obtained for individual clouds, and the average of CBHs was considered as the CBH at the end.

## Results and Discussions

According to the PV plant location coordinates, date, time, camera mapping function and the CBH, the segment of the sky image which creates a shadow on the PV plant was identified. Then, a few points inside each cloud blobs were selected and were undistorted. After that, according to velocities and shadow creating image location, the irradiance drop occurrence time was calculated for each point. According to the minimum and mean occlusion time, the irradiance drop was forecasted 1 min, 5 min, and 15 min ahead of time with 1 min granularity.

Three irradiance drop levels were defined for the three cloud categories in cloud segmentation process. For thick clouds (C3), the percentage irradiance drop was assumed to be 30% of clear day irradiance value, whereas for white clouds (C2), the drop was assumed to be 40% of clear day irradiance level and for the bright white clouds (C1) the drop percentage was assumed as 50% of clear day irradiance value. For the forecast, the irradiance drop percentage for each cloud was defined by the maximum percentage of C1, C2 and C3 pixels in the cloud (e.g. if C1 got the maximum percentage, then the irradiance will be dropped by 30 %). To

obtain the clear day irradiance curve, ASHRAE model [20] was utilized.

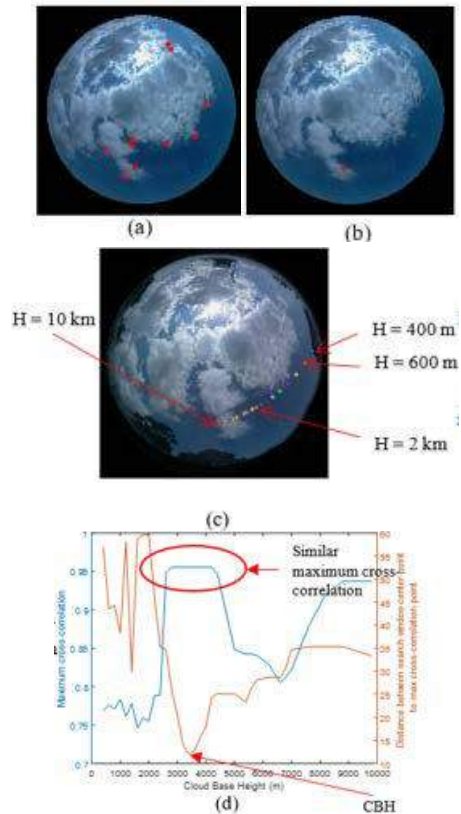


Figure 4: (a) Image taken from the camera at location 1 and selected boundary points, (b) selected single point  $[x, y]$ , (c) Image taken from the camera at location 2 with  $[x,y]$  position for different cloud base heights and (d) the maximum CC for different cloud-based heights (blue) and the distance between search window centre-point to maximum cross-correlation point for the selected boundary point (brown)

To evaluate the results, Root Mean Square Error (RMSE), Mean Absolute Error (MAE), and the percentage of correctly identified irradiance state were calculated. Correctly identified irradiance state (drop or not /1 or 0) percentage of the forecasting methods were calculated using (Eq.1). True state refers to correctly identified irradiance state, and false state

refers to incorrectly identify irradiance state (incorrect drops and missed drops). Correctly identified irradiance state percentage (TS) for the total time period was calculated using (Eq.1).

$$TS = \frac{\text{True states}}{\text{True states} + \text{Fales states}} \times 100\% \quad (\text{Eq. 1})$$

To compare the irradiance forecasts with the actual measurements, the measured power from the rooftop PV systems were converted into the irradiance values using the capacities of the rooftop PV systems. Table 1 shows the calculated errors for a number of selected days. The RMSE, MAE, and TS of the forecasts. For the selected days, the average of the correctly identified irradiance state for the selected days is 75%.

Table 1: Forecasting errors, RMSE, MAE and TS for onsite irradiance forecasts

| Location                          | Date       | Time horizon | Error                |                      |      |
|-----------------------------------|------------|--------------|----------------------|----------------------|------|
|                                   |            |              | RMSE                 | MAE                  | TP   |
|                                   |            |              | /(Wm <sup>-2</sup> ) | /(Wm <sup>-2</sup> ) | /(%) |
| Forecasts obtained for Location 3 | 28/07/2019 | 1 min        | 145                  | 84                   | 85   |
|                                   |            | 5 min        | 110                  | 60                   | 85   |
|                                   |            | 15 min       | 152                  | 85                   | 76   |
|                                   | 29/07/2019 | 1 min        | 114                  | 62                   | 79   |
|                                   |            | 5 min        | 139                  | 77                   | 76   |
|                                   |            | 15 min       | 157                  | 97                   | 61   |
|                                   | 30/07/2019 | 1 min        | 110                  | 62                   | 78   |
|                                   |            | 5 min        | 73                   | 43                   | 70   |
|                                   |            | 15 min       | 66                   | 42                   | 63   |

Figure 5 shows irradiance forecasts for 2 km away location from the camera location. The blue colour curves show the forecasts and the orange colour curves show the measured irradiance.

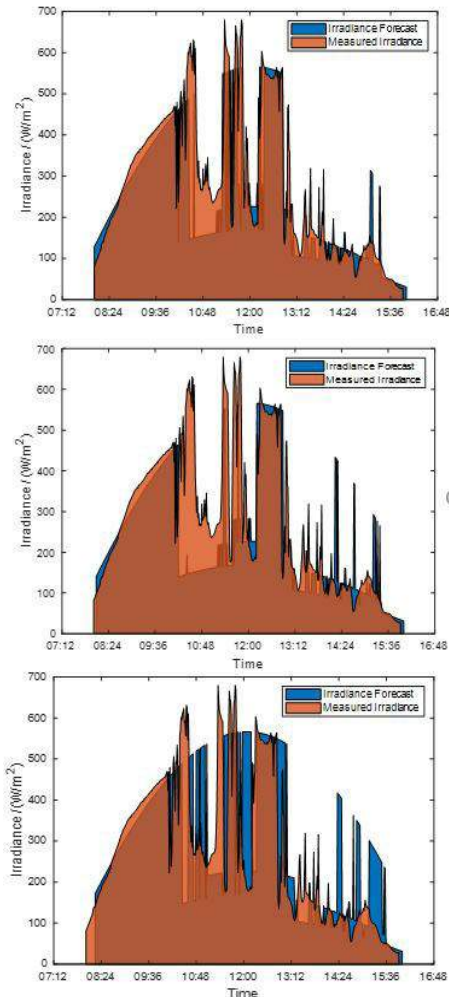


Figure 5: (a) 1 min, (b) 5 min and (c) 15 min forecasts at location 3 on 29th July 2019, blue colour curves show the forecasts and the orange colour curves show the measured irradiance

## Conclusions

A new short-term solar forecasting algorithm was presented, which makes

use of inexpensive ground-based sky imaging systems. 1min, 5min and 15 min ahead irradiance forecasts were obtained using the novel method. The method has the capability of determining the PV power drops a few minutes advance to the actual occurrence.

The wide-angle inexpensive camera captures a large area of the sky, which aids in increasing the forecasting time horizon. Therefore, up to 15 min ahead, forecasts were obtained using the method introduced in this paper. The image distortion removal process at the initial stage limits the maximum possible forecasting horizon due to cropping of the edge of the image, or it reduces the image resolution limiting the forecast accuracy at the centre of the image. The method described in the paper used all visible sky area for the forecast.

The RBR method used for cloud segmentation is unreliable with regard to thick clouds that do not let direct sunlight to pass through them. These clouds have a similar RBR to blue sky pixels. This leads to an under detection of cloud pixels or an overestimation of blue sky. It was more reliable to use different drop percentages according to the cloud properties than using one irradiance drop percentage for the whole cloud since the thickness of the clouds is not the same for each cloud. The results show that the three-level irradiance drop percentage gives relatively more accurate results.

In the work presented, the irradiance/power measurements were not used as input information. Therefore, the proposed method will produce standalone forecasts for onsite and for near locations.

It is known that the cloud shape changes continuously over time. Hence, a cross-correlation based cloud segment tracking algorithm was applied instead of a feature point tracking algorithm. Further, the cloud has multiple layers and has different moving speeds and directions. The proposed cloud segment tracking algorithm allows the establishment of the individual cloud moving velocities. Using this cloud tracking method, irradiance state (increase or decrease) was forecasted correctly for 75% of the time. By adding cloud base height details to the forecasting method, the method was improved. Using this technique, the PV power/irradiance forecasts in multiple sites in the vicinity of the camera location was obtained with the aid of cloud velocity. Further, by incorporating the cloud categorisation details, the results were improved (three different scaling factors were introduced instead of one scaling factor).

The ability to predict clouds locally and being able to extract cloud features are crucial in relation to prediction of solar power output. Further, the short-term forecasting results are useful in mitigating the problems related to solar intermittency in short time periods. Thus, an accurate estimation of solar power derived using the proposed model is useful in scheduling solar power generation in large interconnected networks and it enables active market participation. Thus, the model can be further developed to achieve short-term PV power forecasts in relation to large scale solar farms enabling their active market participation.

### Acknowledgements

The authors would like to acknowledge the financial support provided by the Sri

Lanka Sustainable Energy Authority to carry out this work. Further, the author would like to acknowledge the collaboration between the University of Wollongong and the University of Peradeniya, which set up the program for shared PhDs.

### References

- [1] L. Bird, M. Milligan, and D. Lew, 'Integrating variable renewable energy: Challenges and solutions', National Renewable Energy Laboratory, 2013.
- [2] V. Kostylev, A. Pavlovski, and others, 'Solar power forecasting performance—towards industry standards', in 1<sup>st</sup> International Workshop on the Integration of Solar Power into Power Systems, Aarhus, Denmark, 2011.
- [3] A. Kaur, L. Nonnenmacher, H. T. C. Pedro, and C. F. M. Coimbra, 'Benefits of solar forecasting for energy imbalance markets', *Renewable Energy*, vol. 86, pp. 819–830, Feb. 2016.
- [4] 'Australian Energy Market Operator', Australian Energy Market Operator, 17-Sep-2013. [Online]. Available: <http://www.aemo.com.au/>. [Accessed: 06-Apr-2018].
- [5] Jan Kleissl, *Solar Energy Forecasting and Resource Assessment*. Academic Press, 2013.
- [6] H. M. Diagne, P. Lauret, and M. David, 'Solar irradiation forecasting: state-of-the-art and proposition for future developments for small-scale insular grids', in WREF 2012-World Renewable Energy Forum, 2012.
- [7] N. Zhang and P. K. Behera, 'Solar radiation prediction based on recurrent neural networks trained by Levenberg-Marquardt backpropagation learning algorithm', in 2012 IEEE PES Innovative Smart Grid Technologies (ISGT), 2012, pp. 1–7.
- [8] A. Tascikaraoglu et al., 'Compressive Spatio-Temporal Forecasting of Meteorological Quantities and Photovoltaic Power', *IEEE Transactions on Sustainable Energy*, vol. 7, no. 3, pp. 1295–1305, Jul. 2016.
- [9] C.-L. Fu and H.-Y. Cheng, 'Predicting solar irradiance with all-sky image features via regression', *Solar Energy*, vol. 97, pp. 537–550, Nov. 2013.

- [10] H. Y. Cheng and C. C. Yu, 'Solar irradiance now-casting with ramp-down event prediction via enhanced cloud detection and tracking', in 2016 IEEE International Conference on Multimedia and Expo (ICME), 2016, pp. 1–6.
- [11] J. Alonso-Montesinos, F. J. Batlles, and C. Portillo, 'Solar irradiance forecasting at one-minute intervals for different sky conditions using sky camera images', *Energy Conversion and Management*, vol. 105, pp. 1166–1177, Nov. 2015.
- [12] D. Bernecker, C. Riess, E. Angelopoulou, and J. Hornegger, 'Continuous short-term irradiance forecasts using sky images', *Solar Energy*, vol. 110, pp. 303–315, Dec. 2014.
- [13] M. Cervantes, H. Krishnaswami, W. Richardson, and R. Vega, 'Utilization of Low Cost, Sky-Imaging Technology for Irradiance Forecasting of Distributed Solar Generation', in 2016 IEEE Green Technologies Conference (GreenTech), 2016, pp. 142–146.
- [14] F. Barbieri, C. Riffart, B. T. Vo, S. Rajakaruna, and A. Ghosh, 'Intrahour Cloud Tracking Based on Probability Hypothesis Density Filtering', *IEEE Transactions on Sustainable Energy*, vol. 9, no. 1, pp. 340–349, Jan. 2018.
- [15] H. Huang et al., 'Cloud motion estimation for short term solar irradiation prediction', in *Smart Grid Communications (SmartGridComm)*, 2013 IEEE International Conference on, 2013, pp. 696–701.
- [16] K. Stefferud, J. Kleissl, and J. Schoene, 'Solar forecasting and variability analyses using sky camera cloud detection & motion vectors', in 2012 IEEE Power and Energy Society General Meeting, 2012, pp. 1–6.
- [17] D. M. L. H. Dissawa, G. M. R. I. Godaliyadda, M. P. B. Ekanayake, J. B. Ekanayake, and A. P. Agalgaonkar, 'Cross-correlation based cloud motion estimation for short-term solar irradiation predictions', in 2017 IEEE International Conference on Industrial and Information Systems (ICIIS), 2017, pp. 1–6.
- [18] G. M. Masters, 'Renewable and Efficient Electric Power Systems', p. 676.
- [19] M. J. Ahmad and G. N. Tiwari, 'Solar radiation models—A review', *International Journal of Energy Research*, vol. 35, no. 4, pp. 271–290.
- [20] K. Bakirci, 'Estimation of Solar Radiation by Using ASHRAE Clear-Sky Model in Erzurum, Turkey', *Energy Sources, Part A: Recovery, Utilization, and Environmental Effects*, vol. 31, no. 3, pp. 208–216, Jan. 2009.



# Geographical Area Identification for Concentrated Solar Power (CSP) Plant in Sri Lanka

Ashanka Priyadarshani M.B<sup>#1</sup>, Udayakumar K.A.C<sup>#2</sup>

*# Department of Electrical and Computer Engineering, The Open University of Sri Lanka  
Nawala, Sri Lanka*

<sup>1</sup> ashankadarshani@gmail.com

<sup>2</sup> kauda@ou.ac.lk

## Abstract

This work presents the suitable locations for concentrated solar power (CSP) plant in Sri Lanka. In this work, based on the district wise DNI, three districts have been identified as potential contenders for CSP plants. The suitable locations have been identified based on four criterions: DNI, distance to the water resources, wind speed and topography. Analytical Hierarchy Process (AHP) has been used for assessment of potential zones within the districts. Geographical Information system (GIS) has been used to present the four attribute values of the districts. At the end of this study, based on the results of the AHP the entire land area of the three districts has been divided into four: most suitable, suitable, moderate and not suitable. The land areas of these districts are illustrated graphically with different colours to identify most suitable land area for CSP.

**Keywords:** Concentrated Solar Power (CSP) plant, Direct Normal Irradiation (DNI), Analytical Hierarchy Process (AHP)

## Introduction

Present Sri Lankan electric power system is a hydrothermal one with a small share of energy from renewable sources. As per the long-term generation plan (2018-2037) of Ceylon Electricity Board, demand growth for next ten years has been predicted as 5.4 %. In order to meet this demand new power plants are needed to be introduced to the national grid. On the other hand, remaining potential for new large-scale hydroelectric power plants in the country is limited. Due to high running cost and emission of greenhouse gases construction of new thermal power plants also becomes problematic. Therefore, more attention must be paid for generation of electricity from the alternative sources of energy such as energy from renewable.

Among the renewable sources of energy solar energy is one of the most reliable sources for electricity generation especially for a tropical country like Sri Lanka, where solar irradiance is available throughout the year. As of today considerable amount of solar photovoltaic (PV) has been installed in low voltage distribution systems. However, most of these solar PV contributes only few kilowatts to the national grid. On the contrary, Concentrated Solar Power (CSP) plants, which utilize heat energy of solar radiation are utility-scale power plants which generate electricity even night time using thermal storage system.

Apart from the Direct Normal Irradiation (DNI) requirement, CSP plant locations should satisfy a number of other requirements.

CSP technology is rapidly spreading in many sunniest countries especially in the

Middle-East, North Africa, and Latin America. Most of sunniest countries expect that in future CSP will be one of their main sources of bulk power. In 2017 total installed capacity of CSP was 5.1 GW and It is expected that this number will grow up-to 10 GW by 2022 [1]. There are a number of ongoing projects to construct new CSP plants and it is estimated that by 2030 the contribution from the CSP will be around 7% and by 2050 this will raise up-to 25% [2].

Number of research work has been carried out in many sunniest countries of the world to assess the potential of constructing CSP plants. However, In Sri Lanka still specific studies on centralized CSP plants is few. This study was carried out to assess the possible locations to build CSP plants.

## CSP plants

The CSP plants get the profit of direct irradiation. Direct radiations are the radiations which come directly from the sun without going through clouds or other atmospheric factors. CSP system collects large area of solar irradiation into a small area by using mirrors and lenses with tracking systems. By using the heat energy of concentrated sun light, steam is produced. The energy of heat is converted to mechanical energy either using a conventional steam turbine or using a sterling engine. CSP plants generate electricity during night time by storing the thermal energy which has been collected during the daytime.

CSP plant consists of two main parts. One is collecting sun light and converting it into heat and other one is converting heat energy in to electricity. There are four different CSP systems: parabolic trough, power tower, parabolic dish and linear Fresnel reflector [28]. Each of these types

has different mirror arrangements to collect sun light. Out of these four types, parabolic trough CSP plant is widely used in grid applications.

CSP plants are location specific plants. Other than sufficient solar irradiation which acts as a fuel for the plant, number of other requirements also should be satisfied to construct a CSP plant at a particular location.

### **Direct Normal Irradiation (DNI)**

Since CSP needs heat energy of the sun to covert water or other liquid to steam, DNI at the location is the major requirement. Researchers found that a CSP plant is commercially viable when DNI value is equal or greater than 5.45 kWh/m<sup>2</sup>/day [3]. The capacity of the plant is determined based on the DNI value of the location. DNI value can be obtained from the satellite data or can be measured at the particular location.

The DNI value depends on various factors such as geographic location, time, season, local landscape and local weather. Normally, DNI per day is maximum around 1pm – 3pm. The average DNI value of a very good sunny area where the sun light is falling every day is approximately equal to 6 kWh/ m<sup>2</sup>/day [4]. Sri Lanka is located closer to the equator, therefore receives a supply of solar radiation throughout the year.

### **Water requirement**

The conversion of heat energy to electrical energy in CSP plants is similar to any other type of conventional thermal power plant. Therefore, water is required for converting steam that leaves from turbine to water at the condenser. Apart from this CSP plant needs water for cleaning the mirror surfaces to remove

the dust. In sunny areas there can be more dust in air than other areas. Although DNI values are higher in desert areas, scarcity of water can be a barrier for constructing a CSP plant. Normally, water requirement of CSP plant is about 120 gal/MWh [5]. Therefore, CSP plant should be located at the proximity of source of water such as river, lake, etc.

### **Land requirement**

Large number of concentrated solar collectors needs to be installed to collect heat energy. Therefore, large amount of land area should be available at the CSP location. Land that is not suitable for cultivation and does not have any cultural or historical importance are considered for construction of CSP plants. The land and the area surrounded by the land should be free from trees and any other obstacles. Therefore, effect to the environment also should be considered while selecting the land.

### **Topography**

Two factors are considered under topography: land slope and aspect. The land slope or the flatness of the land affects to the quantity of the sun light captured by mirrors. Different CSP technologies have different conditions regarding the land. For example, parabolic through plant tolerate up to 20 slope of the land and Fresnel reflector plant can tolerate up to 50 slope of the land [6]. Aspect is the azimuth angle. It is the compost direction that slope faces. It can have a strong influence on temperature. Normally a Typical CSP plant requires about 5 – 10 acres of land to generate one megawatt [6]. In addition to this more land is required for thermal storage.

Before selecting a land, long term data should be analyzed to ensure the meteorological background of the area. Strong tendencies of rain, flooding and strong winds can directly affect the power generation. In general, deserts are considered as ideal lands for CSP, if water requirement is met by some means.

### **Wind speed**

When considering the CSP plants, wind availability has negative effect. In CSP plants, flat thin mirrors are located according to a specified angle to concentrate sun light more efficiently. High speed wind can harm those mirrors and can change the mirror angle by attaching to flat surface of mirrors. The tendency of covering mirrors with dust is increasing with wind speed. Apart from this wind causes some thermal losses as well. This means presence of wind reduces the system efficiency

### **Methodology**

The suitable locations for CSP plant need to be determined by considering number of facts, the importance of which are different. This study proposes to use Analytical hierarchy process (AHP) for determination of land suitability.

### **Analytic hierarchy process (AHP)**

AHP is a structured technique proposed by T.L. Saaty (1980) which is used to resolve highly complex decision-making problems involving multiple scenarios, criteria and factors. In AHP there are four step methodologies: modeling, valuation, prioritization and synthesis. At the modeling stage, a hierarchy is constructed including all criteria and the goal which is placed at the top of the hierarchy. After identification of the

criteria those criteria should be weighted considering the relative importance in relation to the desired target. Each criterion should be multiplied by its associated criteria suitability factor to get the result.

In this study AHP was used to determine importance of each of criteria that influences the location of the CSP plant. The influence of each of the criteria has been quantified by assigning a weight to the criteria depending on its importance. This process includes:

- Formulation of pair wise matrix
- Establishment of the relative weight of each of the criteria
- Checking for consistency

### **Calculation of weights and consistency**

All criterions in decision making do not have the same importance. Therefore, relative priorities should be considered. For this purpose Saaty's 9 point weighting scale shown in table 1 was used [7]. The process of converting data to numeric scale is most commonly called standardization.

All the criterions were weighted depending on the importance of criteria for location identification and pair wise comparison matrix has been formed. Saaty's nine-point weight scale given in table 1 has been used for the determination of the weights for the criterion. These judgments were entered into the pair wise comparison matrix. The criterion weights are the average values of the respective row in normalized matrix. To obtain the weight sum vector, each cell in pair wise matrix was multiplied by the relevant criterion weights and the addition of the cells in

the relevant row was calculated. Consistency vector can be determined by dividing weight sum vector by criterion weight. The consistency index (CI) that provides a measure of departure from consistency was calculated by using equation 1.

$$CI = ((\lambda - n)) / ((n - 1)) \quad (1)$$

Where,  
 $\lambda$  = Average value of the consistency vector  
 n = Number of criteria

Table 1: Saaty's nine point weighting scale [7].

| Description of preference  | Scale |
|----------------------------|-------|
| Equally                    | 1     |
| Equal to moderately        | 2     |
| Moderately                 | 3     |
| Moderately to Strongly     | 4     |
| Strongly                   | 5     |
| Strongly to very strongly  | 6     |
| Very strongly              | 7     |
| Very strongly to extremely | 8     |
| Extremely                  | 9     |

The goodness of the CI is determined by using consistency ratio (CR). This was calculated with the help of random index (RI) as shown in equation 2.

$$CR = CI/RI \quad (2)$$

RI is the CI of randomly generated pair wise comparison matrix of order 1 to 10, which is obtained by approximating random indices using a sample size of 500 [8]

### Land suitability index calculation

In this study four attributes have been considered for determination of land suitability for CSP plants. They are:

- DNI
- distance to water resource
- wind speed
- land slope.

For a range of values of each of the attributes, relative weights have been assigned using Saaty's nine-point weighting scale. Pair wise comparison has been carried out to determine criterion weight for each of the attribute.

The land suitability index is determined by getting sum of multiplications of weight assigned to alternative by weight assigned to criteria as below equation 3 [9].

$$\text{Suitability} = \sum Wi * Xi \quad (3)$$

Where,  
 $Wi$  = Weight assign to alternative  
 $Xi$  = Weight assign to criteria

For the attributes listed above pair wise comparison matrix has been formed. This is shown in table 3. Weights for each of the attributes have been assigned using Saaty's nine point weighting scale. Criterion weight, weight sum vector and consistency vector for these attributes have been calculated and given in table 4 The consistency index (CI) is based on this  $\lambda$ . If the pair wise comparison matrix is consistent,  $\lambda$  should be equal or greater than number of criteria. The calculation shows that CI is zero.

For this case RI is equal to 1.12 [20]. In pair wise comparison consistency ratio (CR) should be less than 0.01 [7]. CR is calculated in equation (3)

$$CR = 0 / 1.12 = 0$$

CR < 0.01 shows that the weights are consistent

### Geographic information system

Geographic Information System (GIS) is a computer based tool that analyzes, stores, manipulates and visualizes geographic information usually in a map. GIS enables mapping and analyze the factors affecting to CSP plants location such as direct normal irradiation, land slope and wind speed. GIS provides rich and flexible medium for visualizing and integrating with geographic data. It has many functions for portraying attribute distribution and transforming spatial objects.

Table 2: DNI values of the districts in Sri Lanka(power.larc.nasa.gov, 2018).

| Area         | Annual average DNI<br>(kWh/m <sup>2</sup> /day) |
|--------------|---|
| Vavunia      | 5.45  |
| Mannar       | 5.92  |
| Puttalam     | 5.92  |
| Polonnaruwa  | 4.96  |
| Kurunagala   | 4.31  |
| Matale       | 4.31  |
| Batticaloa   | 4.39  |
| Kandy        | 4.31  |
| Ampara       | 4.39  |
| Gampaha      | 5.63  |
| Kegalle      | 4.31  |
| Nuwara Eliya | 4.03  |
| Badulla      | 4.4   |
| Colombo      | 5.42  |
| Kalutara     | 5.42  |
| Rathnapura   | 4.03  |
| Moneragala   | 4.4   |
| Galle        | 4.3   |
| Matara       | 4.03  |
| Hambantota   | 4.4   |

### Results and Discussion

In order to determine the suitable locations for CSP, DNI values of number of districts have been obtained. This is shown in table 2.

Since the commercial CSP is possible only in areas in which DNI is greater than 5.45 kWh/m<sup>2</sup>/day [3], for further investigation three districts which have highest DNI values have been selected.

- Puttlam
- Mannar
- Vavunia

Other than higher value of DNI, in these three districts population density is low [25] and most of the land is flat and not suitable for agricultural purposes. Therefore, these three districts have been selected for identifying most suitable locations for CSP plants.

DNI, land slope, distance to water resource and wind speed have been obtained for these districts. The variation of these values with the help of GIS software are obtained. They are shown in figures 1, 2, 3, 4 (Puttlam) 5, 6, 7, 8 (Mannar) 9, 10, 11 and 12 (Vavunia).

### Calculation of land suitability index

For each attribute rating has been assigned based on the range of values of the attributes. The weights for each range has been calculated similar to the pairwise matrix calculation described above. This is given in table 5. Land suitability index has been calculated according to the equation 4.

Graphically the suitability of lands in these three districts are shown in figures 13, 14 and 15.

*Table 3: Pairwise comparison matrix*

| <b>Criteria</b>                   | <b>DNI</b> | <b>Land availability</b> | <b>Wind speed</b> | <b>Distance to water resource</b> | <b>Topography</b> |
|-----------------------------------|------------|--------------------------|-------------------|-----------------------------------|-------------------|
| <b>DNI</b>                        | 1          | 3                        | 9                 | 6                                 | 7                 |
| <b>Land availability</b>          | 1/3        | 1                        | 9/3               | 6/3                               | 7/3               |
| <b>Wind speed</b>                 | 1/9        | 3/9                      | 1                 | 6/9                               | 7/9               |
| <b>Distance to water resource</b> | 1/6        | 3/6                      | 9/6               | 1                                 | 7/6               |
| <b>Topography</b>                 | 1/7        | 3/7                      | 9/7               | 6/7                               | 1                 |

*Table 4: Values of consistency vector*

| <b>Criteria</b>                   | <b>Criterion weights</b> | <b>Weight sum vector</b> | <b>Consistency vector</b> |
|-----------------------------------|--------------------------|--------------------------|---------------------------|
| <b>DNI</b>                        | 126/221                  | 630/221                  | 5                         |
| <b>Land availability</b>          | 42/221                   | 210/221                  | 5                         |
| <b>Wind speed</b>                 | 14/221                   | 70/221                   | 5                         |
| <b>Distance to water resource</b> | 21/221                   | 105/221                  | 5                         |
| <b>Topography</b>                 | 18/221                   | 90/221                   | 5                         |

**Puttlam district**

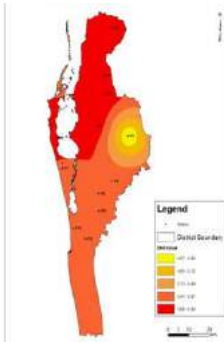


Figure 1: Variation of DNI

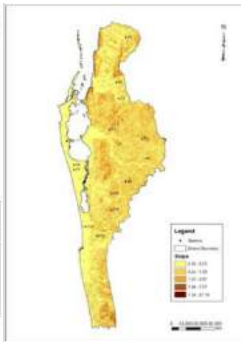


Figure 2: Variation of land slope

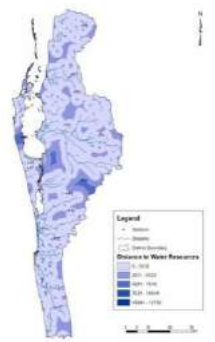


Figure 3: Variation of distance to water resource

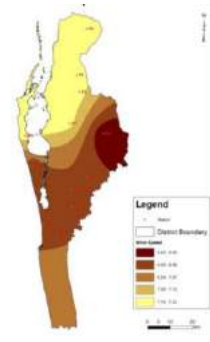


Figure 4: Variation of wind seed

**Mannar district**

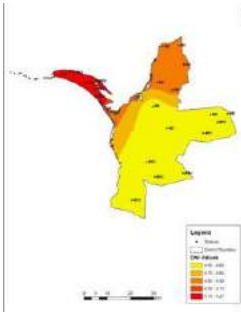


Figure 5: Variation of DNI

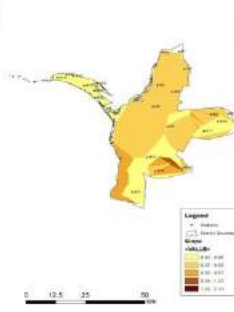


Figure 6: Variation of landslope

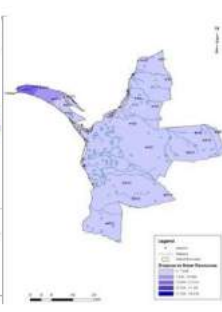


Figure 7: Variation of distance to water resource

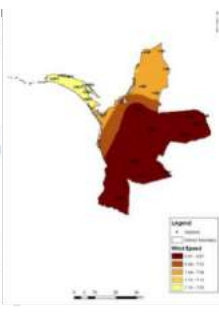


Figure 8: Variation of wind seed

**Vavunia district**

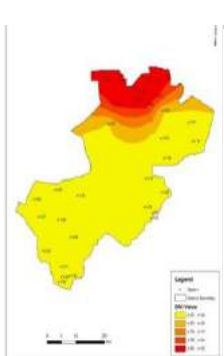


Figure 9: Variation of DNI



Figure 10: Variation of landslope

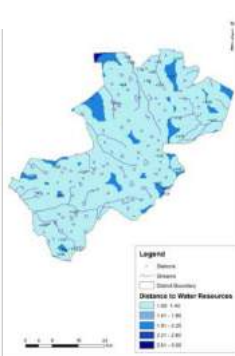


Figure 11: Variation of distance to water resource



Figure 12: Variation of wind seed



Table 5: Calculated weights of attributes

| Criteria                                  | Attribute values                | Ratings | Weights |
|---|---------------------------------|---------|---------|
| <b>DNI<br/>(kWh/m<sup>2</sup>/day)</b>    | 4-3                             | 1       | 0.4380  |
|   | 4-5                             | 2       | 0.2190  |
|   | 5-6                             | 3       | 0.1460  |
|   | 6-7                             | 4       | 0.1095  |
|   | 7-8                             | 5       | 0.0876  |
| <b>Value of land</b>                      | Cultivated land                 | 0       | 0       |
|   | Bare land                       | 9       | 0.5373  |
|   | Natural vegetation              | 4       | 0.2687  |
|   | Near urban area                 | 2       | 0.1343  |
|   | Near cities                     | 1       | 0.0597  |
| <b>Wind speed<br/>(m/s)</b>               | 5.66-5.778                      | 9       | 0.35    |
|   | 5.778-5.956                     | 8       | 0.17    |
|   | 5.956-6.134                     | 7       | 0.11    |
|   | 6.134-6.312                     | 6       | 0.09    |
|   | 6.312-6.49                      | 5       | 0.07    |
|   | 6.49-6.668                      | 4       | 0.06    |
|   | 6.668-6.846                     | 3       | 0.05    |
|   | 6.846-7.024                     | 2       | 0.04    |
|   | 7.024-7.202                     | 1       | 0.04    |
| <b>Distance to water resource<br/>(m)</b> | 130-2055                        | 9       | 0.35    |
|   | 2055-3980                       | 8       | 0.17    |
|   | 3980-5905                       | 7       | 0.11    |
|   | 5905-7830                       | 6       | 0.09    |
|   | 7830-9755                       | 5       | 0.07    |
|   | 9755-11680                      | 4       | 0.06    |
|   | 11680-13605                     | 3       | 0.05    |
|   | 13605-15530                     | 2       | 0.04    |
|   | 15530-17455                     | 1       | 0.04    |
|   | <b>Land slope<br/>(degrees)</b> | 0-0.1   | 9       |
| 0.1-0.2                                   |                                 | 8       | 0.17    |
| 0.2-0.3                                   |                                 | 7       | 0.11    |
| 0.3-0.4                                   |                                 | 6       | 0.09    |
| 0.4-0.5                                   |                                 | 5       | 0.07    |
| 0.5-0.6                                   |                                 | 4       | 0.06    |
| 0.6-0.7                                   |                                 | 3       | 0.05    |
| 0.7-0.8                                   |                                 | 2       | 0.04    |
| 0.8-0.9                                   |                                 | 1       | 0.04    |
| <b>Aspect</b>                             | 0-22.5 (North)                  | 1       | 0.43    |
|   | 22.5-67.5<br>(Notheast)         | 2       | 0.21    |
|   | 67.5-112.5 (East)               | 4       | 0.1     |
|   | 112.5-157.5<br>(Southeast)      | 7       | 0.07    |

|                            |   |      |
|----------------------------|---|------|
| 157.5-202.5<br>(South)     | 9 | 0.06 |
| 202.5-247.5<br>(Southwest) | 8 | 0.05 |
| 247.5-292.5 (West)         | 6 | 0.04 |
| 337.5-360<br>(Northwest)   | 2 | 0.21 |

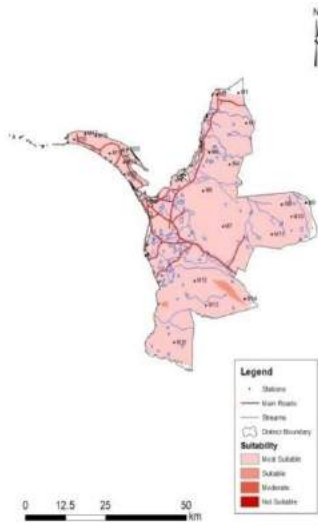


Figure 13: Suitability of selected areas in Mannar district

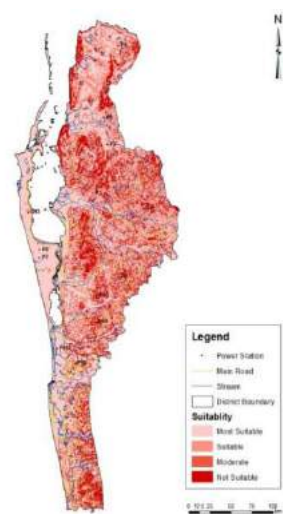


Figure 14: Suitability of selected areas in Puttalam district

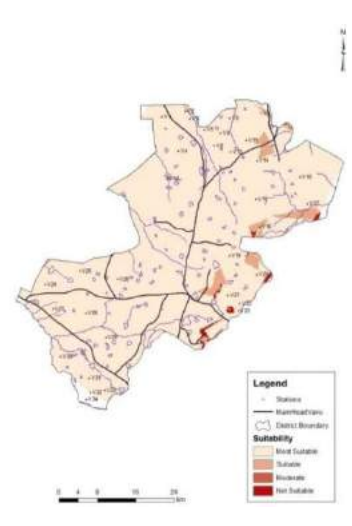


Figure 15: Suitability of selected areas in Vavunia district

## Conclusion

This study shows that in Sri Lanka there are three districts which have potential locations for CSP plants. DNI values of these three districts are sufficient to build commercially viable plants. Land suitability index and graphical representation of suitability of the lands based on the index shows that most of the areas of these districts are good for CSP plants. As it has been revealed in this work the low population density and non-suitability of lands for agricultural purposes provide more population density and non-suitability of lands for agricultural purposes provide more space of the land to construct CSP plants. At the mean time more specific studies need to identify the optimum land area for high capacity CSP. High capital cost and technology may be two barriers for introduction of CSP plants to the national grid. However, the augmentation of some of the existing hydrothermal plants in future can be replaced by the CSP.

## Acknowledgments

Authors wish to gratefully acknowledge Dr. Narendra De Silva, Dr. Gihan Dahanayake and Mrs Kumudu Senanayake for their support at the various stages of this study.

## References

- [1] Govinda R. Timilsina Lado Kurdgelashvili Patrick A. Narbel (2011). A Review of Solar Energy on Web [Online]. Available at <http://documents.worldbank.org/curated/en/546091468178728029/pdf/WPS5845.pdf> Accessed on 26th October 2019.
- [2] DEWA Awards AED14.2 Billion Concentrated Solar Power Project with a Record Bid of USD 7.3 Cents Per kW/h to Generate 700MW Web [Online]. Available at <http://helioscsp.com> Accessed on 26th October 2019.
- [3] Ziuku, S, Seytini, L, Mapurisa, B, Chikodoski, D, Koen Van Kuijk. Brayer and Kines. (2009). Potential of concentrated solar power (CSP) in Zimbabwe, Energy for sustainable development.
- [4] Direct Normal Irradiance on Web [Online]. Available at <http://www.suncyclopedia.com> Accessed on 26th October 2019.
- [5] [www.e-education.psu.edu](http://www.e-education.psu.edu)(2005): utility solar power and concentration on Web [Online]. Available at: <https://www.e-education.psu.edu/eme812/node/780> Accessed on 26th October 2019.
- [6] Concentrating Solar Power on Web [Online]. Available at <https://www.seia.org/initiatives/concentrating-solar-power> Accessed on 26th October 2019.
- [7] V.D.Patil , R.N.Sankhua, R.K.Jain (2012). Analytical Hierarchy Process Framework for Residential Land Use Suitability using Multi-Criteria Decision Analysis.
- [8] Thomas L. Saaty (2008). Decision making with the analytic hierarchy process.
- [9] Sadeeka Layomi, Lalit Kumar, Janaki Sandamali. Assessment of Potential Land Suitability for Tea (*Camellia sinensis* (L.) O. Kuntze) in Sri Lanka Using a GIS-Based Multi-Criteria Approach; 2019.
- [10] Pant Birendra P. and Poudyal Khem (2017). Evaluation of global solar radiation with single and multiple parameter models in midwestern region Jumla, Nepal
- [11] AArora, P.R. (2013). A vital role of concentrating solar power plants of Rajasthan in future electricity demand of India. International Journal of scientific and research publications, volume 3, Issue 6, June 2013, ISBN 2250 – 3153
- [12] [www.nrel.gov](http://www.nrel.gov) (2014). Concentrating solar power projects on Web [Online]. Available [https://www.nrel.gov/csp/solarpaces/project\\_detail.cfm/projectID=264](https://www.nrel.gov/csp/solarpaces/project_detail.cfm/projectID=264) Accessed on 26th October 2019.
- [13] Kevin Ummel(2010). Concentrating solar power in China and India. A spatial analysis of technical potential and the cost of development.
- [14] Power data access viewer (2018) on Web [Online]. Available at

<https://power.larc.nasa.gov/data-access-viewer/> Accessed on 26th October 2019.

[15] Hala Adel effat (2016), Mapping solar energy potential zones, using SRTM and spatial analysis, Application in Lake Nassar Region, Egypt.

[16] Mahsa Liaghat (2013), A multicriteria evaluation using the analytic hierarchy process technique to analyze coastal tourism sites.

[17] E.M. Asanka Jayasundara, K.A.C. udayakumar (2017). Feasibility study of concentrating solar power plant for Sri Lanka.

[18] Helmul Flitter, Robert Weibel, Stephanie Rogers (2014). Introduction to spatial analysis Web [Online]. Available at <http://www.gitta.info/AnalyConcept/en/text/AnalyConcept.pdf> Accessed on 26th October 2019.

[19] Arina Mardoukhi, Nima Kordzadeh (2016). Site location determination using Geographic Information Systems,

[20] Morocco's megawatt solar plant powers up on Web [Online]. Available at

<https://edition.cnn.com/2016/02/08/africa/ouarzazate-morocco-solar-plant/index.html> Accessed on 26th October 2019.

[21] Solar Thermal for Electricity on Web [Online]. Available at <https://greenterrafirma.com/solar-thermal-for-electricity.html> Accessed on 26th October 2019.

[22] J.R Eastman (1993). A procedure for multi-objective decision making in GIS under conditions of conflicting objectives

[23] J R EASTMAN. Multi-criteria evaluation and GIS

[24] Department of Census and Statistics Sri Lankan Web [Online]. Available at <http://www.statistics.gov.lk/> Accessed on 26th October 2019.

[25] Mladen Bosnjakovic(2019). Environment impact of a concentrated solar power plant.

[26] Concentrating Solar Power (CSP) – Technology Web [Online]. Available at <https://energypedia.info> Accessed on 26th October 2019.

# The Effect of Electricity Supply on Economic Growth in Sri Lanka

Peiris W.L.T. <sup>#1</sup>, Kiriella K.K.C.S. <sup>#2</sup>, Samarasingha K.A.T.B. <sup>#3</sup>, Samarakoon W.H.A. <sup>#4</sup>, Wijayapala W.D.A.S. <sup>#5</sup>, Dias M.P. <sup>#6</sup>

*# Department of Electrical Engineering*

*University of Moratuwa, Katubedda, Moratuwa, Sri Lanka.*

<sup>1</sup>lemashapeiris7@gmail.com, <sup>2</sup>chandikasudul@gmail.com,

<sup>3</sup>buddhika.kt92@gmail.com, <sup>4</sup>warunahasun@gmail.com

<sup>5</sup>anuraw@uom.lk, <sup>6</sup>prinathd@yahoo.com

## Abstract

**This research applies two econometric models, Vector Error Correction Model (VECM) and simple econometric model developed by H.Y. Yang (2000), for testing the presence of a long-term relationship between Gross Domestic Product (GDP) and Electricity Consumption in Sri Lanka for the period 1985-2015. Results obtained from both models have been compared and the findings show that the electricity supply has a significant impact on the real GDP growth. According to the results of Granger Causality test, Sri Lanka has a bi-directional long-term relationship between Electricity Consumption and Real GDP.**

**Keywords:** Econometric Model, Electricity Consumption, GDP, Sri Lanka.

## Introduction

Energy, especially electrical energy is one of the key factors that affect economic growth. Electricity is a crucial factor for both developing and developed countries, in achieving and maintaining economic development. Electricity consumption leads to improved productivity and industrial growth and has a direct impact on economic growth.

The relationship between economic growth and electricity consumption of a country depends on the condition of the economy and its economic structure. The causal relationship between these two factors can be categorized as: no causality, unidirectional causality and bi-directional causality. And this can further be categorized as long-term causality and short term causality.

Sri Lankan electricity utilities are operated as a vertically integrated monopoly system. Except for a few power generating units built owned and operated by the private sector, utilities engaged in electricity generation, transmission, distribution and sales are owned by the Government. Due to this direct ownership of the Government, all investments needed for the electricity sector are made by the Government, the prices are set by the Government and all the revenue goes to the Government.

This study is on the effect of electricity supply on the economic growth. The results of this study demonstrate that the investments in electricity sector, though quantitatively large, are fully justified. The causal relationship between economic growth and electricity consumption identified in this research will help the policy makers to take appropriate decisions. Further the results

presented in this paper will be very useful in macroeconomic planning.

## Literature Review

There are very few publications on the relationship between economic growth and electricity consumption in Sri Lanka. R Morimoto and C Hope studied the impact of electricity supply on economic growth from 1960 to 1998 using the model developed by Yang (2000) who found the bi-directional causal relationship in Taiwan for the period of 1954 – 1957. R. Morimoto and C. Hope found that the current and past changes in electricity supply have a significant impact on the economic growth in Sri Lanka. They predicted that for every 1 MWh increase in electricity supply there is an increase in the economic output in the range of LKR 88,000 to 137,000 [1].

Another research study was carried out by Zahid Asghar under the title “Energy GDP Relationship: A causal analysis for five countries of South Asia”. This study investigated causal relationship between GDP and Energy Consumption in five South Asian countries, namely; Pakistan, India, Sri Lanka, Bangladesh and Nepal by using Toda Yamamoto (1995) approach and error correction model. The study found that the electricity consumption and GDP are co-integrated and there is long-term relationship of unidirectional causality from GDP to electricity consumption. The study notes that Sri Lanka has a less energy dependent economy and energy conservation policies have opposite effects [2].

In 1998 Masih and Masih conducted a research for Sri Lanka by applying Johansen’s co-integration tests. Using a trivariate Vector Error Correction Model (VECM) they found the impact of energy

consumption on economic growth. They used energy consumption, real income and price levels and showed that energy consumption is relatively exogenous and it directly influences income and prices of consumer goods [3].

Other literature referred in this study on electricity consumption and economic growth for other countries are in references [4] to [13]. These studies cover both developing as well as developed countries.

## Methodology

This study was conducted using time series data of Electricity Consumption and the Gross Domestic Product (GDP) for the period of 1985 to 2015. Reliable data on electricity consumption and GDP were obtained from the Ceylon Electricity Board (CEB) and the Central Bank of Sri Lanka (CBSL) respectively. Analysis was carried out under four scenarios to check the significance of the impact of the electricity consumption on the economic growth in Sri Lanka. The four scenarios analysed were; Total Electricity Consumption and Total Real GDP, Industrial Sector Electricity Consumption and Industrial Sector Real GDP, Commercial Sector Electricity Consumption and Service Sector Real GDP, Industrial plus Commercial Sector Electricity Consumption and Industrial plus Service Sector Real GDP.

Several econometric models such as Auto Regressive (AR), Moving Average (MA),

Auto Regressive Moving Average (ARMA), Auto Regressive Integrated Moving Average (ARIMA), Auto regressive Distributed Lag (ARDL), Vector Auto Regressive (VAR) and Vector Error Correction Model (VECM), were tested in the Sri Lankan context and the VECM model was selected as the best model to perform the time series analysis for the Sri Lankan data. Raw data should not be stationary and all the data should be integrated in same order to perform the Vector Error Correction Model (VECM). The VECM model is described by the Equation 1.

$$\Delta \text{GDP}_t = C_1(\text{GDP}_{t-1} + \alpha \times \text{ELECT}_{t-1} + \beta) + \sum_{i=1}^n a_i \times \Delta \text{GDP}_{t-i} + \sum_{j=1}^n b_j \times \Delta \text{ELECT}_{t-j} + E_t \quad (1)$$

Where;

$\Delta \text{GDP}_t$  = First differenced real GDP at time t

$\Delta \text{ELECT}_{t-i}$  = First differenced electricity consumption at time t-i

$E_t$  = Error term  $\alpha$ ,  $\beta$ ,  $a_i$ ,  $b_j$ ,  $C_1$  are coefficients

### Scenario 1: Total Electricity Consumption and Total Real GDP

Augmented Dickey-Fuller (ADF) test was used to check the stationarity of the  $\Delta \text{GDP}$  and  $\Delta \text{ELECT}$ . Both are significant at 5% level and the summary of the test results are shown in the Table 1 and Table 2 respectively.

Table 1: Test Results for  $\Delta GDP$ 

|  | t - Statistic    | Probability |
|--|------------------|-------------|
| <b>Augmented Dicky - Fuller Test Statistic</b> | -5.0108          | 0.0019      |
| <b>1% Level</b>                                | -4.3098          |             |
| <b>Test Critical Values:</b>                   | <b>5% Level</b>  | -3.5742     |
|  | <b>10% Level</b> | -3.2217     |

Table 2: Test Results for  $\Delta ELECT$ 

|  | t - Statistic    | Probability |
|--|------------------|-------------|
| <b>Augmented Dicky - Fuller Test Statistic</b> | -6.9378          | 0.0000      |
| <b>1% Level</b>                                | -4.3393          |             |
| <b>Test Critical Values:</b>                   | <b>5% Level</b>  | -3.5875     |
|  | <b>10% Level</b> | -3.2292     |

Johanson co-integration test was used to check whether there is a long-term relationship between the total real GDP and total electricity consumption. It was also significant at 5% level. Results of the Johanson co-integration test for the 1<sup>st</sup> scenario is shown in Table 3.

obtained by using the Akaike's final prediction error criterion. Akaike info Criterion for the 1<sup>st</sup> scenario is 27.66 and Schwarz criterion is approximately 28.25. According to these criteria optimum time lag for Total Electricity Consumption and Total GDP become 5 years.

After performing the unit root test and Johanson co-integration test, the optimal time lag for the econometric model was

The econometric model obtained for t, GDP and Electricity consumption of the 1<sup>st</sup> scenario are given in Table 4.

Table 3: Johanson Co-integration Test

| Hypothesized No. of CE(s) | Eigen value | Trace Statistic | 0.05 Critical Value | Probability ** |
|---------------------------|-------------|-----------------|---------------------|----------------|
| <b>None *</b>             | 0.548       | 32.523          | 15.494              | 0.0001         |
| <b>At most *</b>          | 0.336       | 11.063          | 3.841               | 0.0009         |

Trace test indicates 2 co-integrating eqn(s) at the 0.05 level  
 \*denotes rejection of the hypothesis at the 0.05 level  
 \*\*Mackinnon-Haug-Michelis (1999) p – values



Table 4: Econometric Model for Scenario 1

| $D(\text{GDP}) = C(1) * (\text{GDP}(-1) - 738.1 * \text{ELEC}(-1) - 628583.1) + C(2) * D(\text{GDP}(-1)) + C(3) * D(\text{GDP}(-2)) + C(4) * D(\text{GDP}(-3)) + C(5) * D(\text{GDP}(-4)) + C(6) * D(\text{GDP}(-5)) + C(7) * D(\text{ELEC}(-1)) + C(8) * D(\text{ELEC}(-2)) + C(9) * D(\text{ELEC}(-3)) + C(10) * D(\text{ELEC}(-4)) + C(11) * D(\text{ELEC}(-5)) + C(12)$ |             |                |                              |             |
|---|-------------|----------------|------------------------------|-------------|
|   | Coefficient | Standard Error | t-Statistic                  | Probability |
| C(1)  | -1.246      | 0.393          | -3.167                       | 0.0074      |
| C(2)  | 0.755       | 0.353          | 2.138                        | 0.0520      |
| C(3)  | 1.616       | 0.362          | 4.461                        | 0.0006      |
| C(4)  | 1.847       | 0.538          | 3.432                        | 0.0045      |
| C(5)  | 1.411       | 0.628          | 2.246                        | 0.0427      |
| C(6)  | 0.900       | 0.563          | 1.597                        | 0.1341      |
| C(7)  | -1230.9     | 463.8          | -2.653                       | 0.0199      |
| C(8)  | -1930.7     | 486.5          | -3.967                       | 0.0016      |
| C(9)  | -1773.6     | 623.9          | -2.842                       | 0.0139      |
| C(10)   | -733.5      | 629.4          | -1.165                       | 0.2648      |
| C(11)   | -210.8      | 494.8          | -0.426                       | 0.6770      |
| C(12)   | 355255.2    | 166143.6       | 2.138                        | 0.0521      |
| <b>R-squared 0.768</b>  |             |                | Mean dependent var 346849.9  |             |
| <b>Adjusted R-squared 0.572</b>   |             |                | S.D Dependent var 322271.4   |             |
| <b>S.E of Regression 210727.4</b>   |             |                | Akaike info criterion 27.6   |             |
| <b>Sum squared residual 5.77E+11</b>  |             |                | Schwarz criterion 28.2       |             |
| <b>Log likelihood -333.75</b>   |             |                | Hanan-Quinn criterion 27.8   |             |
| <b>F-statistic 3.9</b>  |             |                | Durbin Watson statistics 1.8 |             |

Thus, the econometric model for the 1<sup>st</sup> Scenario is,

$$\Delta \text{GDP}_t = -1.25(\text{GDP}_{t-1} - 738.17 \times \text{ELECT}_{t-1} - 628585.93) + \sum_{i=1}^5 a_i \times \Delta \text{GDP}_{t-i} + \sum_{j=1}^5 b_j \times \Delta \text{ELECT}_{t-j} + E_t \quad (2)$$

Durbin-Watson test was performed to check whether there is an auto-correlation in the model. To satisfy the Durbin-Watson test, the value should be close to 2. The Durbin-Watson value obtained for 1<sup>st</sup> scenario econometric model was 1.84.

In order to verify the models developed using VECM are satisfactory, the following four specific statistical tests were performed on each model.

- Wald test
- Heteroscedasticity test
- Normality test
- Serial correlation LM test

Table 5 shows the Wald test results for the analysis between the total electricity consumption and total real GDP. Chi-square values are significant in the above case, which mean that the null hypothesis can be rejected at 5% confidence interval.

Table 6 shows the results of the heteroscedasticity test performed for the above model. Chi-square value shows

more than 5% and this reveals that the model has homoscedasticity which is good. Heteroscedasticity test is used to check whether the variance of the model is a time function.

Figure 1 shows the results of the normality test performed for the total electricity consumption and total GDP. The bell shape can be seen in the residual series. The probability value of 0.974 reveals that it is a good model.

Serial Correlation LM test is used for finding the auto correlation of errors in the regression model. A test statistic is derived from use of residuals considering regression analysis.

Table 5: Wald test results

| Wald Test   |        |        |             |
|---|--------|--------|-------------|
| Test Statistic  | Value  | Df     | Probability |
| F-Statistic   | 5.043  | (5,13) | 0.0087      |
| Chi-Square  | 25.216 | 5      | 0.0001      |
| <b>Null Hypothesis : C(7) = C(8) = C(9) = C(10) = C(11) = 0</b> |        |        |             |

Table 6: Heteroscedasticity test results

| Heteroscedasticity Test Breusch-Pagan-Godfrey |        |                      |       |
|---|--------|----------------------|-------|
| F-Statistic                                   | 1.616  | Prob.F(12,12)        | 0.208 |
| Obs*R-squared                                 | 15.443 | Prob.Chi-Square [12] | 0.218 |

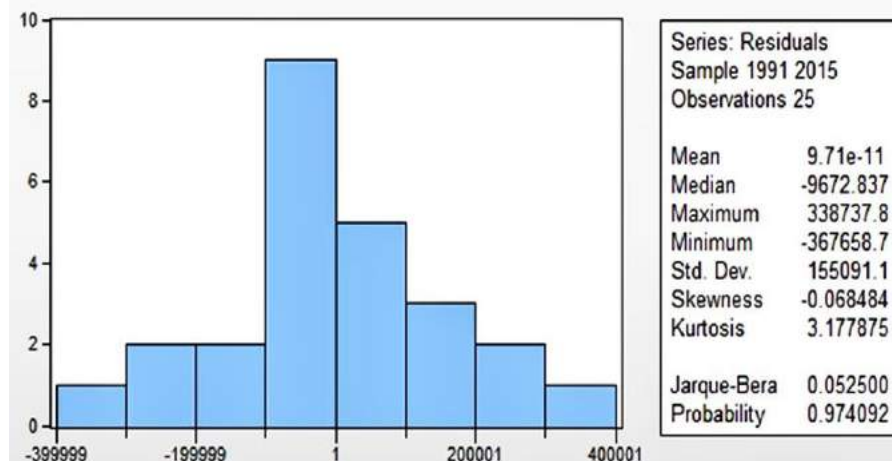


Figure 1: Normality Test

Table 7: Serial Correlation LM test

| <b>Breush-Godfrey Serial Correlation LM Test</b> |        |                    |       |
|--|--------|--------------------|-------|
| <b>F-statistic</b>                               | 1.837  | Prob.F(5,8)        | 0.211 |
| <b>Obs*R-squared</b>                             | 13.364 | Prob.Chi-Square[5] | 0.020 |

Figure 2 shows the validation of the model for the scenario 1 comparing the model output with the actual values. Following a similar procedure as in

Scenario 1, models for the following three additional scenarios were developed and tested.

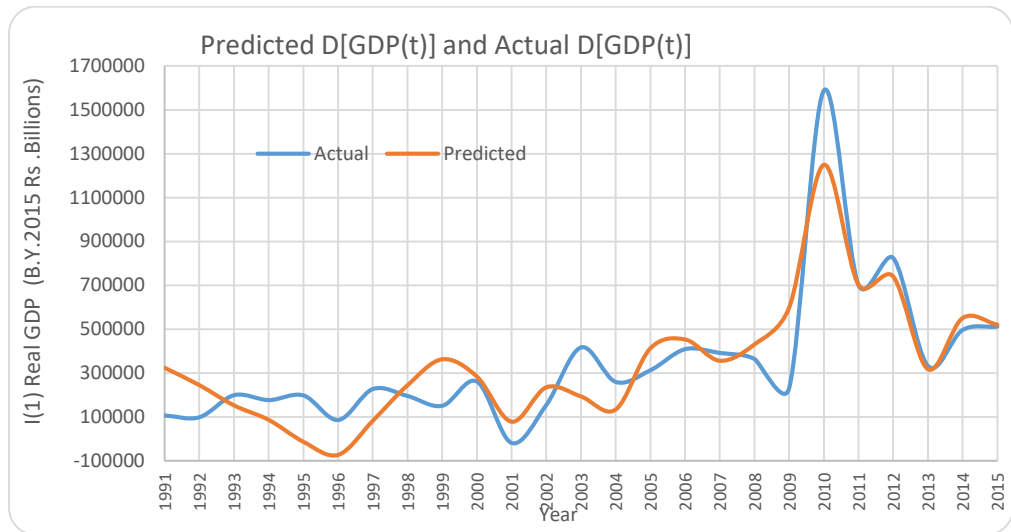


Figure 2: Model for Scenario 1 ( $R^2 = 0.77$ )

**Scenario 2: Industrial sector Electricity consumption and Industrial sector GDP**

**Model**

$$\Delta GDP_t = 0.05(GDP_{t-1} + 1744.81 \times ELECT_{t-1} - 5310230.37) + \sum_{i=1}^3 a_i \times \Delta GDP_{t-i} + \sum_{j=1}^3 b_j \times \Delta ELECT_{t-j} + E_t \quad (3)$$

**Model Output**

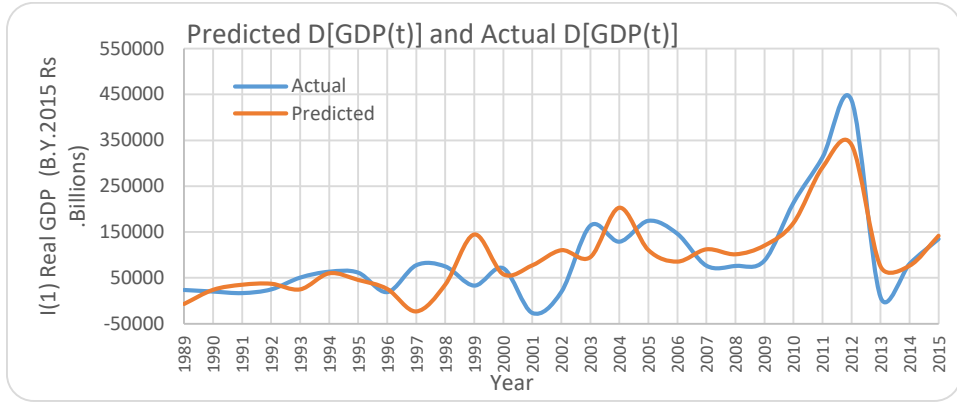


Figure 3: Model for Scenario 2 (R2= 0.68)

**Scenario 3: Commercial Sector Real Electricity Consumption and Service Sector Real GDP**

**Model**

$$\Delta GDP_t = -0.84(GDP_{t-1} - 2037.86 \times ELECT_{t-1} + 99937.98) + \sum_{i=1}^3 a_i \times \Delta GDP_{t-i} + \sum_{j=1}^3 b_j \Delta ELECT_{t-j} + E_t \quad (4)$$

**Model Output**

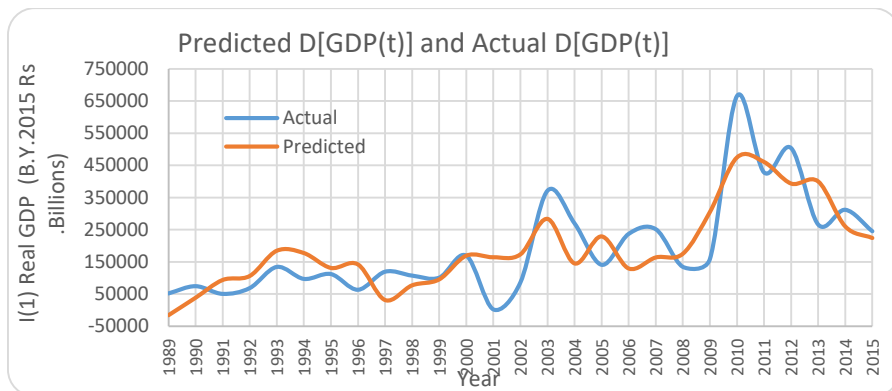


Figure 4: Model for Scenario 3 (R2 = 0.66)

## Scenario 4: (Industrial + Service) Sector GDP and (Industrial + Commercial) Sector Electricity.

### Model

$$\Delta GDP_t = -1.2(GDP_{t-1} - 686.68 \times ELECT_{t-1} - 1844863.37) + \sum_{i=1}^6 a_i \times \Delta GDP_{t-i} + \sum_{j=1}^6 b_j \times \Delta ELECT_{t-j} + E_t \quad (5)$$

### Model Output

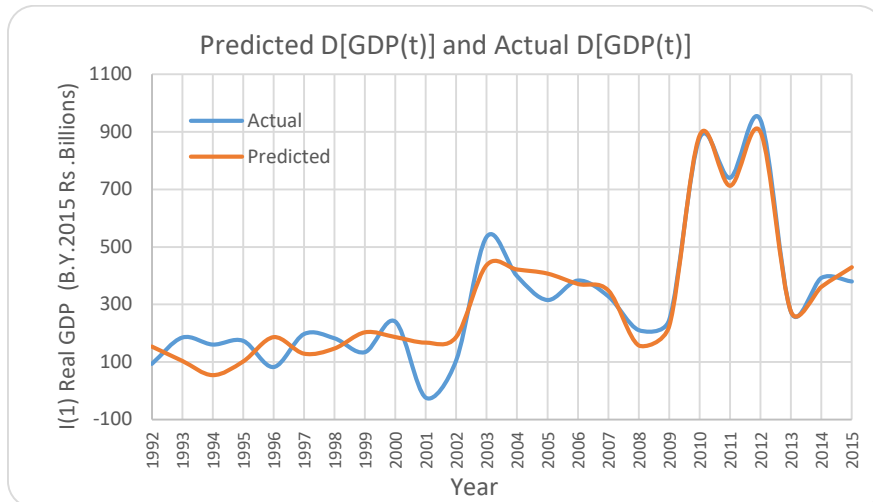


Figure 5: Model for Scenario 4 (R2 = 0.91)

### Conclusion

This study made a comprehensive examination of the impact of electricity supply on economic growth in Sri Lanka for the period 1985-2015, using Vector Error Correction Model (VECM). The findings show that the electricity supply has a significant impact on the real GDP growth.

According to the results of Granger Causality test, Sri Lanka has a bi-directional long term relationship between Electricity Consumption and Real GDP.

When the results of this study are compared with the model developed by H.Y Yang (2000) it can be seen that the

predicted ranges are approximately same and the results of the VECM match with the model developed by H.Y Yang (2000). These findings can be used to estimate the increase in economic output per unit increase of electricity supply in Sri Lanka.

The calculated growth in economic output per GWh of increase in electricity supply for model developed by H.Y Yang and the model developed under this study using VECM are given in the Table 8.

Sri Lanka faced a 26 year of civil ethnic war from 1983 to 2009, which adversely affected economic development. This was further aggravated by the politically driven insurgency during the period 1986 to 1989.

Table 8: Comparison of Results

|  | Model by H.Y Yang<br>(2000) (MLKR)/GWh | VECM Model Results<br>(MLKR)/GWh |
|--|--|----------------------------------|
| <b>Total GDP and Electricity</b>   | 559.8~ 1156.4                          | 484.6~1354.9                     |
| <b>Industrial GDP and Electricity</b>  | 21.4~484.2                             | 47.3~125.8                       |
| <b>(Industrial + Service) GDP and<br/>(Industrial + Service) Electricity</b> | 688.0~1376.6                           | 578.6~1068.0                     |

Due to restoration of law and order from this political insurgency, economy grew with an average growth rate of 5.5% during 1990 to 1993. In 1996 Sri Lanka faced severe drought and the economic growth declined to 3.8% from 5.5%. Drought in 1996 as well as in several subsequent years caused several hour long power cuts causing severe damages to the country's economic growth because Sri Lankan power system heavily depends on hydro power generation [14].

In 2010 Sri Lankan Economy achieved the highest growth of 8.2% because of end of the civil war. Due to global recession, withdrawal of GSP plus, United State's embargo on trade with Iran and adverse weather conditions [14], in the subsequent years, the economic growth declined.

This study confirms the strong relationship between the economic growth and the country's electricity supply. If Sri Lankan policy makers do not pay sufficient attention to make required investments in electricity sector in time, it will be impossible to maintain a healthy economic growth.

## References

- [1] Morimoto R, Hope C. The impact of electricity supply on economic growth in Sri Lanka. *Energy Economics* 2004, vol. 26, No. 1, pp.77-85.
- [2] Asghar Z. Energy-GDP relationship: a causal analysis for the five countries of South Asia. *Applied Econometrics and International Development* 2008, vol. 8, No. 1.
- [3] Sharmin F, Khan M. A causal relationship between energy consumption, energy prices and economic growth in Africa. *International Journal of Energy Economics and Policy* 2016, vol 6, No. 3.
- [4] *Electricity\_Consumption\_and\_Economic\_Growth\_in\_Emerging\_Economies.pdf*, Available: [http://www.scientificpapers.org/wpcontent/files/1453\\_Yilmaz-](http://www.scientificpapers.org/wpcontent/files/1453_Yilmaz-) [Accessed on 15 Dec 2017]
- [5] Tiwari A. The frequency domain causality analysis between energy consumption and income in the United States. *Economia Aplicada* 2014, vol 18, No 1, pp.51-67.
- [6] Seec.surrey.ac.uk. (2018). Cite a Website - Cite This For Me. [online] Available: <http://www.seec.surrey.ac.uk/Research/SEEDS/SEEDS113.pdf> [Accessed 20 Dec. 2017].
- [7] Ameyaw B, Oppong A, Abruquah L, Ashalley E. Causality Nexus of Electricity Consumption and Economic Growth: An Empirical Evidence from Ghana. *Open Journal of Business and Management* 2017, vol 05, No 1, pp.1-10.

- [8] Aktas C, Yilmaz V. Causal relationship between oil consumption and economic growth in Turkey. Available: <https://pdfs.semanticscholar.org/88e7/34f0c386dc862727b043b22dd1f5958d0a97.pdf> [Accessed 1 Nov. 2019]
- [9] Ruhul S, Rafiq S, Hassan A. Causality and dynamics of energy consumption and output: evidence from non-OECD Asian countries. *Journal of Economic Development* 2008, vol. 33, No 2, pp.1-26.
- [10] Isiarticles.com. (2018). Cite a Website - Cite This For Me. [online] Available: <http://isiarticles.com/bundles/Article/pre/pdf/10975.pdf> [Accessed 22 Jan. 2018].
- [11] Hossain S. Multivariate granger causality between economic growth, electricity consumption, exports and remittance for the panel of three SAARC countries. *European Scientific Journal* 2018, ESJ 8(1).
- [12] Yoo SH, Electricity consumption and economic growth: evidence from Korea. *Fuel and Energy Abstracts* 2005, vol. 46 No 6, p.415.
- [13] Cheng B. An investigation of Cointegration and Causality between Energy Consumption and Economic Growth. *Journal of Energy and Development* 1995, vol. 21.
- [14] Sundaytimes.lk. (2018). Economic development and structural changes since independence | The Sundaytimes Sri Lanka. [online] Available at: <http://www.sundaytimes.lk/140202/columns/economic-development-and-structural-changes-since-independence-81903.html> [Accessed 22 Jan. 2018].

# Sustainable Energy Options for Sri Lankan Transport Sector

Gayashika L. Fernando<sup>#1</sup>, M. Afrath Ruzaik<sup>#2</sup>, Migara H. Liyanage. <sup>#3</sup>

<sup>#</sup>Faculty of Engineering, Sri Lanka Institute of Information Technology,  
Malabe, Sri Lanka

<sup>1</sup>gayashika.f@sliit.lk

<sup>2</sup>afrath455@gmail.com

<sup>3</sup>migara.l@sliit.lk

## Abstract

Transport sector of Sri Lanka accounts for 29% of total energy consumption and almost half of greenhouse gas (GHG) emissions in Sri Lanka. This study is to investigate the possible sustainable energy options for the transport sector. Sri Lankan transport sector is modelled using the Asia Pacific Integrated/Endues (AIM Endues) model for the planning horizon from 2015 to 2045. This study analyses four countermeasures along with the business as usual (BAU) scenario. The first countermeasure scenario is promoting residential solar electricity for electric vehicles. Other three scenarios modelled with 20%, 30% and 40% subsidy for electric and hybrid vehicles. Out of the four scenarios, promoting residential solar electricity for electric vehicles is the most effective countermeasure as it could reduce the transport sector energy consumption by 16.4 Mtoe and CO<sub>2</sub> emissions by 35% in 2045. At the current vehicle and electricity prices, providing 20% subsidy will not be effective as 30% and 40% subsidies in achieving significant reduction in energy consumption and CO<sub>2</sub> mitigation Sri Lankan transport sector.

**Keywords:** AIM Endues; Bottom Up Modelling; Transport Sector; Solar Electricity



## Introduction

Increase in energy consumption and subsequent greenhouse gas emissions have become the greatest challenge faced by the mankind in this century. As one of the rapidly developing countries in South Asia, Sri Lanka has to play an important role in reduction of energy consumption and GHG mitigation. Sri Lanka reported its highest Gross Domestic Product (GDP) increase of 9.1% in 2012 [1]. Total energy consumption of Sri Lanka was 9.9 Mtoe in 2015 [2]. As the second largest energy consuming sector in the country transport sector held a 29% of Sri Lankan total energy consumption in 2015 [2]. Sri Lankan transport sector is totally fossil fuel dependent like in most of other developing countries. Thus, it remains as the leading contributor for GHG and other pollutant emissions in the country [3]. Total energy demand of the transportation is expected to increase with the upcoming infrastructure developments, mega projects, expansion of logistics and tourism in the country [4]. Therefore, it is essential to have a well-functioning, sustainable, energy efficient and less-polluting transport system.

Two third of the current vehicles of Sri Lanka are old and most of them have been registered before 2008 [4]. Although there are few electric and hybrid vehicles, it has neither infrastructure nor a plan to promote the use of these vehicles. Furthermore, Sri Lanka clearly lacks policies in importing fuel efficient and emission-controlled vehicles. There have been serious health issues due to local pollutant emissions such as hydrocarbons (HC) and particulate matter (PM). Increased fossil fuel use in the future and lack of energy

policies will further aggravate this problem.

Considering the above facts, it is important to develop a sound policy for environmental mitigation. Sri Lanka is bound by Paris climate agreement to propose Nationally Determined Contributions (NDC) to achieve greenhouse gas emission reduction [5]. Transport sector would be a leading candidate for NDCs. Therefore, such an analysis will provide a framework for developing policy for sustainable pathways in the transport sector.

Energy models have been extensively used in analyzing climate change and global energy crisis as a reason of GHG emission and depletion of conventional energy resources [6]. These energy models serve as tools in energy planning activities and related policy defining for government agencies, academic and research institutes [7].

Asia Pacific Integrated Model (AIM) is one of the predominantly used models to serve this purpose. AIM Endues which is a bottom up recursive dynamic, optimization model of the AIM family has been used by several countries such as Japan, China, Korea, India, Thailand, and Vietnam in their policy making processes [8]. This model is capable of demonstrating energy models in different economic sectors of a country such as residential, commercial, transport and industry. In literature there are several studies which used AIM endues model in order to investigate the transport, environment, and energy nexus at the national level. Several recent studies [6], [8], [9], [10] have been carried out to investigate different policy interventions and various countermeasure scenarios derived under different tax policies,

technology shifting, fuel switching, Bio-fuel introduction, modal shifting, transport demand management, low carbon society measures, and impact on Energy security, marginal abatement costs, and productivity of Thai transport sector. As shown by studies [9]-[11], AIM modeling has extensively used in regional and global transport sector investigations.

According to literature, there are very few sectorial levels in-depth analysis on Sri Lankan transport sector with regard to national policy making, future energy and service demand management and carbon mitigation. The DEMIDEPT Demand Model has been used to estimate the total mobility, total private vehicle fleet, private vehicle use, public transport share and split between bus and rail for the two forecast years 2021 and 2031 on preparation of Sri Lankan transport sector policies [12]. This has not considered individual vehicle technology data such as cost, fuel efficiency, emission factors and fuel types. AIM/Endues modeling for Sri Lanka transport sector had carried out by Selvakkumaran [13]. Nevertheless, it has not considered all three transport modes and detailed technology classification. Fernando *et. al.* [14] has modeled Sri Lankan transport sector using AIM/Endues. The study had been carried out to investigate the mitigation policy options with carbon tax, subsidies for clean energy vehicles and promoting public transport in Sri Lankan transport sector.

Even so, it requires more in-depth studies in terms of alternative policy options acceptable for Sri Lanka to recognize most effective sustainable energy options. Primary objective of this study is

to investigate few countermeasures suitable for Sri Lankan transport sector and quantify the possible emission mitigations along with energy reductions.

## Methodology

The AIM Endues model is used to analyze Sri Lankan transport sector during the period from base year 2015 to 2045. Sri Lankan transport sector has been modeled as two ended services named passenger transport and freight transport. It includes both road and rail transport for passenger and freight. The future transport sector service demands were obtained using multivariate regression method considering transport sector GDP and Sri Lankan population as the independent variables.

Existing vehicle types in the transportation fleet along with potential advanced vehicle options for future years has been considered in the model. The advanced options include efficient models of conventional types, hybrid, plug-in hybrid, electric and fuel cell vehicles. Under railway transport existing diesel engines along with electric railway has been considered as technology options. For water and air transport existing technologies as well as more advanced fuel wise efficient options were considered for future years. Under each existing and potential technology type used energy consumption, service output, emissions, number of units in the base year are considered as inputs to the model. For all existing modes fuel cost, along with operation and maintenance cost was considered. For all future technology options cost of new unit was considered along with the above running costs.

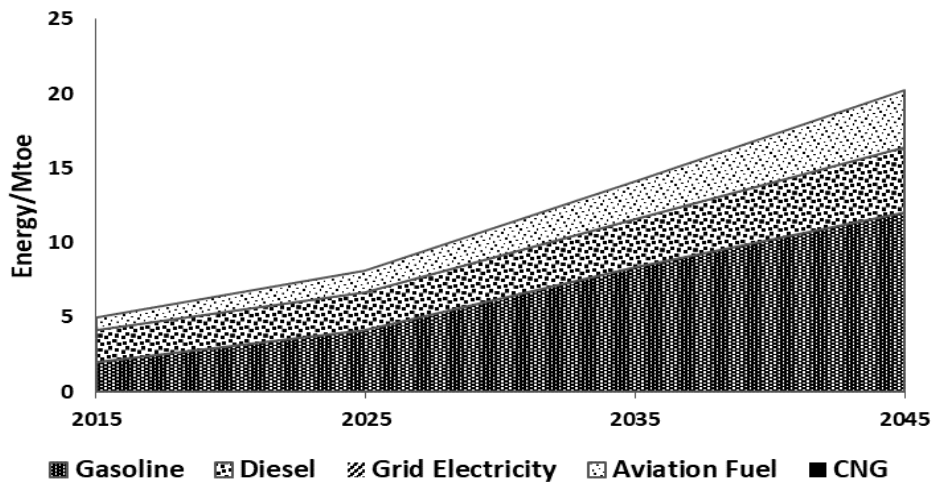


Figure 1: Energy consumption in BAU Scenario

These include possible GHG mitigation under a BAU scenario and three countermeasure scenarios. The BAU scenario considers continuation of current economic, demographic and energy sector trends and policies, and there is no mitigation policy.

The first scenario (CM1) analyzed is considering residential solar electricity in charging. Unit price of solar electricity was calculated by author. All the private electric passenger transport vehicles such as cars, vans, three wheelers and motor bikes will be using residential solar electricity under this countermeasure. A subsidy for electric and hybrid vehicle cost will be considered in the second (CM2), third (CM3) and fourth (CM4) scenarios. A subsidy of 20%, 30% and 40% was considered under CM2, CM3 and CM4 respectively. Average grid electricity prices and emission factors were used in this scenario. Under each scenario changes in energy consumption, CO<sub>2</sub> emission and technology share by vehicle category are analyzed in detail.

The data collection was mainly through governmental sources and independent

research publications. The general macro socio economic data were obtained from Sri Lankan Central Bank publications [1] and the future GDP and population predictions were from privately published sources [15] as there were no proper governmental publications to obtain that information in Sri Lanka. Transport sector technology data were mainly extracted from independent research publications and governmental publications [4],[16]-[20]. Energy data were obtained from [21] and [22].

## Results and Discussions

### Energy and Emissions of BAU Scenario

Figure 1 shows the energy consumption in the BAU scenario. The energy consumption in Sri Lankan transport sector will increase from 5 Mtoe in 2015 to 20.2 Mtoe in 2045 at 1.59% average annual growth rate. Diesel holds the highest share of 42% in 2015 fuel mix and will decline the share by 20% in 2045.

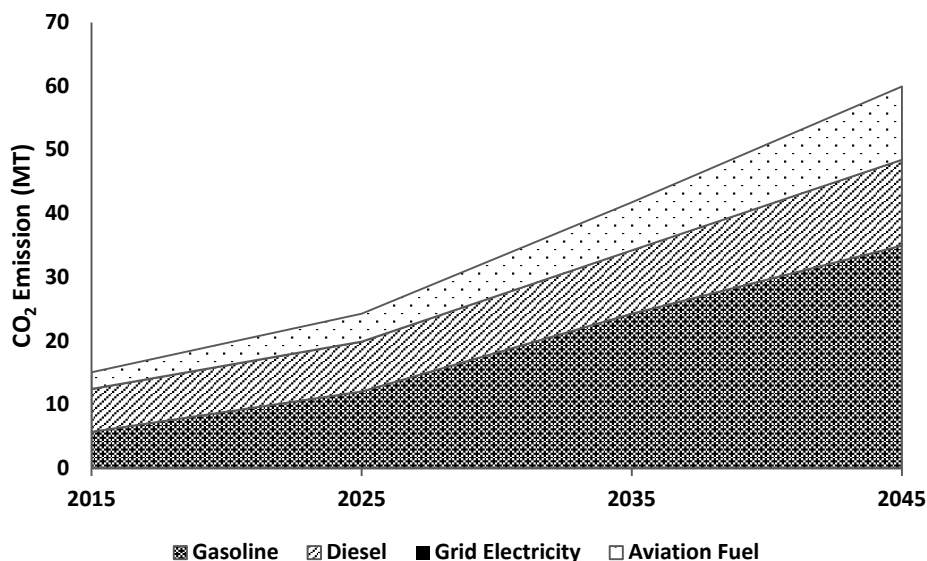


Figure 2: CO<sub>2</sub> Emission in BAU Scenario

After 2025 gasoline becomes the main energy source of transport sector which will account for almost 59% of the transport sector energy supply. Energy supply from electricity and Compressed Natural Gas will remain negligible at the current fuel prices. BAU results insist the requirement of alternative energy policies in promoting cleaner energies such as Compressed Natural Gas and electricity in Sri Lankan transport sector.

The overall CO<sub>2</sub> emissions in the BAU Scenario are presented in Figure 2. The total CO<sub>2</sub> emissions are expected to increase from 15 MT to 60 MT during 2015 and 2045. Diesel has the highest contribution of 44% of total CO<sub>2</sub> emissions in 2015. This is followed by gasoline (38%) and aviation fuel (18%). From 2025 to 2045 gasoline will be the main source in CO<sub>2</sub> emissions in BAU scenario. The contribution of gasoline

raising from 50% to 57% during the period from 2025 to 2045. The share of aviation fuel remains almost constant around 18% in total CO<sub>2</sub> emissions in BAU scenario. Total CO<sub>2</sub> emissions from Electricity and CNG remain negligible throughout the planning horizon. As shown in figure 5, It shows remarkable decline of existing vehicles percentage from 98% in 2015 to 15% in 2045. On the other hand there is a gradual increase of hybrid vehicles from 2% to 15% during 2015 and 2045 period. Most of the existing technologies will be replaced by the efficient vehicles in the BAU scenario.

It can be observed that a considerable increase of hybrid vehicles percentage throughout the period from 2025 to 2045. The electric vehicles share in BAU scenario is negligible due to current tax structure and electricity prices.

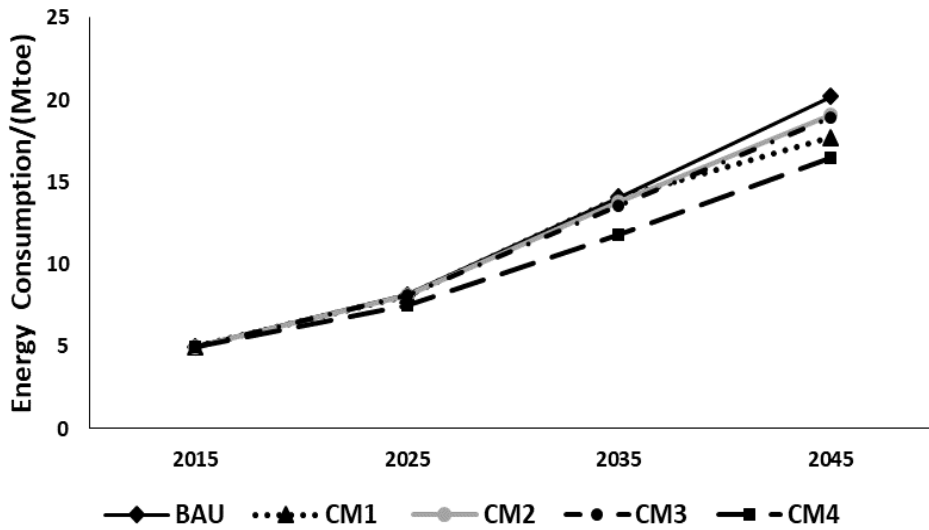


Figure 3: Energy consumptions in countermeasure scenarios

### Energy in Countermeasure Scenarios

Figure 3 presents the total energy consumption figures of all four countermeasure scenarios. As it can be seen all countermeasure scenarios have shown reduction in energy consumption compared to BAU Scenario. CM4 has the lowest total energy consumption with 18.6% (3.7Mtoe) reduction compared to BAU Scenario. It is followed by CM1, CM2 and CM3 with 12.4% (2.5Mtoe), 6.1% (1.24Mtoe) and 5.7% (1.16Mtoe),

cumulative reduction respectively during the planning horizon. The highest energy saving under a 40% subsidy is mainly due to the high penetration of hybrid vehicles from 2025 compared to 20% and 30% subsidies. Usage of residential solar electricity will show significant reduction in energy consumption after 2035 as most of the existing technologies will be replaced by electric and efficient technologies after 2025. In the long run, promoting solar electricity for transport sector would be very effective.

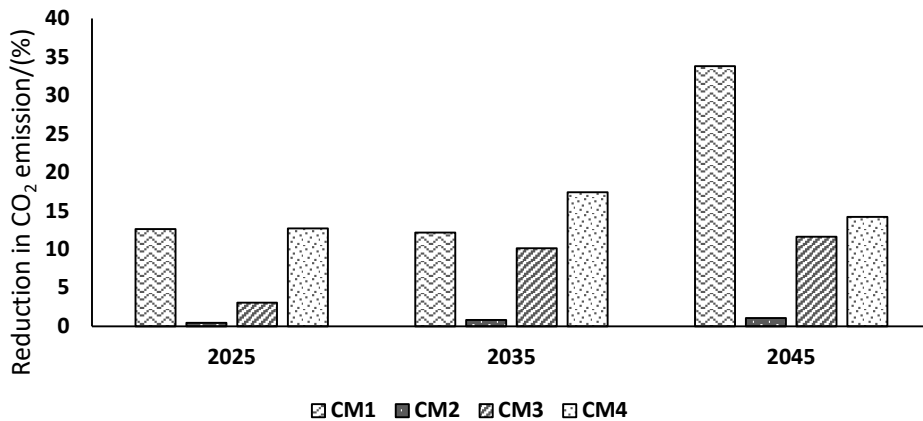


Figure 4: Reduction in CO<sub>2</sub> emission in countermeasure scenarios

CO<sub>2</sub> emission reduction is very prominent from 2015 onwards in all countermeasure scenarios as shown in figure 4. CM1 is the most effective countermeasure out of all scenarios having significant CO<sub>2</sub> mitigation potential from 2025 onwards. It shows 3.4MT, 5.6MT and 22.3MT cumulative CO<sub>2</sub> reductions in 2025, 2035 and 2045 respectively. This is mainly due to less price and zero emissions from the solar electricity compared to grid electricity used in BAU scenario. However, providing 20% subsidy for electric and hybrid vehicles is not an effective policy compared to other countermeasures. As a whole, vehicle subsidy scenarios are not very efficient as CM1 due to more hybrid vehicle penetration compared to electric vehicles under subsidies. It is mainly due to high price and emission factors of grid electricity than petroleum fuels. Figure 5

shows the technology mix in passenger transport share in all countermeasure scenarios compared to BAU scenario. There are two distinguish model structures in CM1 and CM2, CM3, CM4 against Baseline (BL) structure in 2015. BL is consisting of 98% of existing technologies along with 2% hybrid. All vehicle subsidy scenarios consist of existing, hybrid, electric and new efficient technologies whereas in CM1 scenario there are only existing, new efficient and electric technologies only, no hybrid vehicles under CM1 scenario. These findings prove that CM1 is promoting electric vehicles whereas other CMs promote hybrid technologies more compared to electric technologies. Low rate of penetration of electric vehicles compared to hybrid vehicles in vehicle subsidy scenarios along the time line is due to that.

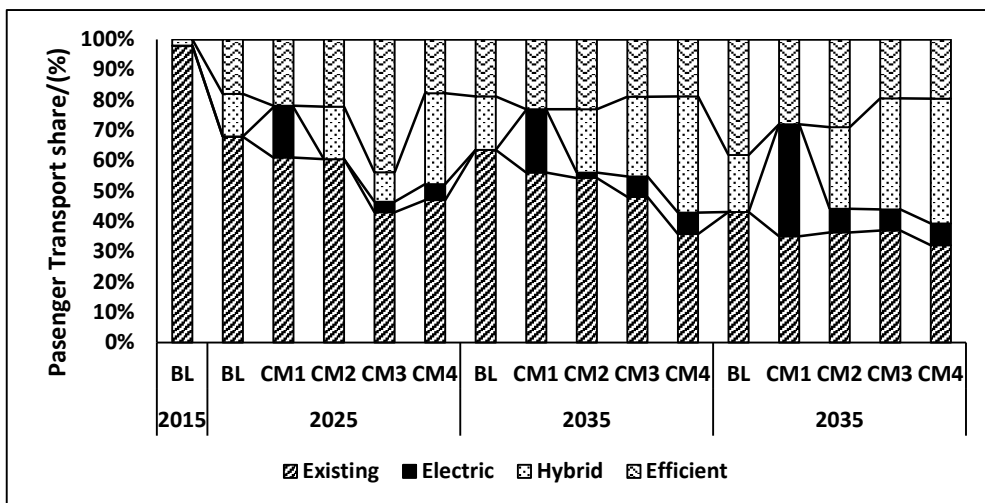


Figure 5: Passenger transport share by vehicle category in Countermeasure scenarios

## Conclusions

This study investigated four countermeasures for energy consumption reduction and CO<sub>2</sub> mitigation in the Sri Lankan transport sector. The countermeasure options include promoting solar electricity in charging electric vehicles and three price subsidies for electric and hybrid vehicle results show that final energy consumption in transport sector will replace diesel as the main fuel used for transport by 2045. Following a similar trend, the CO<sub>2</sub> emissions will also have a fourfold increase, from 15 MT in 2015 to 59.9 MT in 2045. Gasoline will be the main contributor to CO<sub>2</sub> emissions with a share of 55% in 2045. The Efficient technologies and hybrid vehicles together will account for 55% of passenger transport share in BAU by 2045.

Out of the four scenarios, promoting solar electricity was the most effective scenario. It could reduce total energy consumption by 18.6% and CO<sub>2</sub> emissions

by 22.3 Mton compared to the BAU values in 2045. This was followed by CM4, CM3 and CM2 respectively. CM1 and CM4 are very efficient in reducing energy consumption and CO<sub>2</sub> emissions compared to CM3 and CM4.

In the vehicle subsidy scenario the penetration of electric vehicle was comparatively low against the Hybrid vehicles under vehicle subsidy scenarios. However in the solar electricity scenario there is a significant electric vehicle penetration rate compared to hybrid vehicle penetration rate throughout the planning horizon.

## Acknowledgement

The authors would like to thank the National Institute of Environmental Studies of Japan for their technical support with the AIM/Endues model and the Sri Lankan Institute of Information Technology for financial support.

## References

- [1] CBSL, "Sri Lanka Socio Economic Data 2015," Central Bank of Sri Lanka, 2016.
- [2] SLSEA, "Sri Lanka Energy Balance," Sri Lanka Sustainable Energy Authority, 2015.
- [3] MOE, Second National Communication on Climate Change, Ministry of Environment, Sri Lanka, 2011
- [4] NTC, "National Transport Statistics 2016," National Transport Commission, Sri Lanka, 2016.
- [5] MMDE, "Nationally determined contributions submitted for United nations framework convention on climate change," Ministry of Mahaweli development and environment, 2016.
- [6] R.M. Shrestha, S. Malla, M.H.Liyanage, "Climate Policy and Energy Development in Thailand: An Assessment," Regional Energy Resourced Information Center, 2016.
- [7] M. Kainuma, Y. Matsuoka, T. Morita, Climate Policy Assessment: Asia-Pacific Integrated Modelling, Springer Verlag, Tokyo, 2003.
- [8] P. Jayathilaka and B. Limmeechokchai, "Scenario Based assessment of CO2 Mitigation Pathways: A Case Study in Thai Transport Sector," Energy Procedia, 79, PP 969-975, 2015.
- [9] S.Selvakkumaran and B. Limmeechokchai, "Low carbon society scenario analysis of transport sector of an emerging economy — The AIM / Enduse modelling approach," Energy Policy, vol. 81, pp. 199–214, 2015.
- [10] S. Phoulavanh, B. Limmeechokchai "Analysis of Energy Efficiency and Bio-Energy in the Land Transportation in Thailand." Energy Procedia, Vol 79, PP 33-38, Nov 2015
- [11] S. Mittal, H. Dai and P.R Shukla, " Low Carbon transport Scenarios for China and India: A comparative assessment, Transportation research Part D 44, PP266-276, 2016
- [12] A. S. Kumarage, "Sri Lanka Transport Sector Policy Note," Sri Lanka, May 2012.
- [13] S.Selvakkumaran, "Low carbon society and energy security in developing aisa," PhD. dissertation, University of Thammasat, Thailand, 2014.
- [14] Fernando G.L, Liyanage M.H. and Samarasekara G.N, Energy and Environmental Implications of Green House Gas Mitigation Policies in the Transport Sector of Sri Lanka. Proceedings of International conference on green energy for sustainable development (ICUE). Phuket, Thailand. Oct 2018.
- [15] Trading Economics (2018, Feb 12), <https://tradingeconomics.com/sri-lanka/population/forecast>
- [16] K.T.T.P.Karunathilaka, S.P.P. Sanjani, G.G.T Chaminda, G.L. Fernando G.N.Amarasekara, "Estimation of National Level Fuel Consumption and Emissions in Road Freight Transport," Research for Transport and Logistics, Colombo, Sri Lanka, 2018.
- [17] S.P.P Sanjani "Estimation of National level fuel consumption and emissions in road passenger Transport," Unpublished, BSc Thesis, University of Ruhuna, Sri Lanka, 2017
- [18] CAAS, "Annual report 201,5," Civil Aviation Authority, Sri Lanka. 2015.
- [19] DMT, Vehicle Registration Database, Department of Motor Traffic Sri Lanka, 2016
- [20] MFARD, "Fisheries Statistics," Ministry of fisheries and Aquatic Resources Development, Sri Lanka, 2017.
- [21] IMF, (2018, Feb 16), World Economic Outlook [Online], Available [http://www.imf.org/NGDP\\_RPCH@WEO/OEMDC/ADVEC/WEOWORLD](http://www.imf.org/NGDP_RPCH@WEO/OEMDC/ADVEC/WEOWORLD)
- [22] IEA, "World energy outlook," International Energy Agency, 2017



# Importance of Developing a Sri Lankan Wave Energy Resource Assessment According to IEC Standards

R.L.K. Lokuliyana<sup>#1</sup>, Matt Folley <sup>\*2</sup>, S.D.G.S.P. Gunawardane<sup>#3</sup>, P.N. Wickramanayake<sup>#4</sup>

<sup>#1,3</sup> *Department of Mechanical Engineering, University of Peradeniya  
University of Peradeniya Peradeniya, 20400. Sri Lanka*

<sup>1</sup> ravindu.lokuliyana@gmail.com

<sup>3</sup> sdgspg@eng.pdn.ac.lk

<sup>\*2</sup> *School of Planning, Architecture and Civil Engineering, Queen's University Belfast,  
Queen's University Belfast Northern Ireland, UK;*

<sup>2</sup> m.folley@qub.ac.uk

<sup>#4</sup> *Department of Civil Engineering, The Open University of Sri Lanka  
The Open University of Sri Lanka Nawala, Nugegoda, Sri Lanka*

<sup>4</sup> tomwiks@yahoo.com

## Abstract

A good quality dataset obtained through internationally recommended standards for the Sri Lankan wave energy resource is an essential requirement to assess the wave energy potential and to attract potential wave energy developers. This particular requirement arises since the traditional wave resource studies are typically not adequate for a standardized assessment of wave energy capture potentials in wave energy converter deployment projects. This paper introduces the International Electro-technical Committee Technical Specification (IEC TS 62600-101) which establishes uniform methodologies for wave energy resource assessment and characterisation as the major guideline to the study. Then the paper presents a review of the currently existing wave resource studies in Sri Lanka and discusses their importance with reference to strengths and weaknesses for wave energy development in Sri Lanka. Finally, an approach of developing a validated wave model that allows assessment of the Sri Lankan wave energy resource using SWAN third generation wave model is discussed and validation is reported.

**Keywords:** wave energy; IEC standards; Sri Lanka

## Introduction

Wave energy is one of the promising sources of renewable energy and it is particularly important for an island nation like Sri Lanka to achieve sustainable energy mix [1–4]. The requirement of the development of marine renewable energy in Sri Lanka has been comprehensively discussed in a previous study with possible approaches [5]. Worldwide there are large number of companies developing wave energy technologies and are looking for potential deployment sites for both prototypes and commercial wave farms [6,7]. Amongst the many factors that may influence a company's choice of location is the availability of good quality data on the wave resource. Moreover, it is not only that the resource needs to be estimated, but it must also be characterised and presented in a way that allows it to be used effectively for calculation of the annual energy production for a particular technology [8]. This is typically addressed through a wave energy resource assessment which is conducted under a set of internationally recommended standards. As the interest in the exploitation of wave energy, there has been an explosion in the number of studies of the wave energy [9–18], but limited number of them have followed specific standards.

Some established companies in wave energy sector have already shown their interest in deploying wave energy converters in Sri Lankan waters [19–21], but none of those projects have been realized. One of the influential factors for such a drawback is the uncertainty on the annual energy production due to lack of reliable wave resource dataset. So, implementation of wave energy resource assessment under sets of international

standards is a contemporary requirement to assess and characterise the available wave power around Sri Lanka. This can be achieved by the recently published International Electro-technical Committee (IEC) Technical Specification (TS 62600-101) that is designed specifically for the exploitation of wave energy [22].

## IEC Technical Specification

International Electro-technical Committee (IEC) is a well-recognized organization for publishing international standards, Technical Specifications, Technical Reports, Public Available Specifications (PAS) and guides in different electrical and electronic fields. The developed IEC TS 62600-101 category sets recommendations for wave resource assessments by describing the procedures for study planning, data collection, numerical modelling, data analysis and technical report writing. The methodology which describes the wave energy resource assessment in IEC TS 62600-101 can be summarized into six major steps, as shown in Figure 1.

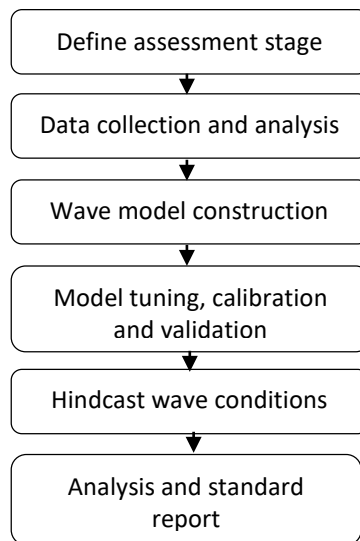


Figure 1 : IEC TS 62600-101 Methodology

The first step focuses on defining the appropriate assessment stage of the resource assessment. There are three main classes of resource assessments; Reconnaissance, Feasibility and Design which are defined on desired level of accuracy and uncertainties of wave energy resource parameter estimations. Next step focuses on the data collection and analysis that involves the collection of required boundary and validation datasets for model development and validation with appropriate spatial and temporal resolutions. The third step involves the development of wave propagation model. Here, numerical model features are defined for each class. The development of numerical model is generally based on the output from a third generation spectral wave model. Then the model tuning, calibration and validation task investigates the uncertainties between wave model prediction and the validation datasets, and modify the model to improve the fidelity of its predictions. The final steps involve wave hindcasting using the validated wave model (minimum 10 years) and reporting the results with standard reporting format. The detailed descriptions of all those steps are available in IEC TS 62600-101.

### **Previously conducted wave resource studies in Sri Lanka**

Annual wave climate of Sri Lanka is affected by two monsoon periods; northeast (December-February) and southwest (May-September). Although the detailed wave analysis is not available for the monsoon periods, some studies clarify that the annual average wave power around the western coastal region of Sri Lanka consist of 10-15 kW/m while southern region has 15-20 kW/m [4]. It is also estimated that the annual average

wave height ranges from 0.5-3 m in different periods where the 80% of 2-3 m heights occur during the June and July [23]. But all of these values are approximated according to the analysis of global wave models [24-25].

The directional wave climatic study that was conducted by Sri Lankan German Corporation under the project of CCD-GTZ (1994), can be considered as one of first comprehensive analysis of wave climatic data in Sri Lanka [26]. The numerical wave propagation model called "REFRAC" was used to transform the deep water wave measurements to locations along the southwest coast at shallower depths. The bathymetric data were defined by digitizing admiralty charts and physically recorded metocean buoy data were used as boundary conditions. The results of this study have been the basis for most of coastal engineering and wave resource studies in the following years [27-29].

The design and implementation of 'WorldWaves' wave model was another earliest wave resource assessment study which was applied Sri Lankan waters as a hypothetical case study. According to the reference, this package has the capability of calculating the wave conditions along the many coasts worldwide [25]. In-situ measurements, satellite measurements and numerical wave model data available in global scale have been used for the wave model construction which contains necessary information for the offshore wave and wind input in time series format.

Another study which was focused on the assessment of the variability of nearshore wave climate off the southern coast of Sri Lanka, using the MIKE 21 SW wave model [30], in a domain covering the entire

southern coast and part of southeast coast of Sri Lanka [31]. The bathymetry used in this study was established by digitizing admiralty charts, which cover the entire south coast and part of the southeast coast as well. Here, the wave data at desired model locations were obtained through a wave transformation matrix approach with respect to three wave measured datasets.

Another application of a wave energy resource study can be found in [32], which was focused on a feasibility study of an ocean wave power generation for southern coast of Sri Lanka. Here, the modeled area was mainly selected by assuming the wave climate of northern and eastern parts of the country restricted due to the geographical location of Sri Lanka. The available seasonal wave climatic data were modeled using WW3 wave model [33]. The paper further describes that the used model data contained wave directions, significant wave heights, peak periods and the wind data. But the sources of those data including bathymetry were not clearly specified in the research publication. Furthermore it addresses the feasibility of implementing wave power plants based on mechanical, electrical and sociological aspects by considering six different sites along the southern coast of Sri Lanka.

A wave energy resource assessment which was conducted for the Indian shelf seas also has consisted some information on Sri Lankan wave resource [14]. This study reveals that the southeast coast of India (northwest part of Sri Lanka) has less than 5 kW/m wave power. The WAM wave model [34], with ECMWF ERA-Interim global atmospheric re-analysis dataset [35], has been used to define the boundary conditions for their model

domain. The variations in wave power at 19 locations were studied with relevant model validation. The illustration related to the distribution of annual mean wave power indicates that the 15-20 kW/m range can be found at the south and southeast regions of Sri Lanka.

Another research which establishes an assessment of wave climate in southwest, south and southeast coasts of Sri Lanka, provides the annual wave power ranges over 100 kW/m for their study locations at 50 m water depth [36]. These estimates deviate from all other reference values which has the annual wave power of 5-20 kW/m. The wave model was developed using Delft 3D model [37] and TOPEX altimeter data [38] has used for the model calibration and validation.

A study based on climate change impacts on seasonal wave climate of the west coast of Sri Lanka is another type of wave resource study which focuses to set up and calibrate a wave model that is capable of predicting the off-shore wave climate around Sri Lanka [39]. Here the global wave model datasets of ECMWF [35], NCEP [40] and NOAA [41] were used as boundary condition data for model development and satellite altimetry TOPEX, JASON, SAR measurements were used for calibration and validation of the wave model which was developed from WW3 [33] and SWAN [42] third generation wave models.

### **Application of IEC TS 62600-101 to Sri Lanka**

According to the previous review, most studies have considered offshore wave climate while few of them focused on the nearshore analysis. None of them have considered both nearshore and offshore

wave climate of the whole Sri Lankan region which is particularly important for the wave resource studies as well as many other subjects including coastal engineering, metrological science, etc. The wave parameter values around Sri Lanka can be estimated using two of above studies which were conducted for the Indian ocean and for the global scale [14],[25]. But they may have consisted higher level of uncertainty where they were not specifically designed for the Sri Lankan region. Moreover, only those two studies have used the measured datasets for the model validation while two other [36],[39] used the satellite altimeter measurements. The wave hindcasting around Sri Lanka is another lacking part of those studies which is highly recommended in any kind of wave resource assessment. None of these studies have discussed the uncertainty estimations of the assessment which is a compulsory requirement of the standards.

Since the previously conducted resource assessment studies have not satisfied most of the basic requirements of wave resource assessment and the IEC TS 62600-101 standards, proper assessment of Sri Lankan wave energy resource is a much needed requirement to address the weaknesses of previous assessments and follow sets of internationally recommended standards. Because of that, a study based on following main objectives have been initiated to study the feasibility of wave energy potential in Sri Lanka.

1. Produce wave resource data to IEC standards, which can be used by developers to assess the potential for their wave energy technologies in Sri Lanka.
2. Identify the most promising deployment locations for wave

energy converters, based on the wave resource characteristics.

3. Calculate the mean annual energy production and its uncertainty for a wave energy converter deployed in Sri Lankan waters.
4. Estimate the total technically available wave energy resource of Sri Lanka.

Following describes the summary of approach of each step defined under Figure 1.

Since this study considers the whole Sri Lankan region which is having a large longshore extent (over 300 km) and probably be the first comprehensive analysis according to IEC TS 62600-101 standards, the appropriate resource assessment is Reconnaissance stage (Class 1) assessment. So, all the assessment features of this study has followed the recommended standards under Reconnaissance stage.

The bathymetry, wind, current and two dimensional wave spectral data were used for the model construction. The recommended maximum horizontal spacing of bathymetric data in water depths for Class 1 Reconnaissance assessment over 200 m, 200 m – 20 m and less than 20 m are 5 km, 500 m and 100 m respectively. To obtain the possible resolutions, GEBCO 30 arc second interval grid [43] has used for the water depths over 200 m while digitized nautical charts interpolated data [44] has used for the water depth less than 200 m. Selection of existing wave data is important as the selection of bathymetric data. It was found that the best available sources of required wave data can be obtained from European Centre for Medium-Range Weather Forecasts (ECMWF) Interim dataset [35] and National Centres for

Table 1: Used wave measured datasets for the model validation

| Dataset | Location  | Deployment         | Period               | Frequency |
|---------|-----------|--------------------|----------------------|-----------|
| CCD-GTZ | 5.936 °N  | Wave buoy          | Feb 1989 – Sept 1992 | 3 h       |
|         | 80.575 °E | (70 m water depth) |                      |           |
| SCSIO   | 6.106 °N  | Wave buoy          | Apr 2013 – Apr 2014  | 1 h       |
|         | 81.080 °E | (10 m water depth) |                      |           |

Environmental Prediction (NCEP) NCAR [40] dataset. So, wind and two dimensional wave spectral data were obtained from ECMWF Interim dataset which have interpolated spatial resolution of  $0.25^\circ \times 0.25^\circ$  and  $1.5^\circ \times 1.5^\circ$  respectively. The current data were obtained from NCEP/NCAR dataset with  $0.5^\circ \times 0.5^\circ$  spatial resolution.

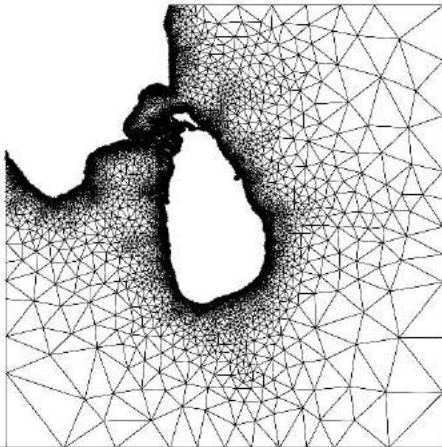


Figure 2: Developed unstructured grid around Sri Lanka

Since all third generation models are following the required recommendations of the standards, selection of a suitable model is based on the model features. SWAN third generation wave model [42] is selected for the model construction task with a developed unstructured grid as shown in Figure 2. The initial model construction of this project involves

coupling SWAN and Matlab, which has the features to define the study area using longitude and latitude coordinates, control the parameter values of the input grids, define the spatial and isolated location outputs using longitude and latitude coordinates.

The model tuning and calibration process has a significant impact on improving the accuracy of model predictions and outputs of final model validation. At the process of model tuning, it was identified that the most sensitive parameters of the model are wind speed, wind direction and bathymetry. Despite of that, all other physical parameters of the model haven't significantly influenced the model results. The final model was developed by choosing the best available input grids for those sensitive parameters with default physical parameter values.

Two wave measured datasets (Table 1) were used for the model validation which were obtained from wave measurement programme that was governed by Coast Conservation Department - Sri Lanka under the Sri Lankan - German Technical Assistant Programme (CCD-GTZ project) [26] and wave observational datasets which were collected in a nearshore area off Matara from the China Harbour Corporation (SCSIO project) [45]. The significant wave height, zero crossing

period and mean absolute wave period of buoy datasets were initially compared according to the minimum validation requirements of the IEC-TS 62600-101. The comparison of the results are shown in Figure 3, Figure 4 and Table 2.

The analysis shows that the obtained results satisfied the minimum requirements for both offshore and nearshore locations. This implies that the developed model has provided significantly accurate outputs at the offshore locations and consisted marginal

deviations at the nearshore locations. Overall, the developed model can be considered as a validated model to assess and characterise the wave resource at other locations with further improvements of the model. This will be focused in the future developments of this project.

### Conclusions

The importance of wave energy resource assessment in accordance with IEC TS

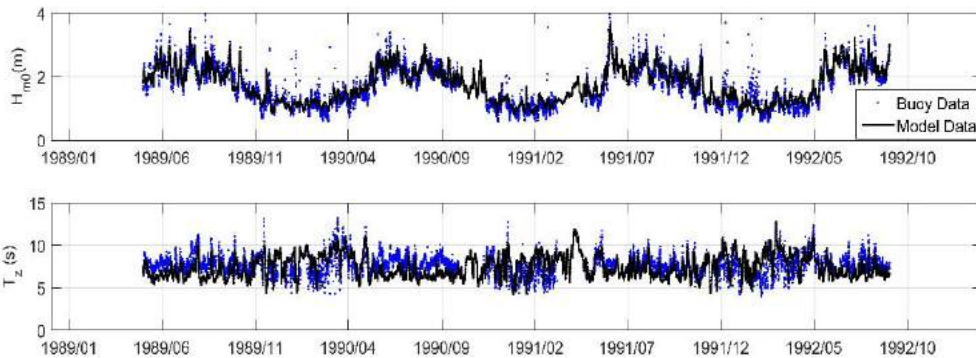


Figure 3: Significant wave height and zero crossing period obtained from CCD-GTZ and SWAN model

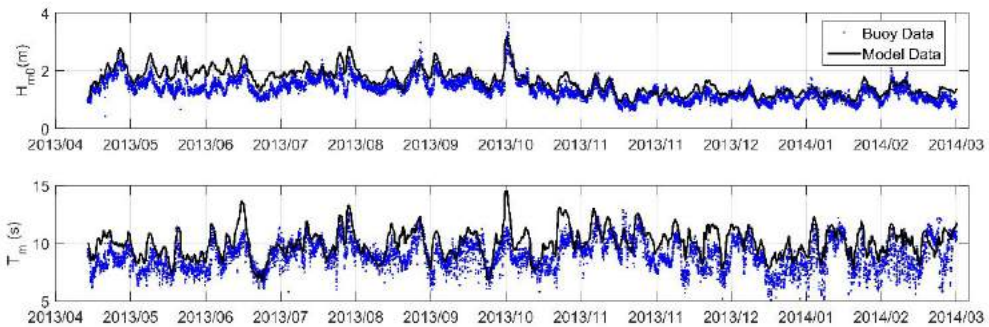


Figure 4: Significant wave height and mean wave period obtained from SCSIO and SWAN model

Table 2 : Model data analysis compared to IEC-TS 62600-101 MVR – Minimum Validation Requirements of IEC TS 62600-101; VR1 –Validation results related to CCD-GTZ buoy dataset; VR2 – Validation results related to SCSIO buoy dataset;

|  | MVR  | VR1     | VR2    |
|--|------|---------|--------|
| <b>Max acceptable weighted mean systematic error, <math>b(e_p)</math></b>      |      |         |        |
| Significant wave height, $H_{m0}$  | 10 % | 2.2 %   | 8.9 %  |
| Zero crossing period, $T_z$  | 10 % | - 6.7 % |        |
| Mean absolute wave period, $T_m$   | 10 % |         | 5.1 %  |
| <b>Maximum acceptable weighted mean random error, <math>\sigma(e_p)</math></b> |      |         |        |
| Significant wave height, $H_{m0}$  | 15 % | 10.6 %  | 13.8 % |
| Zero crossing period, $T_z$  | 15 % | 10.9 %  |        |
| Mean absolute wave period, $T_m$   | 15 % |         | 10.0 % |

62600-101 was highlighted. It has been shown that the currently exist wave resource assessments are not sufficient to study the wave climate around Sri Lanka. Also none of them have followed any internationally accepted standards and need revision comparing to the IEC TS 62600-101 standards. A study has been developed to assess and characterise the Sri Lankan wave energy resource. The approach on developing a validated wave model that allows assessment of the Sri Lankan wave energy resource using SWAN third generation wave model has been discussed with respect to IEC TS 62600-101 standards. The next step of this project will assess and characterise the wave resource by identifying the most promising areas for wave energy exploitation with appropriate illustrations. The findings of the project will help to promote Sri Lanka as one of the small group of nations that are able to provide good quality wave resource data

to prospective investors. This project is a timely needed requirement to create an industry which can significantly contribute to the Sri Lankan economy in future. This will also make a door open to many researchers and local developers who are interested in renewable energy industry where they can expand on the vision and commitment towards the wave energy field.

### Acknowledgement

This study was conducted with the initiative and support of Sri Lanka Sustainable Energy Authority (SLSEA). The authors express their appreciation to SLSEA for providing all necessities and also authors wish to thank to the Coast Conservation Department of Sri Lanka, South China Sea Institute of Oceanology for providing wave measurement dataset and to the anonymous reviewers.



## References

- [1] UNDP, "Sri Lanka: Rapid Assessment and Gap Analysis," Report: Sustainable Energy for all, 2012.
- [2] D. Ranasinghe, "Strategic Importance of Blue Economy to Sri Lanka and Challenges," KDU IRC, 2018
- [3] S. Sayanthan and N. Kannan, "Renewable energy resource of Sri Lanka ! A review," *Int. Journal of Env. & Agri. Research*, vol. 3, no. 4, pp. 80–85, 2017.
- [4] J. Ratnasiri, "Alternative energy – prospects for Sri Lanka," *Journal of the National Science Foundation of Sri Lanka*, 36, pp.89–114, 2008.
- [5] M. Folley, S.D.G.S.P. Gunawardane, "The development of marine renewable energy in Sri Lanka", National Energy Symposium, Colombo, Sri Lanka, 2018.
- [6] E. Rusu and F. Onea, "A review of the technologies for wave energy extraction", *Clean Energy*, vol. 2, no. 1, pp. 10-19, 2018.
- [7] I. López, J. Andreu, S. Ceballos, I. M. De Alegría, and I. Kortabarria, "Review of wave energy technologies and the necessary power-equipment," *Renew. Sustain. Energy Rev.*, vol. 27, pp. 413–434, 2013.
- [8] M. Folley, "The Wave Energy Resource BT - Handbook of Ocean Wave Energy," A. Pecher and J. P. Kofoed, Eds. Cham: Springer International Publishing, 2017, pp. 43–79.
- [9] A. Akpınar and M. Kömürçü, "Wave energy potential along the south-east coasts of the Black Sea", *Energy*, vol. 42, no. 1, pp. 289-302, 2012.
- [10] G. Iglesias, R. Carballo, and C. Pen, "Offshore and inshore wave energy assessment : Asturias ( N Spain )," *Energy*, vol. 35, no. 5, pp. 1964–1972, 2010.
- [11] M. G. Hughes and A. D. Heap, "National-scale wave energy resource assessment for Australia," *Renew. Energy*, vol. 35, no. 8, pp. 1783–1791, 2010.
- [12] M. Gonçalves, P. Martinho, and C. G. Soares, "Assessment of wave energy in the Canary Islands," *Renew. Energy*, vol. 68, pp. 774–784, 2014.
- [13] D. Mollison and M. Pontes, "Assessing the Portuguese wave-power resource", *Energy*, vol. 17, no. 3, pp. 255-268, 1992.
- [14] V. S. Kumar and T. R. Anoop, "Wave energy resource assessment for the Indian shelf seas," *Renew. Energy*, vol. 76, pp. 212–219, 2015.
- [15] M. Gonçalves, P. Martinho and C. Guedes Soares, "Wave energy conditions in the western French coast", *Renew. Energy*, vol. 62, pp. 155-163, 2014.
- [16] R. Alonso, S. Solari and L. Teixeira, "Wave energy resource assessment in Uruguay", *Energy*, vol. 93, pp. 683-696, 2015.
- [17] R. Espindola and A. Araújo, "Wave energy resource of Brazil: An analysis from 35 years of ERA-Interim reanalysis data", *PLOS ONE*, vol. 12, no. 8, p. e0183501, 2017.
- [18] G. Kim, W. Mu, K. Soo, K. Jun, and M. Eun, "Offshore and nearshore wave energy assessment around the Korean Peninsula," *Energy*, vol. 36, no. 3, pp. 1460–1469, 2011.
- [19] "Finland company to help Lanka produce wave energy", *Daily News*, Available: <http://www.dailynews.lk/2017/10/11/local/130920/finland-company-help-lanka-produce-wave-energy>.
- [20] "Carnegie to harness Sri Lanka waves", *Marine Energy*, Available: <https://marineenergy.biz/2016/09/30/carnegie-to-harness-sri-lanka-waves/>.
- [21] "WERPO to make waves in Sri Lanka", *Marine Energy*, Available: <https://marineenergy.biz/2015/07/14/werpo-to-make-waves-in-sri-lanka/>.
- [22] International Electro-technical Committee, "IEC TS 62600-101 Wave Energy Resource Assessment and Characterisation," 2015.
- [23] K. D. R. J. Kumara, D. D. Dias, R. L. Nawagamuwa, and W. M. A. R. Weerasinghe, "Wave Energy Enhancement for Nearshore Electricity Generation," *Engineer: Journal of the Institution of Engineers* no. 2, pp. 43–52, 2018.
- [24] S. Barstow et al., "WORLDWAVES : Fusion of data from many sources in a user-friendly software package for timely calculation of wave statistics in global coastal waters," *Proc 13th ISOPE Conf. Oahu, Hawaii, USA*, 2003.
- [25] S. Barstow, K. Belibassakis, T. Gerostathis, and G. Spaan, "WORLDWAVES : High quality coastal and offshore wave data within minutes for any global site" *COPEDEC VI, Colombo, Sri Lanka*, 2003.

- [26] "H. Scheffer, K.Fernando, "Direcional wave climate study south-west coast of Sri Lanka", CCD-GTZ Coast Conservation project, 1994.
- [27] N. Wikramanayake, P. P. Guneratne, M. M. G. S. Fernando, and I. Ratnayake, "The Coastal Wave Climate of Sri Lanka : Measurements and Modeling," COPEDEC VI, Colombo, Sri Lanka, 2003.
- [28] I. S. K. Wijayawardane, "Coastal Erosion : Investigations in the Southwest Coast of Investigations on Sediment Transport," International Conference on Sustainable Built Environments, Kandy, Sri Lanka, 2010
- [29] T. Thevasiyani and K. Perera, "Statistical analysis of extreme ocean waves in Galle , Sri Lanka," Weather Clim. Extrem., vol. 5–6, pp. 40–47, 2014.
- [30] Danish Hydraulic Institute (DHI), "Mike 21 Wave Modelling," Scientific documentation, 2015.
- [31] P. Gunaratna, D.P.L.Ranasinghe, and T.A.N.Sugandika, "Assessment of Neashore Wave Climate off Southern Coast of Sri Lanka" Engineer: Journal of the Institution of Engineers, Sri Lanka, 44(2), pp.33–42, 2011.
- [32] K. Amarasekara, G. Abeynayake, M. Fernando, and A. Arulampalam, "A prefeasibility study on ocean wave power generation for the southern coast of Sri Lanka : Electrical feasibility," Int. J. Distrib. Energy Resour. Smart Grids, vol.10, pp.79–93, 2014.
- [33] H. L. Tolman, "User manual and system documentation of WAVEWATCH-III version 3.14," Tech. note, no. 3.14, p. 220, 2009.
- [34] WAMDI Group, "The WAM model - A third generation ocean wave prediction model," Journal of Physical Oceanography, vol. 18, no. 12. pp. 1775–1810, 1988.
- [35] "ECMWF ERA Interim dataset.", ECMWF, Available: <https://www.ecmwf.int/en/forecasts/datasets/reanalysis-datasets/era-interim>.
- [36] V. Vithana, "Wave Energy Resource Assesment for the Southern Coast Of Sri Lanka Wave Energy Resource Assesment for The Southern Coast Of Sri Lanka," 6th International Symposium-ACEP, 2018.
- [37] Delft3D , "Delft3D-FLOW User Manual" , 2014."
- [38] "TOPEX altimeter data." Available: <https://www.aviso.altimetry.fr/en/multimedia/publications-and-links/newsletter/newsletter03/tp-data.html>.
- [39] R. M. J. Bamunawala, S. S. L. Hettiarachchi, S. P. Samarawickrama, P. N. Wickramanayakkara, and R. Ranasinghe, "Climate Change Impacts on Seasonal Wave Climate of the Western Coast of Sri Lanka," 3rd International Symposium-ACEP,, 2015.
- [40] "NCEP/NCAR Research Data Archive", NCEP/NCAR Available: <https://rda.ucar.edu/>
- [41] "National Oceanic and Atmospheric Administration." Available: <https://www.noaa.gov/>.
- [42] SWAN, "SWAN Technical documentation," Delft University of Technology: Delft, 2016.
- [43] "Gridded Bathymetry Data", GEBCO Available: [https://www.gebco.net/data\\_and\\_products/gridded\\_bathymetry\\_data/](https://www.gebco.net/data_and_products/gridded_bathymetry_data/).
- [44] "Admiralty Maritime Data Solutions", Admiralty Charts, Available: <https://www.admiralty.co.uk/charts>.
- [45] Y. Luo, D. Wang, T. P. Gamage, and F. Zhou, "Wind and wave dataset for Matara , Sri Lanka," Earth Syst. Sci. Data, pp. 131–138, 2018.

# Wave Energy Resource Assessment for the Coastal Ocean Around Sri Lanka using Satellite Altimeter Data

H.P.V. Vithana<sup>#1</sup>, S.M.D.L.S Wimalarathna<sup>#2</sup>, S.M.Kannangara<sup>#3</sup>

<sup>#</sup> Department of Civil and Environmental Engineering,  
Faculty of Engineering, University of Ruhuna  
Hapugala, Galle, Sri Lanka.

<sup>1</sup>vidura@cee.ruh.ac.lk

## Abstract

Ocean wave energy is an abundant renewable energy source which is untapped and inexhaustible with great potential to be developed in Sri Lanka. Wave energy does not generate harmful solid, liquid or gaseous by-products. Determination of wave energy/power variation as a quantity of the coastal zone is particularly useful for developing the wave power to confront the energy crises and the environmental pollution due to overuse of fossil energy sources. Establishing wave energy resource assessment for the coastal sea around Sri Lanka by quantifying wave energy/power spatially as well as temporally is the main objective of this research. Absence of measured wave statistics around the island is a major challenge in this exercise. Therefore, long term wave climate was established using significant wave height data derived from satellite altimeter data records with verification carried out on the basis of wave buoy measured data offshore of Galle. A map showing wave power per meter of wave crest (kW/m) around Sri Lanka was developed.

**Keywords:** Ocean, Wave energy, Sri Lanka

## Introduction

While wind and solar have been the leading sources of renewable energy up to now, ocean waves are increasingly being recognized as a viable source of power for coastal regions [1]. Being an island nation surrounded by the ocean Sri Lanka offers ideal conditions to develop this abundant energy source.

When considering the wave climate in Sri Lanka, two monsoons, i.e., south west and north east monsoons dominate the climate of the country. The wave climate off the coast of Sri Lanka is characterized by long period swell waves and local wind generated sea waves. The swell waves are those waves generated in the southern Indian Ocean and have propagated out of the generation zones. These waves approach from a more or less southerly direction in deep water [7].

This paper describes results of a wave energy resource assessment in the coastal sea of Sri Lanka. In order to estimate long-term wave climate and available wave power, it is necessary to find the variation in significant wave

height ( $H_s$ ), both spatially and temporally. The objective of this ongoing study is to calculate the available wave energy in the coastal sea of the island.

## Background

### Global wave energy resource

Less wave energetic regions are located close to the equator and poles according to the Figure 1. However, it can be seen that wave energy resources occur in bands across the northern and southern hemispheres. This annual average omnidirectional wave power density will not be able to give a clear idea about the "utility of a particular wave energy resource for particular wave energy converters". Waves are relatively small at the equatorial region due to the small wind speeds of the region. Wave resource is much less variable because Southern hemisphere has much consistent wind than the Northern hemisphere. Therefore, consideration of the local geography and the meteorological conditions give a reasonable qualitative estimate about the wave energy resources [4].

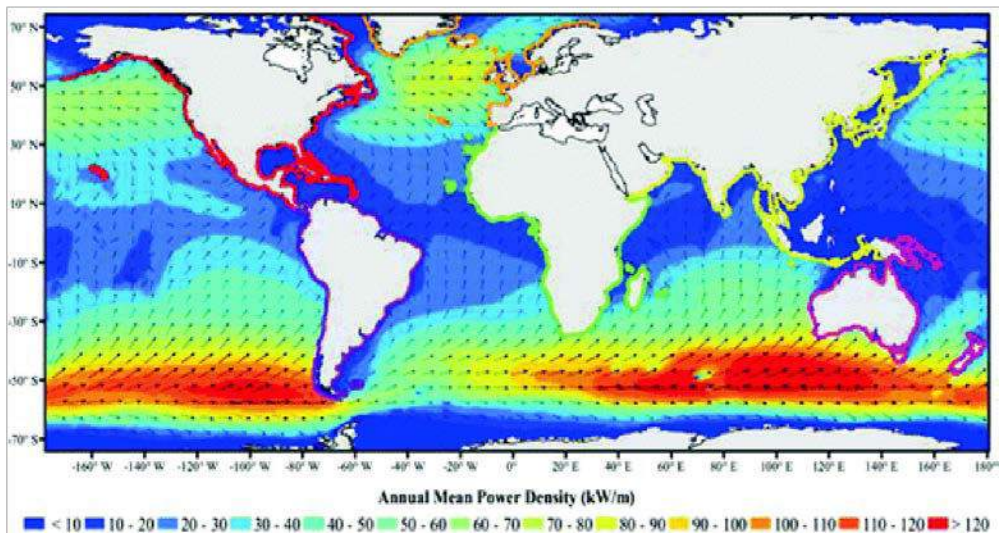


Figure 1: The global wave energy resource [4]

### **Wave height data from satellite altimeter measurements**

Significant wave heights are provided close to the accuracy of a buoy measured significant wave heights by properly interpreted back-scattered signal from satellite altimeters. This accuracy will be given from the satellite having an orbit at 1000 km. Measurements are made each second, whilst the satellite flies over a repeat net of ground tracks at about 6 km/s. At present large amount of steady flow of worldwide data are provided by this process using three or more operational satellites. Therefore, millions of new observations are becoming available each month. Global long-term satellite altimeter measurements have been performed during the period from 1985 to 1989 by the US Navy's Geosat and the Geosat-Follow-on mission (from 2000 to 2008), by ESA's ERS-1 (from 1991 to 1996), ERS-2 (from 1996 to 2003), EnviSat (from 2002) and the US/French Topex/Poseidon mission from 1992 to 2005 augmented by the Topex-Follow-on mission (Jason) which has provided data since 2002 on the same orbit as Topex and, from 2009, Jason-2, also on the Topex orbit [3]. Topex/Poseidon altimeter wave height data have been obtained for this study due to longer data coverage and availability of the data for the research purposes.

### **Wind-wave climate in Sri Lanka**

Sri Lanka being a tropical country is affected by two main annual weather cycles. That is:

(1) The south-west monsoon (from May to September) which brings rain to the southern and western coastal regions and the central hills.

(2) The north-east monsoon (from December to February) which brings rain to the north and east of the island. This is a weaker system and short-lived than the southwest monsoon.

Monthly average wind speed around the coastal zone of Sri Lanka is more than 4 m/s according to the data provided by wind energy resource atlas of Sri Lanka and the Maldives as followed [5], [7].

The most violent sea conditions are observed during the south west monsoon season during which both sea and swell waves occur at maximum strength. Southern and western areas of the island are affected by the south west monsoon. In Sri Lanka, nearshore wave climate is characterized by the simultaneous occurrence of swell waves approaching from a more or less southerly direction and sea waves mainly influenced by monsoonal weather pattern. Some nearshore areas are also vulnerable for occasional impact of cyclonic wave conditions. This complexity and high degree of temporal and spatial variability of waves clearly emphasizes the need for accurate assessment of nearshore wave climate. The lack of wave recordings at nearshore locations restricts the assessment of nearshore wave climate to some extent [7].

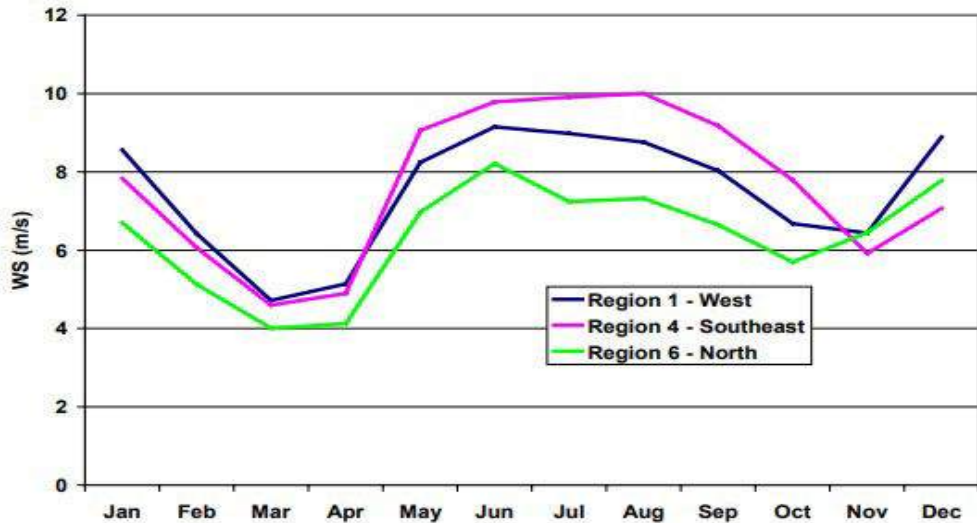


Figure 2: Sri Lanka – Ocean Satellite Monthly Average Wind Speeds and Power Densities  
(Source: <https://www.nrel.gov/docs/fy03osti/34518.pdf>)

## Methodology

### Data collection

The first step of the research project was collecting data to identify the long-term wave climate around Sri Lanka using satellite data and wave buoy measured data. The second and final step is to estimate the wave energy offshore of the main coastal cities.

Two types of wave height data were considered in the research.

### Measured wave data

Directional wave measurements have been carried out on the south west coastal ocean in Sri Lanka by the Coast Conservation Department from February 1989 to September 1992. A pitch and roll type buoy was deployed off Galle harbour at a water depth of 70 m. The sea climate in this region is characterized by a bimodal spectrum with an all year rather strong long period swell wave component and a sea wave component [6]. Both wave systems have different deep-water

Wave systems have different deep-water wave directions. For statistical analysis sea waves were separated from swell waves. The data set obtained from the Coast Conservation Department of Sri Lanka was used for the present wave energy mapping study.

### Satellite wave data

The satellite data was downloaded using TOPEX altimeter sensor data record from physical oceanography distributed active archive centre (PODAAC) which is associated with NASA.

### Data comparison

Data comparison was carried out between satellite data and measured data. Monthly average significant wave heights for the same location and for the same time period were used for this comparison. The purpose of this comparison is to verify the feasibility of using satellite data instead of measured wave buoy data. The comparison is shown in Table 1.

Table 1: Comparison between measured wave height data and satellite altimeter data, Hs (m)

| Month | Satellite wave data (Hs)(m) |       |       |       |       | Galle measured wave data (Hs) | Satellite wave data (Hs) |
|-------|-----------------------------|-------|-------|-------|-------|-------------------------------|--------------------------|
|       | 1989                        | 1990  | 1991  | 1992  | 1993  |                               |                          |
| Jan   | NA                          | 1.020 | 1.020 | 1.200 | 1.300 | 0.939                         | 1.135                    |
| Feb   | NA                          | 1.230 | 1.204 | 0.863 | 1.265 | 0.965                         | 1.140                    |
| Mar   | NA                          | 1.470 | 1.303 | 0.780 | 0.890 | 1.048                         | 1.111                    |
| Apr   | 1.516                       | 1.478 | 1.633 | 1.200 | 1.509 | 0.901                         | 1.467                    |
| May   | 1.768                       | 2.110 | 1.763 | 2.210 | 3.360 | 1.699                         | 2.242                    |
| Jun   | 2.665                       | 2.392 | 2.300 | 2.596 | 1.802 | 2.338                         | 2.351                    |
| Jul   | 1.854                       | 1.891 | 1.891 | 2.500 | 2.785 | 2.206                         | 2.184                    |
| Aug   | 2.777                       | NA    | 2.275 | 2.135 | 2.318 | 2.206                         | 2.376                    |
| Sep   | 2.259                       | 1.998 | 1.874 | 2.14  | 2.275 | 1.913                         | 2.109                    |
| Oct   | 1.366                       | NA    | NA    | 1.704 | NA    | 1.718                         | 1.535                    |
| Nov   | 1.235                       | 1.236 | 1.24  | 2.586 | 1.142 | 1.195                         | 1.488                    |
| Dec   | 0.792                       | NA    | 1.36  | 1.125 | NA    | 1.154                         | 1.092                    |

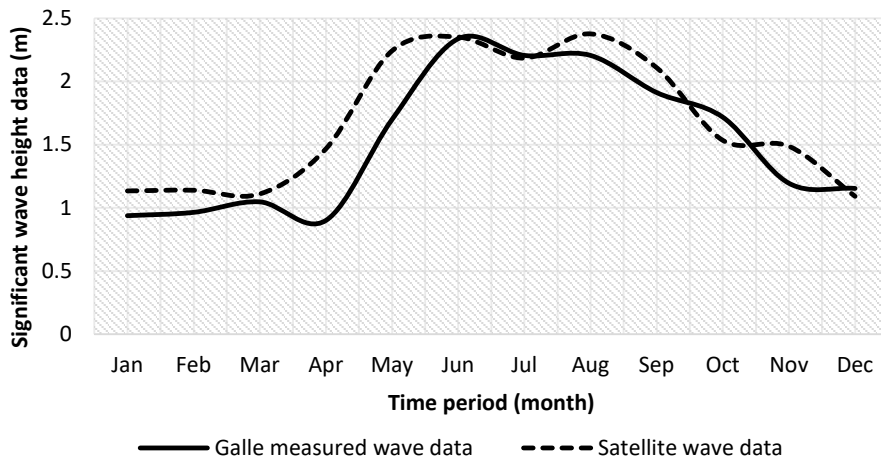


Figure 3: Comparison of measured monthly mean significant wave height data with satellite data

The average monthly significant wave height derived from satellite altimeter and wave buoy measured significant

wave height were plotted as shown in Figure 3.

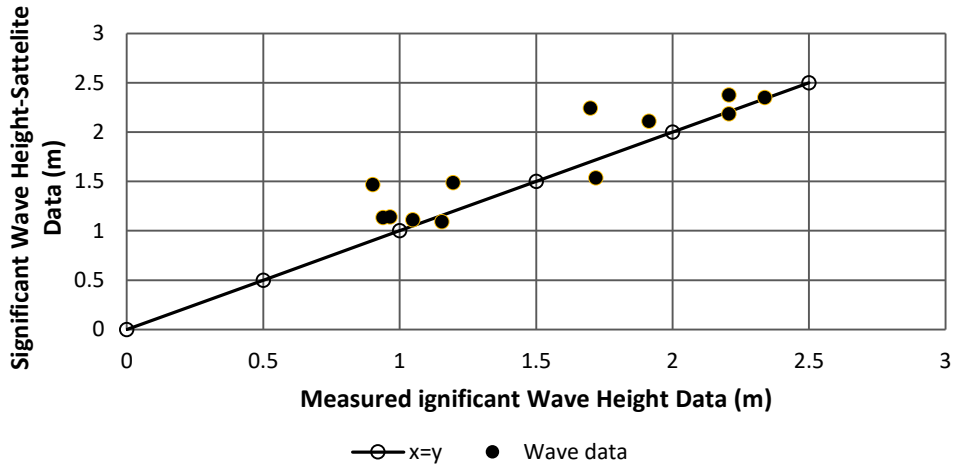


Figure 4: Comparison of measured significant wave height data with satellite data

In this analysis Root Mean Square (RMS) error was found to be 0.027m and  $R^2=0.91$ . According to the results of the comparison, it can be concluded that the satellite measured wave height data can be used for calculating zero-crossing time period and wave power per unit width of wave crest with sufficient accuracy in the absence of buoy measured wave data. Figure 3 shows the monthly mean significant wave height variation (1989-1992) for buoy measured wave data and satellite altimeter measured wave data. The Figure 4 shows the deviation of the same data from  $y = x$  line.

### Wave power calculation

The significant wave height ( $H_s$  or  $H_{m0}$ ), Zero-crossing period  $T_z$ , mean period  $T_m$ , and peak period  $T_p$ , were defined by the following equations.

$$H_s = 4\sqrt{m_0} \quad (Eq 1)$$

Where,

$H_s$  = significant wave height (m)

$m_0$  = initial spectral moment ( $m^2$ )

$$T_z = \sqrt{\frac{m_2}{m_0}} \quad (Eq 2)$$

Where,

$T_z$  = zero crossing wave period (s)

$m_2$  = second spectral moment ( $m^2s^{-2}$ ).

And The energy period of a sea state is defined in terms of spectral moments as,

$$T_E = \frac{m_{-1}}{m_0} \quad (Eq 3)$$

Where,

$T_E$  = energy period

$m_{-1}$  = -1 spectral moment ( $m^2s^{-1}$ ).

The wave power in deep water is expressed by (4). With ( $\rho$ ) sea water density ( $1025 \text{ kgm}^{-3}$ ) and wave energy period,  $T_E$  is defined by (3) The power per unit width of wave crest,  $P$  (kW/m), is given by (4) and can be simplified into (5),

$$P = \frac{\rho g^2}{64\pi} H_s^2 T_E \quad (Eq 4)$$

$$P = 0.49 H_s^2 T_E \quad (Eq 5)$$

In order to determine the wave energy period,  $T_E$  from limited datasets it has been a common practice to employ fixed conversion factors based on a theoretical



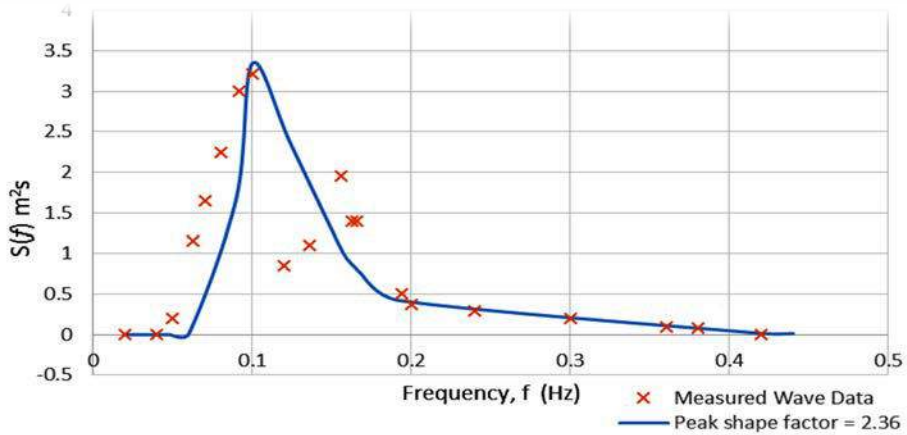


Figure 5: Comparison of measured and JONSWAP Wave Spectra

spectral shape, such as Bret Schneider or JONSWAP, which is deemed to be representative of the dominant wave conditions. The main challenge in this study was lack of measured wave data. Measured data offshore of Galle [8] did not contain the original raw wave data but it consisted of calculated significant wave heights. Therefore, construction of monthly wave energy spectra was not possible to calculate monthly  $T_E$  values. However, the report [8] provided a wave energy spectrum for the whole measurement period [see Figure 5]. This was fitted to JONSWAP spectrum and it was found that the JONSWAP spectrum fits reasonably well to the measured wave energy spectrum when peak shape factor is equal to 2.36.

Cahill and Lewis [2] calculated wave energy period ( $T_E$ ) for different types of spectra on the basis of field measurements and found that the wave energy period varies with peak shape factor. According to previous studies, they give an equation for calculating the wave period ratio by following equation.

$$\frac{T_E}{T_z} = \frac{4.2 + \gamma}{5 + \gamma} * \sqrt{\frac{11 + \gamma}{5 + \gamma}} \quad (Eq 6)$$

Where,

$\gamma$  = peak shape factor

Using this equation, wave period ratio was calculated. For this study it was found that 1.2, then the wave power can be calculated as;

$$P = 0.588 H_s^2 T_z \quad (Eq 7)$$

$H_s$  was extracted for the various locations at 50m water depth and the average of significant wave height was calculated for 15 years from the satellite data. The only unknown parameter  $T_z$  was calculated using the following equation [6]:

$$T_z = \frac{1}{\beta} \ln \left( \frac{1}{\alpha} \left( \frac{c}{H_s + \gamma} \right) \right) \quad (Eq 8)$$

Where,

$c = \sigma_0 - A$  if  $\sigma_0 \leq \delta$  or

$c = \delta - A$  if  $\sigma_0 > \delta$

And  $\alpha, \beta, \gamma, \delta$  are empirically determined constants listed in Table 2.

Table 2: Empirical constants used in the algorithm for calculating  $T_z$   
 (Source: <https://www.sciencedirect.com/topics/engineering/significant-wave-height>) [6]

| Mission  | A     | $\alpha$ | $\beta$ | $\gamma$ | $\delta$ |
|----------|-------|----------|---------|----------|----------|
| TOPEX    | 17.11 | -4.054   | -0.1558 | 1.658    | 12.87    |
| Poseidon | 19.4  | -2.831   | -0.109  | 3.496    | 12.81    |
| Jason-1  | 17.68 | -4.094   | -0.1488 | 1.851    | 12.95    |
| ERS-2    | 17.42 | -3.906   | -0.1422 | 2.072    | 12.39    |
| ENVISAT  | 16.28 | -4.248   | -0.163  | 1.314    | 12.29    |
| GFO      | 17.16 | -4.55    | -0.1648 | 1.669    | 12.88    |

## Results and Discussion

In this study available wave power at twenty-three locations around the island at 50 m water depth has been considered as shown in Table 3. Average annual significant wave height was calculated for each location. Then, zero crossing wave period ( $T_z$ ) for corresponding to average annual wave height was calculated by using Eq. (8), Finally, wave power was calculated using Eq. (7). However, when wave power was calculated on a month by month basis using average monthly wave height and then averaged to obtain annual wave power the resulting wave power was up to 20% higher than that obtained using a single mean annual significant wave height as shown in Figure 6:

Table 3. Locations considered in the study

| Location    | Latitudes | Longitudes |
|-------------|-----------|------------|
| Batticaloa  | 7.73961   | 81.825179  |
| Vakarai     | 8.234637  | 81.58348   |
| Trincomalee | 8.511802  | 81.424178  |
| Pulmudai    | 8.938931  | 81.140289  |
| Mullativ    | 9.352615  | 80.931792  |
| Uduthurai   | 9.787139  | 80.750318  |
| Point Pedro | 10.041462 | 80.437208  |
| Mannar      | 8.860228  | 79.530836  |
| Wilpattu    | 8.428561  | 79.697897  |
| Kalpitiya   | 8.107624  | 79.670028  |
| Chilaw      | 7.592845  | 79.637529  |
| Negambo     | 7.171653  | 79.6747    |
| Colombo     | 6.893613  | 79.637707  |
| Wadduwa     | 6.599036  | 79.813489  |
| Induruwa    | 6.279714  | 79.915112  |
| Galle       | 6.063991  | 80.079907  |
| Matara      | 5.874278  | 80.5117511 |
| Tangalle    | 5.961017  | 80.919619  |
| Hambantota  | 6.051285  | 81.155397  |
| Yala        | 6.272345  | 81.63373   |
| Pottuwil    | 6.7827676 | 81.997435  |
| Thirukkivil | 7.14035   | 81.968712  |
| kalmunai    | 7.51092   | 81.94674   |

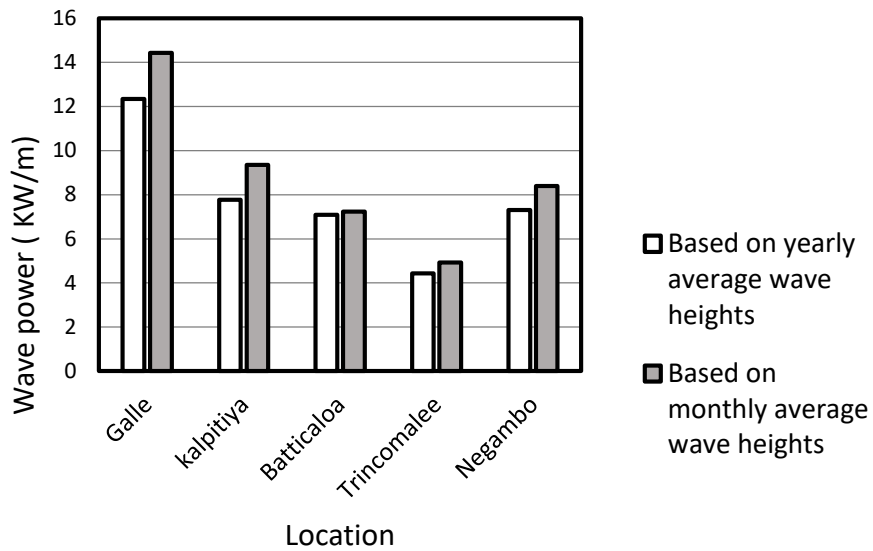


Figure 6: Comparison of Wave power using yearly average values and monthly average values

The variation of wave power (kW/m) in 50 m water depth around Sri Lanka was mapped using 13 years of wave statistics as shown in Figure 7. The maximum wave power was observed offshore of Pottuvil and minimum in Pulmoddai. Maximum wave power observed in

Pottuvil area could be due to that the region is influenced by both south-west and north-east monsoon systems. Variation of wave power around the island w.r.t different locations is shown in Figure 8 and the seasonal variation of wave power is shown in Figure 9.

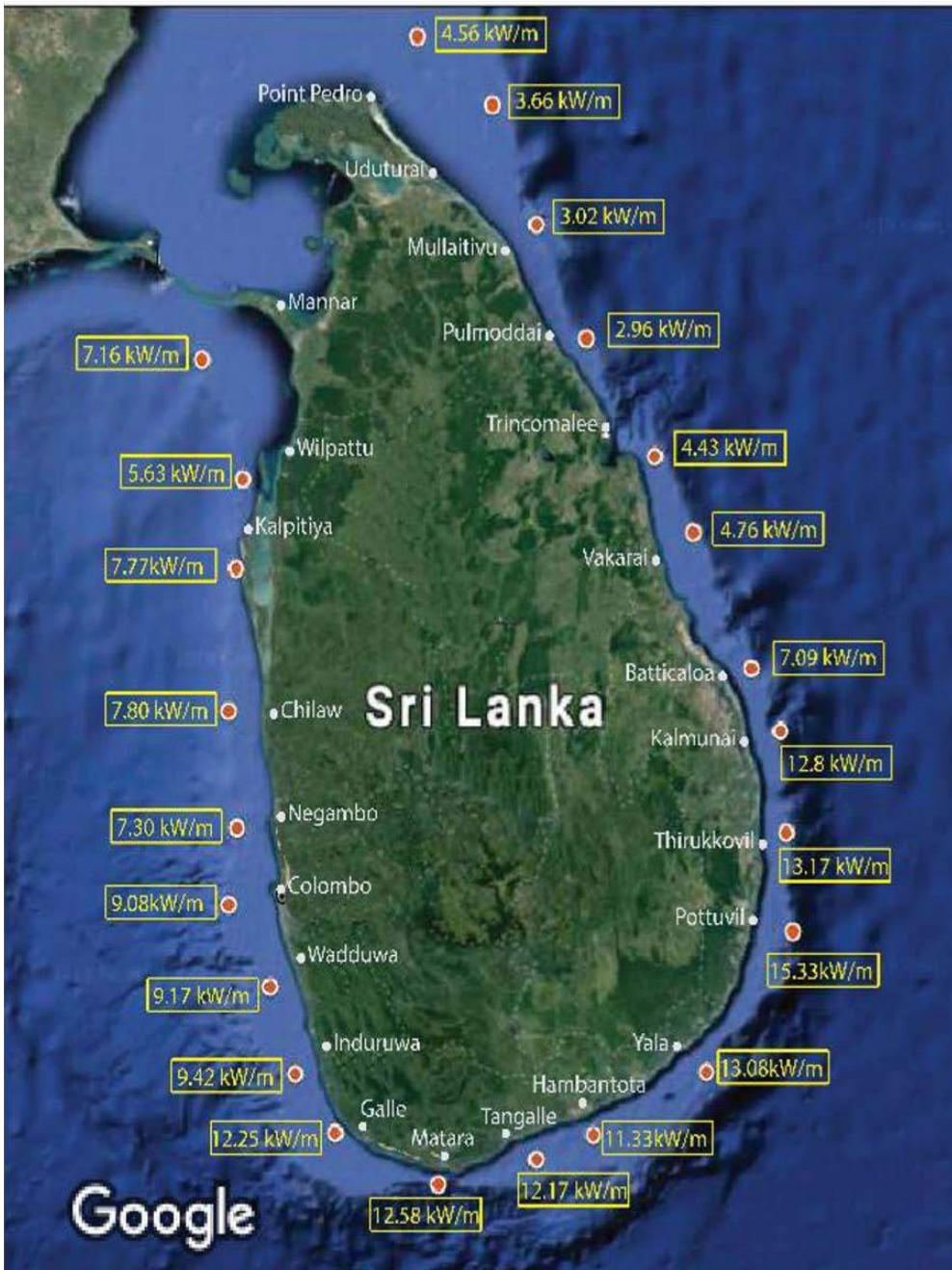


Figure 7. Map showing average wave power (kW/m)

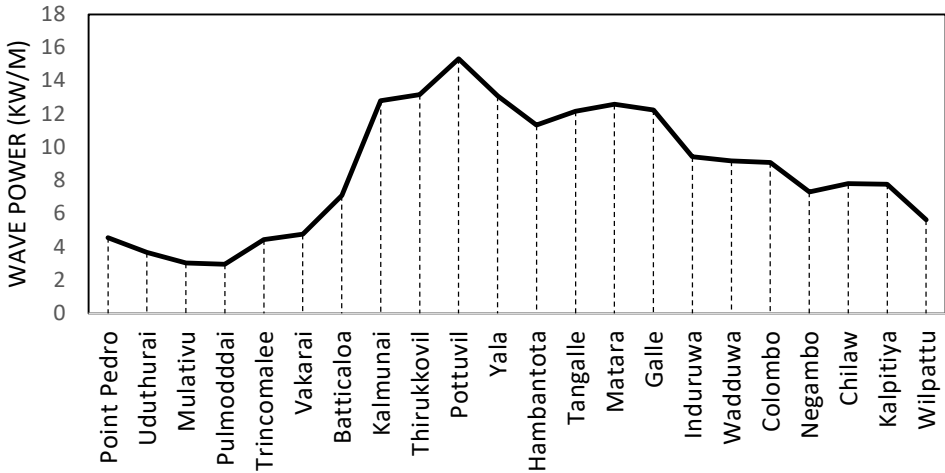


Figure 8: Variation of average wave power around Sri Lanka

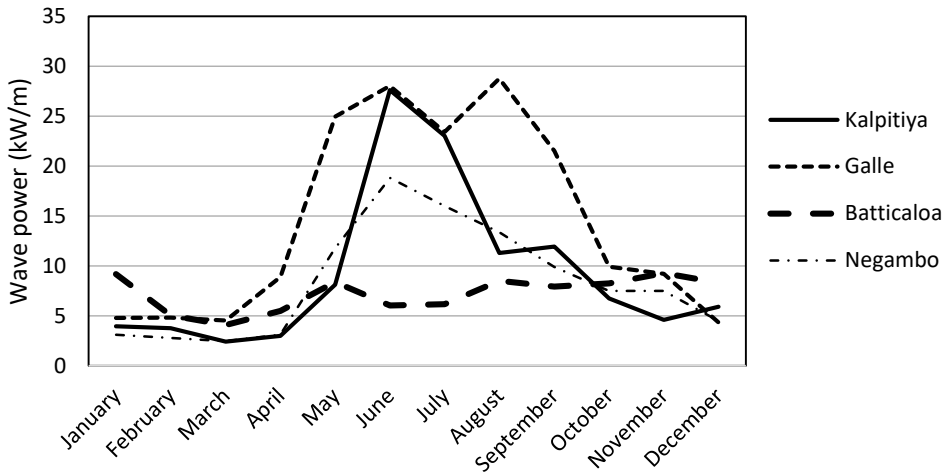


Figure 9: Monthly variation of wave power

## Conclusions

In the absence of measured wave data at sea, wave parameters derived based on satellite altimetry can be used to calculate available wave energy with reasonable accuracy. According to the above results maximum annual wave power can be expected in the southern

and south eastern coastal sea of Sri Lanka with peak energy levels observed in Pottuvil.

## Acknowledgments

The authors express their appreciation to the Coast Conservation and Coastal Resource Management Department for their assistance in securing wave data.

## References

- [1] Cahill, BG, Lewis T. Wave energy resource characterization of the Atlantic Marine Energy Test Site. *Int. J. Mar. Energy* 2013; 1:3–15.
- [2] B.G.Cahill, T. Lewis, “Wave period ratios and the calculation of wave power”, in *Proc. of the 2<sup>nd</sup> Marine Energy Technology Symposium, Mets2014, Seattle, WA, USA, April 15-18, 2014.*
- [3] S. Barstow, G. Mork, L. Lonseth, J.P. Mathisen. Worldwaves wave energy resource assessments from the deep ocean to the coast. [Online]. Available: <https://www.researchgate.net/publication/228644150>.
- [4] Folley M. The Wave Energy Resources. In Pecher A & Kofoed JP (eds). *Handbook of Ocean Wave Energy: Ocean Engineering & Oceanography (7)*, Aalborg, Denmark; 2017, p. 43-61,
- [5] Joseph L. National report of Sri Lanka on the formulation of a transboundary diagnostic analysis and strategic action plan for the Bay of Bengal large marine ecosystem programme. [Online]. Available: [http://www.boblme.org/documentRepository/Nat\\_Sri\\_Lanka.pdf](http://www.boblme.org/documentRepository/Nat_Sri_Lanka.pdf)
- [6] Mackay EBL. Resource Assessment for Wave Energy. In: Sayigh A, (ed.), *Comprehensive Renewable Energy, Vol 8*, pp. 11–77. Oxford: Elsevier; 2012.
- [7] Ranasinghe DPL, Gunaratne PP. Assessment of nearshore wave climate in southern coast of Sri Lanka. *Annual Research Journal of SLSAJ*: 2011; 11: 43-51.
- [8] Scheffer H-J, Fernando KRMD, Fittschen T. Directional wave climate study south west coast of Sri Lanka. Sri Lankan – German Cooperation, CCD-GTZ Coast Conservation project;1994.

# Investigations on Ocean Wave Energy Assessment for Sri Lanka

Pravin Maduwantha #<sup>1</sup>, Harshinie Karunarathna \*<sup>2</sup>, Bahareh Kamranzad \*\*<sup>3</sup>  
Harsha Ratnasooriya#<sup>4</sup>, Kasun De Silva#<sup>5</sup>

# *Department of Civil Engineering, University of Moratuwa,  
Moratuwa, Sri Lanka.*

<sup>1</sup> mgpravim93@gmail.com

<sup>4</sup> ahrr@uom.lk

<sup>5</sup> kasunds@uom.lk

\* *Zienkiewicz Centre for Computational Engineering, College of Engineering, Swansea  
University, Swansea SA1 8EN, UK.*

<sup>2</sup> h.u.karunarathna@swansea.ac.uk

\*\* *Graduate School of Advanced Integrated Studies in Human Survivability (GSAIS), Kyoto  
University, Yoshida-Nakaadachi 1, Sakyo-ku, Kyoto 606-8306, Japan.*

\*\* *Hakubi Center for Advanced Research, Kyoto University, Yoshida Honmachi, Sakyo-ku,  
606-8501, Kyoto, Japan.*

<sup>3</sup> kamranzad.bahareh.3m@kyoto-u.ac.jp

## Abstract

Being an island surrounded by the ocean, a significant potential exists in Sri Lanka to harness ocean wave energy as a renewable energy source. The assessment of wave energy characteristics in coastal waters of Sri Lanka is important in identifying such a potential. A detailed analysis of patio-temporal variability of wave power was carried out by considering computationally projected wave data for the period 1979-2003. Waves were projected using a cascade of computational wave models with increasing resolution where a large-scale Indian Ocean Model provided boundary conditions for a smaller scale model covering the ocean around Sri Lanka. Model outputs were validated using measured wave data off the southwest coast and some other available sources. Projected wave outputs reveal that coastal areas of Sri Lanka from the south-west to the south have a substantial wave power resource, varying between 10-30 kW/m. Wave power reduces when waves travel over the continental shelf towards the shoreline. Offshore wave power throughout the year mostly remains between 10-20 kW/m, although it is significantly modulated by the south-west monsoon. A spatial variation of wave power along the coast was also evident. The study also revealed that inter-annual to decadal scale variability of wave power is largely insignificant, although minor variations are observed.

**Keywords:** Renewable Energy, Ocean Wave Energy, Sri Lanka

## Introduction

Sustainable and clean renewable energy resources have become much more attractive in the energy sector due to various environmental implications of using non-green resources. Ocean wave energy is considered a promising energy source with high predictability with minor environmental impacts.

Though the wave energy essentially depends on the atmospheric conditions, the factors such as wave height, frequency, direction and its seasonal variations should be examined for a proper decision making on wave energy harvesting [1]. Therefore, the spatial and temporal variations of wave energy were analysed to determine the optimum locations for wave energy extraction. Though a rough estimation can be made based on available wave buoy data, the spatial distribution of wave energy and its long term variations cannot be assessed accurately using sparsely available measured data. Hence numerical modelling based on theories of wave generation and propagation can be used to generate ocean waves [2].

Numerically simulated ocean waves were used to a broad scale global wave energy assessment by Cornett [3] to quantify the available wave energy resource in the world. Eventhough with the low resolution of the wave model ( $1.25^\circ$  by  $1.0^\circ$ ), the regions with highest available wave energy in the world were identified by the study. Kamranzad *et. al.* [4] evaluated the available wave energy potential in the Southern Caspian Sea and they have identified wave energy hotspots based on the spatial distribution of wave power in the region. Goncalves *et. al.* [2] investigated the wave energy potential based on spatial distribution of

the resource in Canary Islands using simulated waves over a period of three years. Liang *et. al.* [5] assessed both spatial and temporal variations of wave energy in Shandong peninsula in China by using numerically modelled ocean waves over a period of 16 years (1996-2011). Mirzaei *et. al.* [6] used simulated waves over a period of 16 years since 1979 to assess the wave energy potential in Malaysia and investigated the strong seasonal variation of wave power between winter monsoon period and other seasons. Also, they highlighted the inter-annual wave power fluctuation due to El Niño-Southern Oscillation (ENSO). Other similar studies have been done by Kamranzad *et. al.* [7] for Pursian Gulf region, Folley and Whittaker [8] for UK, Aboobacker [9] for Eastern Bay of Bengal and Malacca Strait, Kamranzad and Mori [10] for Indian Ocean etc.

As an island surrounded by the Indian Ocean, a potential exists in Sri Lanka for wave energy harvesting to satisfy a significant proportion of energy demand in the country. The West, South and South-West coasts of Sri Lanka can potentially be the most effective regions for wave energy harvesting due to the direct exposure to South-West swell approach. Chamara and Vithana [11] assessed wave energy resource along the West, South-West and South coasts of Sri Lanka based on modelled waves developed using DELFT 3D modelling system. Amarasekera *et. al.* [12] carried out a pre-feasibility study on ocean wave power generation for the Southern coast of Sri Lanka using WAVEWATCHIII model and concluded that small scale energy extraction devices can be feasible. Although these studies provide significant insights to wave energy potential of Sri Lanka, a detailed spatio-temporal study is required to establish the resource



availability and its stability over time for making informed decisions on wave energy harvesting.

In this study, computationally projected ocean waves over a period of 25 years were used to simulate wave characteristics around Sri Lanka. The wave energy hotspots were identified based on the spatial distribution of wave power. The temporal variations of available energy resource was investigated over monthly, seasonal and decadal time scales in order to evaluate its stability and sustainability. In addition, variation of wave energy resource from the offshore to nearshore was evaluated.

## Material and Methods

### Study Area

Sri Lanka is an Island with a 1700 km long coastline, located between 5°-10°N latitudes and 79°-82°E longitude, in the Indian Ocean. The South, South-West and West coasts of Sri Lanka are subjected to direct swell waves propagating from the southern part on the Indian Ocean (Figure 1) and energetic long distance swell waves can be observed along these coasts. In addition, Sri Lanka is affected by tropical monsoon climate systems in the Indian Ocean. South-West monsoon which generates energetic waves predominantly in South-West and South coast of Sri Lanka occurs between May and September [11], [13]. North-East monsoon season occurs between December and February generating high waves predominantly in North and East coasts [13].

### Wave Model

The wave characteristics were obtained from an Indian Ocean Wave Model



Figure 1: Location of Sri Lanka in the Indian Ocean (Image reproduced from the GEBCO world map 2014, [www.gebco.net](http://www.gebco.net))

(KU\_IO) [10]. It was developed using the SWAN spectral wave model which has been widely used for ocean wave modelling by the researchers world-wide [14]. Its domain covers the area between 71°-30°N in latitude and 20°-90°E in longitude with 0.5°×0.5° spatial resolution (Figure 2). The wind data input was obtained from Japan Meteorological Agency super-high-resolution global climate model MRI-AGCM3.2S with 20 km and 1 hour spatial and temporal resolutions respectively [15]. The wave model was run for the period of 1979 to 2003 since the wind data were not available after 2003. The Komen's formulation was used in SWAN to simulate the wind field [16]. The Indian Ocean Wave Model (KU\_IO) has been broadly validated using satellite derived wave data. The KU\_IO model was further

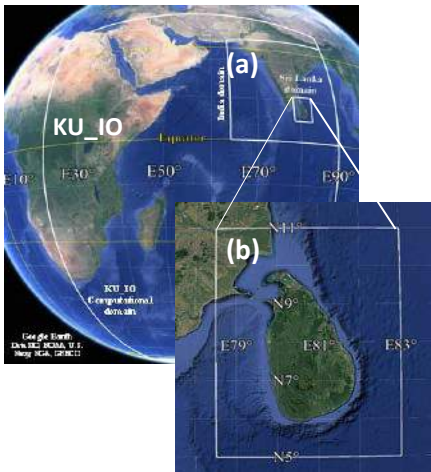


Figure 2: Indian Ocean (KU\_IO), India regional (a) and Sri Lanka local (b) wave model domains (dark white lines) used for wave projections for the Sri Lanka region

used to generate boundary conditions for the Indian regional wave model. The regional wave model domain bounded between  $64^{\circ}$ - $90^{\circ}$ E and  $0$ - $26^{\circ}$ N with computational resolution of  $0.166^{\circ}$ . This model was used to generate wave parameters from 1979 to 2003 at 6 hour intervals. In order to obtain high-resolution wave conditions around Sri Lanka, a small scale Sri Lankan regional wave model was nested in the Indian regional model for the same time period. This Sri Lanka regional wave model domain which covers the area between  $5^{\circ}$ - $11^{\circ}$ N and  $79.5^{\circ}$ - $83.5^{\circ}$ E takes boundary conditions from the Indian regional model. The spatial resolution of the Sri Lankan regional model is  $0.05^{\circ}$  in both directions and model outputs were obtained with the same temporal resolution of 6 hours for the period of 1979 to 2003. GEBCO seabed bathymetry data were used as model input with 30 arc-second spatial resolution for the Sri Lankan regional mode [16].

## Model Validation

Prior to the running the Sri Lankan regional model to obtain long term wave projections, it was validated using measured wave buoy data at Galle and ERA-Interim Global Atmospheric Reanalysis wave data (<https://apps.ecmwf.int/datasets/>). All the relevant locations and details of the data sets which used for the validation are presented in the Figure 3. ERA-Interim reanalysis wave data are published by the European Centre for Medium-range Weather Forecasts (ECMWF) and available since 1979.

The time series of combined significant wave height for all measured, ERA-Interim and modelled data are presented in the Figure 4. The results indicate that the model is able to capture the field reasonably well [Root Mean Square Error (RMSE) = 0.47 m between modelled and measured wave heights]. However, it should be noted that some of the extreme wave heights were not predicted by the model, potentially due to the current model resolution.



Figure 3: Map with all measured/modelled and ERA Interim wave data locations used for wave model validation. GM - Galle (Measured), GE - Galle (ERA-Interim), GMO - Galle (Modelled). P1 and P2 are additional model validation points.

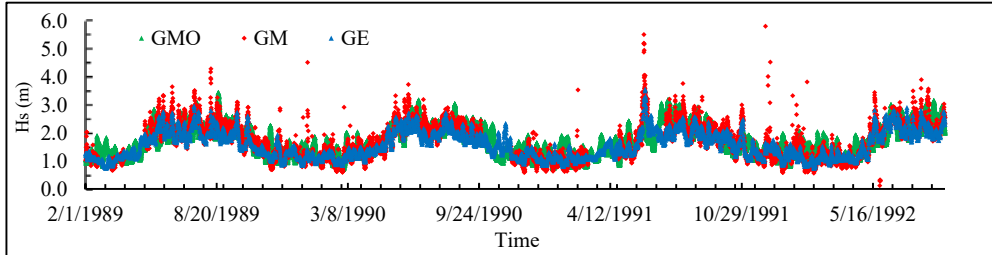


Figure 4: Significant wave height time series of Modelled data (Green), Measured data (Red) and ERA-Interim data (Blue)

Monthly averaged significant wave heights are compared and shown in Figure 5. The modelled wave heights show a good agreement with both measured and ERA-Interim reanalysis data [Root Mean Square Error (RMSE) = 0.12 m between modelled and measured monthly average wave heights]. The ERA-Interim wave data contain only the mean wave period. But, only  $T_{m02}$  (Eq. 1) was available for measured wave data.

$$T_{m02} = \sqrt{\frac{m_0}{m_2}} \quad (\text{Eq. 1})$$

Where,

$m_0$  = zeroth moment of wave the frequency spectrum

$m_2$  = second moment of the wave frequency spectrum

The variation of monthly average mean wave period of ERA-Interim data and monthly averaged  $T_{m02}$  of Modelled and Measured data are shown in Figure 6. During the period from June to August, the modelled  $T_{m02}$  seems to be significantly lower (30% to 35%) than the measured data. This may have been caused by the sensitivity of the  $T_{m02}$  to high frequency waves and the model may not accurately capture the high frequency waves during the South-West monsoon season. Eventhough SWAN is one of the most accurate ocean model in terms of wave heights, it structurally underestimates the wave periods 10%-

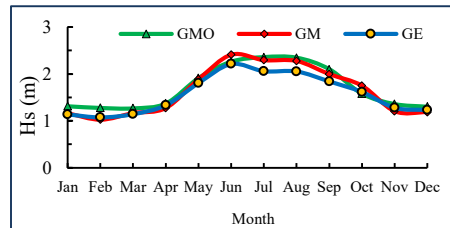


Figure 5: Monthly average significant wave height variation Modelled data (Green), Measured data (Red) and ERA-Interim data (Yellow)

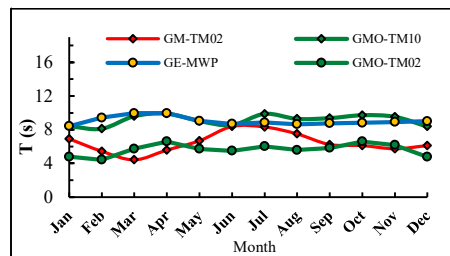


Figure 6: Monthly average wave period variation of Modelled data (Green), Measured data (Red) and ERA-Interim data (Yellow)

20% [20]. The mean wave period of ERA-interim data seems to be higher than both monthly measured and modelled  $T_{m02}$ .

Furthermore, the modelled wave data were compared with ERA interim data at P1 and P2 locations (Fig. 3) for a 5 year period from 1999 to 2003. In both locations, the modelled wave heights are in very close agreement (RMSE values of wave height time series are 0.09 m and 0.23 m for P1 and P2 respectively). The RMSE between mean wave period of ERA-Interim data and  $T_{m-10}$  of modelled

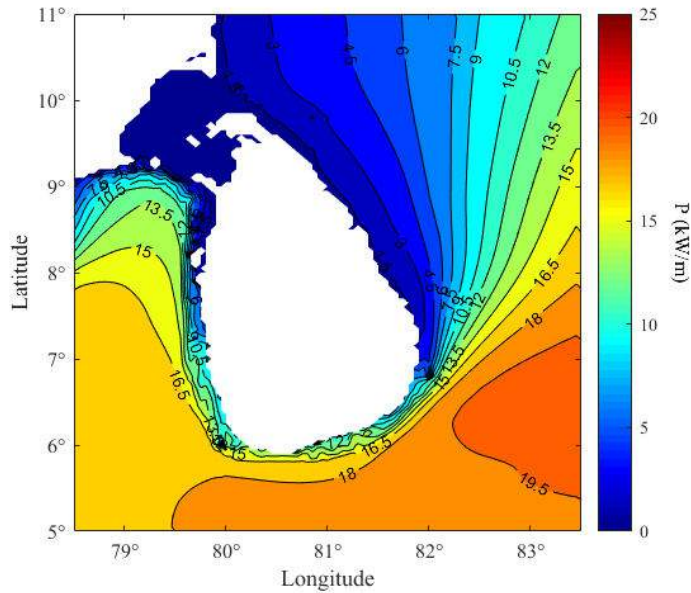


Figure 7: A spatial map of average wave power distribution (averaged over the projected 25-year period between 1979 and 2003) for the entire coastline of Sri Lanka.

waves are 1.6 s and 1.7 s at P1 and P2 respectively.

The above comparisons indicate the fact that the model is able to satisfactorily capture the wave field around Sri Lanka.

### Wave Energy Resource Analysis and Characterization

The significant wave height and wave period of modelled outputs were used to estimate wave power (Eq. 2) required for the spatio-temporal analysis.

$$P = 0.49H_s^2T_{m-10} \quad (\text{Eq.2})$$

Where,  
 $H_s$  = significant wave height (m)

$H_s$  can be calculated from  $H_s = 4\sqrt{m_0}$ , where  $m_0$  is the zeroth moment of frequency spectrum.

Here,  $T_{m-10}$  is introduced to accommodate the randomness of the wave climate and is defined as according to Equation 3 [18].  $T_{m-10}$  can be directly obtained from the model as a wave parameter.

$$T_{m-10} = \frac{m_{-1}}{m_0} \quad (\text{Eq.3})$$

Where,  
 $m_{-1}$  = first negative moment of the wave frequency spectrum

The spatial distribution of total average wave power for 25 years between 1979 and 2003 is shown in the Figure 7. The wave power distribution shows that Sri Lankan coastal region contains a significant amount of wave power, in comparison with many other coastal regions around the world. West, South-West, South and South-East coasts of the Island have the highest average wave power which can be attributed to the exposure of direct swell waves approaching from South-West direction.

The spatial distribution of the monthly average wave power (taking the entire 25-year simulation period) are shown in the Figure 8. Within the South-West monsoon period (May to September), the wave power in the Southern part of Sri Lanka is significantly higher than the other months. The power reaches 25-30 kW/m during the South-West monsoon

season and reduces to 5-15 kW/m in March. West to South-East coast has at least about 10 kW/m monthly average wave power throughout the year. Further analysis was carried out for 18 selected sites located in the West coast to South-East coast, including nine offshore points and nine corresponding near shore points. (Figure 9).

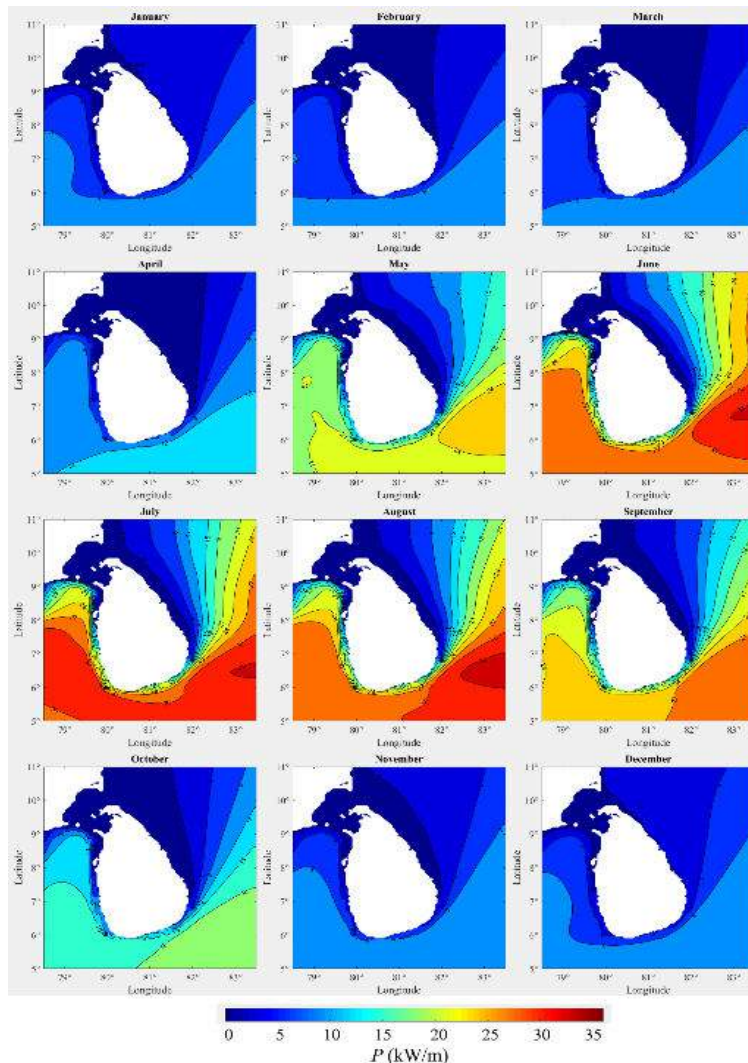


Figure 8: Spatial distribution of monthly average wave power (averaged over the modelled 25-year period between 1979-2003) for the entire coastline of Sri Lanka

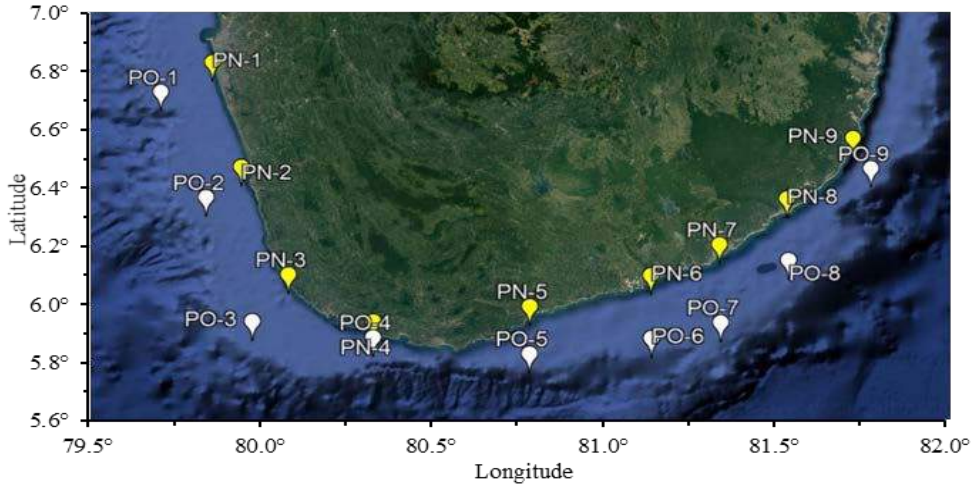


Figure 9: Eighteen nearshore (PN-1 to PN-9) and offshore (PO-1 to PO-9) sites selected along the south-west to south-east coast of Sri Lanka

All selected nearshore sites are located between the 20 m and 30 m water depths and at 2.5 km from the shoreline. All offshore sites are located between 60 m and 100 m water depth and at distances between 7-25 km from the shoreline and within the continental shelf. The stability of the available resource is an important aspect in terms of sustainability and device selection criteria. In order to evaluate the stability, monthly variability indices (MVI) were considered. The MVI were calculated as the ratio of the difference between the maximum and minimum monthly average wave power and the annual average wave power. Lower values of MVI indicate lower variability of the wave resource throughout the year. The Calculated MVI values are shown in Table 1.

The locations from PN-1 to PN-4 and from PO-1 to PO-4 have the highest MVI values which indicate that the West and South-West coasts have higher wave power variation within a year. This can be attributed to the high waves generated during the South-West monsoon season which generates energetic waves in South-West coast of the Island. To examine the wave power variability in the long term, annual average wave power was calculated (Figure 10).

According to Figure 10, a cyclic variability of wave power can be seen with each cycle lasting 5-7 years, which may be attributed to regional climatic variations such as Indian Ocean Dipole (IOD) and Equatorial Indian Ocean Oscillation (EQUINOO) [25]. The figure also shows

Table 1: Calculated MVI values for selected 18 sites

| Site | PN-1  | PN-2  | PN-3  | PN-4  | PN-5  | PN-6  | PN-7  | PN-8  | PN-9  |
|------|-------|-------|-------|-------|-------|-------|-------|-------|-------|
| MVI  | 1.535 | 1.505 | 1.448 | 1.223 | 1.066 | 1.088 | 1.147 | 1.098 | 1.069 |
| Site | PO-1  | PO-2  | PO-3  | PO-4  | PO-5  | PO-6  | PO-7  | PO-8  | PO-9  |
| MVI  | 1.460 | 1.434 | 1.320 | 1.176 | 1.062 | 1.050 | 1.051 | 1.089 | 1.114 |

that almost all the near shore sites have a significantly low annual average wave power in comparison with the corresponding offshore sites.

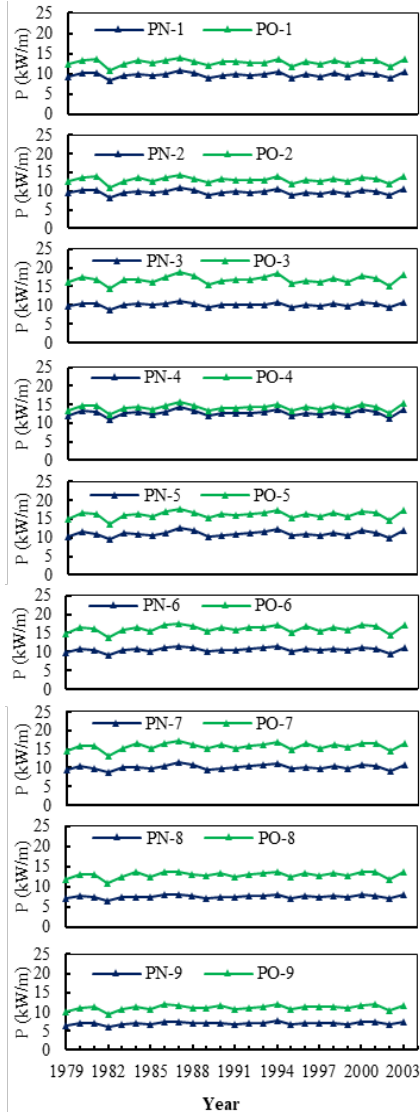


Figure 10: Annual average wave power along the south-west to south-east coast of Sri Lanka, calculated using projected wave climate for the period 1979-2003. Green lines refer to the offshore points while Blue lines refer to the corresponding nearshore points.

## Conclusion

In this study, 25 years of simulated wave data were used to investigate the wave energy potential around Sri Lanka. According to the results, the South-West and the South coast of Sri Lanka have an average amount of wave power between 10 kW/m to 20 kW/m, throughout the year. This is significantly higher than the available wave power in most coastal regions in the world. The direct swell approach from the South-West direction facilitates very favorable conditions for wave energy harvesting, especially in South and South-West coastal areas. The wave climate around the South and South-West of Sri Lanka is strongly modulated by the South-West monsoon which occurs from May to September. As a result, average available wave power can be as high as 20-30 kW/m during the monsoon period, although the resource may be unstable.

The wave power significantly varies along the coastline and towards the shoreline. The South-West coastal areas have the highest wave power, but with a high variability throughout the year. In addition, nearshore areas seem to have 20-50% less wave power than the corresponding offshore locations. A slight cyclic wave power variation can be seen in inter-annual and decadal time scale. Apart from that, the average annual wave power is mostly consistent throughout the 25-year period.

Accordingly, West and South Coasts of Sri Lanka have the potential to produce a significant amount of wave power, when compared to global estimations.

## Acknowledgement

The authors would like to acknowledge the financial support provided for this study by Swansea University, UK through the Global Challenge Research Fund Project on 'Wave energy resource characterization for Sri Lanka in a changing ocean climate'. Dr. Nalin Wickramanayake of the Open University of Sri Lanka is greatly acknowledged for sharing measured wave data and the guidance provided. The Japan Meteorological Agency is acknowledged with gratitude for providing the atmospheric model outputs to run the wave models. Bahareh Kamranzad was supported by the Hakubi Center for Advanced Research at Kyoto University and JSPS Grants-in-Aid for Scientific Research—KAKENHI.

## References

- [1] Portilla J, Sosa J, Cavaleri L., "Wave energy resources: wave climate and exploitation.," *Renew Energy* 2013; 57:594e605., vol. 57, pp. 594-605, 2013.
- [2] Gonçalves M., Martinho P., Soares C.G., "Assessment of wave energy in the Canary Islands," *Renewable Energy*, pp. 774-784, 2014.
- [3] A.Cornett, "A Global Wave Energy Resource Assessment," in *Conference Paper in Sea Technology*, 2008.
- [4] Kamranzad B., Shahidi A. E., Chegini V., "Sustainability of wave energy resources in southern Caspian Sea," *Energy*, pp. 549-559, 2016.
- [5] Liang B., Fan F., Yin Z., Shi H., Lee D., "Numerical modelling of the nearshore wave energy resources of Shandong," *Renewable Energy*, pp. 330-338, 2013.
- [6] Mirzaei A., Tangang F, Juneng L., "Wave energy potential along the east coast of Peninsular Malaysia," *Energy*, pp. 722-734, 2016.
- [7] Mirzaei A., Tangang F, Juneng L., "Wave energy potential along the east coast of Peninsular Malaysia," *Energy*, pp. 722-734, 2016.
- [8] Kamranzad B., Etemad-shahidi A., Chegini V., "Assessment of wave energy variation in the Persian Gulf," *Ocean Engineering*, pp. 72-80, 2013.
- [9] Folley M., Whittaker T.J.T., "Analysis of the nearshore wave resource," *Renewable Energy*, vol. 34, pp. 1709-1715., 2009.
- [10] Aboobacker V.M., "Wave energy resource assessment for eastern Bay of Bengal and Malacca Strait," *Renewable Energy*, vol. 14 (PA), pp. 72-84., 2017.
- [11] Kamranzad B, Mori N., "Future wind and wave climate projections in the Indian Ocean based on a super-high-resolution MRI-AGCM3.2S model projection," *Climate Dynamics*, vol. 53, no. 3-4, p. 2391–2410, 2019.
- [12] "Wave energy resource assessment for the Southern coast of Sri Lanka," in *6th International Symposium on Advances in Civil and Environmental Engineering*, Kuala Lumpur, 2018.
- [13] Amarasekera H.W.K.M., Abeynayake P.A.G.S., Fernando, M.A.R.M., Atputharajah A., Uyanwaththa, D.M.A.R., Gunawardena S.D.G.S.P, "A feasibility study on ocean wave power generation for the Southern coast of Sri Lanka: Electrical feasibility," *International Journal of Distributed Energy Resources and Smart Grids*, vol. 10, no. 2, pp. 79-93, 2014.
- [14] C. C. Department, "Coastal Zone Management Plan, Sri Lanka.," *Coast Conservation Department*, 1997.
- [15] Booij N., Ris R.C., Holthuijsen L.H., , "A third-generation wave model for coastal regions," *JOURNAL OF GEOPHYSICAL RESEARCH*, vol. 104, pp. 1649-1666, 1999.
- [16] Mizuta R., Yoshimura H., and Murakami H., "Climate simulations using MRI-AGCM with 20-km grid," *Journal of the Meteorological Society of Japan*, vol. 90A, pp. 235-260, 2012.
- [17] Weatherall P., Marks K. M. , Jakobsson M., Schmitt T., Tani S, Arndt J. E., "A new digital bathymetric model," *Earth and Space Science*, p. 331–345, 2015
- [18] L. H. a. W. Xiong, "Characteristics and Causes Analysis of Storm Surges under the Effect of Cold Air Outbreaks in the Bohai Sea,"



International Journal of Environmental Science and Development, pp. 85-88, 2013.

[19] S. Team, "SWAN scientific and technical documentation," Delft University of Technology, 2017.

[20] S. Hsu, "A wind-wave interaction explanation for Jelesnianski," open ocean storm surge estimation using hurricane Georges, pp. 1-7, 2004.

[21] C. A.M., "A global wave energy resource assessment," in International offshore and polar engineering conference, Vancouver, Canada, 2008.

[22] Anjali M., Nair and Kumar V. S., "Wave spectral shapes in the coastal waters based on measured data off Karwar on the Western coast of India," Ocean Science, vol. 13, p. 365-378, 2017.

[23] Liberti L., Carillo A., Sannino G., "Wave energy resource assessment in the Mediterranean, the Italian perspective," Renewable Energy, pp. 938-949, 2013.

[24] Sanil K. V., Anoop T. R., "Wave energy resource assessment for the Indian shelf seas," Renewable Energy, vol. 76, pp. 2012-2019, 2015.

[25] Neill N.P., Vogler A., Goward-Brown A.J., Baston S., Gillibrand P.A., Walkdon S., Woolf, D.K., "The wave and tidal resource of Scotland," Renewable Energy, vol. 114, pp. 3-17, 2017.

[26] Yasha Hetzel, Ivica Janekovic, Charitha Pattiaratchi, Wijeratne E.M.S, "Storm surge risk from transitioning tropical cyclones

in Australia," in Transitioning tropical cyclones in Australia, Auckland, New Zealand, 2015.

[27] Komen G.J., Hasselmann S., Hasselmann K., "On the existence of a fully developed wind sea spectrum," Journal of Physical Oceanography, vol. 14, pp. 1271-1285, 1984.

[28] L. Zubair, V. Ralapanawe, U. Tennakoon, "Natural Disaster Risks in Sri Lanka:," Natural Disaster Hotspots Case Studies, pp. 109-136, 2006.

[29] Hughes M.G. and Heap A.D., "National scale wave energy resource assessment in Australia," Renewable Energy, vol. 35, pp. 1783-1791., 2010.

[30] John A., Church, U Peter. Clark, "Climate change," National Hurricane Center, 2013.

[31] Sheffer H.J., Fernando K.R.M.D., Fittschen T., "CCD-GTZ Directional wave climate study South-west coast of Sri Lanka, Report on the wave measurements off Galle," Colombo, 1994.

[32] Gunaratne P.P., Ranasinghe D.P.L., Sugandika T.A.N., "Assessment of Nearshore Wave Climate off the Southern Coast of Sri Lanka," ENGINEER, pp. 33-42, 2011.

[33] F. Hal, Needham, D. Barry, Keim, David, Sathiaraj, "A review of tropical cyclone-generated storm surges," Reviews of Geophysics, pp. 545-591, 2015.

[34] MARINET, "A report on 'Standards for wave data analysis, archival and presentation," 2015

# Geothermal Energy - Potential Applications in Sri Lanka

Bandara, H.M.D.A.H.<sup>1,2</sup> Sooriyarachchi, N.B.<sup>1</sup>, Dissanayake, C.B.<sup>1</sup>,  
Subasinghe, N.D.<sup>\*1</sup>

<sup>1</sup>*National Institute of Fundamental Studies,  
Hanthana Road, Kandy, Sri Lanka*

<sup>2</sup>*Postgraduate Institute of Science, University of Peradeniya,  
Peradeniya 20400, Sri Lanka*

*\*Deepal.su@nifs.ac.lk*

## Abstract

Sri Lanka has seven major hot springs with outflow temperatures ranging between 35- 72 °C and possible reservoir temperatures ranging between 140 - 150 °C. Hence, they are categorized as low enthalpy geothermal systems. In the past research work, little attention was given to the geothermal energy potential, whereas priority has been given to study the origin of the geothermal systems. Hence this work focuses on understanding the potential of using geothermal energy in Sri Lanka. For geothermal energy exploitation, heat source and reservoir are vital to be located in depth, which is reachable economically. Recent studies carried out by our team using modern geophysical and geochemical techniques revealed that the heat sources of Nelumwewa, Mahapelessa, Kanniya and Kapurella hot springs are situated at depths which can be considered as suitable for economical drilling. Therefore, these sites can be earmarked as suitable locations for geothermal power plants supplying electricity. The other hot springs, which may not be suitable for electricity generation due to the high cost of drilling, can be used for direct heat utilization such as, drying of agricultural products (fish, rice, etc), steaming in sugar production from canes, direct use of heated water as recreation and medicinal applications.

**Keywords:** Geothermal Energy, Hot Springs, Low enthalpy, Sri Lanka, Geophysical

## Introduction

The energy demand of the world is increasing day by day due to the growth of industrial and household requirements of energy. This is a common situation in Sri Lanka as well. According to statistics of Sustainable Energy Authority, Sri Lanka's total energy demand in 2012 was 38.3 PJ. A large amount of fossil fuel, biomass and hydropower had been used. The involvement of these energy sources has also made a considerable contribution to environmental pollution in Sri Lanka. Hence, the need for environmental-friendly, pollution-free, renewable energy is very important.

Geothermal resource is a reservoir inside the earth from which heat can be extracted and utilized for generating electric power. This contains heat both in solid rock and fluids that fill the fractures/ pore spaces within the rock.

Geothermal resources can be estimated based on geological and geophysical data such as: (1). Depth, thickness, and extent of geothermal aquifers. (2). Properties of rock formations (3). Salinity and geochemical fluids likely present in the aquifers. (4). Temperature, porosity, and permeability of rock formations.

In the earth the natural geothermal gradient is 20-60 °C/km. However, with the occurrence of geological boundaries and hotspots, heat locally transferred within a few kilometers from the earth's interior through the process of convection by magma or molten rocks. These hot magmas or molten rocks interact with near-surface rocks giving rise to geothermal activities such as; hot springs, geysers or fumaroles. Essential requirements for geothermal system exist are; (1). A large source of heat. (2). A

reservoir to accumulate heat. (3). A barrier to hold the accumulated heat.

The main types of geothermal systems include vapor dominated, hot water, geopressed hot dry rock (HDR) and magma systems.

Though there are several types of geothermal resources, the ideal conventional geothermal system requires heat, permeability, and water. The heat from the earth's core continuously flow outward, sometimes as magma, coming out of the surface as lava or it remains below the earth's crust, heating nearby rocks and water. This hot water or steam can be trapped in permeable and porous rocks under impermeable rock and confined to form a geothermal reservoir. The important physical parameters in a geothermal system are; temperature, porosity, permeability, chemical content of the fluid and pressure [1].

Sri Lanka has seven major known hot springs with surface outflow temperatures varying from 35- 74 °C. Their source temperatures have been calculated and range from 140 – 170 °C [2],[3]. Hence those are categorized as low enthalpy geothermal systems. Even though most Sri Lankan hot springs have lower temperatures, some of the hot springs like Nelumwewa and Kapurella have much higher temperatures. Hence, they can be utilized to generate electricity. Even though other hot springs have lower temperatures they can be utilized as direct geothermal energy sources, like hot water for agriculture, food drying, recreational medicinal applications etc. Therefore with proper studies and infrastructure developments hot springs in Sri Lanka can be utilized as geothermal energy sources.

## **General Applications of Geothermal Energy**

Geothermal energy is used in three main methods, (1). Direct use and district heating systems (2). Electricity generation power plants (3). Geothermal heat pumps. In Direct use and district heating systems. Hot water is used from geothermal springs or reservoirs located near the surface for bathing, and many people believe the hot, mineral-rich waters have natural healing powers. Ancient Roman, Chinese and Native American cultures used hot mineral springs for bathing, cooking and heating. Industrial applications of geothermal energy include food dehydration, gold mining, and milk pasteurizing. Dehydration, or the drying of vegetable and fruit products, is the most common industrial use of geothermal energy. To heat buildings through district heating systems, hot water near the earth's surface is piped directly into buildings for heating. The district heating system provides heat for most of the buildings in Iceland, Italy, and Greece.

Geothermal electricity generation requires water or steam at high temperatures (150 °C to 350 °C). Geothermal power plants are generally built where geothermal reservoirs are located, within a kilometer or two of the earth's surface. Geothermal power plants contribute a significant amount to the electricity demand in countries like Iceland, El Salvador, New Zealand, Kenya and the Philippines and more than 90% of heating demand in Iceland.

The main advantages are that it does not depend on weather conditions and has very high capacity factors; for these reasons, geothermal power plants are capable of supplying baseload electricity, as well as providing ancillary services for short and long-term flexibility in some cases.

In geothermal heat pumps, constant temperatures near the surface of the earth is used to heat and cool buildings. Geothermal heat pumps transfer heat from the ground (or water) into buildings during the winter and reverse the process in the summer.

## **Geothermal Springs in Sri Lanka**

Hot water springs in Sri Lanka do not have any relationship with volcanic activities, in view of the fact that Sri Lanka is not situated in an active volcanic region or at an active plate boundary. Recent volcanism is not likely the heat source for the thermal springs [2] because the youngest igneous activity in Sri Lanka had occurred in Jurassic or late Cretaceous time [4, 5]. Geothermal springs in Sri Lanka occur in Eastern part of the country along Highland Complex (HC) and Vijayan Complex (VC) boundary extending northward as ~350 km thermal spring line [8]. All geothermal water springs have variable flow rates and discharge temperatures, and springs are located in the lower altitude regions (<100m) of the island except the spring at Wahawa, Padiyathalawa which is located around 100 m altitude.

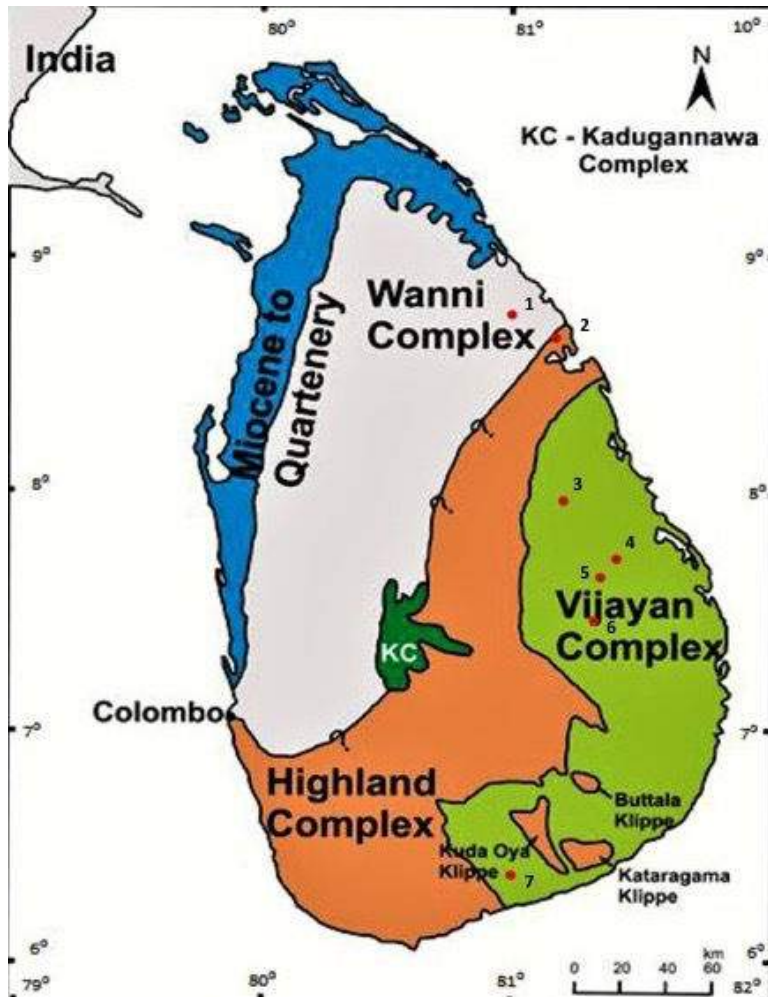


Figure 1: Geothermal hot springs in a generalized geological and tectonic map of Sri Lanka. The locations of hot springs are marked in red (Modified after [4]). The springs: 1-Rankiriulpotha; 2-Kanniya; 3-Nelumwewa; 4-Kapurella; 5-Mahaoya; 6-W W

The discharge temperatures of springs varied from 39.1 °C (Rankihiriya) to 74 °C (Kapurella). And pH vary from 5.7 (Kanniya) to 8.0 (Kapurella) [2],[7]. On account of the presence of a line of serpentine bodies, granites and anomalous uranium bearing regions, some considered them to be the source of heat for the hot springs. Chemical

geothermometers reveal the temperatures of the heat sources of some hot springs near to 150 °C [8] From the chemical geothermometers of the Na- K- Ca and silica subsurface temperatures reported for the hot springs are, Kapurella, Mahaoya, Wahawa, Padiyathalwa ,143 °C and for others 102-131 °C [9], [10].

*Table 1: Thermal springs identified in Sri Lanka, temperatures and lithological unit (After [6, 2, 7])*

| No | Hot spring            | Temperature °C | Lithological Complex |
|----|-----------------------|----------------|----------------------|
| 1  | Rankihiriya           | 39             | Highland Complex     |
| 2  | Kanniya               | 41             | Highland Complex     |
| 3  | Nelumwewa             | 62             | Vijayan Complex      |
| 4  | Kapurella             | 70             | Vijayan Complex      |
| 5  | Mahaoya               | 55             | Vijayan Complex      |
| 6  | Wahawa, Padiyathalawa | 50 – 60        | Vijayan Complex      |
| 7  | Mahapelessa           | 45             | Vijayan Complex      |

Most geothermal springs are closely associated with the Highland and Vijayan Complex boundary, which is a thrust zone based on the presence of shear zones, wrench faults and mylonites. The thrusting produces the heat in the nature of a deep mantle plume consisting crustal uplift and releasing a thermal flux, producing a high heat zone along the HC-VC boundary act as the source for the thermal spring line which appeared to align with the boundary line orientation [8] Multiple thrust zones and tectonically active zones which are connected with deep-seated mega lineament present in the area generate heat to increase the geothermal gradient [11]. Neo- tectonic activities along the HC – VC boundary, which is also evident by microseismicity observed in the Highlands and Sri Lanka due to the slow vertical movement in the Highlands [11] cause a thermal anomaly by increasing the geothermal gradient [12].

The Vijayan Complex is considered as a priority region as it consists of the

youngest intrusions of dolerite dikes of K-Ar age of 150 Ma. The presence of thermal springs in association with dyke swarms indicate thermal components that have been added from relatively young intrusions. In the Wahawa and Padiyathalawa area, dolerite dykes having the K- Ar ages of  $152 \pm 7.6$  Ma [13] are observed near westward of the thermal spring (Senaratne and Chandima, 2011). For the Wahawa and Padiyathalawa thermal springs, [14] were of the view that the meteoric water percolated from the Mahaoya River through the upper fractures of the shear zone to deep-seated fracture zones. This provides a continuous flow of water and the less fractured impermeable cap rock which over lies the reservoir, prevents the escape of hot reservoir fluids and acts as a barrier.

There is close proximity between HC- VC boundary and the Uranium anomalous regions reported in Sri Lanka and the Serpentinite occurrences. [8], suggested that the decay of uranium and highly

exothermic reaction of serpentinization of ultramafic rocks may also act as the heat source for some of the hot springs in Sri Lanka.

## Geothermal Exploration in Sri Lanka

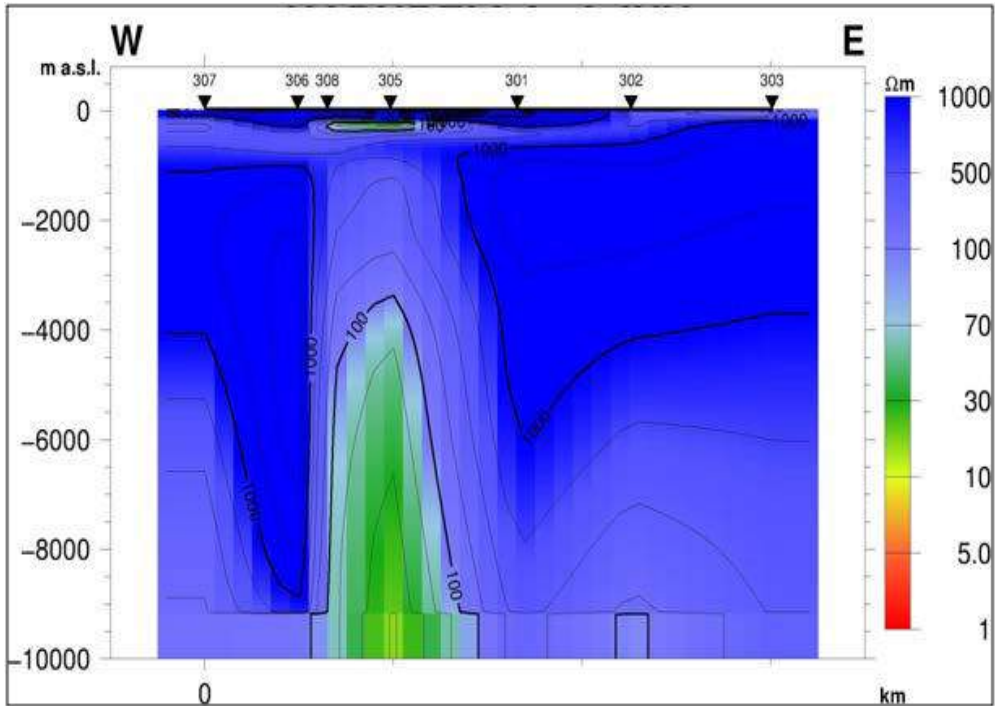
### Geophysical Explorations

An imager resistivity, self-potential, magnetic and gravity survey carried out by [15], at the Mahapalessa and Mahaoya hot springs in Sri Lanka suggests, near subsurface resistivity structure to a maximum depth of a few hundred meters indicating no evidence for the existence of a sizable thermal water accumulation, but evidence for an upward flow path with the results of low resistive ground at the surface and very high resistivity at the depth. Very low resistivity regions ( $<30 \Omega\text{m}$ ) have been detected by the magnetotelluric (MT) method at many thermal springs within very high resistive rocks with the resistivity greater than  $10,000 \Omega\text{m}$  [7], Low resistivity regions at depths greater than 10- 12 km, and of a few square kilometers in cross sections occur at Padiyathalawa, Mahaoya and Kinniya. MT computed 2D resistivity models indicates connection from low resistivity regions at the depth towards the hot springs through the less resistive bands [7].

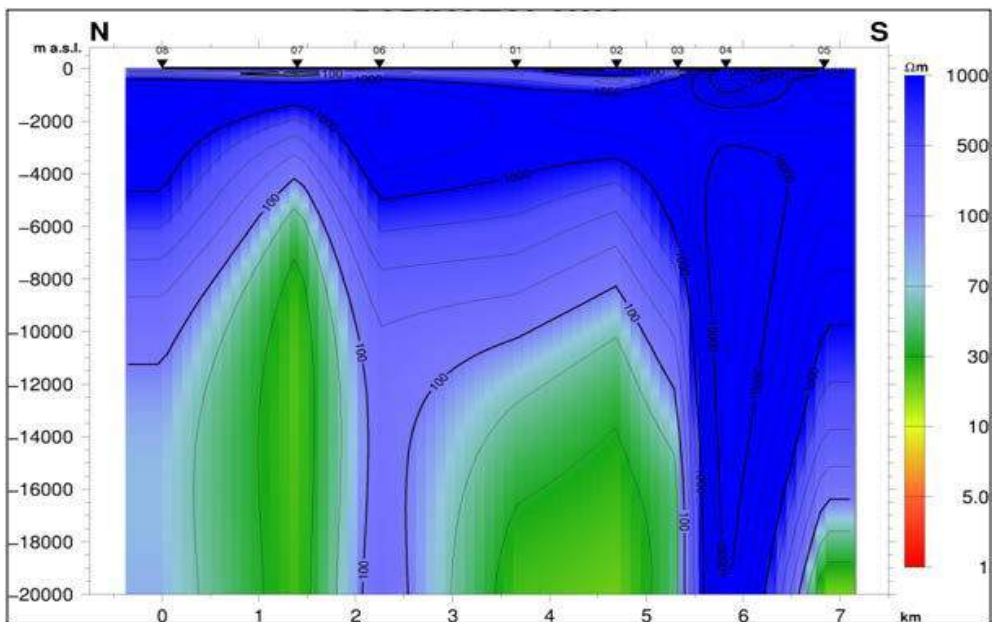
The extremely low resistive conditions observed around 150 m depth at the Kapurella area has been interpreted as an indication of water accumulation or

aquifer. By the study using time domain electromagnetic (TDEM) method, the occurrence of vertical low resistive regions starting right below the Wahawa hot spring has been interpreted as the deep fractures circulating the thermal water to the surface.

One vertical line represents a regional fault [16], In Mahaoya, nearly vertical low resistive zone is attributed to the composite results by the three structural discontinuities, one lineament and two faults [16]. The geophysical study using magnetotellurics (MT) method in the Kapurella thermal spring, near subsurface indicated a low resistive pocket and SW dipping extension interpreted as the feeding fracture zone. Here the higher resistive impermeable metamorphic basement occurs in both sides of the fracture and reservoir of the kapurella thermal spring is suggested to have occurred at the 7.5 km depth [3]. Many hot springs are close to the eastern flanks of the garben, river Mahaweli and topographic channels through Badulla and Ella flank the western side of the garben (Hatherton et al, 1975). As the hot spring waters are of meteoric origin [17],[2] and if deep normal faults are interconnected, the garben water enters through the western garben and returns upward as heated water along the eastern garben. In most locations dolerite dykes closely occur with the hot springs in the Kapurella and Padiyathalawa, and magnetic and resistivity surveys reveal that they are interconnected by deep fractures [18].



(a)



(b)

Figure 2: Deep resistivity profiles of kapurella and Padiyathalawa hot spring fields. (a). Resistivity profile for 10,000 m (10 km) depth, Kapurella area. (b). Resistivity profile up to 20,000 m depth, Padiyathalawa hot spring area.



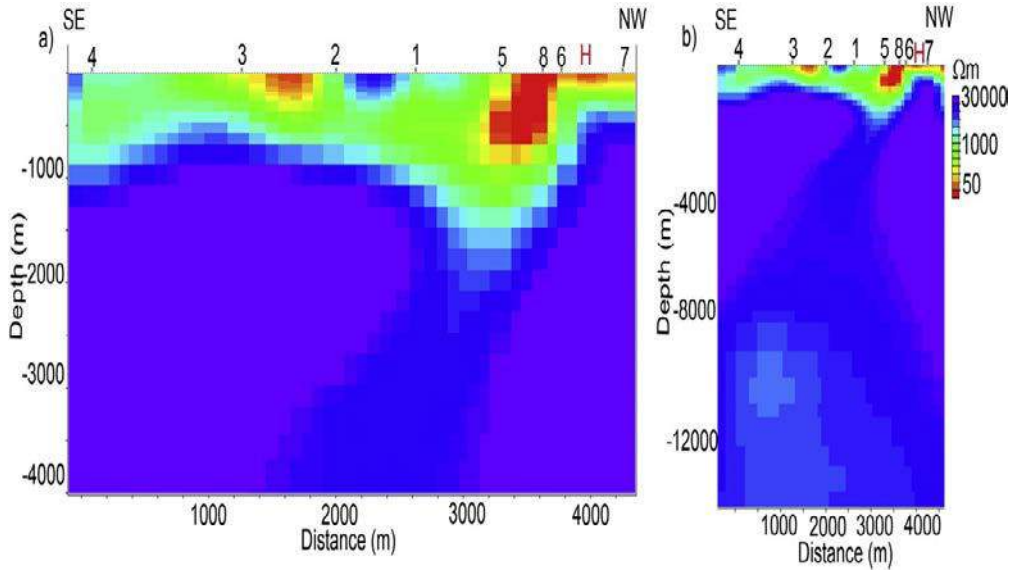


Figure 3: Deep resistivity profiles of Kapurella hot spring field. (a). 4000m deep profile. (b). 12000m deep profile [3].

Figure 4 represents the recent studies on the Mahapelessa hot spring field and its relationship to the HC/VC boundary [20]. This resistivity image clearly shows the low resistivity zones extending, starting from the hot spring and to the deep subsurface. Another very low resistive

one interpreted as [20] geothermal water accumulation zone can be identified in 500 m depth. Therefore, the Mahapelessa geothermal field can be utilized for electricity generation as geothermal water accumulation has occurred at shallow depths from the surface. It is

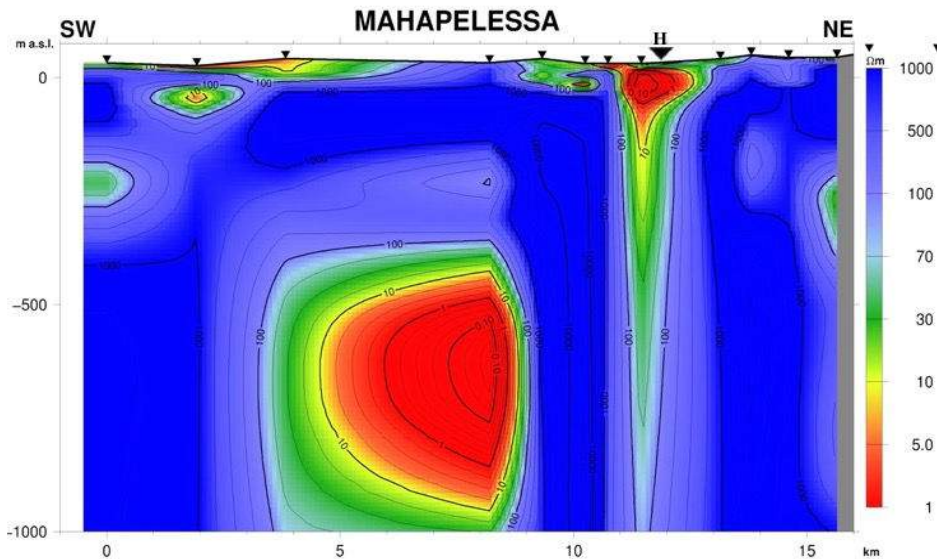


Figure 4: 1 km deep resistivity structure of the Mahapelessa hot spring field generated from MT method

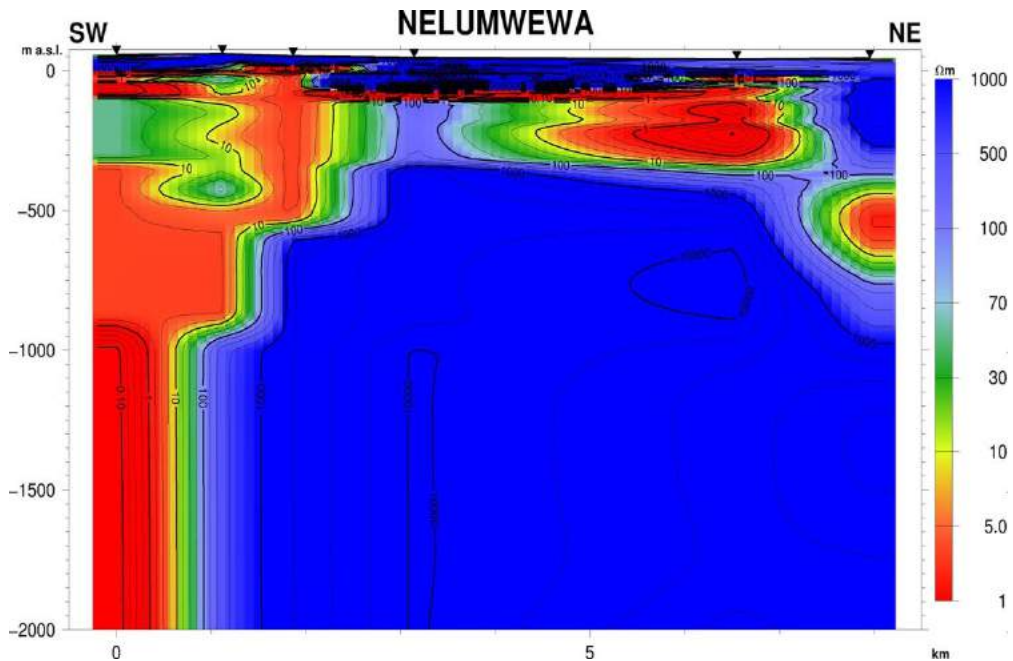


Figure 5: 2 km deep resistivity structure of the Nelumwewa hot spring field generated from MT method

therefore economically suitable for deep drilling.

In the resistivity profile of the Nelumwewa hot spring field generated from MT method, it is observed that low resistive zones occur at shallow depths from the surface (~500 m), which are interpreted as geothermal water accumulation zones [20]. Even the magnetic surveys conducted in the same field reveal possible shallow geothermal water circulation paths in the area. Hence the Nelumwewa spring field is also a possible future geothermal electrical plant.

From geological studies and vertical electrical sounding (VES) carried out at the Nelumwewa thermal spring, a geostructural model has been proposed for the formation of Nelumwewa hot

spring indicating deep percolating of groundwater through a regional fault zone, heated up by Hot Dry Rock beneath the Dimbulagala Mountain and returning to the surface through a regional vertical fault [19].

#### Geological and Geochemical Studies of Sri Lankan Geothermal Fields

According to the geological, geochemical and geographical settings, hot water springs in Sri Lanka can be divided into three groups;

- Group 1: Mahapalessa
- Group 2: Kapurella, Mahaoya, Padiyathalawa, Palanoya and springs around Mahiyangana and Ampara
- Group 3: Kanniya, Rankihiriya and Adampane springs.

Group 1 is located in the Southern part of the Sri Lanka, near the HC- VC boundary and has a high salt content. Group 2 lies in the Eastern part and is mostly located in the VC, at a considerable distance from the HC- VC boundary and contain a low content of salt. Group 3 is located in the Northern part and in the HC having very low salt content [12].

The electrical conductivity of geothermal water varied from 532  $\mu\text{S}/\text{cm}$  (Kanniya) to 7300  $\mu\text{S}/\text{cm}$  (Mahapalessa), indicates the low mineralization of geothermal water except at the Mahapalessa spring [2].

Based on the major element compositions, hot springs can be classified in to three groups as, Na – Cl–  $\text{HCO}_3^-$  type (Mahapelessa), Na – Cl –  $\text{SO}_4$  type (Nelumwewa, Mahaoya, Marangala and Kapurella) or Ca–Cl– $\text{SO}_4$ -type (Rankihiriya and Kanniya) [2].

Geothermal springs located in the Northeastern part (Rankihiriya and Kanniya) are mostly dominated by high bicarbonate contents; Özler (2000) indicates that the  $\text{HCO}_3^-$  content can increase with the time and travel distance in underground. Both these springs show lower discharge temperatures [2].

Table 2: Geothermometric calculations of geothermal heat sources in Sri Lanka (modified after, [8], [2])1 [8] 2 [2] a Temperature estimated by chalcedony geothermometer b Temperature estimated by chalcedony geothermometer based on field study

| Geothermo<br>meter                         | Calculated Heat source temperatures (°C) |         |           |        |           |            |         |
|--|--|---------|-----------|--------|-----------|------------|---------|
|  | Rankihiriya                              | Kanniya | Nelumwewa | Wahawa | Kapurella | Madunagala | Mahaoya |
| Thermal Spring                             |  |         |           |        |           |            |         |
| Na-K-ca (1)                                | 102-131                                  | 102-131 | 102-131   | 143    | 143       | 102-131    | 143     |
| Silica geo<br>thermometer<br>(1)           | 102-131                                  | 102-131 | 102-131   | 143    | 143       | 102-131    | 143     |
| Silica–quartz<br>conductive<br>cooling (2) | 131                                      | 97      | 132       | 97     | 126       | 116        | 131     |
| Silica quartz<br>max. steam loss<br>(2)    | 127                                      | 99      | 128       | 98     | 124       | 114        | 128     |
| Silica–<br>Chalcedony a<br>(2)             | 92                                       | 57      | 92        | 57     | 87        | 76         | 92      |

|  |     |     |     |     |     |     |     |
|--|-----|-----|-----|-----|-----|-----|-----|
| <b>Silica–<br/>Chalcedony b<br/>(2)</b>            | 103 | 69  | 103 | 68  | 98  | 87  | 103 |
| <b>Modified silica<br/>geothermomet<br/>er (2)</b> | 133 | 105 | 137 | 138 | 128 | 118 | 121 |
| <b>Na–Li f (2)</b>                                 | 99  | 103 | 129 | 122 | 124 | 96  | 127 |

The springs in the middle part of the Sri Lanka (Nelumwewa, Mahaoya, Marangala and Kapurella) are concentrated in high sulfate water, while Mahapalessa in the Southern Sri Lanka with higher chloride- Sodium contents.

The modified silica geothermometers of Verma and Santoyo (1993) yielded the highest reservoir temperatures that range from 105°C (Kanniya) to 138°C (Marangala) for all geothermal springs in Sri Lanka. Silica based geothermometers reveal the highest reservoir temperatures of 97 °C (Kanniya) to 132 °C (Nelumwewa) while Na – Li geothermometers reveals 96 °C (Mahapalessa) to 129 °C (Nelumwewa). The average reservoir temperatures vary from 88 °C (Kanniya) to 120 °C (Nelumwewa) [2].

The geochemical composition of natural shallow groundwater in nearby terrains closely matches with the hot spring waters, indicating that all water should stem from a common circulation. As the geochemical values, isotopic data from geothermal and non- geothermal water are almost identical; the hypothesis of a common source of recharge and internal circulation pattern can be confirmed [2].

From the isotopic and geochemical similarities of shallow groundwater and geothermal spring water, a fast circulating system, is indicated. Hence the hot springs are much likely to be heated at much shallow depths, because fast

conduit circulation systems do not reach down to much higher depths. This suggests a much steeper geothermal gradient which may be related to the residual heat along the HC – VC boundary zone [2].

### **Potential Applications of Geothermal Energy in Sri Lanka**

There are many potential applications using the geothermal hot springs in Sri Lanka. Even though the heat source or reservoir origins are not clearly identified, their temperatures have been calculated already. The temperatures of the sources indicate (~ 150-170 °C) which means t they can be utilized to generate electricity, as a direct use of a geothermal energy.

As Sri Lanka has many agricultural and tourism impacts, there are many direct uses of geothermal springs. some of the most common uses which can be applied to Sri Lanka are discussed in the following section.

#### **Direct use**

The areas around geothermal manifestations have a dry climate and the major economic activity in the areas is agriculture. It is also a popular tourist destination because of the wildlife and beach (specially Trincomale to Hambanthota). These sectors can be benefited immensely from the

geothermal energy through direct utilization. The possible applications include drying of agricultural products (cereal), sugar processing, papermill operation and in recreational facilities such as warm pools, saunas and steam baths.

### **Steaming and drying of agricultural products**

The geothermal springs have been located in Trincomalee (Kanniya, Rankiriulpotha), Polonnaruwa (Nelumwewa), and Hambanthota (Mahapelessa) districts. The area is extensively agricultural especially, rice, maize, soya, peanut, etc. being grown. For rice and cereal production industries, hot spring water can be used as thermal energy for steaming and drying. At least a part of energy consumption of this production can be supplied using these geothermal energy systems.

### **Sugar processing**

geothermal energy can be used in sugar processing. Cane sugar production requires considerable amounts of steam; The geothermal heat energy can be used for evaporation in multiple effect evaporators. It is reported that natural heat is already used in several countries for brewing and distillation. Cane cultivation in the area can be used as a cost effective and easy process to manufacture sugar or other valuable products using this geothermal energy. In Sri Lanka cane sugar industry is limited to areas like Trincomalee and Moneragala. Hence Hot springs such as Kanniya, Padiyathalawa, can be used as geothermal energy sources for the cane industry in Sri Lanka.

### **Recreational and health applications**

Hot springs and warm mineral springs have been used for recreational and health purposes from many countries, even in Sri Lanka. There are records of many geothermally heated swimming pools, mineral baths, mud baths, steam baths and specially organized recreational centers from several countries. In Sri Lanka, the tourism industry has shown great progress in recent times, including the areas where there are hot springs. There is a great potential for attention for herbal and local medicinal therapy by the tourists. Hence. Combining tourism and these local medicines would give much higher profits to the country. As in many other countries, hot spring waters can be used for herbal and steam baths before some medicinal treatments. Therefore, additional infrastructures such as hotels, recreational facilities have to be developed for better tourist attractions at such places.

### **Indirect use (electricity)**

By assuming that the 350 km long highland Vijayan boundary zone a potential geothermal energy source, estimation to a thickness of 2 km and a width of 2 km, A potential of 1335 MWe generating capacity for 50 years and 723 MWe generating capacity for 100 years were concluded by a Monte Carlo simulation [6]. Even though [6] is the only comprehensive study done about potential electricity generation estimations, some of the assumptions cannot be justified. For example, assuming that the whole 320 km long HC/VC boundary as a geothermal belt may not be correct. Hence considering the hot spring fields as point sources rather than a continuous belt might give a more accurate and precise estimations.

## References

- [1] Georgsson L.S., (2009). Geophysical methods used in geothermal exploration. Presentation in short course IV on exploration for geothermal resources, UNU-GTP, KenGen, GD, Naivasha, Kenya.
- [2] Chandrajith, R., Barth, J.A.C., Subasinghe, N.D., Merten, D., Dissanayake, C.B., (2013). Geochemical and isotope characterization of geothermal spring waters in Sri Lanka: evidence for steeper than expected geothermal gradients. *Journal of Hydrology* 476, 360–369.
- [3] Nimalsiri, T., Suriyaarachchi, N., Hobbs, B., Manzella, A., Fonseka, M., Dharmagunawardena, H. and Subasinghe, N. (2015). Structure of a low-enthalpy geothermal system inferred from magnetotellurics — A case study from Sri Lanka. *Journal of Applied Geophysics*, 117, 104-110.
- [4] Takigami, Y., Yoshida, M., Funaki, M., (1999).  $^{40}\text{Ar} - ^{39}\text{Ar}$  ages of dolerite dykes from SL. *Polar Geosciences*, 12, 176–182.
- [5] Yoshida, M., Kunaki, M., Vitanage, P.W., (1989). A Jurassic – Cretaceous Dolerite dyke from Sri Lanka. *Journal of Geological Society of India*. 33-1, 71-75.
- [6] Wijetilake, S., (2011) The potential of geothermal energy resources in Sri Lanka. United Nations University, Geothermal Training Programme. Report 34
- [7] Hobbs, B.A., Fonseka, G.M., Jones, A.G., De Silva, S.N., Subasinghe, N.D., Gawes, G., Johnson, N., Cooray, T., Wijesundara, D., Suriyaarachchi, N., Nimalsiri, T., Premathilake, K.M., Kiyan, D., Khoza, D., (2013). Geothermal Energy Potential in Sri Lanka: A Preliminary Magnetotelluric Survey of Thermal Springs. *Journal of Geological Society of Sri Lanka* 15, 69-83.
- [8] Dissanayake, C. and Jayasena, H. (1988). Origin of geothermal systems of Sri Lanka. *Geothermics*, 17(4), 657-669.
- [9] 22. Fournier, R. and Rowe, J. (1966). The deposition of silica in hot springs. *Bulletin Volcanologique*, 29(1), 585-587. 10. Fournier, R. and Truesdell, A. (1973). An empirical Na-K-Ca geothermometer for natural waters. *Geochimica et Cosmochimica Acta*, 37(5), 1255-1275.
- [11] Fernando, M. J. & Kulasinghe, A. N. S. (1986). Seismicity of Sri Lanka. *Physics of the Earth and Planetary Interiors*, 44, 99-106.
- [12] Premasiri, H.M.R., Wijeyesekera, D.S., Weerawarnakula, S., Puswewala, U.G.A., (2006). Formation of Hot Water Springs in Sri Lanka. *ENGINEER*, XXXIX, 04, 07-1.
- [13] Yoshida, M., Kunaki, M., Vitanage, P.W., (1989). A Jurassic – Cretaceous Dolerite dyke from Sri Lanka. *Journal of Geological Society of India*. 33-1, 71-75.
- [14] Senaratne, A., Chandima, D., (2011). Exploration of a potential geothermal resource at Wahawa Padiyatalwa area Sri Lanka. Thirty-Sixth Work shop on Geothermal Reservoir Engineering Stanford University, Stanford, California.
- [15] Fonseka, G.M. (2000). Geological and geophysical investigations for geothermal energy, study of Mahapelessa and Mahaoya thermal springs, NARESA report RG/94/EP/02 with National Science Foundation Sri Lanka.
- [16] Subasinghe, N.D., Nimalsiri, T.B., Suriyaarachchi, N.B., Hobbs, B.A., Fonseka, G.M., Dissanayake, C.B., (2014). Study of thermal water resources in Sri Lanka using time domain electromagnetics (TDEM). *Advanced Materials Research*, (955-959), 3198-3201.
- [17] Dharmasiri, J. & Basnayake, S. (1986). Origin of thermal springs of Sri Lanka. *Sri Lanka Association of Advancement of Science*, 42, 156-157.
- [18] Samaranyake, S., De Silva, S., Dahanayake, U., Wijewardane, H. and Subasingha, D. (2015). Feasibility of Finding Geothermal Sources in Sri Lanka with Reference to the Hot Spring Series and the Dolarite Dykes. In: *Proceedings World Geothermal Congress 2015*. Melbourne, Australia.
- [19] Kumara, S.M.P.G.S., Dharmagunawardhane, H.A., 2014. A geostructural model for the Nelumwewa thermal spring: north central province, Sri Lanka. *Journal of Geological Society of Sri Lanka* 16, 19–27.
- [20] Bandara, H.M.D.A.H., (2020). Petrological and Geophysical study of geothermal springs in Sri Lanka with special emphasis on the Highland/Vijayan boundary in Sri Lanka. MPhil Thesis, University of Peradeniya.

# Greenhouse Gas Emissions in the Energy Sector and Mitigation by Shifting from Coal to Natural Gas

Janaka Ratnasiri<sup>1</sup> and Sumudu H. Kuruppu<sup>2</sup>

<sup>1</sup>*27 Sudarshana Mawatha, Nawala, Rajagiriya*

<sup>2</sup>*Sri Lanka Climate Fund, Sampathpaya, Battaramulla*

<sup>1</sup>*janakaratnasiri@gmail.com*

<sup>2</sup>*sumuduharshanee8@gmail.com*

## Abstract

The emission of greenhouse gases (GHG) from fossil fuel combustion in the energy sector is computed for the period from 2000 to 2016. The emissions of GHGs comprising CO<sub>2</sub>, CH<sub>4</sub> and N<sub>2</sub>O were computed using fossil fuels consumed in different sub-sectors comprising power, transport, industrial, commercial and households along with corresponding emission factors given for each of the GHGs in the 2006 IPCC Guidelines for National GHG Inventories. Emissions of individual gases were converted to Carbon Dioxide Equivalent (CO<sub>2eq</sub>) values using their Global Warming Potentials. Results show that overall CO<sub>2eq</sub> has increased from 11.1 Tg to 23.7 Tg during the period 2000–2016, with sectoral emissions increasing from 2,061 Gg to 8,069 Gg in the power sub-sector, from 1,091 Gg to 1,800 Gg in the industry sub-sector, from 5,237 Gg to 10,239 Gg in the transport sub-sector. Projections are also made for emissions in the power sub-sector based on CEB's Generation Expansion Plan 2015-2034 Base Case for Business-as-Usual scenario and No-Coal Case in 2018-2037 Plan as the mitigated scenario, yielding mitigation from 196.8 Tg to 147.9 Tg or 25% reduction, during 2020–2030 period. This meets easily Sri Lanka's obligations towards the Nationally Determined Contributions (NDC) in the Energy Sector making Sri Lanka eligible for external funding.

**Keywords:** Greenhouse gases, Carbon Dioxide, Methane, Nitrous Oxide, GHG Inventory

## Introduction

Growing concern about the anticipated global climate change with adverse impacts on the people, induced by global warming due to burning of fossil fuels and large-scale deforestation resulting in the emission of greenhouse gases (GHG) into the atmosphere, prompted the nations to adopt the UN Framework Convention on Climate Change (UNFCCC) in June 1992. The objective of the UNFCCC is to get the Parties to take measures for the stabilization of GHG concentrations in the atmosphere at a level that would prevent dangerous anthropogenic interference with the Earth's climate system [1].

Under the Convention, Parties listed in Annex 1 to the Convention text comprising developed country Parties and countries with transition economies, mostly Eastern European countries, are required to reduce their GHG emissions to their pre-1990 levels by the end of the decade. Obligation of non-Annex I Parties is only to take climate change considerations into account, to the extent possible, in their relevant social, economic and environmental policies and actions.

All Parties were required to develop national inventories of anthropogenic emissions and sinks of GHGs using methodologies recommended by the Intergovernmental Panel on Climate Change (IPCC). Annex I Parties are required to submit these inventories to the Convention Secretariat regularly while Non-Annex I Parties are required to do so depending on the availability of funding to them by developed country Parties. The GHG Inventory comprises one Chapter in the National Communication on Climate Change (NCCC) that every Party is required to

submit to the Convention Secretariat. Sri Lanka submitted its initial NCCC in 2000, second in 2011 and the third is under preparation.

The objective of the present study is to determine the GHG emissions and sinks in the energy sector in Sri Lanka from 2000 to 2016, and to find means of mitigation of GHG emission.

## Greenhouse gases and their sources

A GHG is defined in the UNFCCC document as a gaseous constituent in the atmosphere, both natural and anthropogenic, that absorbs and re-emits infrared radiation. The main GHGs which are directly emitted and controlled by the Convention are carbon dioxide (CO<sub>2</sub>), Methane (CH<sub>4</sub>) and Nitrous Oxide (N<sub>2</sub>O). There are several other precursor gases including Carbon Monoxide (CO), Oxides of Nitrogen (NO<sub>x</sub>) and Non-Methane Volatile Organic Compounds (NMVOC) which get converted into GHGs in the presence of sun light after their release into the atmosphere.

A series of chemically inert compounds commonly known as Chloro-Fluoro-Carbons (CFC) are also known to have high global warming potential (GWP) but they are not controlled by the UNFCCC since they are being phased out under the Montreal Protocol on Substances that Deplete the Ozone Layer.

The main sources of CO<sub>2</sub> emissions are combustion of fossil fuels such as coal, petroleum oil and natural gas in the energy sector. Fossil fuels are burnt to generate energy required to operate thermal power plants, furnaces and ovens in industries, road and off-road vehicles, railways, domestic airlines and thermal appliances in households and



commercial establishments. CO<sub>2</sub> is also emitted and absorbed in land-use changes and forestry sector while CH<sub>4</sub> and N<sub>2</sub>O are emitted in agriculture and waste sectors as well. Methane is emitted mostly from agricultural activities such as paddy cultivation and rearing of ruminant animals. It is also emitted during waste disposal. Nitrous Oxide is emitted mostly from agriculture soils.

However, these emissions are not considered in this study. Combustion of biomass for energy generation also emits CO<sub>2</sub> as well as CH<sub>4</sub> and N<sub>2</sub>O. Since CO<sub>2</sub> emitted is off-set by the amount absorbed during the biomass growing process, CO<sub>2</sub> emission is not included in the GHG inventory, but the other two gases CH<sub>4</sub> and N<sub>2</sub>O are included.

The latest GHG Inventory available for Sri Lanka is its Second National Communication on Climate Change (SNC) submitted in 2011 [2]. According to this inventory, the energy sector has the highest contribution of 61%, while agriculture, waste and industrial sectors follow with 25%, 11% and 3% contributions, respectively. In this paper, only the emissions from the energy sector comprising emissions due to energy generation in power, industry, transport, household and commercial sub-sectors are considered.

### **Computation of GHG emissions**

The IPCC, in 2006, has developed detailed guidelines [3] for the computation of GHG emissions and removals, which both developed and developing countries are expected to follow. The computation of GHG emissions require two factors, activity factor (AF) and the emission factor (EF). In the energy sector, AF is the amount of fuel burnt for energy

generation in various applications; power generation, heat generation in industries, operation of vehicles and in cooking and space heating in domestic & commercial establishments. The EF is the amount of individual gases emitted when a unit amount of fuel is burnt. For CO<sub>2</sub> emissions, EF depends only on the carbon content in the fuel and does not depend on how the fuel is burnt.

Hence, a knowledge of overall fuel consumption is adequate to estimate the amount of CO<sub>2</sub> emitted in the sector. However, for CH<sub>4</sub> and N<sub>2</sub>O, EF depends on both the type of fuel as well as the type of appliance where the fuel is burnt, be it the type of power plant or the type of vehicle. Hence, the amount of fuel burnt in different types of applications is necessary for estimating CH<sub>4</sub> and N<sub>2</sub>O emissions. In Sri Lanka, the Ceylon Petroleum Corporation (CPC) had the monopoly of importing, distributing and refining crude petroleum oil up to 2003 when the Indian Oil Company (IOC) was granted license to enter into the petroleum market. Currently, diesel, gasoline and lubricants are marketed by Lanka IOC. A Statistical Digest giving CPC's annual sales under different applications and end-users for each type of fuel were published up to 2007. Thereafter, annual overall sales figures of each type of fuel were published in the CPC Annual Reports without giving any sectoral breakdown. The Central Bank Annual Reports give in their Statistical Appendices [4] the overall annual quantities of different fuel types sold by both CPC and Lanka IOC. However, primary data from these two sources were not made available even upon request.

The Sri Lanka Sustainable Energy Authority (SLSEA) prepares annually the Energy Balance Statement giving the

imports, exports, production, conversion and consumption of different fuels in different sectors. The values are given in both original units and common units of tonnes of oil equivalent (TOE) as well as in Tera Joules (TJ). The sub-sectors covered are power, industries, transport, household & commercial and agriculture. In the present study, the consumption data given in original units in SLSEA database are used. There are, however, discrepancies between these data and those given in CBSL data when total consumption data are compared. Since gasoline is used only for transport, data given for gasoline in SLSEA data and CBSL data could be compared. It was noted that SLSEA data match with Central Bank data in most years, but in some there have been some deviations and these were adjusted. There were also discrepancies between values given in excel sheets and PDF versions.

*Table 2: Emission factors (EF) for CH<sub>4</sub> and N<sub>2</sub>O*

| Sector    | Fuel     | EF (g/GJ)       |                  |
|-----------|----------|-----------------|------------------|
|           |          | CH <sub>4</sub> | N <sub>2</sub> O |
| Power     | Oil      | 3               | 0.6              |
|           | Coal     | 1               | 1.5              |
|           | LPG      | 1               | 0.1              |
| Industry  | Oil      | 3               | 0.6              |
|           | Biomass  | 30              | 4                |
| Transport | Gasoline | 15              | 5                |
|           | Diesel   | 4               | 4                |
|           | LPG      | 5               | 0.1              |
| HH & Com  | Kerosene | 10              | 0.6              |
|           | Biomass  | 300             | 4                |

An error that has gone into the Balance Sheet is that in converting fuel consumed in power plants given in million litres (ML) into mass values in kilo tonnes (kt). The PDF reports give separately the volume of different fuels consumed by power plants in ML. The Balance Sheets also give the identical figures for the fuel consumed in power plants expressed in original units

of kt. This means, a density of 1 kg/l has been assumed for all oils, diesel and heavy oils. In this study, for the power-sub-sector, mass values were estimated from the volume values using corresponding density values for different fuels. There are also discrepancies in the total diesel and fuel oil consumed in respect of some years between SLSEA data and CBSL data, but these could not be adjusted as no sectoral data are available in CBSL data.

The Guidelines prepared by IPCC give basic data such as net calorific value (NCV) and carbon content in different fuels which are necessary for the computation of GHG emissions [5]. table 1 gives these data taken from the IPCC Guidelines for different fuels and used in the present study. Further the Guidelines give emission factors (EF) in respect of CO<sub>2</sub>, CH<sub>4</sub> and N<sub>2</sub>O for different sectors such as energy industries, manufacturing industries, transport, residential and agricultural activities.

*Table 1: Properties of fuels (IPCC 2006)*

| Fuel type         | NCV<br>GJ/t | Carbon<br>content<br>kg/GJ | CO <sub>2</sub> |
|-------------------|-------------|----------------------------|-----------------|
|                   |             |                            | EF<br>kg/TJ     |
| <b>Gasoline</b>   | 44.3        | 18.9                       | 69,300          |
| <b>Kerosene</b>   | 43.8        | 19.6                       | 71,900          |
| <b>Diesel oil</b> | 43.0        | 20.2                       | 74,100          |
| <b>RO/ FO</b>     | 40.4        | 21.1                       | 77,400          |
| <b>LPG</b>        | 47.3        | 17.2                       | 63,100          |
| <b>Naphtha</b>    | 44.5        | 20.0                       | 73,300          |
| <b>Coal</b>       | 25.8        | 25.8                       | 94,600          |
| <b>Nat gas</b>    | 48.0        | 15.3                       | 56,100          |
| <b>Biomass</b>    | 15.6        | 30.5                       | 112,000         |

Emission of CO<sub>2</sub> depends solely on the amount of fuel burnt and the relevant EF values for different fuels are also given in table 1.

The IPCC guidelines give three sets of methodologies referred to as Tier I, Tier II and Tier III for estimating emissions of CH<sub>4</sub> and N<sub>2</sub>O. Tier I is a simplified version intended for use by developing countries who may not have detailed data in different applications.

In the present study, Tier I methodology was used in which a single set of EFs is given for CH<sub>4</sub> and N<sub>2</sub>O for each sub-sector, eg. A single EF value for the entire transport sector. Whereas in Tier II, different EFs are given for different types of vehicles and models. The EF values for CH<sub>4</sub> and N<sub>2</sub>O corresponding to Tier I methodology given in IPCC 2006 Guidelines for different fuels and sub-sectors and used in the study are given in table 2 [6].

### Total Energy Supply

Sri Lanka's energy mix comprises biomass, petroleum oil, coal, hydropower and non conventional renewable sources such as small hydropower plants, wind turbines, dendro power plants and solar photovoltaic (PV) systems. The total primary energy supply in 2016 has been 481 PJ with its share of each source shown in table 3.

*Table 3: Primary energy sources in 2016*

| Source          | PJ/y         | PC           |
|-----------------|--------------|--------------|
| <b>Oil</b>      | 220.6        | 45.8         |
| <b>Coal</b>     | 53.7         | 11.2         |
| <b>Biomass</b>  | 190.3        | 39.5         |
| <b>Hydro</b>    | 12.5         | 2.6          |
| <b>Other RE</b> | 4.2          | 0.9          |
| <b>Total</b>    | <b>481.3</b> | <b>100.0</b> |

*Table 4: Matrix of fuel consumption in 2016*

| Fuel                     | Power  | Industry | Transport | HH & other | Total  |
|--------------------------|--------|----------|-----------|------------|--------|
| Fuel consumption in PJ/y |        |          |           |            |        |
| <b>LPG</b>               |        | 3.32     | 0.05      | 13.47      | 16.84  |
| <b>Gasolene</b>          |        |          | 51.83     |            | 51.83  |
| <b>Naphtha</b>           | 5.53   |          |           |            | 5.53   |
| <b>Avgas</b>             |        |          | 0.01      |            | 0.01   |
| <b>Kerosene</b>          |        | 0.25     |           | 7.30       | 7.55   |
| <b>JetA1</b>             |        |          | 0.12      |            | 0.12   |
| <b>Diesel</b>            | 14.19  | 0.93     | 86.61     | 0.02       | 101.75 |
| <b>Fuel oil</b>          | 14.14  | 15.17    | 0.01      | 0.01       | 29.33  |
| <b>Residual</b>          | 7.65   |          |           |            | 7.65   |
| <b>Total oil</b>         | 41.51  | 19.67    | 138.63    | 20.80      | 220.61 |
| <b>Coal</b>              | 51.70  | 2.01     |           |            | 53.71  |
| <b>Sub-Total</b>         | 93.21  | 21.68    | 138.63    | 20.80      | 274.32 |
| <b>Biomass</b>           |        | 74.12    |           | 116.16     | 190.28 |
| <b>Hydro &amp; RE</b>    | 16.71  |          |           |            | 16.71  |
| <b>Total</b>             | 109.92 | 95.80    | 138.63    | 136.96     | 481.31 |

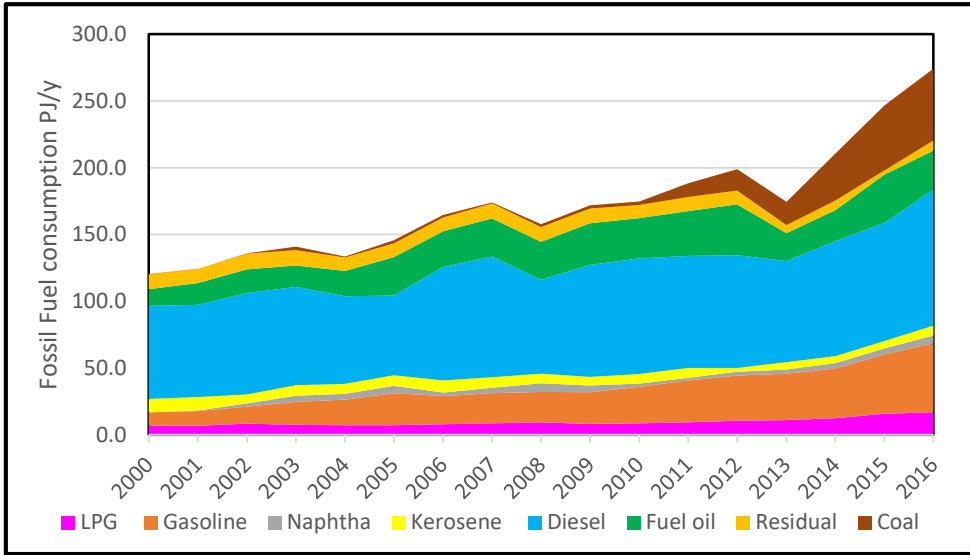


Figure 1: Growth of consumption of different fuels during 2000 – 2016 (SLSEA and CBSL)

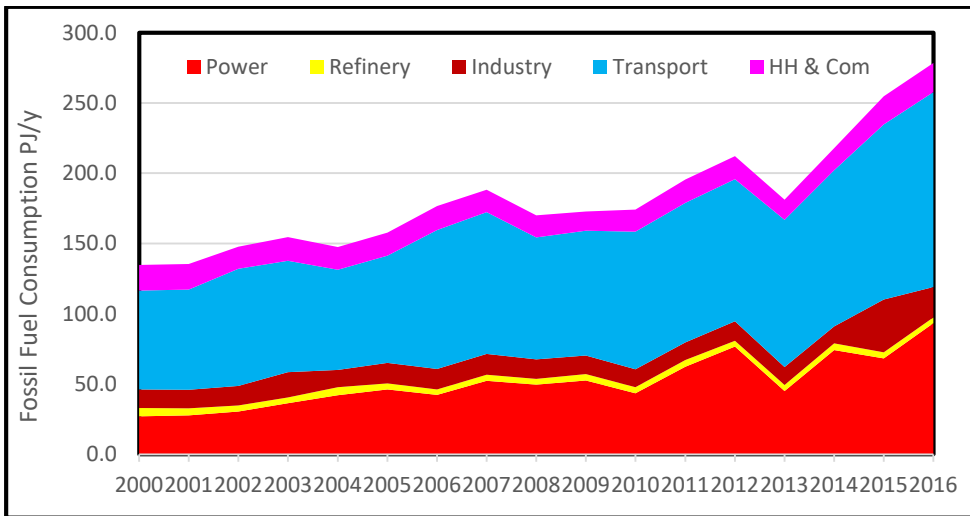


Figure 2: Growth of overall fossil fuel combustion in different sub-sectors during 2000 – 2019

In converting the amount of hydro power generation given in GWh into a common unit of GJ, their direct relationship of 1 GWh = 3,600 GJ was used. However, Sri Lanka’s utilities use the oil substitution method which inflates the hydro power component to about 9%, instead of about 3% obtained when using the direct equivalent method. The breakdown of fossil fuel consumption in different sub-sectors are shown in Table 4 for 2016. The

contribution from all oils has been 274 PJ while the gross consumption including biomass and renewables has been 481 PJ. Though these renewables are shown in the Table, these do not cause any GHG emissions.

The growth of consumption of different fossil fuels in all sub-sectors during 2000-2016 is shown in Figure 1, while their

overall consumption in different sub-sectors is shown in figure 2.

There has been a rapid increase in the fuel consumption in the transport sub-sector in recent years due to the increase in the population of motor cycles, 3-wheelers and motor cars. This has contributed to the increase in the consumption of gasoline.

There has also been a significant increase in the diesel oil and fuel oil consumption for power generation in recent times. This has contributed to the increase in the consumption of diesel oil.

### Emission of Greenhouse gases

The emission of GHG was computed using the Tier I methodology given in IPCC 2006 Guidelines. table 2 gives the emission factors (EF) for different gases emitted from combustion of different fuels in different sub-sectors, given for Tier I methodology. Under this methodology, a single EF is used for the entire sub-sector for each fuel. Using the fuel properties given in Table 1, emission factors given in table 2 and the fuel consumption values given in Table 4, the emissions were computed for 2016.

Table 5: GHG emissions by sub-sector 2016

| Sub-Sector   | GHG Emission<br>MtCO <sub>2</sub> Eq | 2016<br>PC   |
|--------------|--------------------------------------|--------------|
| Power gen    | 8.07                                 | 35.6         |
| Petro Ref    | 0.31                                 | 1.4          |
| Industries   | 1.81                                 | 8.0          |
| Transport    | 10.24                                | 45.1         |
| HH & Com     | 2.26                                 | 10.0         |
| <b>Total</b> | <b>22.68</b>                         | <b>100.0</b> |

The emissions from individual gases were converted to a common unit of CO<sub>2</sub>Eq values by multiplying the individual

emissions by their global warming potential values which are 21 for CH<sub>4</sub> and 310 for N<sub>2</sub>O. These emissions from each sub-sector are given in table 5 for 2016.

The highest contribution of 45% has come from the transport sub-sector, while the power sub-sector has contributed 35%, followed by household & commercial sub-sector and industries sub-sector contributing 10% and 8%, respectively. The low emission from the industrial sub-sector is a reflection of the poor status of industrialization of the country.

The emissions of individual gases from all sub-sectors in 2016 are shown in table 6.

Table 6: Emissions of GHGs in energy sector 2016

| GHG              | MtCO <sub>2</sub> eq | PC           |
|------------------|----------------------|--------------|
| CO <sub>2</sub>  | 21.40                | 94.4         |
| CH <sub>4</sub>  | 0.81                 | 3.6          |
| N <sub>2</sub> O | 0.47                 | 2.0          |
| <b>Total</b>     | <b>22.68</b>         | <b>100.0</b> |

The above computations were repeated for each year from 2000 to 2015, using sectoral fuel consumption data shown in figure 2. The results are shown in figure 3.

As expected, the GHG emission growth pattern follows closely the growth of fossil fuel consumption pattern. The dip in the emissions from the power sector could be attributed to the fact 2013 has been a high rainfall year generating more hydropower and less thermal power. The increase in the transport sector since 2013 has been the high growth of vehicular population during this period. The stagnant growth of emissions in the household and commercial sector has been the decline in kerosene consumption despite the increase in LPG consumption. Between 2000 and 2016, there has been a four-fold increase in the GHG emissions in the power sector,

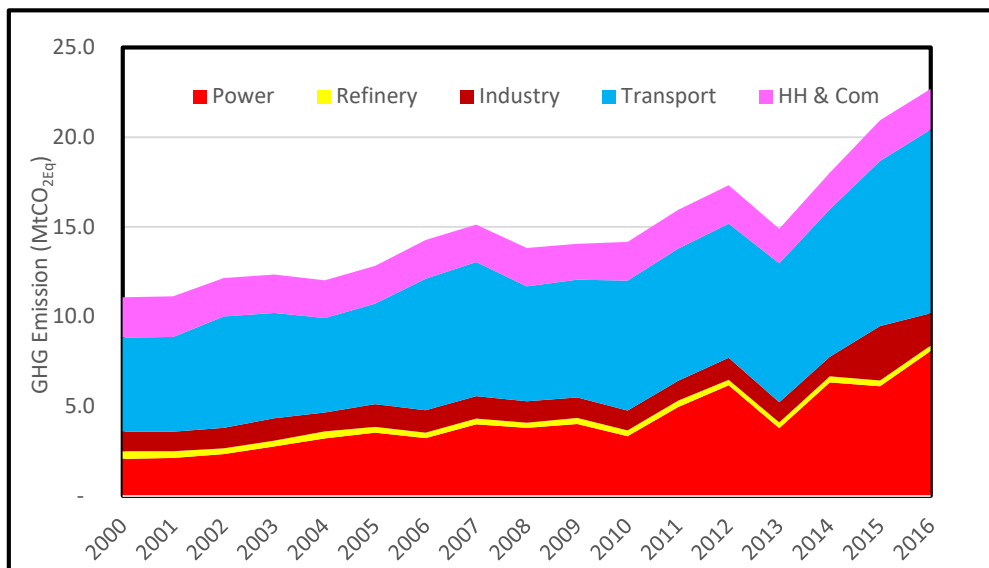


Figure 3: Growth of GHG emission during 2000 – 2016 in different sub-sectors

also increase in the transport sector with zero growth in House-hold & Commercial sector, with an overall two-fold increase as shown in Table 7. Industrial sub-sector shows a low growth reflecting the absence of energy intensive industries in the country.

Table 7: Growth of emissions between 2000 and 2016

| Sector          | Mt(CO <sub>2</sub> Eq) |              | Ratio      |
|-----------------|------------------------|--------------|------------|
|                 | 2000                   | 2016         |            |
| Power           | 2.06                   | 8.07         | 3.9        |
| Refinery        | 0.43                   | 0.31         | 0.7        |
| Industry        | 1.09                   | 1.81         | 1.7        |
| Transport       | 5.24                   | 10.24        | 2.0        |
| HH & Com        | 2.25                   | 2.26         | 1.0        |
| <b>Total/Av</b> | <b>11.07</b>           | <b>22.68</b> | <b>2.0</b> |

### Option for mitigation of emissions

Under the Paris Agreement on Climate Change [7], Parties have agreed to reduce GHG emissions voluntarily as pledged to the UN Framework Convention on

Climate Change (UNFCCC) on condition that adequate funding will be made available to developing countries to meet their obligations least partly. The Ministry of Environment has given an undertaking in September 2016 in a report titled “Nationally Determined Contributions” (NDC) to the UNFCCC Secretariat [8] to reduce by 20% (estimated as 39,383Gg) of the cumulative emissions in the power sub-sector during 2000 – 2030 (estimated as 196,915 Gg) possible with the implementation of the Ceylon Electricity Board’s (CEB) 2015-2034 Long-Term Generation Expansion (LTGE) Plan [9] considered as the business-as-usual (BAU) scenario, which comprises power plants operated with diesel and coal. In the CEB’s 2018-2037 LTGE Plan [10] that has been approved, an optional scenario has been proposed in Annex 8 comprising a “no-coal” case where all coal power plants (CPP) are to be replaced with combined cycle gas turbine (CCGT) natural gas power plants (NGPP). These power plants emit only about 1/3 the emissions from a CPP of similar capacity in view of low carbon content in NG and

their high efficiency. Hence, shifting to NG from coal for power plant operation is an emission mitigation option that has been adopted in many countries. In this study, GHG emissions are estimated for power plants added under CEB 2015-34 Plan as BAU case and the “no-coal” case. Table 8 gives the proposed capacity additions under these two cases.

*Table 8: Capacity additions under BAU and “No-coal” cases (CEB LTGE Plans)*

| Year | BAU Case    | “No-coal” case        |
|------|-------------|-----------------------|
| 2019 | 35 MW GT    | 70 MW GT<br>300 MW NG |
| 2020 | 500 MW Coal | 35 MW GT              |
| 2021 |             | 300 MW NG             |
| 2022 | 600 MW Coal |                       |
| 2023 |             | 463 MW NG             |
| 2024 | 300 MW Coal | 300 MW NG             |
| 2025 |             | 300 MW NG             |
| 2026 |             | 300 MW NG             |
| 2027 | 300 MW Coal | 300 MW NG             |
| 2028 |             |                       |
| 2029 | 300 MW Coal | 300 MW NG             |
| 2030 | 300 MW Coal | 300 MW NG             |

The emissions are estimated assuming that each power plant operates at 80% plant factor, burning fuel whose NCVs are given in Table 1. Thermal efficiencies assumed are 35% for sub-critical CPP, 40% for super critical CPP and 55% for CCGT type NGPP. The gas-turbine and diesel power plants included in the CEB Plans are also considered. The resulting emissions under the two case are given in table 9.

It is seen that shifting from coal to NG to operate base load power plants will save 48.9 MtCO<sub>2Eq</sub> of GHG emissions during the period 2000-2030 or 25% relative to the emissions under BAU case for the same period.

*Table 9: Emissions under BAU and No-coal cases*

| Year         | Emission MtCO <sub>2Eq</sub> |              |
|--------------|------------------------------|--------------|
|              | BAU                          | No-coal      |
| 2021         | 14.5                         | 13.5         |
| 2022         | 18.6                         | 13.5         |
| 2023         | 17.5                         | 12.5         |
| 2024         | 19.2                         | 13.6         |
| 2025         | 19.1                         | 14.2         |
| 2026         | 19.1                         | 15.0         |
| 2027         | 20.9                         | 15.8         |
| 2028         | 20.9                         | 15.8         |
| 2029         | 22.6                         | 16.6         |
| 2030         | 24.4                         | 17.3         |
| <b>Total</b> | <b>196.8</b>                 | <b>147.9</b> |

### Assistance under the Paris Agreement

Under the Paris Agreement adopted in 2015, countries have voluntarily agreed to reduce GHG emissions to the extent possible by each country. The reduction of emissions envisaged by Sri Lanka as given in the NDC report includes 4% unconditional (with internal funding) and 16% conditional (with external funding) reduction”. Since Sri Lanka could achieve more than the minimum mitigation pledged in its NDC Report by shifting from coal to natural gas in the power sector, Sri Lanka could claim external funding made available to developing countries to meet any additional incremental costs incurred in shifting from coal to NG from for base load power plants.

### Financial implications

The CEB has released its latest draft LTGE Plan for 2020-2039 where it has considered a mix of coal and NG power plants. The levelized costs of generation from super critical CPP and CCGT type

NGPP were estimated assuming the plant capital costs to be USD/kW 2,000 for super-critical CPP and USD/kW 950 for NGPP. The fuel costs were assumed to be USD/t 110 for coal and USD/MBtu 10 for LNG, along with data for operation and maintenance (O&M) for the two types of power plants taken from the CEB's Draft LTGE Plan for 2020-2039 [11].

The results are given in Table 10. It is seen that the direct generation costs are more or less the same with the two technologies, subject to price fluctuations of the two fuels. However, the high level of pollution taking place even with the high-efficient super critical CPPs, and the high expenditure incurred to control such pollution generated from flue gas emissions and large amounts of coal ash accumulated over the years and their impact on the health of exposed people and the environment, give rise to external economic costs which are estimated to be about UScts/kWh 3 for CPP and UScts/kWh 1 for NGPP, based on a

European Commission study adapted to Sri Lanka [12]. When these costs are added to the generation costs, the NGPP comes out as the cheaper option by a wide margin. Such a margin could accommodate any fluctuations in the fuel prices.

## Conclusion

Introduction of NG in the power alone could enable Sri Lanka to meet its obligations towards the Paris Agreement while maintaining a clean local environment. Utilization of NG in other sub-sectors such as transport and industries could replace expensive oil resulting in enhancing the saving of GHG emissions and expenditure, because transport sub-sector is the highest contributor of GHG emissions. Once the on-going arrangements are completed for importing liquefied NG into the country, market forces will enable its introduction to other sub-sectors thus saving much money spent on oil imports.

*Table 10: Levelized costs of generation for Coal and natural gas power plants*

| Plant          | Annual plant cost<br>UScts/kWh | Annual Fuel cost<br>UScts/kWh | Fixed O&M cost<br>UScts/kWh | Variable O&M cost<br>UScts/kWh | Total gene'n cost<br>UScts/kWh |
|----------------|--------------------------------|-------------------------------|-----------------------------|--------------------------------|--------------------------------|
| <b>Super</b>   |                                |                               |                             |                                |                                |
| <b>CPP</b>     | 3.56                           | 3.89                          | 0.77                        | 0.60                           | 8.82                           |
| <b>CCGT NG</b> | 1.70                           | 6.20                          | 0.07                        | 0.50                           | 8.47                           |



## Acknowledgement

Authors thank the staff of SLSEA for providing clarifications on their database and the Sri Lanka Climate Fund for permitting one author to work on this study.

## References

- [1] UNEP/WMO. UN Framework Convention on Climate Change, Climate Change Secretariat, Geneva, 1992
- [2] Ministry of Environment, Second National Communication on Climate Change, Battaramulla, 2011
- [3] IPCC, 2006 IPCC Guidelines for National Greenhouse Gas Inventories, Intergovernmental Panel on Climate Change,

Geneva, 2006

- [4] CBSL. Annual Report Statistical Appendix, Central Bank of Sri Lanka, Colombo, 2010 and 2016
- [5] *ibid* [3] Chapter 1
- [6] *ibid* [3] Chapter 2
- [7] UNFCCC. Paris Agreement Text, 2015
- [8] Ministry of Environment, Report to the UNFCCC Secretariat on Nationally Determined Contributions, 2016
- [9] CEB, Long-Term Generation Expansion Plan 2015-2034, Colombo, 2015
- [10] CEB, Long-Term Generation Expansion Plan 2018-2037, Colombo, 2018
- [11] CEB, Long-Term Generation Expansion Plan 2020-2039 (Draft), Colombo, 2019
- [12] EU European Commission, External Costs - Research results on socio-environmental damages due to electricity and transport, European Commission, Brussels, 2003.

# Determination of Suitable Concentration of Non-Digested and Digested Dairy Wastewater for Growing *Nannochloropsis* Spp. for Biodiesel Production

R.P.C. Samanthika<sup>#1</sup>, C.P. Rupasinghe<sup>\*2</sup>, P.W.A. Perera<sup>#3</sup>

Faculty of Agriculture, University of Ruhuna,  
Matara, Sri Lanka

<sup>2</sup>chintha@ageng.ruh.ac.lk

## Abstract

Algal bio diesel production is considered as one of the sustainable solutions for increasing energy demand. Use of animal manure wastewater as a medium for algae is economically profitable and environmentally sound solution. Objective of the study was to select the suitable concentration of non-digested and digested dairy wastewater for growing microalgae, *Nannochloropsis spp.* Microalgae were grown in digested and non-digested wastewater media which were diluted into three concentrations (i.e. 25%, 50% and 100% on total dissolved solid (TDS) content) under local climatic conditions. Guillard and Ryther's modified F2 media was used as the control treatment. Experimental design was CRD, and treatments were replicated three times. Dry matter content of harvested *Nannochloropsis spp.* was measured and, oil content was estimated using Soxhlet method. Dry matter content of *Nannochloropsis spp.* in 25% TDS, 50% TDS and 100% TDS of non-digested and digested dairy wastewater media were observed as 1.96 g/l  $\pm$ 0.24, 1.20 g/l  $\pm$ 0.06, 0.55g/l $\pm$ 0.05, and 1.38 g/l  $\pm$ 0.33, 0.94 g/l  $\pm$ 0.08, 0.51 g/l  $\pm$ 0.05 respectively. Oil content in the same were estimated as 14.19%  $\pm$ 0.77, 9.39%  $\pm$ 0.85, 4.27%  $\pm$ 0.44, and 9.87%  $\pm$ 1.65, 5.44%  $\pm$ 0.61, 3.15%  $\pm$ 0.22 respectively. Dry matter and Oil content in F2 media was estimated as 1.35 g/l  $\pm$ 0.13 and 5.42%  $\pm$ 1.20 respectively. Dry matter content and oil percentage of 25% TDS of non-digested wastewater media was significantly higher ( $P < 0.05$ ). *Nannochloropsis spp.* can be successfully grown in 25% TDS of non-digested dairy wastewater under local conditions for getting higher oil yield.

**Keywords:** Algal biodiesel, *Nannochloropsis spp.*, Dairy wastewater

## Introduction

Fossil fuel consumption is now accepted as an unsustainable solution to compensate the world's energy demand. Solution is to find economically and environmentally sustainable production processes that are renewable, and capable of sequestering atmospheric CO<sub>2</sub>. So, microalgae bio fuel production is considered as a good solution that can successfully address above two criteria [1].

Small and industrial scale microalgae cultivation and production have evolved over the last five decades [2]. Mass cultivation of microalgae biomass using various simple and derived methods, ensure a high productivity of microalgae lipids. In commercial microalgae production systems, photoautotrophic microalgae are mostly cultivated by using solar energy. As microalgae bio fuel production is a complex process that is technologically challenging and economically expensive, currently four main cultivation technologies are used for commercial production i.e. (I) microalgae cultivation in a low-cost nutrient medium, (II) harvesting the cells from cultivation medium, (III) separation of the cells from growth medium by cell drying & cell disruption, (IV) efficient and low-cost lipid extraction through transesterification for biodiesel production, fermentation & distillation, starch hydrolysis.

Nutrient quantity and quality, temperature, light, salinity, turbulence and pH, are the most important parameters of regulating algal growth. As cell concentrations in phytoplankton cultures are generally higher than in natural conditions, algal cultures must be enriched with nutrients to make up for

deficiencies in seawater. Macronutrients [nitrate: phosphate (approximate ratio 6:1) and silicate (utilized by diatoms for external shell production)], and micronutrients [various trace metals, vitamins (thiamin, cyanocobalamin and sometimes biotin)] are generally utilized to enrich the production media. Walne medium and Guillard's F/2 medium are two suitable enrichment media that have extensively been used for the growth of most algae. Availability of commercial nutrient solutions may reduce labor usage for preparation. Complexity and cost of above culture media often excludes their usage in large-scale culturing operations. Suitable alternative enrichment media for mass microalgae production in large-scale extensive systems are composed of agriculture-grade fertilizers rather than laboratory-grade fertilizers and contain only the most essential nutrients.

As wastewater feeding for algae is not new a new concept, algal biofuel production can be successfully combined with wastewater treatment. Therefore, different types of wastewater (i.e. dairy manure, animal urine, winery wastewater, raw municipal wastewater, partially treated sewage, industrial and wastewater) have been already tested as the medium of growth.

Though, wastewater from livestock/cattle industries is one of the nutrient sources, major problem with most cattle wastewaters is the high nutrient concentration (specially the concentration total N and total P). Capability of microalgae to be effectively grown in nutrient-rich environments and, to efficiently consume the nutrients and accumulated metals in wastewater, have ensured their use as sustainable and low cost means of wastewater treatment [3].

As a sustainable solution for the energy crisis, world is now moving towards renewable energy sources. And, algal biodiesel production is considered as one of the environmental friendly solutions for that. Usage of artificial nutrient media such as Walne medium and Guillard's F/2 medium, are two suitable enrichment media that have extensively been used for the growth of most algae. But, the complexity and cost of above culture media often excludes their usage in large-scale culturing operations. And wastewater from livestock/cattle industries has high nutrient concentration. Capability of microalgae to be effectively grown in nutrient-rich environments and to consume the nutrients and accumulated metals in wastewater, have caused to use them as a sustainable, low cost means of wastewater treatment. Therefore, this study was conducted to select the suitable concentration of non-digested and digested dairy wastewater to be used as a growth medium for microalgae *Nannochloropsis spp.* for biodiesel production. This study was focused to select the suitable concentration of non-digested and digested dairy wastewater for growing *Nannochloropsis spp.* under local conditions.

## Methodology

Experiment was conducted in the Department of Agricultural Engineering, Faculty of Agriculture, University of Ruhuna, Sri Lanka.

*Nannochloropsis spp.*, marine micro algae samples were collected from shrimp culture farm, Chilaw and were grown under laboratory conditions.

## Preparation of Nutrient Media for Algae Growing

Guillard & Ryther's modified F2 medium was selected as the suitable medium for microalgae cultivation [4]. F2 medium is a common and widely used enriched seawater medium which is designed for growing coastal marine algae (especially diatoms) [5].

Stock solution "A" was prepared by dissolving 84 g of  $\text{NaNO}_3$ , 10 g of  $\text{NaH}_2\text{PO}_4$  and 10 g of Disodium EDTA in a volumetric flask and the volume was increased up to 1 L using distilled water. Stock solution "B" was prepared by dissolving 2.9 g of  $\text{FeCl}_3$  in a volumetric flask and the volume was increased up to 1 L using distilled water. Stock solution "C" was prepared by dissolving 0.2 g of Vitamin B1, 10 ml of Vitamin B12 and 10 ml of Biotin in a volumetric flask and the volume was increased up to 1 L using distilled water.

Preparation of trace metals stock solution (Solution "D"): Firstly, primary stock solutions were prepared to make trace metal stock solution. Primary stock solution "a" was prepared by dissolving 1.96 g of  $\text{CuSO}_4$  and 4.4 g of  $\text{ZnSO}_4$  in a volumetric flask and the volume was increased up to 100 ml using distilled water. Primary stock solution "b" was prepared by dissolving 1.26 g of  $\text{Na}_2\text{MoO}_4 \cdot 2\text{H}_2\text{O}$  in a volumetric flask and the volume was increased up to 100 ml using distilled water. Primary stock solution "c" was prepared by dissolving 36 g of  $\text{MnCl}_2$  in a volumetric flask and the volume was increased up to 100 ml using distilled water. Primary stock solution "d" was prepared by dissolving 2 g of  $\text{CaCl}_2$  in a volumetric flask and the volume was increased up to 100 ml using distilled water. After preparation of primary stock

solutions, trace metal solution was prepared by dissolving 1 ml of each primary stock solution (a, b, c & d) in a volumetric flask and, the volume was increased up to 1 L using distilled water.

#### **Preparation of Wastewater Media:**

Digested wastewater was collected from well-functioning biogas digester located in Walgama and, non-digested wastewater was collected from cattle shed of the faculty. By adding fresh water, digested and non-digested wastewater samples were diluted in to three concentrations based on their total dissolved solids (TDS) content. New concentrations of digested dairy wastewater were: 0.67g/l (25%TDS) - T1, 1.35g/l (50%TDS) - T2, 2.7g/l (100%TDS) - T3 and New concentrations of non-digested dairy wastewater were: 0.9g/l (25%TDS) - T4, 1.8g/l (50%TDS) - T5, 3.6g/l (100%TDS) - T6 respectively.

#### **Cultivation of Pure Culture (*Nannochloropsis Spp.*)**

Sea water solution of 35 ppt was taken, and it was diluted up to 25 ppt. Then 1 ml of each prepared stock solution was added per 1L of sea water of 25 ppt. The 10 ml of pure culture growing media of *Nannochloropsis* spp. was inoculated with above prepared culture medium inside the laminar flow (Conical flasks were plugged with cotton wools), and the samples were kept under normal light conditions in the laboratory. They were shaken and mixed well once a day.

After two weeks, color of the culture media was into dark green color and those were transferred into another 1 L of the same culture medium and experiment was established in the indoor cultivation unit under artificial light conditions (20 W) with single artificial

aeration devices (air pump 1.5 L/min) in each 1 L bottle. After another two weeks, when above culture media were changed into dark green color, they were mixed with 4 L of wastewater culture medium in outdoor cultivation unit. As the control treatment, F2 media was selected. Experiment was established in the outdoor cultivation unit under normal light conditions with artificial aeration for 2 weeks. At this stage, experiment was designed according to the complete randomized design (CRD). Treatments were replicated 3 times.

#### **Data Collection and Instrumentation**

EC (EC meter - Wagtech international) and pH (pH meter – Cyberscan pH 300) of each replicate were measured every other day for period of two weeks. Temperature (Dry bulb Thermometer, accuracy  $\pm 0.1^\circ\text{C}$ ), Relative Humidity (RH) (Dry and Wet bulb thermometer) was measured inside the green house every day. Light intensity was taken as lux meter (Lux meter – CRM DT 1308, accuracy  $\pm 5\% + 2$  digits) reading for both inside and the outside of the green house every day. Bright sunshine was taken daily using Sunshine recorder. Rainfall of the day was taken using Rain Gauge daily. Well grown algae were harvested by flocculation method using NaOH. The dry weight and oil content (as a percentage) were taken.

Water soluble nitrates in wastewater media were determined by using spectrophotometer under the wave length of 410 nm. Wastewater samples from each container were taken at the outlet and orthophosphate was analyzed according to the Ascorbic acid method.

## Results and Discussion

Consider the variation of climatic factors in experimental site during the experimental period, average temperature, average relative humidity, maximum rainfall and average daily sunshine were observed as 31° C, 71%, 80 mm and 5.8 hours respectively.

### Microalgae Growth Media Properties:

According to the pH variation, nearly the same pattern of pH variation was observed for all treatments. Salinity levels of wastewater treatments are lower than control treatments as control treatment includes sea water. Salinity of control treatment was changed in 30-40 ms/cm range. But wastewater salinity remains 2-8 ms/cm range.

### Dry weights of microalgae in both culture systems:

Harvested dry matter content of microalgae *Nannochloropsis spp.* in 25%TDS, 50%TDS and 100%TDS of non-digested dairy wastewater media were observed as 1.96 g/l, 1.20 g/l and 0.55 g/l respectively. Also, dry matter content of *Nannochloropsis spp.* in 25% TDS, 50% TDS and 100% TDS of digested dairy wastewater media were observed as 1.38 g/l, 0.94 g/l and 0.51g/l respectively. Dry matter in F2 media was observed as 1.355g/L (figure 1). Harvested dry matter in treatment 1 (algae grown in 25% TDS non-digested wastewater) was significantly higher than other treatments. ( $P < 0.05$ ). Highest

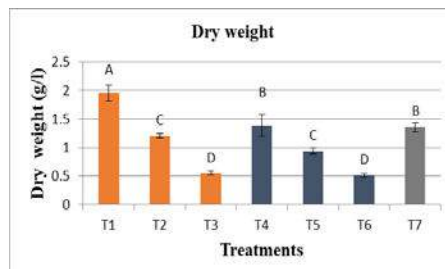


Figure 1. Dry weights of *Nannochloropsis spp.* of different treatments

dry matter yield of 25% TDS non-digested dairy wastewater (T1) was significantly different from other treatment. Dry matter content was decreasing with the increasing concentration of Digested and Non-digested wastewater. Comparatively higher dry matter yield was observed in Non-digested wastewater.

### Oil content of *Nannochloropsis spp.*:

As shown in figure 2, oil content of in 25% TDS, 50% TDS and 100% TDS of non-digested dairy wastewater media were estimated as 14.19%, 9.39%, and 4.27% respectively in dry basis. Oil content of in 25% TDS, 50% TDS and 100% TDS of digested dairy wastewater media were estimated as 9.87%, 5.44% and 3.15% respectively in dry basis. Oil content in F2 media was estimated as 5.42%. Highest oil content was observed in 25%TDS of non-digested wastewater.

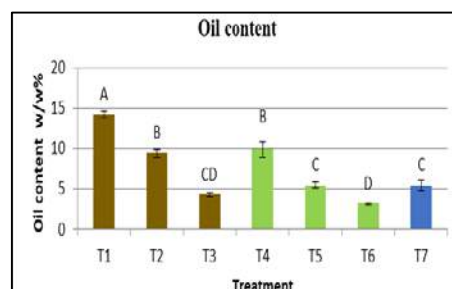


Figure 2. Oil content of *Nannochloropsis spp.* of different treatments.

The highest oil content of 25% TDS non-digested dairy wastewater (T1) was significantly different from other treatment. When comparing oil content of different concentrations of each wastewater media (non-digested, digested) lower concentrations showed higher oil content. High nutrient availability or toxicity in higher concentrations can be caused to these results. Oil content was significantly higher in 25% TDS non-digested dairy wastewater ( $P < 0.05$ ).

### Conclusions

When comparing with Guillard and Rither's modified F2 media, dry matter and oil content were significantly higher in 25% TDS concentration of non-digested dairy wastewater. 25% TDS concentration of non-digested dairywastewater is the

most suitable concentration for *Nannochloropsis* spp. growth.

### References

- [1] Lund Henrik, 2007. Renewable energy strategies for sustainable development, Energy, Volume 32, Issue 6, June
- [2] Lundquist, T.J., Woertz, I.C., Quinn, N.W.T. and Benemann, J.R., 2010. A realistic technology and engineering assessment of algae biofuel production. Energy Biosciences Institute, p.1.
- [3] Hena, S., Fatimah, S. and Tabassum, S., 2015. Cultivation of algae consortium in a dairy farm wastewater for biodiesel production. Water Resources and Industry, 10, pp.1-14.
- [4] Fox, J.M., 1983. Intensive algal culture techniques. CRC Handbook of mariculture, 1, pp.43-69.
- [5] Lavens, P. S. P., 1996. Manual on the Production and Use of Live Food for Aquaculture. Rome: Food and Agriculture Organization of the United Nations.

# A Rechargeable Banana Pith Bio-Battery

C. N. Nupearachchi<sup>#1</sup>, V. P. S. Perera<sup>#2</sup>

<sup>#</sup> *Department of Physics, The Open University of Sri Lanka,*

*Nawala, Nugegoda, Sri Lanka*

<sup>1</sup>chathunilnupe@gmail.com

## Abstract

A rechargeable bio-battery was made from banana pith as functional organic substrate which acts as the redox electrolytic mediator along with carbon and mild steel electrodes. The functionality is based on the equilibrium between  $\text{Fe}^{2+}$  and  $\text{Fe}^{3+}$  ions in the redox mediator during charging and discharging process. This specific study investigated the bio-battery charging variations using the pith of a Sri Lankan banana variety [Musa AAA Group (Cavendish Subgroup) 'ambun'] when  $\text{Fe}^{3+}$  ions are introduced into the electrolytic media.

It was achieved by introducing  $\text{Fe}^{3+}$  ions into the electrolytic media by two ways; a) either addition of Fe containing salt in an optimized ratio or b) allowing the mild steel electrode to stand alone in contact with the electrolyte for a day. Then  $\text{Fe}^{3+}$  ions diffuse to the banana pith from the mild steel by oxidation. This process can be expedited by connecting the mild steel to positive and carbon electrode to negative terminal of a power supply of about 2 V for one hour.

Spontaneous oxidation of  $\text{Fe}^{2+}$  ions to  $\text{Fe}^{3+}$  that complexed with phenolic groups are responsible to deliver a current after charging the battery. The average  $V_{oc}$  and  $I_{sc}$  values for a cell with  $\text{Fe}^{3+}$  ions were 605.1 mV and 3.08 mA respectively whereas values of 596.5 mV and 2.99 mA were recorded for a cell without  $\text{Fe}^{3+}$  ions.

**Keywords:** ambun, banana pith, electrode, electrolyte, phenolic groups, rechargeable bio-battery



## Introduction

In the recent past, numerous research and development have received the attention to harvest sustainable energy to produce electricity via power devices mainly as production/storage of energy using batteries, although they are diverse depending on the different application niches. Yet, there are many challenges ahead to develop batteries while meeting the current demands of high energy density, prolonged cycle life, less toxicity, less fabrication costs and less production complexity. Even it is essential that environmental constraints should be addressed in a methodical way while affecting the sustainability.

In this respect, the technology of batteries has evolved further towards bio-batteries for power generation with rapid advances and inexpensive energy solutions from the initial research curiosity of Galvani [1]. As a result, different modifications have been introduced [2, 3] into the structure of bio-battery design while optimization by the usage of new alternative materials [4, 5] are in practice. Even the focus has been diverted to the selection of various natural electrolytes by the researchers [6] with a major concern in ease of fabrication, affordability and safety.

Moreover, there is a practical need for bio-batteries with important characteristics such as, less weight, reusable with environmentally safe disposable practices and increased battery life. In fact, further improvements are needed to push the technology even further to enhance durability due to the inherent barrier of biodegrading nature of the bio-batteries. So, after multiple investigations [7-12],

the present study was aimed to understand the bio-battery charging variations using the pith of a Sri Lankan banana variety [Musa AAA Group (Cavendish Subgroup) 'ambun'] as the electrolytic media when Fe ions are introduced.

## Material and Methods

### Preparation of banana pith electrolyte

First, the trunk of ambun banana variety was cut into small cubes ( $1 \times 1 \times 1 \text{ cm}^3$ ) where it was chopped using an electric blender afterwards. Then, the blended pith was kept on a hot plate set at  $120 \text{ }^\circ\text{C}$  for 30 minutes with an intention to concentrate the liquid content. Fe ions were introduced in a very minute quantity of 1:100,000 mass ratio to the banana pith electrolytic media. For this purpose, 99% ferric chloride hexahydrate ( $\text{FeCl}_3 \cdot 6\text{H}_2\text{O}$ ) purchased from Thomas Baker was used. The cell without  $\text{Fe}^{3+}$  ions was used as the control of this experiment.

### Fabrication of cell

Next, banana pith with mass ratio of  $\text{FeCl}_3$  1:100,000 was sandwiched between two concentric electrodes configured with a carbon rod (diameter 0.7 cm) in the middle of a mild steel (ferrous) cylinder with 1 cm of separation and pith was filled up to a height of 4 cm in between.

### Characterization of cells

The initial open circuit voltage ( $V_{oc}$ ) and short circuit current ( $I_{sc}$ ) of the cells were checked using a digital multimeter.

Normal discharge without charging and the discharge after connecting to a power supply with constant voltage of 2 V for one hour were monitored for the cells with FeCl<sub>3</sub> and banana pith for total eight hours by recording the current and voltage separately. Above mentioned procedure was carried out for another cell without the inclusion of Fe ions as a control with identical dimensions and electrodes.

## Results and Discussion

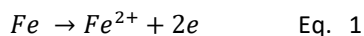
The average  $V_{oc}$  and  $I_{sc}$  values for a cell with Fe ions were 605.1 mV and 3.08 mA respectively whereas values of 596.5 mV and 2.99 mA were recorded for a cell without Fe ions. There was an increment of the conductivity of the electrolytic medium after introducing Fe<sup>3+</sup> ions in minute quantity. Numerically it is evident in average  $V_{oc}$  and  $I_{sc}$  values as expected.

Fe<sup>3+</sup> ions are needed to be in the electrolytic media for the functionality of this rechargeable bio-battery. It can be achieved by introducing Fe ions into the electrolytic media by the means of either

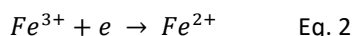
- a) addition of Fe containing salt chemically or
- b) allowing the mild steel electrode in contact with the electrolyte of the bio-battery for some time, at least 24 hours.

This allows Fe<sup>2+</sup> ions to diffuse into the banana pith from the mild steel at the interface by oxidation. This process can be expedited and achieved in a short period by connecting the mild steel to positive terminal and carbon electrode to negative terminal of a power supply of constant voltage of about 2 V for one hour. Galvanic mode operation of this

cell by connecting cathode and anode across a load resistor also introduces Fe<sup>2+</sup> ions to the electrolytic media. Fe<sup>2+</sup> ions diffuse to the electrolyte from mild steel according to the Equation 1.



These Fe<sup>2+</sup> ions further oxidise to Fe<sup>3+</sup> ions and complexation of Fe<sup>3+</sup> ions with phenolic groups in banana pith makes it into black blue colour. Introduction of Fe<sup>3+</sup> ions to the banana pith electrolytic media in any of the two methods mentioned above are reduced to Fe<sup>2+</sup> ions near the mild steel electrode during the charging process of the bio battery, which makes pale pink colour (Equation 2).



Thus, two specific colours of pale pink and black blue are observed near the mild steel anode and carbon cathode respectively. The cells were charged by connecting mild steel electrode to the negative and carbon electrode to the positive terminal of 2 V power supply for one hour. A thin brownish black layer was delaminated in between the electrodes after charging for one hour providing a demarcation boundary to the two colours. It is believed to be indicating the equilibrium of non-spontaneous redox reaction occurring in the electrolyte of banana pith.

Spontaneous oxidation of Fe<sup>2+</sup> ions to Fe<sup>3+</sup> that complexed with phenolic groups are responsible to deliver a current after charging the battery.

Figure 1 shows the variation of the circuit voltage and current with time under discharge of the two types of cells across a 50 Ω resistor without charging.

Here the cells operated in galvanic mode.

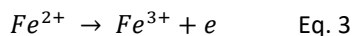
Although both voltage and current decreases exponentially in the first few minutes, after 30 min, there is a plateau of constant voltage and current for about two hours in each case. Afterwards, voltage and current of the cell without  $Fe^{3+}$  ions gradually increases with time whereas the cell with  $Fe^{3+}$  ions gradually decreases over the time.

Initial drop in the voltage and current of both the cells is due to interruption of double layer due to accumulation of electrons on the mild steel and  $Fe^{3+}$  ions in the electrolyte close to the electrode. The reaction in Equation 1 is not favoured in the cell where  $Fe^{3+}$  ions are introduced due to the existence of excess  $Fe^{3+}$  ions in the electrolyte. Thus, the gradual decrement of current and voltage is observed with time in this cell. But current and voltage in the cell without  $Fe^{3+}$  ions tend to increase because  $Fe^{3+}$  ions from the mild steel tend to diffuse towards the cathode that accumulated close to mild steel in the process due to repulsion of common ion favouring the forward reaction of Equation 1.

Figure 2 shows the discharge circuit voltage and current with time after two

types of cells were connected to a constant 2 V power supply for one hour of charging.

For the cell without  $Fe^{3+}$  ions, carbon electrode was initially connected to the negative while mild steel electrode was connected to the positive end of the power supply of 2 V to aid the presence of  $Fe^{3+}$  in the electrolyte by oxidation of iron for one hour. After that this cell and the cell already with  $Fe^{3+}$  ions by addition, were charged by connecting mild steel electrode to the negative while carbon electrode to the positive for 2 V power supply of one hour where the reduction of  $Fe^{3+}$  ions to  $Fe^{2+}$  ions occur. Then both cells were allowed to discharge under a load where  $Fe^{2+}$  ions tend to release electrons and form  $Fe^{3+}$  ions (Equation 3).



Both the voltage of the discharge curves of the bio-cells with and without  $Fe^{3+}$  ions showed a sudden increment in the second minute (Figure 2a inset). Recorded voltage increments of the bio-cells with and without  $Fe^{3+}$  ions were 91 mV and 90 mV respectively.

When the banana pith electrolyte is within contact with the electrodes,

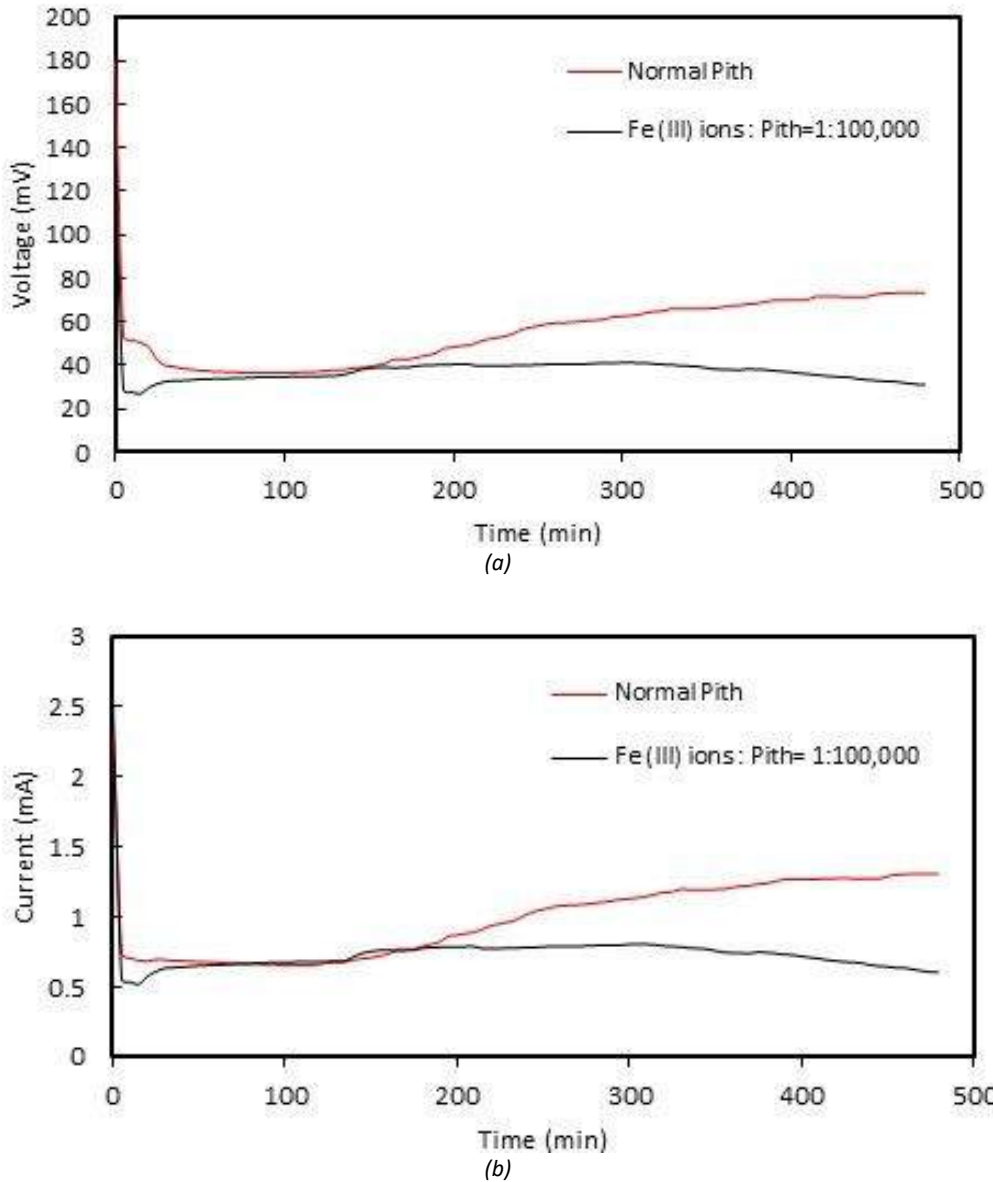


Figure 1 a) circuit voltage and b) current variation of the bio-cell with normal pith and with  $Fe^{3+}$  ions without charging

accumulation of access charge at the electrode surface is balanced by the accumulation of ionic species in the electrolyte close to the surface of electrode forming a double layer. This polarization causes potential drop due to activation polarization ( $\eta_a$ ) and concentration polarization ( $\eta_c$ ) along

with ohmic losses due to internal resistance ( $IR$ ). Hence, voltage of the cell  $V_{cell}$  differs (Equation 4) from cell potential  $E_{cell}$  due to the formation of double layer at the anode and cathode. Therefore,

$$V_{cell} = E_{cell} - \eta_a - \eta_c - IR \quad \text{Eq. 4}$$

When the sudden increment of voltage was noted, the recorded current was 1.6 mA and 1.8 mA for the bio-cells with and without  $\text{Fe}^{3+}$  ions respectively. The double layer formed was interrupted due

to the high current delivered by the cell, so that the voltage of the cell was increased initially. but when the circuit current decreasesd, stabilization of the double layer drop the voltage again.

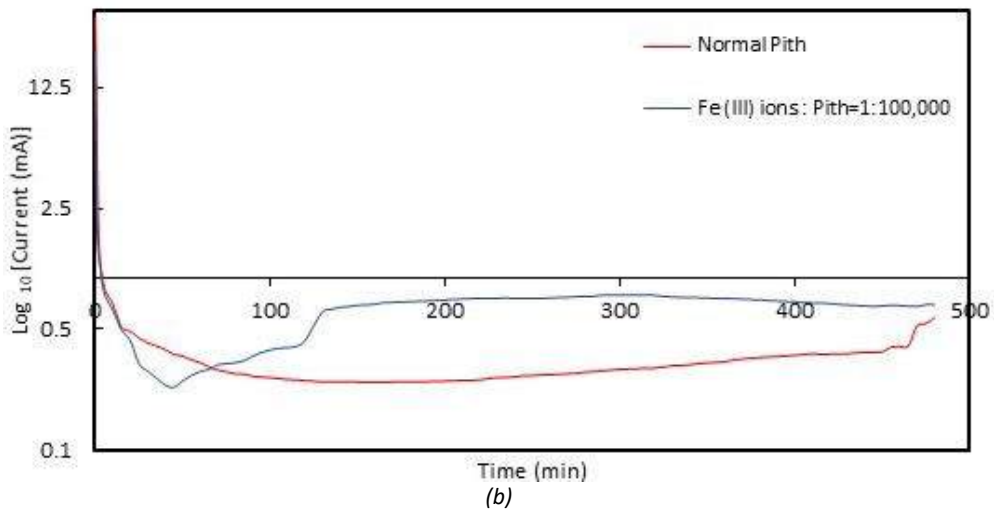
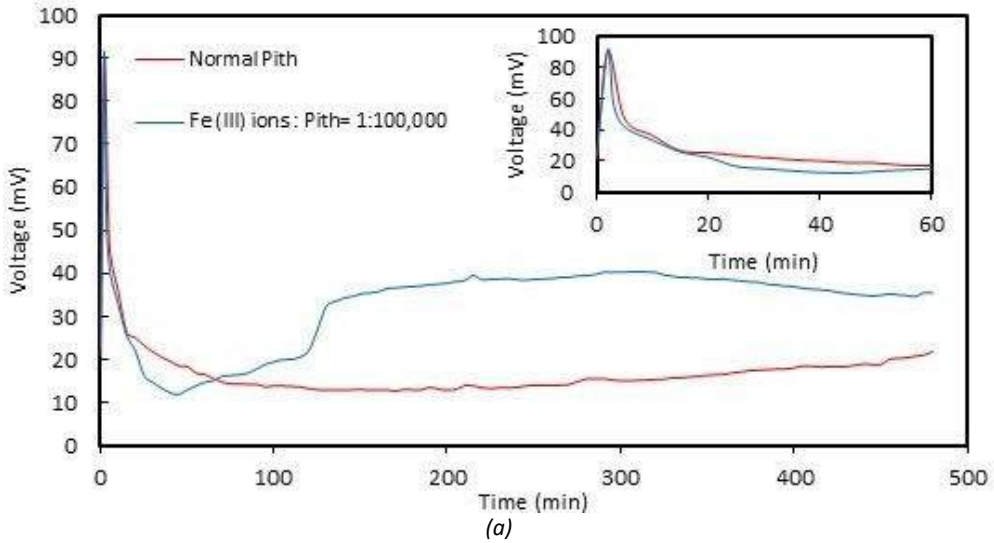


Figure 2 Discharged a) circuit voltage and b) current variation of the bio-cell with and without  $\text{Fe}^{3+}$  ions after connected to a 2 V power supply

After that, there was an exponential decay of the current for both cells. Yet, for the bio cell without  $\text{Fe}^{3+}$  ions started to show a slight increment in the current after 150 minutes and continued to increase till the end of 8 hours. The bio-cell with  $\text{Fe}^{3+}$  ions also started to increase the current after 45 minutes where after 5 hours, it started to decrease. This could be due to the same reason observed in galvanic discharge as well.

The specific values and time to observe the voltage increment tend to change due to the concentration of  $\text{Fe}^{3+}$  ions in the electrolytic media according to a previous study done by us [11]. It was observed that when the  $\text{Fe}^{3+}$  ions concentration is increased in the electrolytic media, the time to observe the voltage increment also took more time.

## Conclusion

A rechargeable bio-battery was made from banana pith as functional organic substrate which acts as the redox electrolytic mediator along with carbon and mild steel electrodes. The functionality is based on the equilibrium between  $\text{Fe}^{2+}$  and  $\text{Fe}^{3+}$  ions in the redox mediator during charging and discharging process. The average  $V_{oc}$  and  $I_{sc}$  values for a cell with  $\text{Fe}^{3+}$  ions to banana pith mass ratio 1:100,000 were 605.1 mV and 3.08 mA respectively. Comparatively, the values of 596.5 mV and 2.99 mA were recorded for a cell without  $\text{Fe}^{3+}$  ions. The sudden voltage increment in the discharge curves was noticed at 91 mV and 90 mV in two minutes for the bio-cells with and without  $\text{Fe}^{3+}$  ions respectively due to the interruption of the double layer.

This bio battery is an ideal replacement of chemical batteries for any device which require electric power in mW

range for its operation such as toys, LED light torches etc. in the area of consumer electronics as this invention facilitates the rechargeability in the long-term usage as an inexpensive and non-toxic power source.

## References

- [1]. Galvani, L. De viribuselectricitatis in motumuscolari. Commentarius. Bon. Sci. Art. Inst. Acad. Comm. 1791; 7:363-418. (English translation by M. G. Foley, 1953, Burndy, Retrieved from <http://www.bo.infn.it/galvani/de-vir-eng.html>)
- [2]. Baptista, A.C., Martins, J. I., Fortunato, E., Martins, R., Borges, J. P. and Ferreira, I. Thin and flexible bio-batteries made of electrospun cellulose-based membranes. Biosens. Bioelectron. 2011; 26 (5): 2742-2745.
- [3]. Hoffman, A.B., Suresh, S., Evitts, R.W., Kennell, G. F. and Godwin, J. M. Dual-Chambered Bio-Batteries Using Immobilized Mediator Electrodes. J. Appl. Electrochem. 2013; 43 (7): 629-636.
- [4]. Golberg, A., Rabinowitch, H. D. and Rubinsky, B. Zn/Cu vegetative batteries, bioelectrical characterizations and primary cost analyses. J. Renew. Sustain. Energy. 2010; 2: 033103.
- [5]. Muske, K. R., Nigh, C. W. and Weinstein, R. D. A Lemon Cell Battery for High Power Applications. J. Chem. Educ. 2007; 84 (4): 635-638.
- [6]. Jayashantha, N., Jayasuriya, K.D. and Wijesundara, R. P. "Biodegradable Plantation Pith for Galvanic Cells." in Proc. 28<sup>th</sup> Tech. Sess. Inst. Phy. Sri Lanka, 2012, pp 92-99.
- [7]. Nupearachchi, C.N., Perera, V.P.S., Samarasingha, K. A and Arawwawala, L. D. A. M. "Analysis of Selected Varieties of Banana Piths as Electrolyte in Bio Batteries." in Proc. 5th Int. Conf. on Ayurveda, Unani, Siddha and Traditional Medicine, Colombo, 2017, pp 217.
- [8]. Nupearachchi, C.N., Wickramasinghe, G. C. and Perera, V.P.S. "Investigation of Applicability of Banana Pith as Electrolytic Media for Bio-Batteries." in Proc. 15<sup>th</sup> Open University Res. Sess., Colombo, 2017, pp 509-512.

[9]. Nupearachchi, C.N., Wickramasinghe, G. C. and Perera, V.P.S. "Analysis of Performance of Bio-Battery Made of Banana Pith by Introducing Baker's Yeast." in Proc. 34<sup>th</sup> Tech. Sess. Inst. Phy. Sri Lanka, Colombo, 2018, pp 80-86.

[10]. Nupearachchi, C.N. and Perera, V.P.S. "Characterization of Banana Pith as Electrolytic Media of a Bio-Battery Using Electrochemical Techniques." in Abstracts of 11<sup>th</sup> Int. Res. Conf. of General Sir John Kotelawala Defence University, Colombo, 2018, pp13.

[11]. Nupearachchi, C.N. and Perera, V.P.S. "Oxidation and Reduction of Fe Ions Introduced to Banana Pith Electrolytic Media of A Bio-Battery." in Extended Abstracts of Open University Int. Res. Sess., Colombo, 2018, pp 305-308.

[12]. Nupearachchi, C.N. Wickramasinghe, G. C. and Perera, V.P.S. "Effect of Fe<sup>3+</sup> Ion on the Performance of a Bio-Cell Made of Banana Pith Electrolyte and Ferrous Anode" in Proc. 35<sup>th</sup> Tech. Sess. Inst. Phy. Sri Lanka, Colombo, 2019, pp 1-8

# Development of Cathode Material for Sodium-ion Rechargeable Battery in Sri Lanka

H.D.W.M.A. M.Wijeisnghe<sup>#1</sup>, C.H. Manathunga<sup>#2</sup>, V.P.S. Perera<sup>\*3</sup>, K.S. Mannatunga<sup>#4</sup>, R.A.D.D. Dharmasiri<sup>#5</sup>.

*#Department of Physics, University of Sri Jayewardenepura,  
Nugegoda, Sri Lanka.*

*\*Department of Physics, Open University of Sri Lanka,  
Nawala, Nugegoda, Sri Lanka.*

<sup>2</sup> chandimavc@sjp.ac.lk

## Abstract

Sodium-ion batteries are a hot topic in the modern scientific world. Because of the rapid depletion of Lithium resources, a replacement for the Lithium-ion batteries should be a great investment in future world. Considering the similar rock and chair mechanism with the Lithium, one can expect that inexpensive Sodium will be a potential candidate for a replacement. Even though number of cathode materials that were accommodated in Lithium-ion batteries was also tested with Sodium-ion batteries, a similar performance was not achieved with each and every material. Sodium-ion battery development field is relatively young in Sri Lanka. However, considering the sodium supply and mineral resources in Sri Lanka, one can expect it to have a great potential for further advancements within the country. In here we review the work previously done on Oxide, Silicate and Phosphate based transition metal compounds as cathode materials for the Sodium-ion batteries in Sri Lanka. It further discusses the performance and drawbacks when they are accommodated as cathode materials for sodium-ion batteries.

**Keywords:** Sodium-ion, XRD, Cyclic Voltammetry, Solid state reactions, Capacity



## Introduction

Rechargeable Lithium-ion batteries (LIB) are largely used as the main power supplying source in modern portable electronic devices. The first commercialization of them is reported (carbon//LiCoO<sub>2</sub> cell), in 1991. Though LIBs were originally developed as a high-energy power source for portable electronic devices their energy is typically limited to less than 100 Wh as a single battery pack [1].

The limited availability of the reserved Lithium deposits and the increasing demand has made the price of these batteries getting increased rapidly [2]. Due to this inflation, scientists are looking for alternative sources since last decades. [3]. Both sodium and Lithium are first group elements and they share some common chemical and physical properties. Another important fact is that these two battery types are associated with the same identical rocking chair mechanisms hence provide additional support [4]. Sodium, being the fourth most abundant element on earth, has a great feasibility to be employed as an unlimited source for battery production material. In parallel, an alternative to lithium is needed to realize large-scale applications; Sodium-ion Batteries (SIB) have attracted considerable research attention in recent years [3].

Having said that SIB has similar properties as LIBs does, it is pretty obvious that the cathode materials which were employed in LIBs are also feasible in using SIBs. Number of cathode materials was tested to be employed in LIBs. As usual transition metal compounds were

accommodated as the first choice. Lithium-oxide compounds such as LiCoO<sub>2</sub>, LiNiO<sub>2</sub> and LiMnO<sub>2</sub> and phosphates and silicates of the same have employed successfully in LIBs [5]. Similarly, number of cathode materials which were employed in Lithium-ion batteries was also tested with sodium-ion batteries as well. There are number of cathode materials, which were tested for sodium-ion cathodes. Most of the cathode materials are fabricated using transition metal oxides. Not only metal oxides polyanions such as phosphates, pyrophosphates, flurosulfates, oxychlorides, and sodium super ionic conductor types [1].

Although there are number of cathode types, the capacity of sodium-ion batteries are not up to the standards of the Lithium-ion batteries. In the basic stages the achieved capacity was nearly 20% of the capacity of the Lithium-ion batteries. According to experts in this area, the major reason behind this reduction is that the atomic size of the sodium ion is higher than the lithium-ion and it decreases the mobility of the ion. This is the main drawback of modern sodium-ion batteries which is needed to be solve and hence sodium-ion battery development is a quest which is not easy [3].

High capacities for SIBs are reported using Sodium Vanadium Fluorophosphates [6], Na<sub>2</sub>MnPO<sub>4</sub>F [7] carbon and aluminum oxide co-coated Na<sub>3</sub>V<sub>2</sub>(PO<sub>4</sub>)<sub>2</sub>F [8]. However, the battery life and number of charge-discharge cycles which were calculated regarding SIBs are comparatively lower than the LIBs. On

the other hand, durability and lower resistance to water vapor are another two problems that the sodium-ion battery industry has to face today. However, the sustainability and the environmental friendliness of SIB have not led down the hopes of researchers to build up a well working SIB [9].

The modern world energy crisis should be managed through the sustainability. Renewable Energy sources such as solar cells are the top competitors in renewable energy development. Sodium-ion cells have the ability to accommodate not only in mobile power devices such as in mobile phones or in but in stable power devices such as solar cells. On the other hand, sodium is less toxic than Lithium. Sodium-ion battery technology has recently aroused great interest, among all the scientific community, as a valid and more environmentally friendly alternative to Li-ion, owing to the abundance of sodium all over the planet [10].

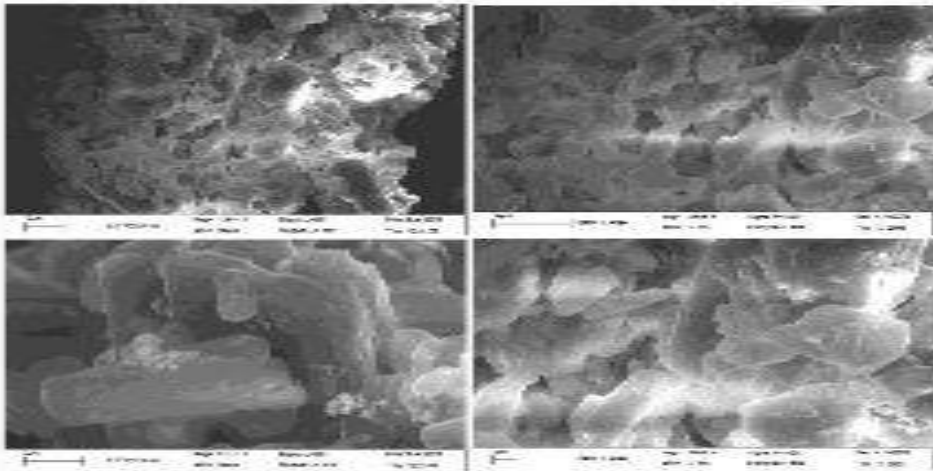
In this article, we are looking through some of the recent research development of cathode materials which were designed to accommodate in Sodium-ion batteries. This research field is relatively young in Sri Lanka as well. However, it should not be neglected that there is a great potential to develop sodium-ion battery industry in Sri Lanka. First of all, Sri Lanka has a great potential in an unlimited sodium supply being an Island. Secondly the country has rich minerals such as Ilmenite in Pulmoddai which contains Titanium and Seruwila iron ore which contains Copper and Iron which are still not totally utilized. On the other hand, Sri

Lanka owns the best graphite resource in the world at Kahatagaha. Hence a sodium-ion battery development trend in world will lead to economic development within the country.

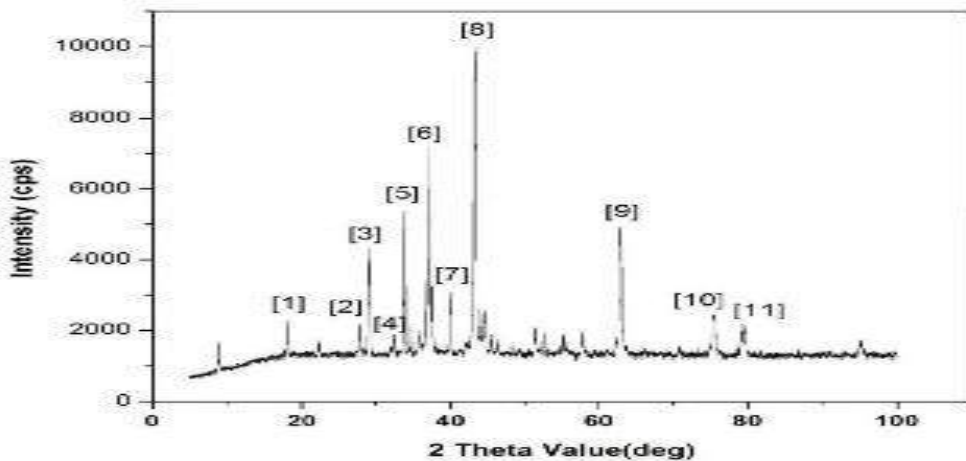
### **Oxide Based Cathode Materials in SIBs.**

Oxides are the most common type of cathode materials which has accommodated in SIBs throughout the world. In Sri Lanka, previously known work has related to Nickel Oxide[11], Manganese dioxide [12] and Magnetite which contains  $\text{Fe}_3\text{O}_4$ . [13]. Magnetite samples were prepared using the raw magnetite from Buththala.

Cathode material development has done by using solid state reactions [11] [12] and by directly applying magnetite into the cathode [13]. For the solid state reactions temperatures of 700 °C for 24 hours [11] and 850 °C for 10 hours [12] had used. Figure 1.(a) shows the (XRD) X-Ray Diffraction pattern compared with the standards for the sample prepared by the solid state reaction between  $\text{Na}_2\text{CO}_3$  and  $\text{Ni}(\text{NO}_3)_2$  in order to prepare the active material of  $\text{NaNiO}_2$  and Figure 1.(b) the scanning electron microscopic (S.E.M) view for the sample which clearly shows the micron level cavities formed when the cuboid shaped particles constructed with hexagonal unit cells, attached with each other. This enables the Na ions to intercalate in the cathode material. Here the molar ratio has been selected to be stoichiometric ratios of 1:2.



(a)



(b)

Figure 1: (a) The SEM view (b) The XRD pattern for the prepared sample of Sodium nickel oxide

However in the case of preparing a battery using  $\text{NaMnO}_2$ , the research team has experimented difference mole ratios of sodium in active material identify the best mole ratio to

prepare the desired material as in the Figure 2. Magnetite samples have directly accommodated as the active material after it has hammered and powdered as the active material.

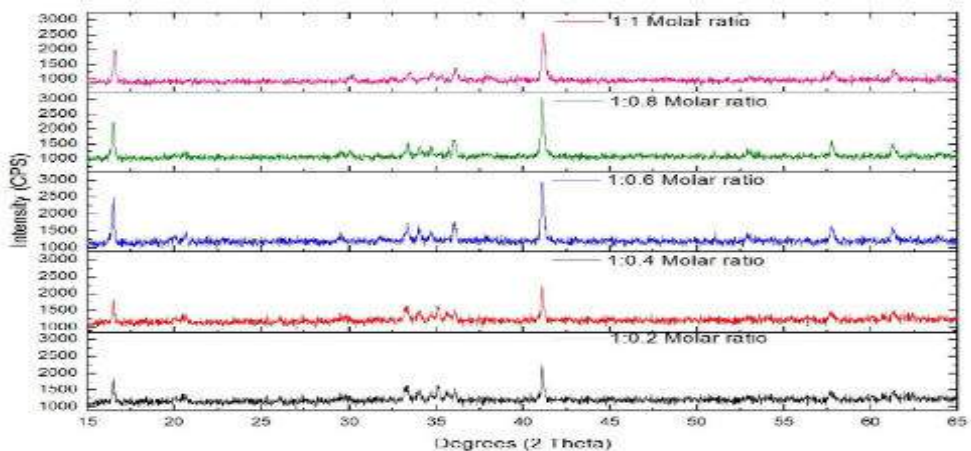
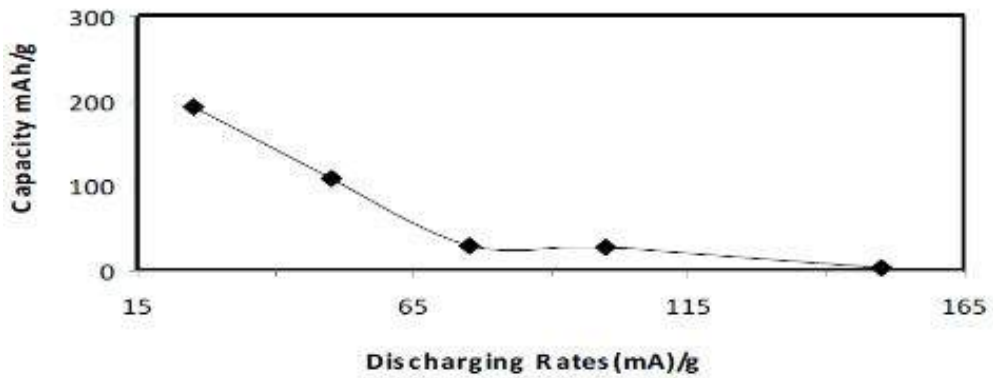


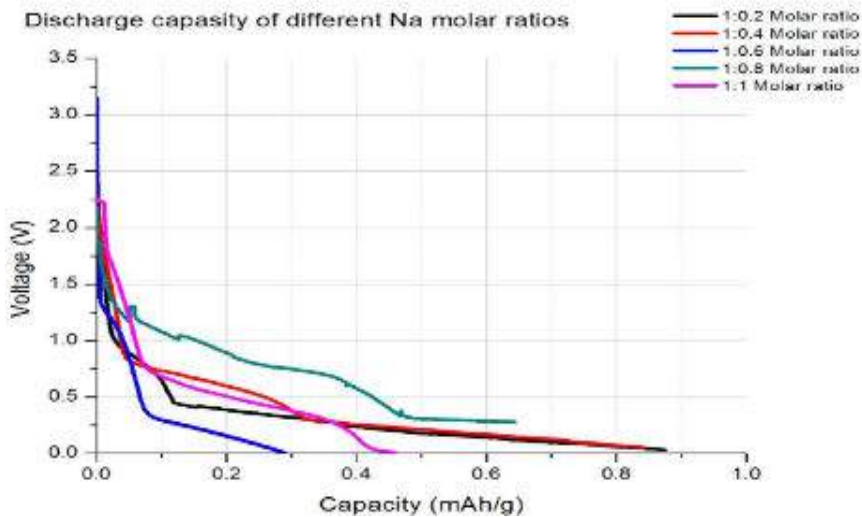
Figure 2: XRD pattern of  $\text{NaMnO}_2$  for different sodium mole ratios [12]

In cell preparation, the doctor blade method [14] was the desired fabrication method in each case. In general prepared active material samples are mixed with carbon black[12, 13] or acetylene black[11] and with polyvinylidene fluoride (PVdF) in 85%:5%:10% ratios with respect to mass. Cell fabrication should be done in an inert condition since sodium is highly reactive with oxygen and water vapor. For this purpose, a glove box is used. [13]

Figure 3.(a) discharging curve shows the ability of Sodium nickel oxide material to retain a high discharging capacity. Figure 3.(b). shows a relative comparison of obtained discharge capacities with respect to each molar ratio for the Sodium manganese oxide cell. The charging capacity and discharging capacity shows that maximum discharging capacity is with active material of 1:0.8 molar ratio of sodium. Magnetite based cathode materials have to be more explored since its capacity was  $8.09 \text{ mA h g}^{-1}$  and haven't done a further detailed study.



(a)

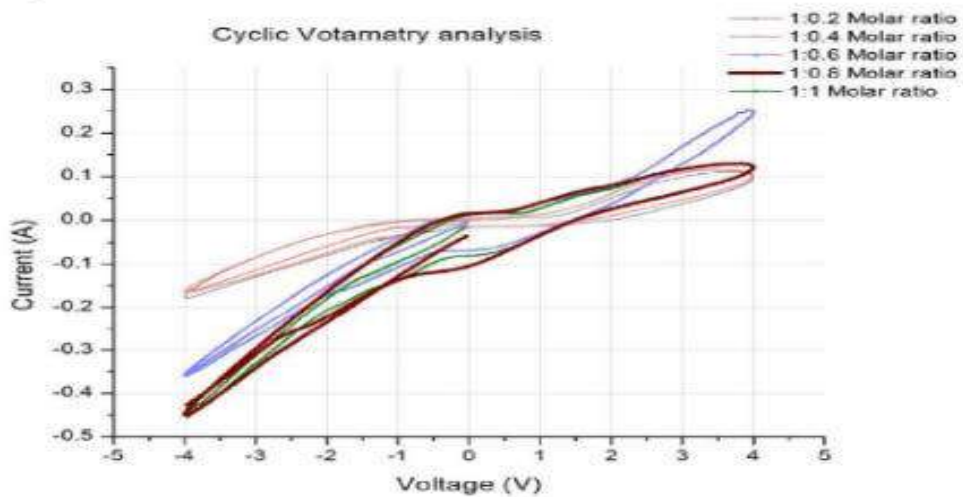


(b)

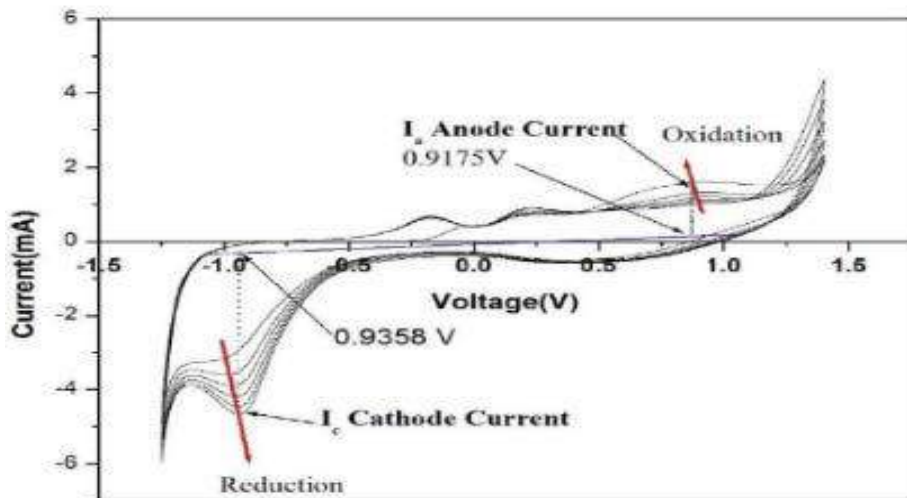
Figure 3: (a) The discharging curve for the sodium nickel oxide cell [11] (b) Discharging curves for different molar ratios  $\text{NaMnO}_2$  cell [12].

Considering the cyclic voltammetry, the oxidation and reduction peaks Nickel oxide based battery half-cell has shown (in Figure 4.b) more clear peaks. The cyclic results for the different ratios in Manganese dioxide based cell was or in the magnetite

based cell cyclic voltammetry results (in figure 4.a) were not that much promising. Any type of Oxidation or reduction peaks was not visible in this case. This may have resulted to the lower capacity of the battery.



(a)



(b)

Figure 4: (a) The cyclic voltammetry analysis for the different ratios for the  $\text{NaMnO}_2$  cell [12] (b) The cyclic voltammetry analysis for the different ratios for the  $\text{NaNiO}_2$  cell [11]

### Silicate based cathode materials for SIBs

Transition metal orthosilicates ( $\text{Na}_2\text{MSiO}_4$ , M=transition metal), which might possess a two-electron electrochemical reaction, open up the possibilities for high-capacity polyanion cathodes.  $\text{Na}_2\text{FeSiO}_4$  is currently attracting attention due to

its high theoretical capacity of  $276 \text{ m Ah g}^{-1}$  assuming a two-electron reaction occurred and its low cost nature due to the component consists of earth-abundant elements [15]. When considering Sri Lankan minerals silica sand is to be found easily in the areas like Matale, Jaffna, Madampe and Akurala. Hence these can be well utilized as cathode materials for SIBs with a low cost. In the Silicate based

scope, researches were carried out using the Sodium Manganese Silicates. The active material for the batteries had synthesized using a solid state reaction between  $\text{Na}_2\text{CO}_3$ ,  $\text{MnO}_2$  and  $\text{SiO}_2$  in  $800^\circ\text{C}$  for six hours [16]. Another method used was [17] earth abundant  $\text{Na}_2\text{SiO}_3$  and  $\text{MnCO}_3$  taken in 1:1 ratio at a temperature of  $800^\circ\text{C}$  for 4 hours. Both cases the battery fabrication has done using active material, PVDF and activated carbon into 7:1.5:1.5 ratios with respect to weight.  $\text{NaClO}_4$  was the electrolyte in each case. Battery fabrication as usual was done inside a glove box filled with argon. XRD of the prepared material in

[17] was compared with pure  $\text{SiO}_2$ . The XRD pattern of the pure  $\text{SiO}_2$  used in this synthesis and it is found to be in amorphous form. The amorphous nature of silica disappeared after synthesizing active material confirmed by the sharp peaks appearing in the XRD pattern (Figure 5.(a)). The Energy Dispersive X-Ray spectroscopy (EDX) of the prepared material [16] (Figure 5.(b)) depicts the peaks for the presence of Sodium, Manganese and silica with a molar ratio of  $\text{Na}:\text{Mn}:\text{Si}:\text{O}=2:1:1:4$ . Here, a high percentage of Na, Si and O may be due to unreacted  $\text{Na}_2\text{SiO}_3$  present in the sample.

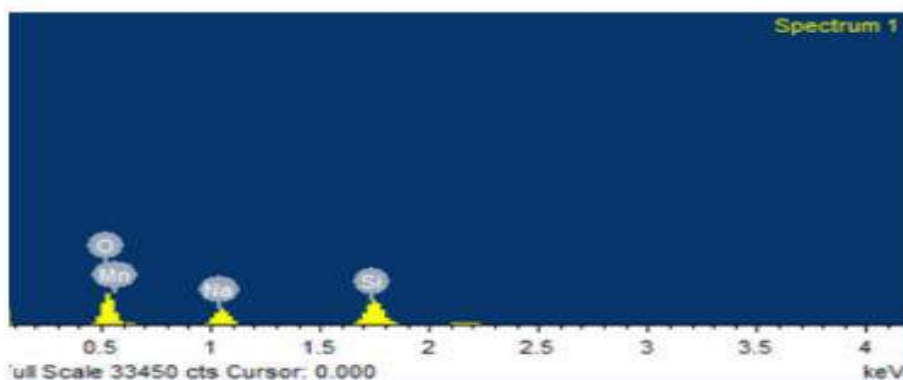
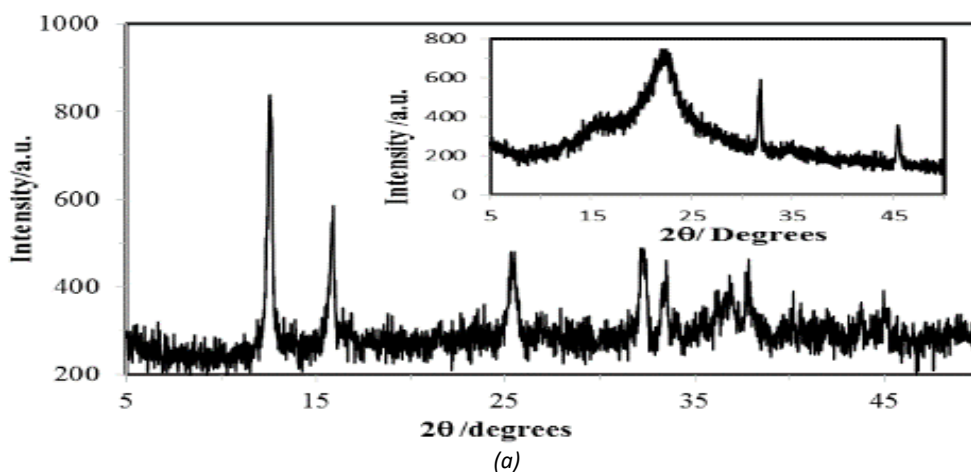


Figure 5: The XRD results for the prepared sample by [17] (b) The EDX results for the prepared sample prepared sample [16]

Considering the battery capacities of  $1.63 \text{ mA h g}^{-1}$  [17] and  $1.89 \text{ mA h g}^{-1}$  [16], it is clear that these capacities should be further developed in order to accommodate in practical applications. The less capacity may have resulted due to the intercalation chemistry to be the principle method of releasing the charged particles rather than the oxidation and reduction. However, from the obtained results and the theoretical implications above it can be deduced

that the orthosilicates are cost effective materials for cathode materials used in sodium-ion batteries [17]. Therefore, conducting further researches on these cells will be a great investment which can be expected to give great results in future. Since the silicates are dielectric materials, the composition of carbon in the electrode also needs to be optimized [17]. In this purpose the carbon percentages were varied, in order to find out the best composition.

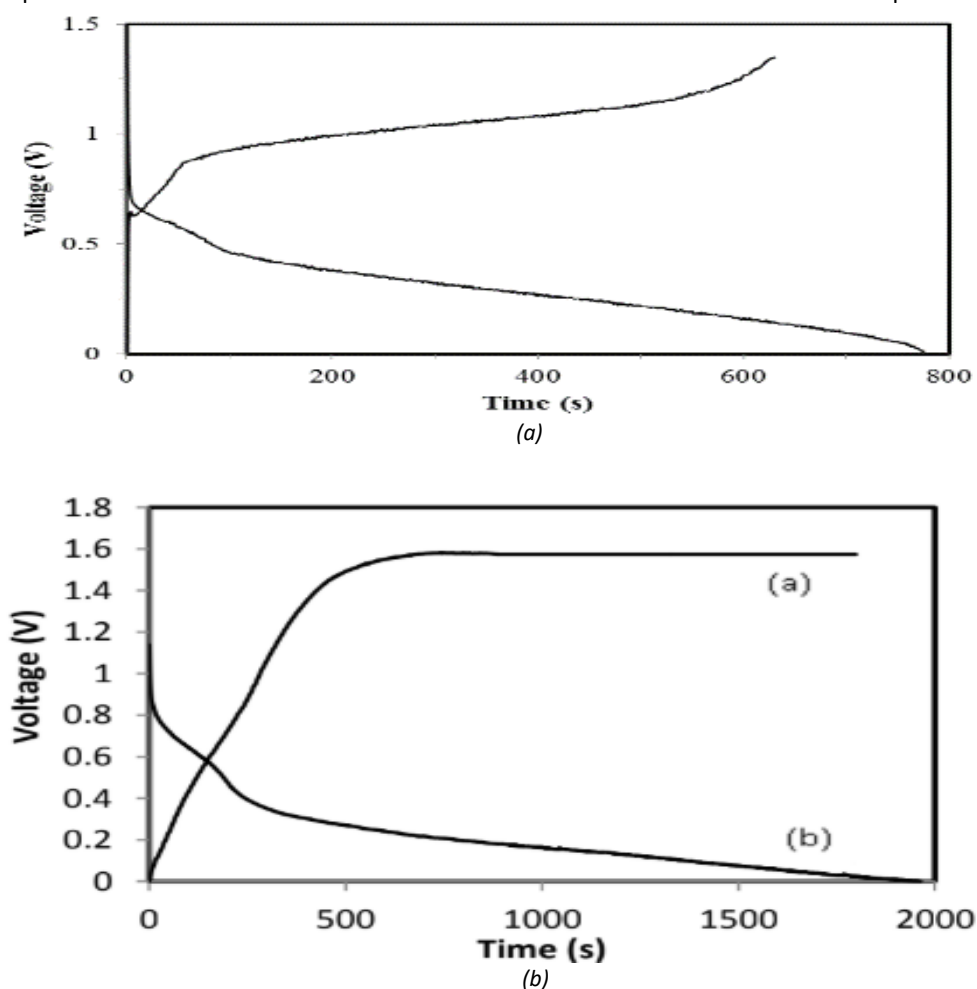


Figure 6: The comparison of charge discharge cycles by (a) cells by [17] and (b) The charge and discharge by [16]



## Phosphate based cathode material development

Phosphate based cathode material designing is relatively young and still needed to be developed. In contrast,  $\text{MxPO}_4^{2-}$  is a promising class of conversion cathode materials because of its thermodynamic stability (where M is a metal). In literature, the research group has reported that  $\text{Cu}_3(\text{PO}_4)_2/\text{C}$  can be used as a cathode material [18]. One can predict that these phosphate-based composites can be employed in the production of sodium-ion batteries. When concerning transition metal compounds containing polyanions such as  $\text{PO}_4^{3-}$  are intensively investigated because the strong P-O covalent bonds can stabilize the lattice oxygen even at highly charged state. The phosphate framework materials show very low thermal expansion (the coefficient of thermal expansion is around  $10^{-6}\text{C}^{-1}$ ), this has lead them to be have high structural stability at high temperature [19].

In the phosphate based material development, the common procedure to develop the materials is to conduct a solid state reaction between the transition metal compound and sodium phosphate at  $700\text{ }^\circ\text{C}$ -  $800\text{ }^\circ\text{C}$  for around 4-6 hours. In one such case, Cobalt Oxide was mixed with sodium phosphate and grinded using the ball mill until it mixed together [20]. The material of Sodium cobalt phosphate was synthesized using a solid state reaction, at a temperature of  $800\text{ }^\circ\text{C}$ . The XRD pattern of this material was compared with the previous literature [21] and confirmed the presence of sodium cobalt phosphate. However, the presence of noise peaks in XRD indicates that such solid state reactions can contain impurities other than the desired material. The cell was fabricated using the mixture of active material, activated carbon and PVDF 18:1:1 ratio inside a glove box filled with Argon gas. The obtained cyclic voltammetry graph shows oxidation and reduction peaks which are different in size. This is one of the reasons behind the less capacity reported  $9.58\text{ mA h g}^{-1}$ . This will also impact negatively on the cyclability of the cell.

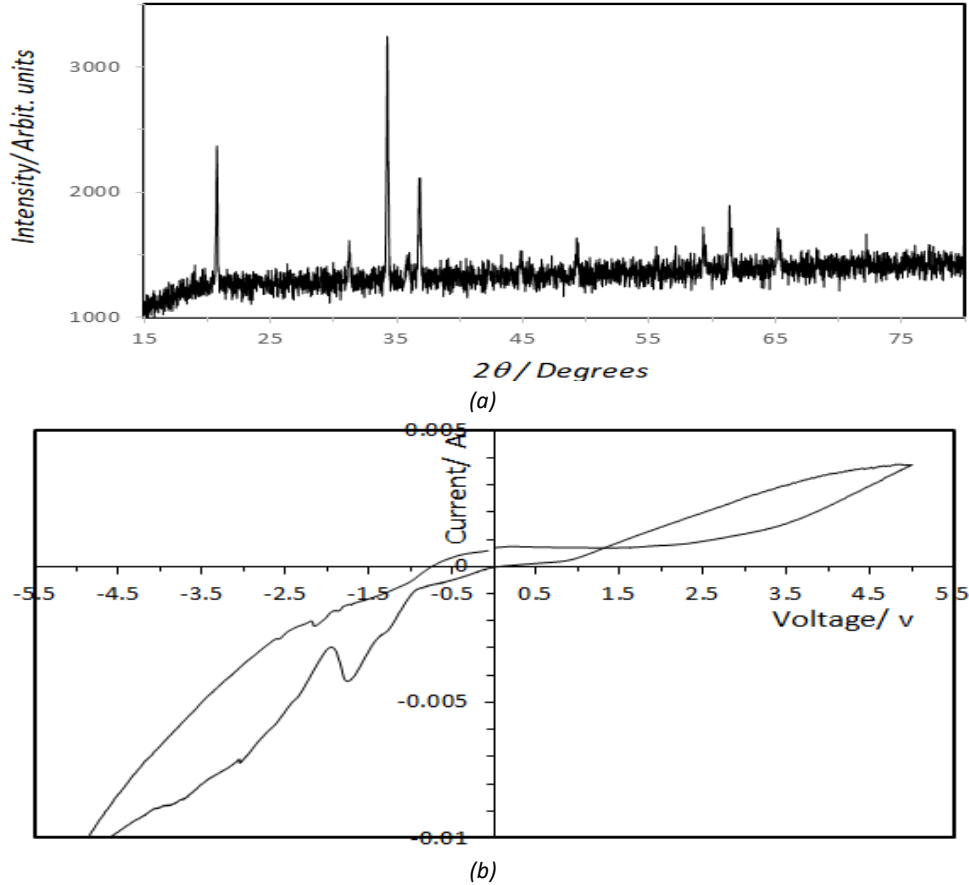


Figure 7: (a) XRD pattern for the prepared material of Sodium cobalt phosphate, (b) The cyclic voltammetry pattern for the prepared cell [20]

A sophisticated cell was fabricated using a Sodium cobalt phosphate cathode [22]. This cathode approached a higher capacity of  $103.12 \text{ mAhg}^{-1}$ . The cathode material preparation was done using a solid state reaction between Sodium phosphate and Copper iodide in  $600^\circ\text{C}$  as Copper oxide was relatively expensive and hard to find. When considering the XRD pattern and the EDX results, it was evident that the desired material was synthesized

using the proposed method by authors. The cyclic voltammetry graph has shown a clear indication of oxidation and reduction peaks. It has played a major role in achieving a high capacity from the prepared cell. In some of the previously discussed cells, the oxidation reduction process was not successfully visible in the cyclic voltammetry graphs. Since they were based only on intercalation of sodium ions the achieved capacities were relatively low.

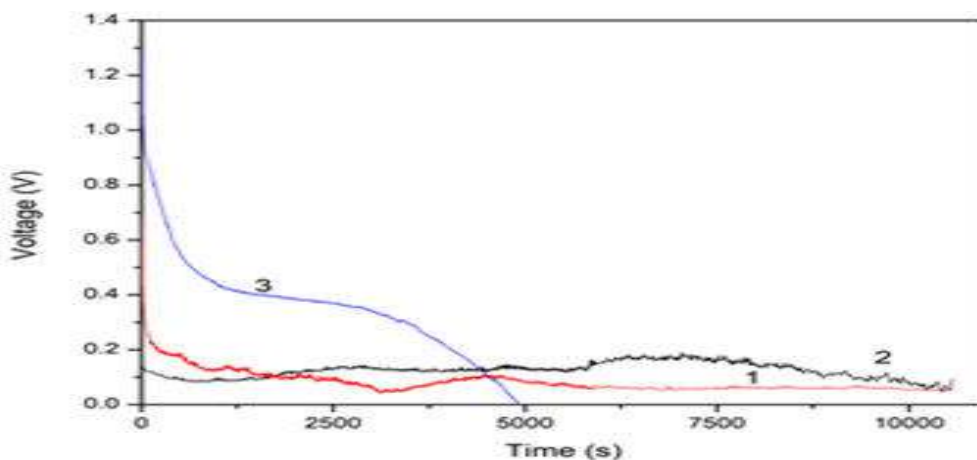


Figure 8: The discharging curves- 1-first cycle, 2-fifth cycle, 3-tenth cycle [22]

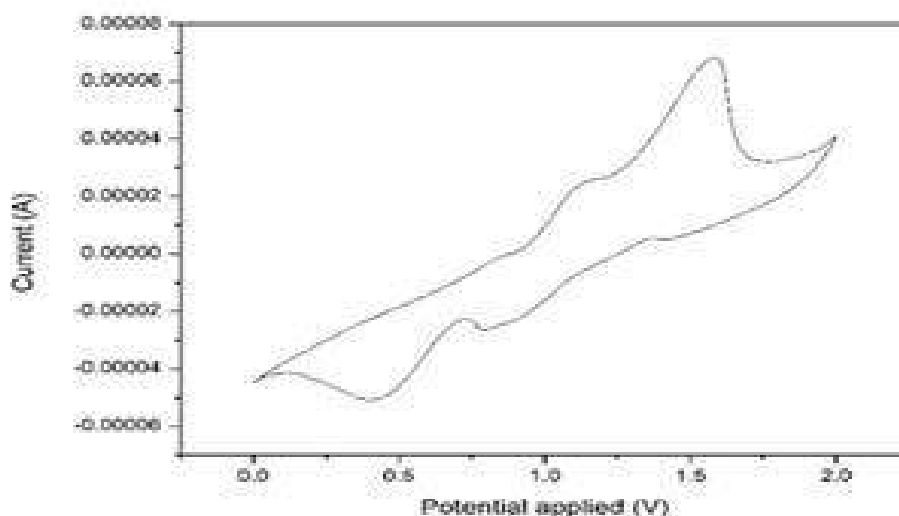


Figure 9: The cyclic voltammetry graph for the prepared cell [22]

## Conclusions

The research interest on sodium-ion batteries in Sri Lanka is relatively new. There is a feasibility to use minerals abundant in Sri Lanka in sodium-ion batteries and sodium could be also purified from seawater. Cathode material development is very important in order to develop a sophisticated sodium-ion battery

which can be accommodated as a commercial product. Although both Sodium-ion and Lithium-ion batteries hold some similar properties each and every cathode material suitable for Lithium-ion batteries cannot be directly accommodated in Sodium-ion batteries. Transition metal oxide, silicates and phosphates had tested as cathode materials in reported literature and these cathode

materials based batteries should be further developed in order to achieve high capacities and cyclability. For achieving such high capacities, the oxidation and reduction process plays a major role than the intercalation chemistry. However, there is a great potential to develop sodium-ion batteries in commercial standards within the country if further researches are carried out.

## References

- [1] Yabuuchi, N., et al., Research Development on Sodium-Ion Batteries. *Chemical Reviews*, 2014. 114: p. 11636–11682.
- [2] Ali, B., et al., Interconnected mesoporous  $\text{Na}_2\text{FeSiO}_4$  nanospheres supported on carbon nanotubes as a highly stable and efficient cathode material for sodium-ion battery. *Journal of Power Sources*, 2018. 396: p. 467-475.
- [3] Hwang, J.Y., Myung, S.T. and Sun, Y.K., Sodium-ion batteries: present and future. *Chem Soc Rev*, 2017. 46(12): p. 3529-3614.
- [4] Wang, D., et al., Sodium vanadium titanium phosphate electrode for symmetric sodium-ion batteries with high power and long lifespan. *Nature Communications*, 2017: p. 1-7
- [5] Zubi, G., et al., The lithium-ion battery: State of the art and future perspectives. *Renewable and Sustainable Energy Reviews*, 2018. 89: p. 292-308.
- [6] Serras, P., V. Palomares, and Rojo, T., High-Voltage Cathodes for Na-Ion Batteries: Sodium–Vanadium Fluorophosphates. 2016.
- [7] Lin, X., et al., Exploiting  $\text{Na}_2\text{MnPO}_4\text{F}$  as a high-capacity and well-reversible cathode material for Na-ion batteries. *RSC Adv.*, 2014. 4(77): p. 40985-40993.
- [8] Ma, D., et al., Enhanced electrochemical performance of carbon and aluminum oxide co-coated  $\text{Na}_3\text{V}_2(\text{PO}_4)_2\text{F}_3$  cathode material for sodium ion batteries. *Electrochimica Acta*, 2018. 283: p. 1441-1449.
- [9] Dahbi, M. and Komaba S., Fluorine Chemistry for Negative Electrode in Sodium and Lithium Ion Batteries. 2015: p. 387-414.
- [10] Yan, G., et al., Higher energy and safer sodium ion batteries via an electrochemically made disordered  $\text{Na}_3\text{V}_2(\text{PO}_4)_2\text{F}_3$  material. *Nature Communications*, 2019. 10(1): p. 585.
- [11] De Silva, R.C.L., et al., Sodium nickel oxide nanoporous cathodes used for sodium-ion rechargeable batteries. *Sri Lankan Journal of Physics*, 2014. 15: p. 19-29.
- [12] Rathnayake, R.R.D.V., Perera, V.P.S., and Manathunga, C.H., Synthesis and characterization of  $\text{Na}_x\text{MnO}_2$  as a cathode material for Sodium-ion rechargeable Batteries. *Proceedings of the Technical Sessions Institute of Physics – Sri Lanka 2017*, 2017. 33: p. 39-44.
- [13] Rathnayake, R.R.D.V., Perera, V.P.S., and Manathunga, C.H., Capability of Using ore magnetite directly as cathode material for Sodium-ion Rechargeable Battery. in *International Conference on Multidisciplinary Approaches*. 2017. University of Sri Jaywardenepura.
- [14] A., B., M. M., and S. H., Doctor Blade. In: Aegerter M.A., Mennig M. (eds) *Sol-Gel Technologies for Glass Producers and Users*. . 2004: Springer, Boston, MA
- [15] Guan, W., et al., A High Capacity, Good Safety and Low Cost  $\text{Na}_2\text{FeSiO}_4$  Based Cathode for Rechargeable Sodium-Ion Battery. *ACS Applied Materials & Interfaces*, 2017. 9(27): p. 22369-22377.
- [16] Alahakoon, T.N., et al., Sodium Manganese Silicate as cathode material for Sodium-ion Rechargeable batteries. *Proceedings of the Technical Sessions Institute of Physics – Sri Lanka 2018*, 2018. 34: p. 87-91.
- [17] Alahakoon, T.N., et al. Fabrication of Sodium Ion Rechargeable Battery Using Earth Abundant Orthosilicates in *Proceeding of the 15<sup>th</sup> Open University Research Sessions (OURS 2017)* 2017.
- [18] Zhao, W., et al.,  $\text{Cu}_3(\text{PO}_4)_2/\text{C}$  composite as a high-capacity cathode material for rechargeable Na-ion batteries. *Nano Energy*, 2016. 27: p. 420-429.

[19] Fang, Y., et al., Phosphate Framework Electrode Materials for Sodium Ion Batteries. *Adv Sci (Weinh)*, 2017. 4(5): p. 1600392.

[20] Wijesinghe, H.D.W.M.A.M., Manathunga, C.H., and Perera, V.P.S., Development of sodium-ion rechargeable battery using sodium cobalt phosphate cathode. *International Journal of Multidisciplinary Studies (IJMS)*, 2019. 6(1): p. 1-6.

[21] Gond, R., et al., Bifunctional Electrocatalytic Behavior of Sodium Cobalt Phosphates in Alkaline Solution. *ChemElectroChem*, 2017. 5(1): p. 153-158.

[22] (press) Wijesinghe, H.D.W.M.A.M., Manathunga, C.H., and Perera, V.P.S., Development of sodium-ion rechargeable battery using sodium copper phosphate cathode (2019).

# Fabrication and Characterization of CuO Nanocrystalline Thin Films Prepared by Using Colloidal Suspension

Wickramasinghe G.C.\*<sup>1</sup>, Wickramasinghe W.M.H.G.S.\* , Perera V.P.S.\* ,  
Senthilnithy R.#

*\*Department of Physics, The Open University of Sri Lanka, Nawala,  
Nugegoda, Sri Lanka*

*#Department of Chemistry, The Open University of Sri Lanka, Nawala,  
Nugegoda, Sri Lanka*

<sup>1</sup>*gim.chathu@gmail.com*

## Abstract

Increasing energy requirements for worldwide population, along with global warming and environmental pollution issues drive a search and growth of clean and renewable energy technologies such as solar cells. The applications of CuO nanoparticles in quantum dot solar cells are the most interesting research area in this context. Copper oxide thin films were fabricated on Fluorine-doped Tin Oxide (FTO) glass plates by spin and doctor blade method using colloidal suspension of nanocrystalline CuO dispersed in mixture of methanol and chloroform. CuO nanoparticles were synthesized by adding trimethylamine into copper acetate dissolved in 96% (V/V) methanol subsequent heating at 45-50 °C. The x-ray diffraction analysis revealed that the synthesized CuO has nanocrystalline structure. The CuO films were also analyzed using electrochemical impedance spectroscopy and capacitance-voltage (Mott- Schottky) measurements. The negative slope of the Mott-Schottky plot confirmed that the synthesized CuO is p-type. Although the reported value of the flat band potential of CuO is at around 0.79 V, the synthesized CuO film of the current study was 1.04 V. This facile cost-effective method of synthesis of CuO nanocrystalline material and simple fabrication technique of thin films find many applications as efficient antimicrobial agent, biological catalyst, chemical and gas sensors, and specially in light harvesting in the global world. The above synthesized CuO in this study could be used quantum dot solar cells by reducing the particle size further.

**Keywords:** Copper oxide; Triethylamine; Nanocrystalline material

## Introduction

The application of metal oxide nanoparticles is most interesting research area in the development of novel science and technology innovations. Among them, solar cell technologies based on metal oxide nanoparticles can enable the realization of low-cost and high-throughput photovoltaic production [1]. Currently solar power is more cost effective than the other forms of alternative energy sources which provide a clean, renewable and low cost energy for the increasing demand. Multiple junctions are used in solar cell technology to enhance the throughput. But the problem with nanoparticle multiple junctions solar cell due to its high cost of production and toxicity of some of the materials used for the fabrication. While much work has previously been focused on organic semiconductor materials, colloidal inorganic green semiconductor nanocrystals (NCs) are the recent attention by researchers for photovoltaic applications [2]. NCs have the advantages of being solution-processable, capable of absorbing a large fraction of the solar spectrum, and tunable band-gap due to its quantum-confinement effects.

In this study, facile cost effective method of synthesis of CuO nanocrystalines and simple fabrication technique of thin film with this material is investigated. Compared to the other p-type semiconductor materials with a narrow band gap, copper oxide (band gap 1.2 eV) is useful in various applications [4]. CuO being a green semiconductor material finds in many applications as efficient antimicrobial agent, biological catalyst, chemical and gas sensors, and specially in light harvesting. There is a need to find other renewable energy sources to

overcome the increasing energy requirement globally.

In this present study, an alternative procedure is introduced for synthesizing CuO nanoparticles via modified alcoholic-triethylamine method. CuO thin films were made on Fluorine-doped Tin Oxide (FTO) glass plates by spin coating and doctor blade method for characterization using colloidal suspension of the synthesized CuO nanoparticles dispersed in mixture methanol and chloroform. The characteristics were compared with the commercially available CuO powder.

## Methodology

### Synthesis of CuO nanoparticles

CuO was synthesized using the following procedure. 0.6 g of copper acetate was added to 60 ml of 96 % (V/V) methanol at 45-50 °C with vigorous stirring using a magnetic stirrer for 30 min. 4 ml of triethylamine (TEA) was added to the above reaction mixture and was allowed to continue the reaction at 45-50 °C for 1 hour. A black brown colour CuO precipitate was obtained which was separated out from the reaction mixture and washed with deionized water three times followed by centrifugation at 3600 rpm for 2 min. The washed precipitate was collected into a petri dish using acetone and dried at 150 °C for 30 min. A black brown precipitate of CuO obtained was kept in a desiccators until use.

### Preparation of CuO films

A Fluorine-doped Tin Oxides (FTO) glass plates were cut into the size of 1 cm × 2 cm which were cleaned in an ultrasonic bath using 1 drop of conc. HNO<sub>3</sub> in deionized water and again with deionized water for 5 minutes

respectively. Then the glass plates were boiled with acetone and with isopropyl alcohol solution respectively in a beaker on a hot plate at 80 °C for 15 minutes. 0.002 g of CuO sample and Methanol and chloroform in 1:2 ratio were placed into a mortar. The mixture was grinded in the mortar using a pestle for 15 min until a fine paste of sample was obtained. The CuO paste was spread on the FTO glass using doctor blade method. The CuO films were sintered on a hotplate at 300 °C for 30 min.

### Characterization of samples

The structural properties of the CuO particles were investigated using high energy X-Ray Diffraction (XRD) analysis. XRD pattern was obtained using a Rigaku Ultima IV. Cu K $\beta$  radiation with a scanning angle (2 $\theta$ ) range from 20 ° to 80°. The films of commercial and synthesized CuO were characterized with the mott-shottky measurements and impedance spectroscopy to find the flat band potential and impedance of the films respectively. The photocathodes were served as working electrode while a platinum wire and a saturated Ag/AgCl electrode served as counter and reference electrodes, respectively.

## Results and Discussion

### Determination of flat band potential

The mott-schottky measurement was carried out on the CuO thin films deposited on FTO glass as shown in figure 1. The flat band potential was determined from the intercept of the potential vs reciprocal square capacitance axis. The negative slope of the Mott-Schottky plot confirmed that the synthesized CuO is p-type. The values of the flat band potential of the synthesized CuO and commercial CuO were 1.04 V and 1.5 V respectively. Mott-Schottky relationship for a p-type semiconductor is describe by the following equation [5].

$$\frac{1}{C^2} = \frac{2}{e\epsilon\epsilon_0 N_A} \left( E - E_{fb} - \frac{kT}{e} \right) \quad (\text{eq 1})$$

Where,

C = capacitance of the space charge region

$\epsilon_0$  = vacuum permittivity

$\epsilon$  = relative dielectric constant of the sample

e = electron charge

V = applied potential

K = Boltzmann constant

T = absolute temperature

$N_A$  = acceptor concentration

With a  $\epsilon$  value of 18.1 for CuO [5], the acceptor concentrations of the samples were determined from the slope of Mott-Schottky plots as shown in Table 1.



Table 1: Flat band potential and acceptor concentration of commercial CuO and Synthesized CuO films.

|                 | Flat band potential (V) | Acceptor concentration (cm <sup>-3</sup> ) |
|-----------------|-------------------------|--|
| Commercial CuO  | 1.5                     | $5.17 \times 10^{19}$                      |
| Synthesized CuO | 1.04                    | $1.37 \times 10^{20}$                      |

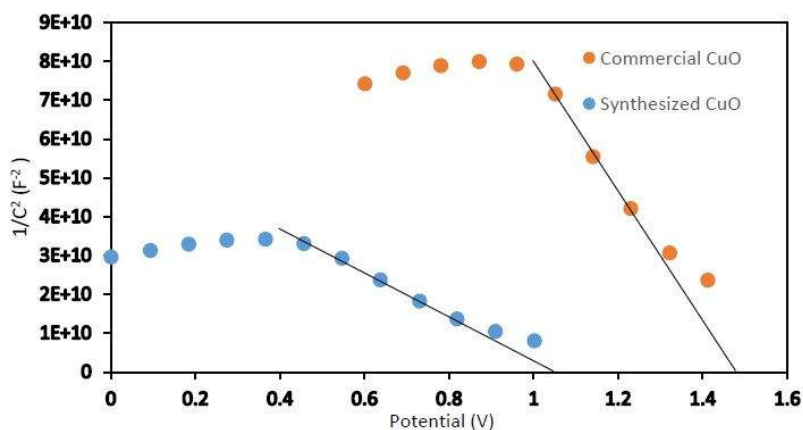


Figure 1 : Mott-Schottky plot of commercial CuO and synthesized CuO in 0.1M sodium acetate (pH = 6.84) at the frequency of 1000Hz.

### Impedance of the Films

Figure 2 (a) shows the electrochemical impedance spectroscopy (EIS) spectra for commercial CuO and synthesized CuO. Figure 2 (b) shows the equivalent circuit model for the both type of CuO. The series resistance and charge transfer

resistance of synthesized CuO is lower than those values of commercial CuO. As well as bulk capacitance of the synthesized CuO is lower than the commercial CuO. Table 2 shows the summary of the values obtained from equivalent circuits of the EIS measurements.

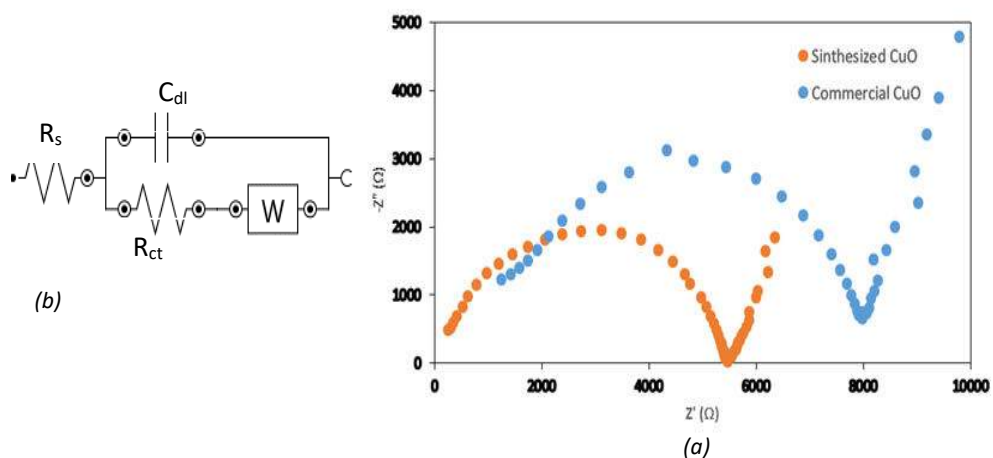


Figure2: (a) EIS spectra of commercial CuO and synthesized CuO in 0.1M sodium acetate (b) Equivalent circuit model

Table2: Simulated results of series resistance ( $R_s$ ), bulk capacitance ( $C_{bl}$ ), and charge transfer resistance ( $R_{ct}$ )

|                 | $R_s$ ( $\Omega$ ) | $R_{ct}$ ( $\Omega$ ) | $C_{bl}$ (F)           | $Y_0$ ( $\mu\text{Mho}\cdot\text{s}^{1/2}$ ) |
|-----------------|--------------------|-----------------------|------------------------|--|
| Commercial CuO  | 340                | 5440                  | $1.09 \times 10^{-9}$  | 14.2   |
| Synthesized CuO | 312                | 4830                  | $0.516 \times 10^{-9}$ | 598  |

## XRD Analysis

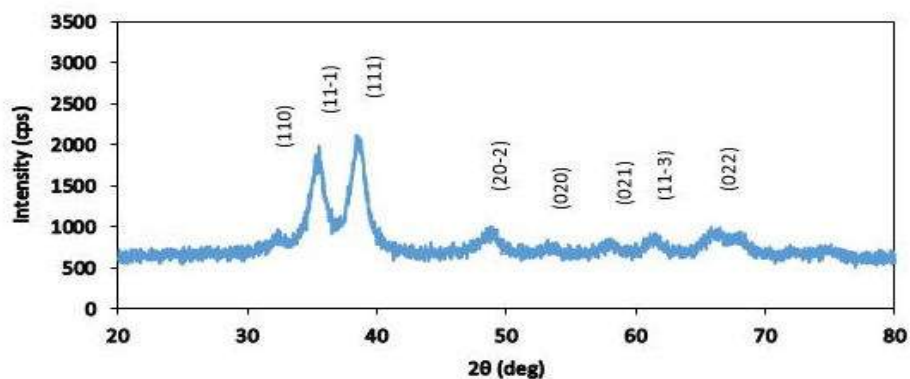


Figure 2: XRD-pattern of synthesized CuO nanoparticles

The XRD pattern of prepared CuO (figure 3) is well matched with the monoclinic phase of CuO nano particles and well consistent with Joint committee on Powder Diffraction Standards (JCPDS) card files No. 80-1916. No characteristics peaks of impurities were detected. The crystallite size was calculated by using Debye Scherrer equation.

$$D = \frac{0.9\lambda}{\beta \cos\theta} \quad (\text{Eq 2})$$

Where,

$\lambda$  = X-ray wave length

$\beta$  = line broadening at the maximum intensity in radians

$\theta$  = Bragg angle

From the calculations the average crystallite size of synthesized CuO nano particle is found to be around 5.7 nm.

## Conclusion

In this study a simple method was introduced for synthesis of nanocrystalline p-type CuO with average particle size of 5.7 nm. The flat band potential of the synthesized CuO was 1.04 V. The flat band potential of the valence band has shifted upwards or in other words become more negative because of the higher concentration of acceptors in the synthesized CuO. Some of the triethylamine used in the synthesis may

be still attached on the surface where N+ sites may be acting as acceptors. Hence it could be concluded from the impedance measurement, the series resistance of the film has decreased as a result of improvement in the conductivity.

## Acknowledgment

The authors are grateful for the financial support received from the competitive research grant (GRCS201801) of the Open University of Sri Lanka.

## References

- [1] Brabec C. J. and Durrant J. R. , Solution-processed organic solar cells, MRS Bulletin, 2008, 670:675-33,
- [2] Tang J. and Sargent E. H., Infrared colloidal quantum dots for photovoltaics: fundamentals and recent progress, Advanced Materials, 2011, 29:23-12,
- [3] Radhakrishnan, A.A. and Beena, B. B., Structural and Optical Absorption Analysis of CuO Nanoparticles, Indian Journal of Advances in Chemical Science, 2014, 158:161-2
- [4] Yang Y., Di Xu, Qingyong Wu and Diao P, Cu<sub>2</sub>O/CuO bilayered composite as High – Efficiency Photocathode for photochemical Hydrogen Evolution Reaction, Nature, 2016
- [5] Jiang T., Zhao Y., and Xue H, Boosting the performance of delafossite photocathode through constructing a CuFeO<sub>2</sub>/CuO heterojunction for photoelectrochemical water reduction, J Mater Sci 2019 ,11951:11958-54

# Torrefied Biomass Combustion in Biomass Powered Boilers: Process Simulation-Based Case Study Analysis of Power Generation and Thermal Energy Generation

U.M.A. Devaraja <sup>#1</sup>, S.D.S. Supunsala <sup>#2</sup>, S.W. Abeywardane <sup>#3</sup>, R.M.D.S. Gunarathne <sup>#4</sup>

*# Department of Chemical and Process Engineering, University of Moratuwa, Sri Lanka.*

<sup>1</sup> [udya1991madavi@gmail.com](mailto:udya1991madavi@gmail.com)

## Abstract

Torrefaction is a thermochemical pre-treatment carried out at 200-300 °C in an inert atmosphere. This can upgrade not only energy density, but also physicochemical properties of raw biomass. Therefore, raw biomass can be replaced by torrefied biomass for industrial thermal requirements and power generation purposes. This study is on the evaluation of the performance of torrefied biomass in 3.3 MW power plant and one of Industrial thermal energy generating system by using the Aspen Plus simulating model. Gliricidia and Rubber wood, most abundant woody biomass sources in Sri Lanka were torrefied at 300°C for 60 min under an inert atmosphere and used to replace raw biomass. It shows LKR 51,400.00 saving per day by reducing 14.6% of raw Gliricidia usage in thermal power plant whereas, LKR 32,700.00 saving per day by reducing 25.3 % of raw Rubber wood usage in the Industrial boiler.

**Keywords:** Torrefaction, Biomass, Aspen plus

## Introduction

Renewable and non-renewable energy sources are the main two categories used for power generation and thermal energy generation. Non-renewable energy sources will eventually run out while the renewable energy sources are re-produced. The main source of non-renewable energy that will eventually run out is fossil fuels. Fossil fuels are the major source of energy for a vast amount of industries, though environmental pollution, global warming, emission of greenhouse gases, liberation of hazardous products such as arsenic, mercury, particulate matter, SO<sub>x</sub> and NO<sub>x</sub>, public health issues and non-renewable nature are the negative impacts related to the above mentioned energy sources. Therefore, alternative energy sources which are renewable, sustainable and cost effective are essentially should be considered as a solution for the prevailing energy scarcity. Moreover, energy sources that are environmentally sustainable and that prevent health risks are more favored. Biomass is one of such alternatives, renewable energy sources which can be converted to solid, liquid and gaseous fuels. Energy from biomass is commonly used throughout the world. It is a sustainable feedstock and supports the reduction of greenhouse gas emission and low impact on climate. But due to their hydrophilic nature, high moisture and low density, it is difficult to gain high energy output in its original form. Therefore, raw biomass needs proper treatment when it is used as an energy source in large scale applications.

Biomass pretreatments techniques can be classified as chemical, mechanical, thermal, hydrothermal and biological. Torrefaction is the latest thermal pretreatment technology, which can

upgrade the chemical and physical properties of raw biomass. It is carried out at moderate temperatures (200–300 °C) in an inert environment resulting a dark color solid product along with non-condensable gases and liquid products [1]. Solid products are represented typically 72- 60% of total output of Torre faction [2] and it consists of original and modified sugar structure, newly synthesized polymeric structure and ash [1][2]. Several researches have shown [3][4] advantages of torrefied biomass compared to raw biomass such as high heating value, high energy density, low hydrophilic nature, resistance to biological decay and better grindability [5].

The torrefied biomass can be used for co-firing in coal power plants and it may not only improve energy security and reduce emissions, but also economically favorable if properly implemented with good torrefied biomass supply chain. Industries with biomass boilers, furnaces, etc. can also be benefited by using torrefied biomass due to improved combustion process and reduction of the logistic cost. Any type of biomass can be considered for Torre faction including woody biomass, forestry by-products, agricultural biomass and even municipal solid wastes.

The largest share of Sri Lankan industrial energy requirement which is 68% is fulfilled by biomass [7] which is nearly 4,573,000 MT per year [8]. Agricultural residue, municipal and industrial waste and fuelwood are the most common forms of biomass [8] and among them, the highest share of biomass energy sources comes from fuelwood. It is nearly 63.4% of total biomass consumption [8]. Rubber wood and Gliricidia are commonly used woody biomass in Sri

Lanka, and the government has introduced, *Gliricidia* as the fourth plantation crop of the county due to their multi-functional ability as energy crop and supporting crop [6]. Rubberwood is abundantly available as an agricultural residue. On the other hand, uprooted rubber trees could be utilized for fuel purpose after their latex yielding period of around 25 years. According to the statistics, presently there are 133668 ha of rubber plantations available in Sri Lanka [10].

Although these two types of wood are most abundantly available in Sri Lanka, studies on the Torrefaction performance of those is still lacking. Therefore, these two types of biomass were considered in this study. The effect of using torrefied biomass over the non-torrefied biomass for power generation and thermal energy generation are discussed considering two local scenarios.

## Methodology

### Experimental

#### Torrefaction process

In this study, both Rubber and *Gliricidia* wood were torrefied at 300 °C, atmospheric pressure under inert environment for 60 min. A horizontal stainless-steel cylindrical reactor was used and it consists nickel-chrome coil which covered by porcelain insulation. The temperature controlling system and inert gas feeding system were maintained required temperature and inert gas flow rate. For proper thermal insulation, the K-wool was used in surrounding the inner tube.

#### Fuel analysis

First, the thermogravimetric analysis (TGA) was performed for raw *Gliricidia*

and Rubber wood from room temperature to 800°C in inert media, to identify the thermal decomposition behavior of two types of biomass. Further, proximate and ultimate analysis were conducted to get a better understanding of thermal properties of both untreated and treated rubber and *gliricidia* samples. C, H and N content of biomass was determined using solid Perkin Elmer 2400 Series II CHNS analyzer taking the balance as the O content. The moisture, volatile matter and ash content were determined by using ASTM E871, E872 and E830 standard test methods respectively taking the balance as the fixed carbon content.

The calorific value was determined by empirical equations

$$HHV = 34.91Y_C + 117.83 Y_H - 1.51Y_N - 10.34 Y_O \quad (\text{Eq 1})$$

$$LHV = HHV - h_v \times (Y_H + H_2O) \quad (\text{Eq 2})$$

Where,

HHV = Higher heating value

LHV = Lower heating value

$Y_C$  = mass fraction of C

$Y_H$  = mass fraction of H

$Y_N$  = mass fraction of N

$h_v$  = Latent heat of water

The solid yield of torrefied product calculated as below.

$$\eta_m = \left( \frac{m_{treated}}{m_{raw}} \right) \times 100 \quad (\text{Eq 3})$$

Where,

$\eta_m$  = mass yield

$m_{treated}$  = mass of torrefied product

$m_{raw}$  = dry mass of untreated product

Process description and modeling

3.3 MW power generation plant and 12.5 MW capacity thermal energy generation boiler selected for this study to evaluate the performance of torrefied biomass using Aspen simulation software.

### Power plant

#### Process description

Vidul Biomass (Pvt) Limited, a subsidiary of Vidullanka PLC has implemented the Dehiattakandiya Dendro Power Project to supply power to the National Electricity Grid with installed capacity of 3.3 MW. The Power Plant is expected to generate approximately 24 million kWh annually. The biomass fuel source is mainly sustainable grown *Gliricidia*, a fast-growing tree available in abundance in the dry zones.

The grown fuel wood, notably *Gliricidia*, a fast-growing tree legume, which is available in abundance in the country's dry zones expressly in Mahaweli System areas. The fuel-wood is obtained from plantations of *Gliricidia* and from farmers in the region who grow these trees as their out-grower's agricultural programs [10].

#### Process model

First, biomass (*Gliricidia*) is defined as a non-conventional solid and the ultimate and proximate analysis were used to define the composition. The fraction of

Table 1: Dehiattakandiya Dendro Power plant

|                           |   |
|---------------------------|---|
| <b>Installed capacity</b> | <b>3.3 MW</b>                               |
| <b>Location</b>           | Dehiattakandiya, Eastern Province           |
| <b>Fuel type</b>          | <i>Gliricidia</i> , Ipil Ipil, Coconut Husk |
| <b>Configuration</b>      | One Steam Boiler and One Turbo Generator    |
| <b>Steam Parameter</b>    | 46 bar(g) and 440 OC                        |
| <b>Annual Generation</b>  | 24 GWh                                      |

N,+S and other trace elements were neglected in the model. To breakdown the biomass to its elemental components RYield reactor is used. Then it is linked to a RGibbs reactor. Ryield and Rgibbs together represent the combustion chamber. The flue gas emitting from the RGibbs is connected to a cooler in order to depict heat loss from the furnace walls. The outlet of the cooler is connected to three countercurrent heat exchangers in order to depict the boiler. The three heat exchangers serve as one for producing saturated water at given pressure, another for producing saturated steam from saturated water and the other for producing superheated steam from saturated steam. The cycle, which connects the heat exchangers is linked with a turbine for power generation and turbine exhaust is passed through a condenser and a pump back to the boiler. The simulation was carried out based on the operational data provided by the power plant. The biomass flow rate to the Ryield reactor is then fixed at 4200 kg/h

in ash free basis. Since actual air supply is such that 3% oxygen in the flue gas, the design specification feature in Aspen Plus was used to estimate the air flow rate required, by setting the oxygen volume fraction in the flue gas as the target value. Further, the same feature was used to estimate the % boiler wall and other losses (sum of all the losses except flue gas loss), by setting the flue gas temperature as the target value. The turbine inlet and outlet steam conditions were set at 47 bar and 0.9 bar respectively, whereas the isentropic efficiency is 88%. The power output of the turbine is the target simulation result which was compared with the design data of the system for the model validation. For the case with torrefied biomass combustion, the required torrefied

biomass flow rate was estimated for the same power output of the turbine and same flue gas temperature at the exit. Here, the % boiler wall and other losses (sum of all the losses except flue gas loss) was assumed to be similar to the raw biomass case. The design specification feature in Aspen Plus was used to estimate the air flow rate required, by setting the oxygen volume fraction of 3% in the flue gas as the target value. The torrefied biomass flow rate is the target simulation result which was then used to calculate the raw biomass requirement based on the composition and mass yield data of the Torrefaction experiments. The calculation of the cost saving is based on the expected biomass saving.

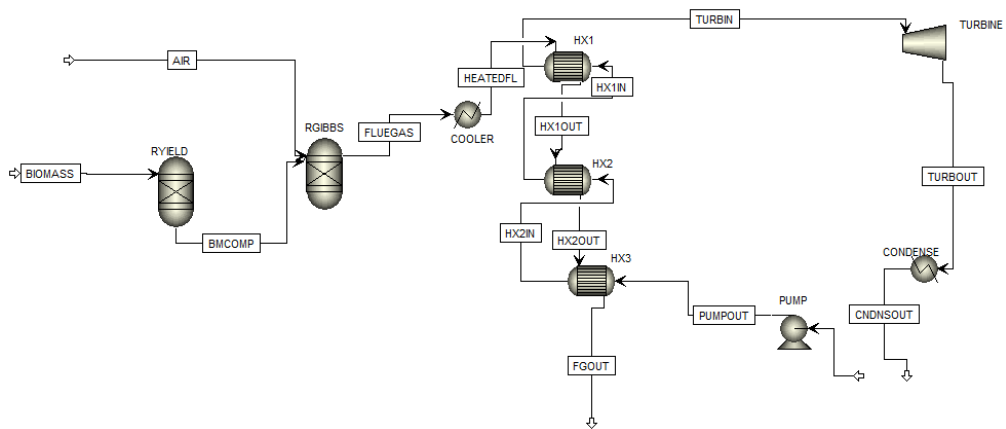


Figure 1: Aspen plus flow sheet for Gliricidia combustion and power generation



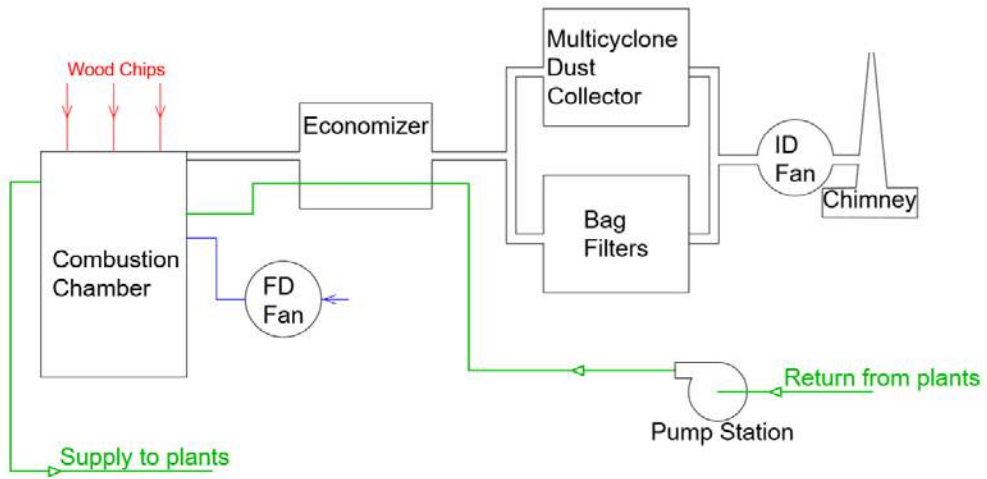


Figure 2: The schematic flow of flue gas and high-pressure hot water heater

### Thermal plant

#### Process description

In a multinational glove manufacturing company in Sri Lanka, high pressure hot water is to be made for the in-plant purposes which is mainly for heat exchangers. In the circulation scenario, the pressure of hot water is 12 bar at a

temperature of 180 °C which is in the compressed liquid state.

#### Process model

The process model was developed in a similar manner to the power plant. Here, the outlet of the cooler is connected to a single heat exchanger in order to represent the hot water boiler.

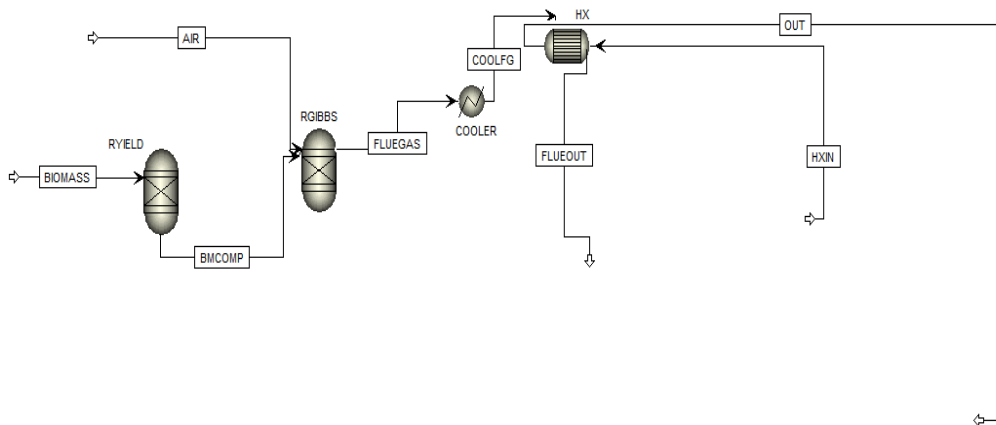


Figure 3: The schematic flow of flue gas and high-pressure hot water heater

The simulation was carried out based on the operational data provided by the thermal plant. The biomass flow rate to the Ryield reactor is then fixed at 5400 kg/h in ash free basis. Since the operating air/fuel mass ratio is 6, the air flow rate was determined accordingly. Further, the design specification feature in Aspen Plus was used to estimate the % boiler wall and other losses (sum of all the losses except flue gas loss), by setting the flue gas temperature as the target value. The hot water inlet condition was set at 12 bar and 155 °C. The hot water outlet temperature is the target simulation result which was compared with the design data of the system for the model validation.

For the case with torrefied biomass combustion, the required torrefied biomass flow rate was estimated for the same hot water outlet temperature and same flue gas temperature at the exit. Here, the % boiler wall and other losses

(sum of all the losses except flue gas loss) was assumed to be similar to the raw biomass case. The design specification feature in Aspen Plus was used to estimate the air flow rate required, by setting the oxygen volume fraction in the flue gas similar to the raw biomass case. Here also, the torrefied biomass flow rate is the target simulation result which was then used to calculate the raw biomass requirement and the cost saving similar to the power plant case.

## Results and discussions

### Fuel analysis

Thermogravimetric analysis of *Gliricidia* and Rubber are shown in Figure 4 and 5 respectively, and they present the mass loss (TG) and derivative mass loss (DTG) curves for thermal decomposition of both fuels.

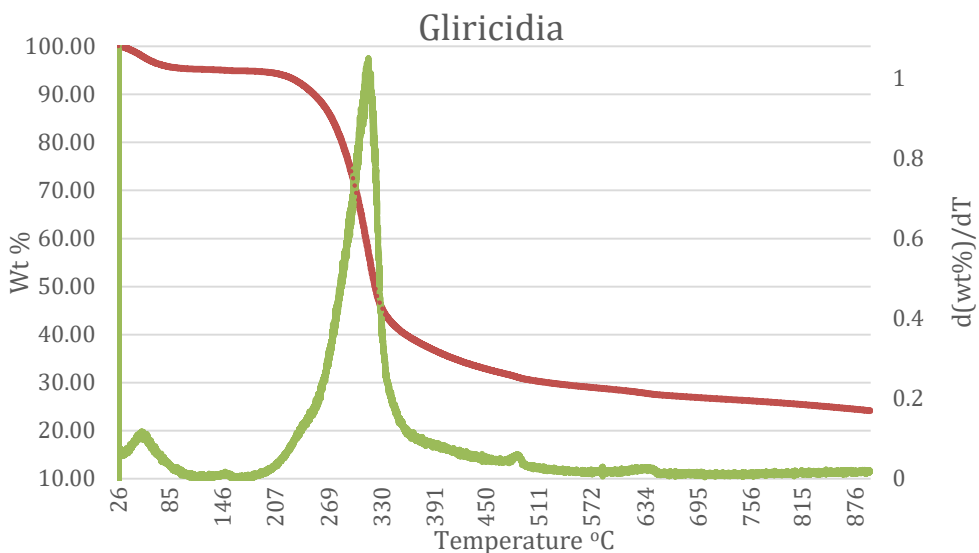


Figure 4: TGA curve of *Gliricidia* wood

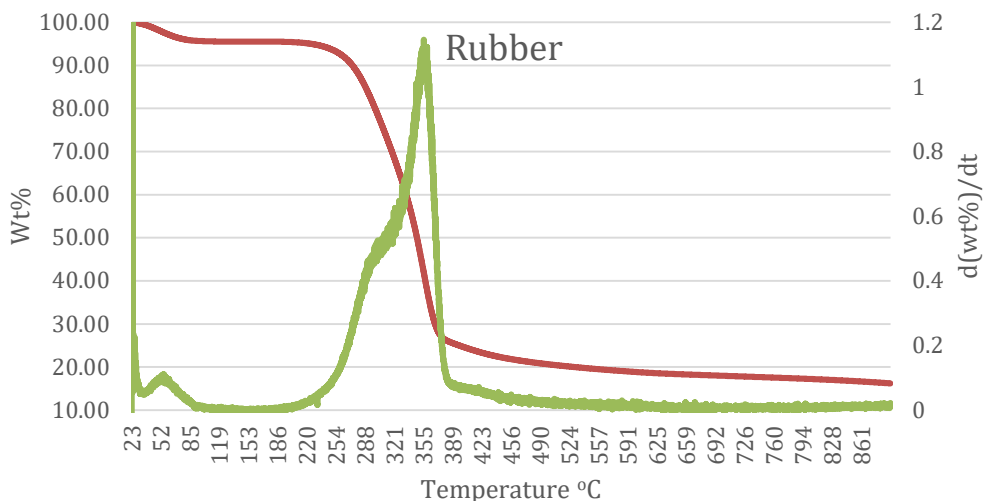


Figure 5: TGA curve of Rubber wood

Gliricidia shows a single asymmetric peak, revealing the overlapping hemicellulose and cellulose decomposition, whereas the Rubberwood shows a shoulder, followed by a distinct peak due to less overlapping nature of the hemicellulose and cellulose decomposition. Up to 250°C, only 10% mass loss exhibits in Gliricidia whereas rubber wood shows a similar mass loss at 275°C. This is mainly due to the evaporation of moisture and the decomposition of a fraction of hemicellulose [11]. A significant mass loss was observed within 250 °C - 330 °C and it corresponds to a reduction of approximately 70% of the total mass of Gliricidia. Rubber shows nearly 80% mass loss at 275 - 380 °C temperature range. Cellulose decomposition is happening in

these ranges [11]. According to these results, rubber wood is more thermally stable than Gliricidia. At 300 °C, which is the reported maximum operating temperature of Torre faction, 28% of Gliricidia and 22% of rubber wood has decomposed.

In the lab scale Torre faction reactor operated at 300 °C and 60 minutes residence time, 7% mass loss was observed for Gliricidia and 12% mass loss in the case of Rubber wood. The lower mass loss observed in the lab scale reactor compared to TGA study at the same temperature is due to heat and mass transfer limitations of the lab scale reactor.

Ultimate analysis results of both torrefied and non torrefied product are shown in Table 2.

Table 2 : Ultimate analysis

| Wood type                   | Ultimate analysis (wt% dry basis) |     |      |     | Lower heating value (MJ/kg) |
|-----------------------------|-----------------------------------|-----|------|-----|-----------------------------|
|                             | C                                 | H   | O    | N   |                             |
| <b>Gliricidia</b>           | 42.1                              | 6.7 | 50.4 | 0.8 | 15.01                       |
| <b>Torrefied Gliricidia</b> | 45.6                              | 6.3 | 47.4 | 0.7 | 16.91                       |
| <b>Rubber</b>               | 44.1                              | 6.7 | 48.9 | 0.3 | 15.89                       |
| <b>Torrefied Rubber</b>     | 47.6                              | 6.2 | 45.9 | 0.3 | 17.76                       |

During the Torrefaction process, oxygen and hydrogen components are partially removed due to hemicellulose decomposition and the resulting solid

product has lower O/C and H/C ratios and higher heating value. Variation of H/C and O/C ratios are represented in van-Kreylen diagram (Figure 6).

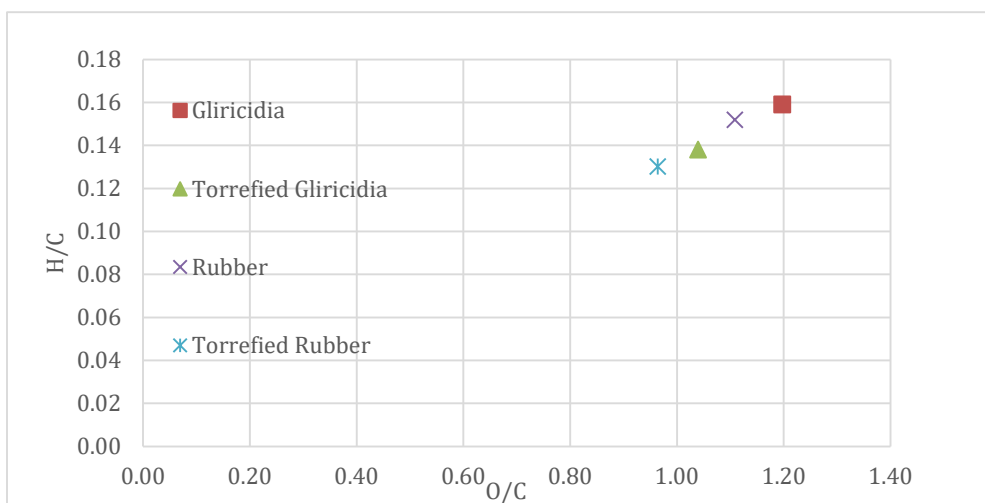


Figure 6: Van-Kreylen diagram

Table 3: Actual data vs simulation results

|                             | Power Plant |                   | Thermal Plant |                   |
|-----------------------------|-------------|-------------------|---------------|-------------------|
|                             | Design data | Simulated results | Design data   | Simulated results |
| Power output                | 3.3 MW      | 3.0 MW            | 12.5 MW       | 11.6 MW           |
| Flue gas outlet temperature | 180 -190 °C | 194 °C            | 300-320 °C    | 322°C             |

**Model validation**

Both models were first simulated for existing parameters and results obtained from simulation are shown in Table 3. The simulation results show excellent agreement with the design data of both plants.

**Expected saving**

The comparison of simulation results of the torrefied and non torrefied biomass are presented in Table 4

Table 4: Simulation results of raw and torrefied biomass

|                                    | Power Plant          |                      | Boiler           |                  |
|------------------------------------|----------------------|----------------------|------------------|------------------|
|                                    | Untreated Gliricidia | Torrefied Gliricidia | Untreated Rubber | Torrefied Rubber |
| <b>Inlet raw fuel flow rate</b>    | 4200 kg/hr           | 3588 kg/hr           | 5400 kg/hr       | 4334 kg/hr       |
| <b>Flue gas outlet temperature</b> | 194 °C               | 196 °C               | 322 °C           | 324 °C           |

In the power plant, by maintaining output power generation as a constant parameter for both torrefied and non torrefied cases, required inlet torrefied fuel flow rate was obtained using the Aspen Plus simulation model. It shows that 14.6% of biomass consumption can be reduced and it gives LKR 51,400.00 saving per day. Also, the flue gas temperature was maintained at approximately 190°C in both cases.

In the thermal plant, 12 bar hot water at 180 °C is produced with a boiler capacity of 12.5 MW using rubberwood as the energy source. The flue gas temperature is maintained at a constant value and the fuel flow rate for both torrefied and non torrefied cases were studied. From the results obtained it can be seen that the overall efficiency increased by 25.7% for torrefied biomass over non torrefied biomass and also, LKR 37,700.00 can be saved by saving approximately 1366 kg of rubberwood which is 25.3% by mass.

## Conclusion

The two separate case studies were carried out to evaluate the performance of torrefied biomass over raw biomass considering two local scenarios. Gliricidia and rubberwood are the biomass types considered in this modeling study. According to the results obtained from the Aspen plus simulation, it can be seen that the efficiency has increased in both cases and 612 kg of Gliricidia is saved in the power plant analysis while 1366 kg of rubber wood is saved in the thermal plant analysis. Also, it can be seen that the flue gas temperatures of both cases are approximately around 200 °C - 300 °C, thereby the emitted flue gas can be used as an energy source to produce torrefied biomass within itself. Thereby an extra cost to produce torrefied biomass can be eliminated. Therefore, by considering these favorable factors, it can be shown that the use of torrefied biomass for power and thermal energy generation is economical, efficient and sustainable.

## Acknowledgement

The authors would like to acknowledge the Senate Research Council of University of Moratuwa, Sri Lanka for the financial support under the grant number SRC/LT/2019/08. The support given by Vidullanka PLC and the Glove manufacturing company providing required data is highly appreciated.

## References

- [1] D. Nhuchhen, P. Basu, and B. Acharya, "A Comprehensive Review on Biomass Torrefaction," *Int. J. Renew. Energy Biofuels*, vol. 2014, pp. 1–56, 2014.
- [2] Y.-H. Chen et al., "The By-products and Emissions from Manufacturing Torrefied Solid Fuel Using Waste Bamboo Chopsticks," *Environments*, vol. 4, no. 2, p. 36, 2017.
- [3] D. Nhuchhen, P. Basu, and B. Acharya, "A Comprehensive Review on Biomass Torrefaction," *Int. J. Renew. Energy Biofuels*, vol. 2014, pp. 1–56, 2014.
- [4] L. J. R. Nunes, J. C. De Oliveira Matias, and J. P. Da Silva Catalão, "Torrefaction Technologies," *Torrefaction Biomass Energy Appl.*, pp. 161–172, 2018.
- [5] J. Meligu, C. Ribeiro, R. Godina, L. Jorge, and R. Nunes, "Future Perspectives of Biomass Torrefaction : Review of the Current State-Of-The-Art and Research Development," pp. 1–17.
- [6] IEA, "Energy Balance 2016," *Energy Balanc.*, pp. 14–18, 2016.
- [7] "MULTIMEDIA CENTER – BIOMASS ENERGY 2022 – "FUELING THE ECONOMY-PROTECTING FOREST"", *Biomassenergy.lk*, 2019. [Online]. Available: <http://www.biomassenergy.lk/multimedia-center/>. [Accessed: 05- Nov-2019]
- [8] A. Abeygunawardana, "GLIRICIDIA-Fourth Plantation Crop of Sri Lanka," pp. 1–2, 2005
- [9] P. Perera, "Forest Certification," no. May, 2014
- [10] "Biomass – Vidullanka PLC", *Vidullanka.com*, 2019. [Online]. Available: <https://www.vidullanka.com/power-projects/biomass/>. [Accessed: 03-Nov-2019]
- [11] A. E. Eseyin, P. H. Steele, C. U. Pittman, K. I. Ekpenyong, and B. Soni, "TGA Torrefaction Kinetics of Cedar Wood," *J. Biofuels*, vol. 7, no. 1, p. 20, 2016.

# Investigation of the Suitability of on-site Cogeneration Power Plants for Sri Lankan Upcountry Hotels

N. G. Tennakoon<sup>#1</sup>, M. A. Wijewardane<sup>#2</sup>

## Abstract

Tourism industry in post-war Sri Lanka has experienced a remarkable boom, while driving local and international investors to construct new hotel facilities around the island. As a result, the electricity demand of the country has significantly increased. However, the hotels need electricity, heating as well as cooling simultaneously and the amount of those three forms vary due to different factors, i.e. size of the hotel, star category, location of the hotel. In general, heating requirement of the upcountry hotels is much higher than a low country hotel. Majority of the hotels fulfil their electricity requirements from the national grid and separate boilers are used to meet the heating requirements. Although, almost all the hotels own a stand-by generator to supply electricity whenever needed, none of them uses on-site advanced efficient technologies i.e. cogeneration or tri-generation to provide either electricity and heating or electricity, heating and cooling respectively. This study mainly focuses on analysing the economic benefits and the reduction of carbon footprints by implementing on-site cogeneration power plants in up-country hotels. Calculations were performed for fulfilling the maximum electricity demand and the maximum heat demand separately, from the cogeneration power plant. Results show that, whichever the cogeneration plant configuration, energy cost reduction can be expected for hotels, those have 50-150 room space. Moreover, the Carbon footprint also reduces significantly. When examine the energy demand of the upcountry hotels, pattern of both electrical and heat energy demand is ideal for accompanying a cogeneration plant. However, heat demand has some sudden increments, and hence, it is advised to propose a thermal storage in addition to the cogeneration system to cater for the additional heat demand requirement without any interruption.

**Keywords:** Waste heat recovery, recovery boilers, hotel industry, co-generation, energy management

## Introduction

Currently, the tourism industry is the third largest foreign income earner of Sri Lanka. Its contribution for the Sri Lankan economy is significant and continuously growing, while contributing to more than 11% of the gross Domestic Products (GDP) in 2014 [1]. Since the recent past, in post-war Sri Lanka, the tourism industry has experienced a remarkable boom while driving local and international investors to construct new hotel facilities island-wide. As a result, the electricity demand of the country has significantly increased and currently, it is growing at a rate of 6% per annum [2]. In year 2011, the hotel industry consumed 196 GWh of electricity sold by Ceylon Electricity Board (CEB) and Lanka Electricity Company (LECO) [3], whereas in year 2017 the electricity consumption increased to 292 GWh, 2% of the total electrify consumption of the country [2].

According to Sri Lanka's electricity generation statistics, there is no more potential left to use hydro-power as it is almost producing the full predicted capacity. More than 75% total electricity requirement of the country is fulfilled using fossil fuels; coal and oil [4]. As a result, the electricity prices of the country are highly fluctuating depending on the fossil fuel prices in the world market. This could significantly affect domestic tariff system as well as commercial tariff system of the country i.e. office buildings and hotels. As the tourism industry significantly contributes to the country's GDP, this study mainly focuses on investigation and viability of an energy saving strategy to reduce the energy costs of the hotel sector.

A hotel requires electricity (for lighting and all other ancillary work), heat (for hot

water, laundry, etc.) and cooling. Use of energy efficient equipment and implementation of energy efficient technologies can be identified as the main cost reduction actions. In Sri Lanka, majority of the hotels are provided with grid electricity which can be considered as a reliable electricity supply. However, each hotel has a stand-by electricity generator to cater to the full electrical demand in a sudden power interruption. Moreover, majority of the hotels facilities have hot water boilers and rest have heat pumps, hot water heaters to provide the hot water requirement. On contrary, the countries associated with poor grid power supply i.e. Maldives, use only onsite generators to obtain the required electricity demand [Aarah Resort at Raa Atto]. In Bangladesh they have unreliable grid power, so they use LNG operated onsite power generators (Bangal Plastic Pvt. Ltd.).

There are three main electricity generation techniques. Power plants, cogeneration systems and tri-generation systems. Thermal efficiency of power plants varies from 30-40% whereas efficiencies of cogeneration and tri-generation systems vary from 65-80% and 80-90% respectively. Power plants are designed only to produce electricity, whereas cogeneration systems are designed to produce both electricity and heat and, tri-generation systems are designed to produce electricity, heating as well as cooling [5]. Majority of the developed countries use efficient cogeneration systems to fulfil the electricity and heat demands. However, in Sri Lanka, use of cogeneration systems is only limited to few industries and unfortunately, none of the hotels are facilitated with an onsite cogeneration power plant.



Hotels located in upcountry areas i.e. Hatton and Nuwaraeliya requires more heating than a similar capacity hotel situated in low country. On contrary, a hotel located in low country area requires more cooling than a similar capacity hotel situated in upcountry. This study mainly focuses on investigation of technical and economic viability of implementation of efficient power generation systems in hotels, which requires both electricity as well as heating. This paper will first present the data collected from few selected hotels located in up country on electricity, heating and cooling. Then will discuss the cogeneration theory and cogeneration modes that are currently available. Later, economic viability and environmental feasibility will be discussed based on the analytical calculations.

### Energy consumption of upcountry hotels in Sri Lanka

Primary data collection of the study is presented in this section. Five upcountry hotels (those experience average ambient temperatures of 15-20°C) were selected (Table 1) for the analysis and obtained the average electricity utilization, space heating consumption and hot water consumption from the respective maintenance departments. As shown in Table 2, further summarizes the monthly maximum electricity consumption and maximum heat consumption of each hotel.

Table 1: Information of Hotels

| Hotel                | Location    | No. of Rooms | Energy cost/month |
|----------------------|-------------|--------------|-------------------|
| Heritage Tea Factory | Kandapola   | 52           | 1,334,750         |
| Jetwing St. Andrews  | Nuwaraeliya | 56           | 1,720,040         |
| Earls Court Hotel    | Nuwaraeliya | 73           | 1,300,000         |
| Black Pool Hotel     | Nuwaraeliya | 65           | 1,150,000         |
| Grand Hotel          | Nuwaraeliya | 154          | 2,784,065         |

Table 2: Electricity, hot water and space heating consumption information

| Hotel                | Electricity (avg kWh/ month) | Hot water (avg CUM/ month) | Space heating capacity (TR) |
|----------------------|------------------------------|----------------------------|-----------------------------|
| Heritage Tea Factory | 52,883                       | 224,640                    | 36                          |
| Jetwing St. Andrews  | 66,790                       | 241,920                    | 56                          |
| Earls Court Hotel    | 57,115                       | 433,620                    | 64                          |
| Black Pool Hotel     | 45,000                       | 205,920                    | 41                          |
| Grand Hotel          | 105,619                      | 792,120                    | 56                          |

Based on the above utility consumption details, the utility consumption values were estimated as follows. Table 7 summarizes specimen calculation for proposed plant for the Grand Hotel.

## Cogeneration Principle

### Introduction

Cogeneration technology is very well understood and already in operation elsewhere in the world, although the Sri Lankan hotel industry has not used it. A normal power plant is designed to produce only electricity and rejects 30-70% of the energy will become waste heat. However, cogeneration plants can be designed to operate over 60-85% thermal efficiency by introducing different techniques to efficiently use this waste heat as shown in the Figure 1. In general, a cogeneration system is

implemented in a facility which requires both heat and electricity.

Thermal efficiencies of a standard power plant and a cogeneration power plant are shown in the Equation 1 and Equation 2 respectively.

$$\eta_{\text{thermal, powerplant}} = \frac{\text{Electricity generated}}{\text{Total heat input}} \quad \text{Eq.1}$$

$$\eta_{\text{thermal, cogen plant}} = \frac{\text{Electricity+Heat}}{\text{Total heat input}} \quad \text{Eq.2}$$

Consider a hotel facility which requires 25 units of electricity and 35 units of heat. Following analysis can be performed by considering electricity and power are produced either by a combination of standalone power plant and a separate hot water boiler or, using a cogeneration power plant.

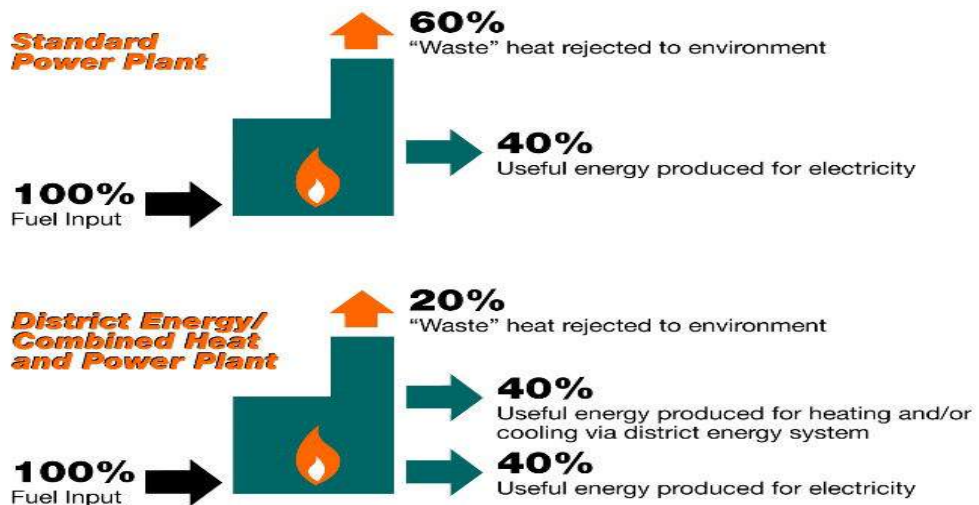


Figure 1: Energy breakdown of a standard power plant and a combined heat and power (CHP) plant [6]

Table 3: Comparison of the benefits of using standard power plant and a CHP power plant for a facility requires both electricity and heat

|                                  | <b>Total input power to produce<br/>25 units of electricity and 35<br/>units of heat</b> | <b>Waste</b>        |
|----------------------------------|--|---------------------|
| Power station (efficiency = 40%) | =25/0.40<br>=62.50   | =62.50-25<br>=22.50 |
| Boiler (efficiency = 85%)        | =35/0.85<br>=41.18   | =41.18-35<br>=6.18  |
| CHP Plant (efficiency = 85%)     | =(25+35)/80<br>=75.00  | =75.00-60<br>=15.00 |

Accordingly, the total waste when producing electricity and heat separately is 28.68 units and, when producing electricity and heat using a CHP is 15.00 units, implies use of cogeneration in hotels is efficient and cost effective.

There are many benefits of using on-site cogeneration power plants (CHP) in a facility. As the CHPs have greater thermal efficiencies, the emission of greenhouse gases (GHGs) is significantly reduced. Moreover, the burden on utility networks and transmission line losses are significantly reduced. Cogeneration plants can be designed to operate on solar energy as the primary energy source (i.e. concentrating solar power plant) instead of fossil fuels.

### Operation modes of cogeneration power plants

A cogeneration power plant can be designed to cater to either base electricity load or, base thermal load or, full electricity load or full thermal load. Table 4 differentiates and discusses the 4 different techniques in-detail. When choosing a co-generation solution for a site, several other important parameters should also be taken into account [7, 8 and 9].

- Heat-to-power ratio: Varies depending on the industry. Measures in terms of kWth/kWe. For example food industry – 1.2, pharmaceuticals – 2.0 and breweries – 3.1

Table 4: Cogeneration operation modes

|                                      | <b>Description</b>   |   |
|--------------------------------------|--|---|
|                                      | <b>Electricity</b>   | <b>Heat</b>   |
| <b>Base electrical load matching</b> | <ul style="list-style-type: none"> <li>• Meets the base electrical load</li> <li>• Electricity purchase from grid during peak demand time</li> </ul> | <ul style="list-style-type: none"> <li>• Meets by the cogeneration system</li> <li>• If lower than the peak demand, meet the difference by an auxiliary boiler</li> <li>• Excess, sell to the others or discards</li> </ul> |
| <b>Base thermal load matching</b>    | Meets by the cogeneration system   | <ul style="list-style-type: none"> <li>• Meets the base thermal load</li> <li>• Peak demand will be met by an auxiliary boiler</li> </ul>   |

---

|                                 |  |   |
|---------------------------------|--|---|
| <b>Electrical load matching</b> | <ul style="list-style-type: none"> <li>• If lower than the peak demand, purchase from national grid</li> <li>• Excess, sell to the national grid</li> <li>• Maximum capacity is met by the cogeneration system</li> <li>• Electricity does not purchase from the national grid instead sell the excess during off-peak time</li> </ul> | <p>Meets by the cogeneration system</p> <ul style="list-style-type: none"> <li>• If lower than the peak demand, meet the difference by an auxiliary boiler</li> <li>• Excess, sell to the others or discards</li> </ul> |
| <b>Thermal load matching</b>    | <p>Meets by the cogeneration system</p> <ul style="list-style-type: none"> <li>• If lower than the peak demand, purchase from national grid</li> <li>• Excess, sell to the national grid</li> </ul>  | <ul style="list-style-type: none"> <li>• Maximum capacity is met by the cogeneration system</li> <li>• Excess during the off-peak sell to the others or discard</li> </ul>  |

---

- Quality of thermal energy: Required pressure and temperature of thermal energy. For an example, sugar industry requires 120°C whereas, cement industry requires 1,450°C.
- Load patterns: The heat and power demand patterns are very important when deciding the type and size.
- Availability of the fuel
- System reliability
- Grid dependent vs. independent
- Retrofit vs. new installation
- Electricity buy-back
- Local environmental regulation

Different cogeneration systems can be identified with some already identified technical parameters as shown in Table 4.

As explained above and following the design criteria, an efficient cogeneration system can be designed to obtain electricity and heat simultaneously. However, few drawbacks can be identified in cogeneration systems and are, system complexity, higher initial investment regardless to the convincing payback periods, operation and maintenance cost. However, considering the fuel saving and the significantly minimized GHG emissions convincing the installation of these systems in hotel industry. The next section is dedicated to present and discuss the propose cogeneration techniques for the selected upcountry hotels in Sri Lanka.

## Cogeneration systems for Sri Lankan up-country hotels

### Selected cogeneration configurations

Figure 2 illustrate the selected cogeneration configurations for this analysis. Electricity of the power plant is expected to generate from a diesel generator equipped with diesel fired reciprocating engine considering the heat to power ratio of the selected hotels in Section 2. The System is designed to cater to the electrical demand so that the generated heat can be stored in a hot

water vessel throughout the day. By having thermal storages the system has an ability to cater to the peak heat demand at any peak without deficient to obtain from a separate hot water generator.

There are two common methods by which the waste heat can be recovered to obtain the required heat demand when using a diesel generator and are low temperature water (around 60°C) that is obtained from jacket cooling water and, tap the flue gas with waste heat recovery boiler (WHRB) at the exhaust system to obtain the high temperature water (around 80°C).

Table 5: Technical parameters of different cogeneration techniques

| CHP system                          | Heat to power ratio (kW <sub>th</sub> /kW <sub>e</sub> ) | Power output (%of fuel input) | Overall efficiency |
|-------------------------------------|--|-------------------------------|--------------------|
| Back-pressure steam turbine         | 4.0-14.3   | 14-28                         | 84-92              |
| Extraction-condensing steam turbine | 2.0-10.0   | 22-40                         | 60-80              |
| Gas turbine                         | 1.3-2.0  | 24-35                         | 70-85              |
| Combined cycle                      | 1.0-1.7  | 34-40                         | 69-83              |
| Reciprocating engine                | 1.1-2.5  | 33-53                         | 75-85              |

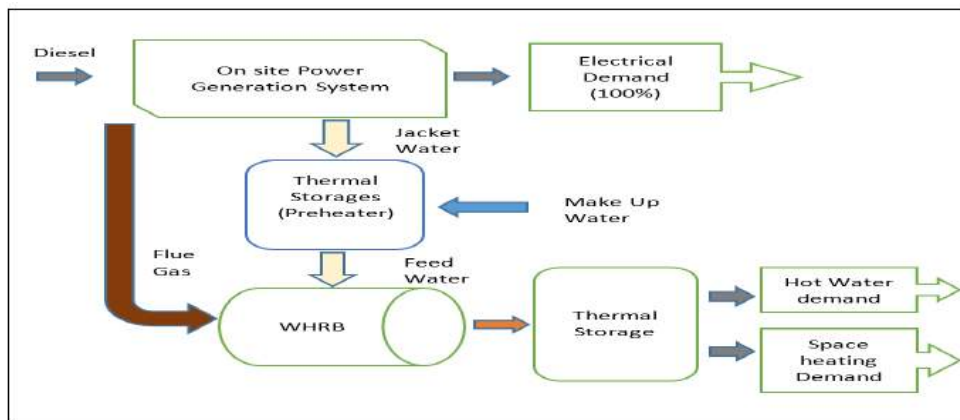


Figure 2: Proposed Plant Architecture

## Calculations

To perform the calculations following assumptions were made. Electrical efficiency of the generator – 98%, Efficiency of the waste heat recovery boiler – 95%, Make-up water temperature – 14°C, Pressure drops were

neglected, Boiler feedwater temperature – 70°C.

Calculation results shown in the Table 6 shows energy data of the Grand Hotel Nuwaraeliya considering the existing power supply configuration against the proposed cogeneration configuration.

Table 6: Available data – The Grand Hotel

| Category                               | Description                      | Quantity               | Units     |
|--|----------------------------------|------------------------|-----------|
|  | Name                             | Grand Hotel            |           |
| <b>General</b>                         | Official category                | 4                      | Star      |
|  | Location                         | Nuwara Eliya City      |           |
|  | Ambient temperature              | 14                     | C (deg)   |
|  | Ambient RH (Relative humidity)   | 68                     |           |
|  | Availability of grid power       | yes                    | Yes/No    |
| <b>Occupancy</b>                       | Average occupancy                | 78                     | %         |
|  | No of staff in day time          | 221                    | No's      |
|  | No of staff in night time        | 40                     | No's      |
|  | No of Beds                       | 154                    | No's      |
| <b>Hotel facilities &amp; Services</b> | SPA (Treatment Beds)             | 1                      | No's      |
|  | Laundry                          | 120                    | kg/Day    |
|  | Staff accommodation              | 185                    | Beds      |
|  | Pool area                        | 300                    | Sqm       |
| <b>Electrical</b>                      | Power Demand                     | 105,619                | kWh       |
|  | Transformer capacity             | 630                    | kVA       |
|  | Generator capacity               | 550                    | kVA       |
|  | Electricity bill                 | 1,819,036              | LKR/Month |
|  | Solar PV capacity                | 0                      | kw/day    |
|  | Diesel consumption for generator | 2550                   | l/month   |
|  | Average Power cut                | 3                      | Hr./Month |
|  | Diesel Cost for generator        | 162,428.00             | LKR/Month |
| <b>Space Conditioning</b>              | Conditioned area                 | Rooms, Restuarent, Spa |           |
|  | Cooling                          | N                      | Y/N       |
|  | Heating System                   | Y                      | Y/N       |

|                  |                                  |                  |            |
|------------------|----------------------------------|------------------|------------|
|                  | Cooling/Heating System           | 56               | TR         |
|                  | Capacity                         |                  |            |
|                  | Demand                           | 22800            | Cum/day    |
|                  | supply temperature               | 55               | C (Deg)    |
|                  | storage                          | 10,000           | Cum        |
|                  | heating equipment                | Hot water Boiler |            |
| <b>Hot water</b> | Boiler fuel type                 | diesel           |            |
|                  | Boiler Diesel demand             | 7870             | l/month    |
|                  | Heat Recovery option             | N                | Y/N        |
|                  | Diesel Cost for Hot water boiler | 802,601.00       | LKR/Month  |
|                  | Demand                           | 1.5              | Ton/Hr.    |
|                  | Boiler capacity                  | 1.5              | Ton/Hr.    |
|                  | Boiler fuel type                 | diesel           |            |
| <b>Steam</b>     | Boiler Diesel demand             | 7,480            | l/month    |
|                  | Heat Recovery option             | N                | Y/N        |
|                  | Diesel Cost for Hot water boiler | 762,925.00       | LKR/ Month |

*Table 7: Energy calculation based on existing system – The Grand Hotel*

|  |                     |                  |
|--|---------------------|------------------|
| <b>Electricity bill from National Grid</b> | <b>1,819,036.00</b> | <b>LKR/Month</b> |
| <b>Diesel Cost for backup generator</b>    | 162,428.00          | LKR/Month        |
| <b>Diesel cost for Hot water boiler</b>    | 802,601.00          | LKR/Month        |
| <b>Total Cost for conventional System</b>  | <b>2,784,065.00</b> | <b>LKR/Month</b> |

Table 8: Energy calculation for proposed– The Grand Hotel

| <b>Electrical Demand</b>                       | <b>105,619</b> | <b>kWh</b> |
|--|----------------|------------|
| <b>Predicted Electrical demand for heating</b> |                |            |
| Heater capacity for each room                  | 1.20           | kW         |
| Operating hours                                | 8              | Hrs./Day   |
| Average Operating room                         | 123            | No's/Day   |
| Average Operating room nights                  | 28             | Days       |
| Electrical Demand for heating                  | 33,062         | kWh        |
| Predicted Electrical demand without heating    | 72,557         | kWh/month  |
| <b>Diesel cost for generator</b>               |                |            |
| Average fuel consumption of generator          | 3.25           | l/kWh      |
| Predicted fuel consumption of generator        | 22,325         | l/month    |
| Unit Cost of Diesel                            | 103            | LKR/Liter  |
| Predicted fuel cost of generator               | 2,299,486      | LKR/month  |
| <b>Heat Generation of Generator</b>            |                |            |
| Average power generation per day               | 2,591          | kWh/day    |
| Predicted heat generation per day              | 3,110          | kWh/day    |
| <b>Heat Demand</b>                             |                |            |
| <b>Hot Water</b>                               |                |            |
| Hot water consumption per head per day         | 115            | l/day/head |
| Hot water demand per day                       | 28,290         | l/day      |
| Feed water temperature                         | 10             | C deg      |
| Hot water supply temperature                   | 55             | C deg      |
| Heat Demand per day                            | 1,485          | kWh        |
| <b>Space Heating</b>                           |                |            |
| Heater capacity for each room                  | 1.20           | kW         |
| Operating hours                                | 8              | hrs./Day   |
| Average Operating room                         | 123            | No's/Day   |
| Electrical Demand for heating                  | 1,181          | kWh        |
| <b>Total Heat Demand</b>                       | <b>2,666</b>   | <b>kWh</b> |

As shown above, it is well understood that the hotel situated in upcountry requires a substantial amount of heating

And the electricity to heat ratio is around 1.02. Currently the heating requirement is fulfilled using additional hot water boilers operated on fuel oil (Diesel).



Table 9: Carbon Footprint calculation for – The Grand Hotel

| Conventional System  |           |           |
|--|-----------|-----------|
| <b>Electrical Consumption for month</b>                                | 105,619   | kWh/month |
| <b>Electrical Consumption for year</b>                                 | 1,267,428 | kWh/Year  |
| <b>Carbon foot print for electrical consumption from national grid</b> | 899.87    | Ton/Year  |
| <b>Diesel consumption for month</b>                                    | 9,471     | l/month   |
| <b>Diesel consumption for year</b>                                     | 113,652   | l/year    |
| <b>Carbon foot print for diesel consumption</b>                        | 311.41    | Ton/Year  |
| <b>Total carbon foot print for conventional system</b>                 | 1,211.25  | Ton/Year  |
| Proposed system  |           |           |
| <b>Diesel consumption for month</b>                                    | 22,325    | l/month   |
| <b>Diesel consumption for year</b>                                     | 267,900   | l/year    |
| <b>Carbon foot print for diesel consumption</b>                        | 734.05    | Ton/Year  |

### Performance evaluation of the cogeneration plants with the capacity of a hotel

Proposed configuration of cogeneration system was designed to cater to the maximum electricity demand. Then effects of various economic and environmental factors of generating on-site electricity and excess generation

management were evaluated. As shown below, the energy cost and environmental facts of the cogeneration systems were evaluated for varied hotel capacities. The operational cost and the environmental impact were also calculated and shown in the Figure 3 and Figure 4.

Operational cost and the carbon foot print were calculated as follows.

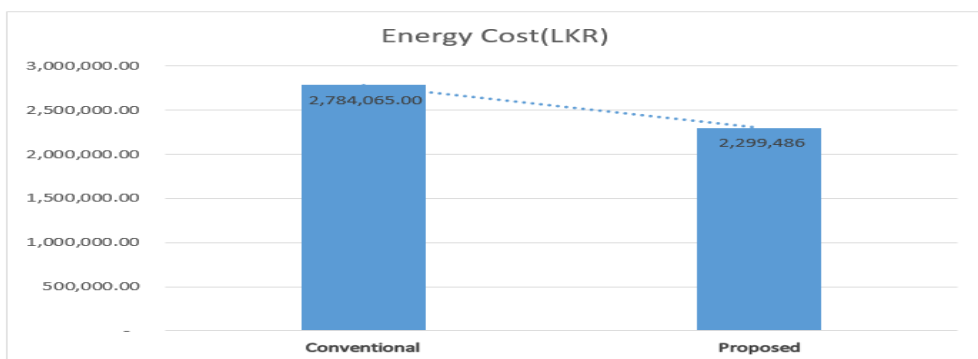


Figure 3: Energy cost

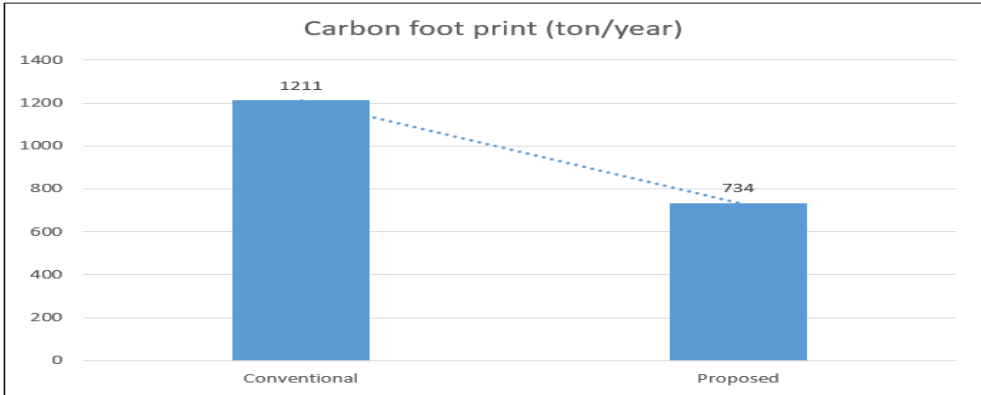


Figure 4: Carbon Footprint

Similar to figure 3, indicates that generation combinations reduce the energy cost by about 11%. Therefore, it can be safely assumed that recover the waste heat requirements from the onsite is more economical in terms of savings. However, impact of capital needs to be studied in detail after optimizing the system.

As shown in figure 4, in this setup too, the CO<sub>2</sub> emission is much lower than the existing setup. With waste heat recovery option, the amount of carbon footprint of emissions is 40% lesser than the conventional

### Capacity Analysis for other facilities

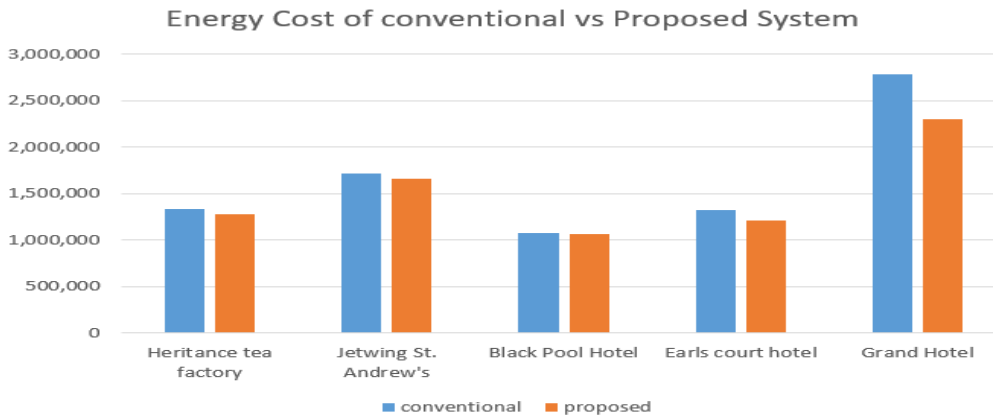


Figure 5: Energy Cost of Conventional Vs. Proposed System

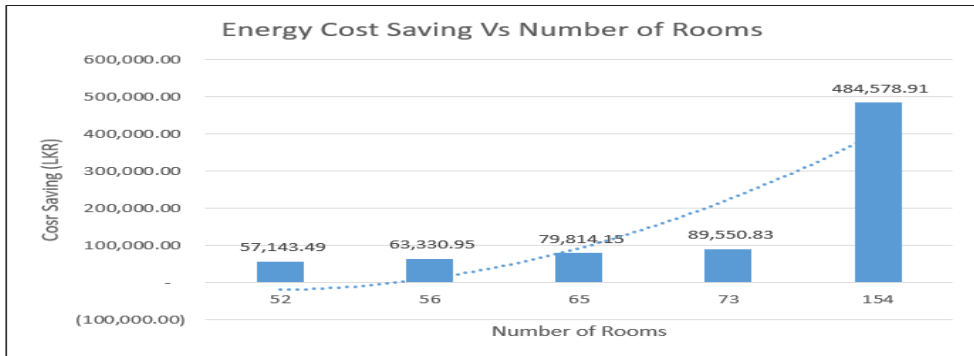


Figure 6: Energy cost saving vs. number of rooms

AS indicated in the trend line, there is no significant saving for the small-scale hotel such as below 100 rooms. On the other hand, the calculation doesn't reflect the maintenance cost and labour cost too. So the actual saving of the facilities will be less than the indicated value.

## Conclusions

When considering the fuel cost in the study it was identified as the most suitable type of co-generation plant for above 100 rooms' hotels. Small-scale hotels below 100 rooms have no significant profitable operation cost when considered the maintenance and labour costs.

The fuel cost can reduce further, if cheap fuel such as furnace oil is used. But it is not technically viable to apply furnace oil running generators for the facilities which have electricity demand below 1MW. For a facility which exceeds which exceed the electricity demand of 1MW, it will be more profitable than the diesel running system.

One of the most prominent facts in the results is the extremely favourable

economic and environment result for the above 100 room hotels Co-Generation plants. Such systems are technically not much sophisticated. Diesel driven generators are the most common equipment in Sri Lankan buildings and operating and maintenance the waste heat recover boilers much simpler than the diesel boiler. Another important area to study is how to create a certificate system for self-generated electricity that would encourage the industry to implement Co-generation. Study on implementing methodologies to obtain benefits from carbon credits is also important.

Finally, it is evident that the Sri Lankan upcountry hotels can be benefited from implementing co-generation plants meeting economical targets in a sustainable manner.

## Acknowledgements

We would like to thank Mr. Chinthaka Jagodarachchi, EnergySolve Intentional (Pvt) Ltd. for providing technical information and other relevant literatures for the completion of this thesis work.

## References

- [1] 'Chinese tourist numbers in Sri Lanka: a case for improving growth'. Online Available: <https://blogs.lse.ac.uk/southasia/2018/02/27/chinese-tourist-arrivals-to-sri-lanka-a-case-for-improving-growth/>, Accessed on: 15/05/2019
- [2] 'Performance 2017 and Programmes for 2018', Ministry of Power and Renewable Energy. Online Available: <http://powermin.gov.lk/english/wp-content/uploads/2017/10/MoPRE-2017.2018-03-English.pdf>, Accessed on: 12/05/2019
- [3] 'Ensuring sustainability on Sri Lanka's growing hotel industry'. Online Available: <https://www.ifc.org/wps/wcm/connect/30f331004fddd89eb9d8ff23ff966f85/Mapping+Report+++Ensuring+Sustainability+in+Sri+Lanka%E2%80%99s+Hotel+Industry.pdf?MOD=AJPERES>. Accessed on: 12/05/2019
- [4] 'Electricity Generation Facts'. Online Available: <http://www.energy.gov.lk/index.php> Accessed on: 20/05/2019
- [5] 'Cogeneration'. Online Available: [https://cset.mnsu.edu/engagethermo/systems\\_cogen.html](https://cset.mnsu.edu/engagethermo/systems_cogen.html). Accessed on: 15/05/2019
- [6] Online available: <https://www.prweb.com/releases/2012/2/prweb9204937.htm>, Accessed on 18/08/2019
- [7] Online available: <https://www.sciencedirect.com/topics/engineering/cogeneration-plant>, Accessed on 18/08/2019
- [8] Online available: <https://www.sciencedirect.com/topics/engineering/cogeneration-system>, Accessed on 18/08/2019
- [9] Online available: <https://biomasspower.gov.in/document/download-leftside/Biomass%20Cogeneration.pdf>, Accessed on 18/08/2019

# A Tunnel Dryer for Clay Roof Tile; Preliminary Evaluation of Pilot Unit

J.A.A.D.Jayasuriya <sup>#1</sup>, A.S.K.Warahena <sup>\*2</sup>, E.A.N.K. Edirisinghe <sup>#3</sup>

*# Energy & Environmental Engineering Department, National Engineering Research & Development Centre of Sri Lanka  
Industrial Estate, Ekala, Sri Lanka*

<sup>1</sup> ajithjaya@nerdc.lk

<sup>3</sup> nandana@nerdc.lk

*\* Department of Manufacturing Technology, University of Vocational Technology  
No. 100, Kandawala Road, Ratmalana*

<sup>2</sup> aruna.warahena@gmail.com

## Abstract

The traditional clay roof tile draws a special interest as a roofing material due to its aesthetic character and good thermal comfort it provides. However, the market share of these tiles is only 10-15% in Sri Lanka as there are several imported roofing materials. The process of tile manufacturing includes raw material processing, tile forming, drying and firing. Drying is the most critical stage as long as quality is concerned. Improper drying causes tile to be deformed. The traditional practice is to allow the tiles to lose its surface moisture content in ambient conditions by stacking them in open racks. On average, rate of deformed products (rejects) is 20% and the drying time is around 8 days. But in dry seasons, drying is faster, but causes more rejects due to deformation. During the rainy seasons drying takes prolonged periods extending to about 2 weeks. The tunnel type clay roof tile dryer designed to process 1080 numbers of tiles at a time was fabricated installed and tested for functionality at a tile factory at Waikkal Sri Lanka. Trial runs indicated that warping of tiles occur due to uneven drying of two faces of the tile. The dryer was operated on both continuous mode and batch mode while controlling the temperature and air flow. Preliminary evaluation of the dryer indicated that 1080 numbers of tile could be dried in 60 hours by maintaining drying temperature 33.50C – 350C in the dryer with no deformation or warping of tiles when ambient humidity is around 76 – 83 %.

The results indicate that the tunnel type dryer has a greater potential to replace the existing primitive type of drying practice. The user friendliness of functions of loading, unloading and moving of trays requires to be improved.

**Keywords:** Drying, Clay roofing tiles, Tunnel dryer

## Introduction

Clay roof tiles dominated the market as the elegant and standard roofing material at certain times in history and today face some setback due to the competition from cheaper alternative roofing materials. Yet the traditional clay roof tile draws a special interest as a roofing material due to its aesthetic character and good thermal comfort it provides. However, the market share of these tiles is only 10-15% in Sri Lanka as there are several imported roofing materials. Earlier the main clay tile profile type was Calicut but now profiles come in various shapes [1]. In Sri Lanka there are about 290 numbers of small scale tile factories, having monthly capacity less than 150,000 tiles while only 5 numbers of large scale factories in operation with monthly capacity more than 150,000 tiles [2]. The quality of clay tiles is governed by the Sri Lanka Roofing Tile standards (SLS2:2016). The standard covers Calicut, Roman, Euro, Spanish, Plain and Sinhala tiles. In addition, SLS2:2016 extends to cover the European export tile requirements [2].

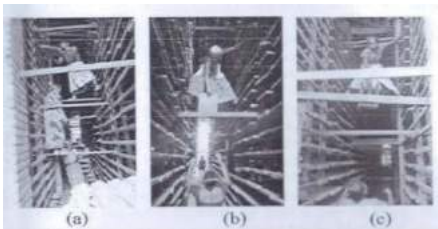


Figure 1: Conventional method of drying of clay tile

In the process of manufacturing of clay tiles drying is the most critical stage as long as quality is concerned. Improper drying causes tile to be deformed. The traditional practice is to allow the tiles to lose its surface moisture content in ambient conditions by stacking them in

open racks [4]. On average, rate of deformed products (rejects) is 20% and the drying time is around 8 days. But in dry, drying is faster, but causes more than 20% rejects due to deformation. During the rainy season drying takes prolonged periods extending to about 2 weeks [2].

## Process of Roofing Tile Production

The basic process steps in clay roof tile manufacturing are as follows. [3]

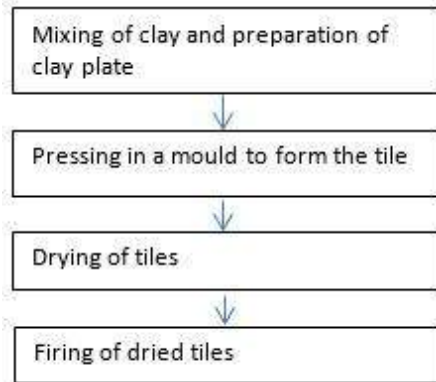


Figure 2: Basic process steps in clay tile manufacturing

Raw material processing and forming are done using machines and firing is done in a biomass fired kiln. In small scale industries clay tiles are dried using sun drying.

## Drying of Roof Tiles

The drying of the tile should be done at a controlled rate, as otherwise they will warp in the heat of the sun and due to effect of the wind. Therefore, in small scale clay tile manufacturing, tiles are dried after staking in shelves under a shade. Rapid drying causes tile to be warped or deformed.

Therefore, usually it takes a week to get dry during dry season and even two weeks are not enough in a rainy climate [3]. In the Indian subcontinent, and as

especially witnessed in Sri Lanka, the formed raw tile is quite wet and an extensive drying process and practice is desired [4]. "It is not possible for the tiles to undergo rapid drying. It would cause the surface hardening and the moisture inside would be trapped, which is undesirable. If the drying rate is too slow, the dryer output would be reduced which affect the production capacity and productivity. Till the moisture diffusivity reaches the beginning of falling the drying has to be controlled" [4]. It is very important to allow removing water from clay tiles until them stiffen up before entering the dryer [5].

### Development of a Roof Tile Dryer

National Engineering Research and Development Centre (NERDC) designed and developed a tunnel type clay roof tile dryer suitable for small/medium scale tile manufactures on a request of the Ministry of Industry and Commerce of the government of Sri Lanka. The pilot unit of the dryer was installed at the Pathiraja Tile mill at waikkal.

Objective of the project was to conduct a preliminary evaluation of performance of the Pilot unit of the tile dryer installed at the tile factory at Waikkal.

### Material and Methods

#### Tunnel Type Roof Tile Dryer

The tunnel type clay roof tile dryer tested under this study, had been designed to

process 1080 numbers of tiles at a time. The dryer was fabricated and installed at the Pathiraja Tile Factory at Waikkal, Sri Lanka (Figure 3). The dryer consists of 12 numbers of movable trolleys with each trolley capable of carrying 90 numbers of tiles.

The forced draft type fuel wood burning furnace provides necessary heat for the dryer. Flue gasses generated from the furnace are directed through a set of pipes located in the lower compartment of the dryer and exit to the atmosphere through a chimney (Figure 4). Ambient air enters in to the dryer through adjustable air ports located at both sides of the lower compartment of the dryer, get heated by heat carrying pipes. Humid air exits the drying chamber through vanes located at the top. (Figure 2). Trolley is so designed that the tiles are placed at an angle to the incoming air flow for even distribution of air in both sides of a tile (Figure 5).

The dryer could be operated in continuous mode by loading trolleys loaded with tiles at predetermined time intervals at the cold end of the dryer so that tile gets dried while they move on towards hot end of the dryer. The tile laden trolleys are moved mechanically by pulling them along the dryer. This dryer could also be operated in batch mode by loading all the trolleys laden with raw tiles and keeping without being moved until drying is completed.



Figure 3: The pilot plant of Tunnel type tile dryer



Figure 4: Pilot unit of Roof tile dryer



Figure 5: Trolley and heat pipe arrangement in the dryer



Figure 6: Un-loading of a trolley

### Conducting Preliminary Drying Tests

Trail A was conducted by operating the dryer in continuous mode. In this preliminary test run, all the trolleys were loaded to the dryer but only every other trolley was loaded with tiles. Therefore, in Trial A, 540 tiles loaded in to six trolleys

with ninety tiles per trolley, were dried. After operating the furnace, trolleys with tiles were loaded to the dryer from the cold end and moves forward in a predetermined time period.

Trail B was conducted by operating the dryer in batch mode. In Trial B, 1080 tiles were dried using twelve trolleys with ninety tiles loaded to each trolley.

In both tests before feeding to the dryer tiles were kept outside for some time period ranging from 20 to 24 hours for the purpose of avoiding formation of a high moisture gradient within a tile at the beginning of the drying, which may leads to warping or cracking of tiles. Completion of drying was decided by manual scratching method by an expert in the field, which is the traditional practice.

In conducting test operations, the furnace was fed with fuel wood manually by monitoring the temperature of the drying compartment at the hot end of the dryer. Temperature and humidity data loggers were fixed to every other trolley, starting from the hot end. The ambient temperature and humidity were also recorded.

## Results and Discussion

### Test A

Test A was conducted by operating the dryer on continuous mode and 540 numbers of tiles were dried. Retention time in the dryer varied from 54.5 – 61 h (Table 1). Because tiles were kept outside the for 20 -24 h time period before entering to the dryer, total drying time was approximately from 78.5 h (3.3 days) – 85 h (3.5 days). In this drying test operation no warped or deformed tiles were observed.



Table 1: Summary of performance Test A of Roof tile dryer

| Trolley No | Ave. Temp. (°C) | Ave. RH (%) | Retention time (h) |
|------------|-----------------|-------------|--------------------|
| 1          | 31.2            | 70.18       | 54.5               |
| 3          | 32.1            | 68.8        | 63.5               |
| 5          | 32.4            | 68.7        | 61.5               |
| 7          | 32.5            | 69          | 65                 |
| 9          | 32.1            | 70.8        | 63                 |
| 11         | 32.6            | 69.7        | 61                 |

In operating the dryer in Test A, the average ambient temperature and humidity were 29.2 °C and 76.8% respectively. Rate of fuel wood consumption 4-5 kg/h.

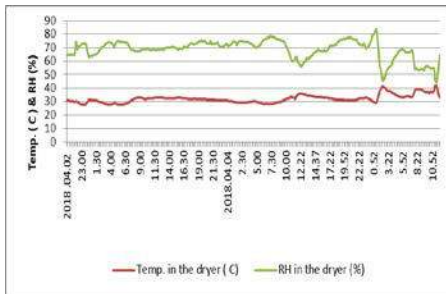


Figure 7: Test A; Trolley No 3; Variation of temperature and humidity in the dryer when operate on continuous mode

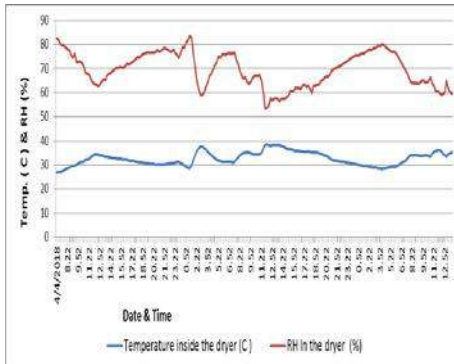


Figure 8: Test A; Trolley No 11; Variation of temperature and humidity in the dryer when operate on continuous mode

**Test B**

Test B drying operation was conducted on batch mode. Dryer was operated at comparatively high temperature in order to observe and study the effect of temperature on the drying time. Twelve numbers of trolleys with altogether 1080 numbers of tiles were loaded to the dryer. Trolleys were kept stationary until time of completion of the drying. Retention time in the dryer of tiles were 24.5 to 36 h. Considering the time period outside the dryer, as 24 h, total drying time were 48.5 h (2.02 days) – 60 h (2.5 days). Tiles in 1<sup>st</sup> trolley which is located at the hottest end of the drier were deformed. Approximately 5% of tiles in 2<sup>nd</sup> and 3<sup>rd</sup> trays were deformed. No warping of tiles in rest of the trays were observed.

Table2: Summary of performance Test B of Roof tile dryer

| Trolley No | Ave. Temp. (°C) | Ave. RH (%) | Retention time (h) |
|------------|-----------------|-------------|--------------------|
| 1          | 38.8            | 53.8        | 24                 |
| 3          | 36.8            | 59.7        | 24.5               |
| 5          | 35              | 64.81       | 30                 |
| 7          | 33.5            | 71.5        | 32                 |
| 9          | 33.3            | 73.4        | 33.5               |
| 11         | 33.5            | 71.5        | 36                 |

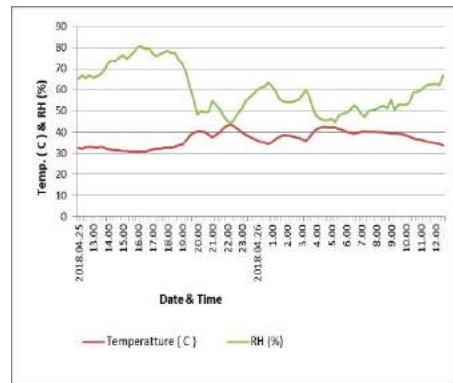


Figure 9: Test B; Trolley No 3; Variation of temperature and humidity in the dryer when the dryer operates on batch mode

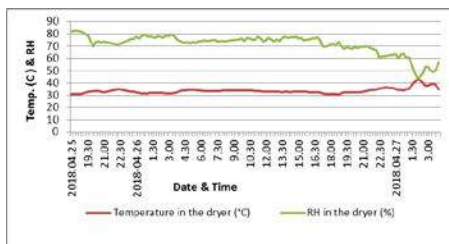


Figure 10: Test. B; Trolley No.11; Variation of temperature

In the Test B, the temperature of trolley No.3 (Figure 9) has gone up above the 33 °C, 7 hours after entering to the dryer. But none of the tiles in both of these trollies had been warped. Although the average temperature of trolley No. 3 is 36.8 °C, the average temperature in the first 7 hours was 32 °C. That is before exposing to a temperature in excess of 32 °C, tiles had been dried 24 h outside the dryer at ambient conditions and 7 h in the dryer. It gives indication on the critical time period of drying of a tile. In operating the dryer in Test B, the average ambient temperature and humidity were 27.4 °C and 83.1 % respectively. The average rate of fuel wood consumption was 10 kg/h.

## Conclusions

In operating the tunnel type dryer in continuous mode, dryer performed without any warping or deformed tiles with retention time in the dryer 54.5 h to 61 h at an average temperature in trollies ranging from 31.2 °C – 32.6 °C with average relative humidity in drying compartments 70.18 % - 69.7 %. Total period of drying, taking in to account of the period of keeping the tiles outside the dryer, was 78.5 h – 85 h. No deformed tiles were observed in this configuration

In the batch mode operation, the retention time in the dryer was 24.5 to 36 h, at an average temperature 33.5 °C- 35

°C with average RH 59.7 - 71.5 %. Total drying time was 48.5 h – 60 h. Total of 10 % tiles was deformed. The results indicate that by avoiding exposing the tiles to a temperature in excess of 35°C and by maintaining the temperature within the first 7 h less than or equal to 32 °C, amount of deformation of tiles could be reduced.

Operating continuously needs attention of labour to load and unload trollies approximately by 2 h time periods. Results suggest that by operating the dryer at a higher temperature than 33.5 – 35 °C after initial 7 h of drying, the drying time on continuous mode could also be reduced.

These preliminary drying trials were conducted on average ambient RH value 76.8 % - 83.1 %. Under these environmental conditions generally in conventional natural drying, it takes about 14 days for completion of drying of tiles.

It was observed that further improvement of mechanisms of loading, unloading and moving of tiles through the dryer is required in order to make it more user-friendly.

## Acknowledgement

The authors greatly appreciate the Financial assistance and support provided by the NERDC management, Ministry of Industry and Commerce and also to Pathiraja Tiles Company at Waikkal facilities afforded for implementing this project. Facilities provided by the Energy and Environmental Management Centre of NERDC for collecting data, is also thankfully acknowledged. A Presentation of this research work has been made at NERDC.

## References

- [1] Ariyaratna G.L.M. et.al., Investigating the physical, mechanical and thermal properties of common roofing materials in Sri Lanka, NBRO Symposium 2015- "Innovations for resilient environment"
- [2] Kularathna Wipul, Use of red clay roofing tiles in the construction industry, Business Lanka Vol.30 –Issue 04/2017
- [3] W.D.S.M. Costa, A.L.M. Mouroof, Properties of flat clay tiles, Annual Transactions of IESL, 2005, Institution of Engineers of Sri Lanka
- [4] Aruna S.K. Warahena et al. Development of a "Roof-tile drier" for traditional roof industry- a feasible technological transformation step for productivity improvement, towards revival of a traditional industry, University of Peradeniya, 2016
- [5] <https://ceramicartsnetwork.org/daily/pottery>

**SRI LANKA SUSTAINABLE ENERGY AUTHORITY**

1<sup>st</sup> Floor, Block 5, BMICH, Baudhaloka Mawatha, Colombo 07.

E-mail : [symposium@energy.gov.lk](mailto:symposium@energy.gov.lk) | Telephone : 0112 677 445

Web : [www.energy.gov.lk](http://www.energy.gov.lk)

Facsimile : 0112 682 534



**SRI LANKA SUSTAINABLE ENERGY AUTHORITY**

1<sup>st</sup> Floor, Block 5, BMICH, Baudhaloka Mawatha, Colombo 07.

E-mail : [symposium@energy.gov.lk](mailto:symposium@energy.gov.lk) | Telephone : 0112 677 445

Web : [www.energy.gov.lk](http://www.energy.gov.lk)

Facsimile : 0112 682 534

